Purification and Structural and Functional Characterization of Major Donkey Seminal Plasma Proteins, DSP-1 and DSP-3

A Thesis
Submitted for the Degree of

DOCTOR OF PHILOSOPHY

By
Sk Alim
(Reg. No. 16CHPH26)





School of Chemistry
University of Hyderabad
Hyderabad, Telangana- 500046
India
December 2022

Dedicated to My Beloved Parents and Family

Contents

Statement		i
Certificate		ii
Declaration		v
Acknowledgm	nents	vi
Abbreviations		X
Chapter 1:	Introduction	1
Chapter 2:	Purification, Molecular Characterization and Ligand Binding Properties of the Major Donkey Seminal Plasma Protein, DSP-1.	25
Chapter 3:	Chaperone-like Activity of the Major Donkey Seminal Plasma Protein DSP-1 is Modulated by Ligand Binding, Polydispersity and Hydrophobicity.	58
Chapter 4:	Probing the Chemical Unfolding of and Phospholipid Binding of the Major Protein of Donkey Seminal Plasma, DSP-1 by Fluorescence Spectroscopy.	82
Chapter 5:	Primary Structure Determination and Physicochemical Characterization of DSP-3, a Phosphatidylcholine Binding Glycoprotein of Donkey Seminal Plasma.	106
Chapter 6:	General Discussion and Conclusions.	135
References		140
Plagiarism Re	port	156
List of Publications		



School of Chemistry University of Hyderabad Hyderabad-500046

STATEMENT

I hereby declare that the matter embodied in this thesis is the result of investigations carried out by me in the School of Chemistry, University of Hyderabad, Hyderabad, under the supervision of **Prof. Musti J. Swamy**.

In keeping with the general practice of reporting scientific observations, due acknowledgements have been made whenever the work described is based on the finding of other investigators. Any omission which might have occurred by oversight or error is regretted.

Hyderabad

December 2022

Sk Alim



School of Chemistry University of Hyderabad Hyderabad-500046

CERTIFICATE

This is to certify that the thesis entitled "Purification and Structural and Functional Characterization of Major Donkey Seminal Plasma Proteins, DSP-1 and DSP-3" submitted by Mr. Sk Alim bearing the registration number 16CHPH26 in partial fulfillment of the requirements for the award of the Doctor of Philosophy (Ph.D.), is a bonafide work carried out by him under my supervision and guidance in the School of Chemistry, University of Hyderabad, India. This thesis is free from plagiarism and has not been submitted previously in part or in full to this or any other University or Institution for the award of any degree or diploma.

Further, the student has five publications before submission of the thesis for adjudication and has produced evidence for the same in the form of reprints.

Parts of this thesis have been published/communicated for publication (or under preparation) as indicated below:

- 1. <u>Alim, S.</u>; Chappali, S.K.; Laitaoja, M.; Talluri, T.R.; Janis, J. and Swamy, M.J., Purification, Molecular Characterization and Ligand Binding Properties of the Major Donkey Seminal Plasma Protein DSP-1, *Int. J. Biol. Macromol.* 2022, **194**, 213–222. (Chapter 2)
- 2. <u>Alim, S.</u> \$; Cheppali, C.K.\$; and Swamy, M.J., Chaperone-like Activity of the Major Donkey Seminal Plasma Protein DSP-1 is Modulated by Ligand Binding, Polydispersity and Hydrophobicity, (To be Communicated). (\$These two authors equally contributed). (Chapter 3)
- 3. <u>Alim, S.</u>; Das, S. and Swamy, M.J., Probing the Chemical Unfolding of and Phospholipid Binding to the Major Protein of Donkey Seminal Plasma, DSP-1 by Fluorescence Spectroscopy, *J. Photochem. Photobiol. A: Chemistry* (Under Review). (Chapter 4)

4. <u>Alim, S.;</u> M. Laitaoja, Pawar, S.S.; Talluri, T.R.; Janis, J. and Swamy, M.J., Primary Structure Determination and Physicochemical Characterization of DSP-3, a Phosphatidylcholine Binding Glycoprotein of Donkey Seminal Plasma Protein, *Int. J. Biol. Macromol.* (Under Review). (Chapter 5)

The student has also made presentations in the following conferences:

- Poster presentation at International Conference on Frontier Area of Science and Technology (ICFACT-2022), 12th India-Japan Science and Technology Seminar organized by Indian JSPS Alumni Association (IJAA), 9-10 September, 2022, University of Hyderabad, Hyderabad, India.
- 2. Poster presentation at **CHEMFEST-2022**, 19th Annual in-house Symposium, 22-23 April, 2022, School of Chemistry, University of Hyderabad, Hyderabad, India.
- 3. Poster presentation in the 44th Indian Biophysical Society Annual Meeting, 30th March–1st April, 2022 (hybrid mode) at ACTREC, Navi Mumbai, India.
- 4. Oral presentation at **CHEMFEST-2021**, 18th Annual in-house Symposium, 19-20 March, 2021, School of Chemistry, University of Hyderabad, Hyderabad, India.
- 5. Poster presentation in the 43rd Indian Biophysical Society Annual Meeting, 15-17 March, 2019, IISER Kolkata, Kolkata, India.
- 6. Poster presentation at **CHEMFEST-2019**, 16th Annual in-house Symposium, 22-23 February, 2019, School of Chemistry, University of Hyderabad, Hyderabad, India.
- 7. Poster presentation at **CHEMFEST-2017**, 14th Annual in-house Symposium, 3-4 March, 2017, School of Chemistry, University of Hyderabad, Hyderabad, India.

Further, the student has passed the following courses towards the fulfillment of the coursework requirement for Ph. D. degree:

Sl. No.	Course	Title	Credits	Status	
1.	CY-801	Research Proposal	3	Pass	
2.	CY-551	Biological Chemistry	3	Pass	
3.	CY-805	Instrumental Methods-A	3	Pass	
4.	CY-806	Instrumental Methods-B	3	Pass	

Hyderabad

December 2022

Dean

School of Chemistry

University of Hyderabad

Dean SCHOOL OF CHEMISTRY University of Hyderabad Hyderabad-500 046 Prof. Musti J. Swamy

(Thesis Supervisor)

Prof. Musti J. Swamy School of Chemistry University of Hyderabad Hyderabad – 500 046, India



School of Chemistry University of Hyderabad Hyderabad-500046

DECLARATION

I, Sk Alim hereby declare that the thesis entitled "Purification and Structural and Functional Characterization of Major Donkey Seminal Plasma Proteins, DSP-1 and DSP-3" submitted by me under the supervision of Prof. Musti J. Swamy is a bonafide research work which is free from plagiarism. I also declare that it has not been submitted previously in part or in full to this University or any other University or Institution for the award of any degree or diploma. I hereby agree that my thesis can be deposited in Shodganga/INFLIBNET.

A report on plagiarism from the University Library is enclosed.

9/1/2022

Sk Alim

Reg. No.: 16CHPH26

5k Alin 2022

Prof. Musti J. Swamy

(Thesis Supervisor)

Prof. Musti J. Swamy School of Chemistry University of Hyderabad Hyderabad – 500 046, India

ACKNOWLEDGEMENTS

This is a pleasant obligation to express my heartful thanks to all those who contributed in different ways to accomplish the thesis. It wouldn't be complete without thanking their contributions.

First, I would like to express my heartfelt gratitude to my doctoral supervisor, Prof. Musti J. Swamy, for his continuous cooperation, encouragement, and kind guidance. I am highly indebted to him for allowing me to work under his supervision and giving me complete freedom to express my thoughts and explore the area I wanted. His continuous encouragement helped me to stay positive even when my Ph.D. work was not going smoothly. It has been an unforgettable educative experience for me to work with him.

I extend my heartiest thanks to the present and former Dean(s) and Faculty members at School of Chemistry for their valuable suggestions at various stages and the infrastructure available at the school. My sincere thanks to doctoral committee members, Prof. Lalitha Guruprasad and Prof. Tushar Jana, for their cooperation and support during Ph.D. journey.

I want to thank all the non-teaching staff of the SoC for being very helpful and supportive, Mr Abraham, Mr Gupta, Mr Venkate, Mr Durga Prasad, Mr Anandam, Mr Mahendra, Ms Gita, Ms Rani, and Ms Radhika, in particular. I am also grateful to the Central Instrumental Laboratory, VoH, for providing an excellent instrumentation facility. My special thanks to Dr Maqbool Ahmed, Mr Prasad, and Mr K. Dasaradha (Dept of Plant Science, SLS) for their assistance and cooperation during various experiments.

I express thanks to our collaborators, especially Prof. Janne Jänis and his student Mikko Laitaoja (Department of Chemistry, University of Eastern Finland, Joensuu, Finland) for mass spectrometry facilities and Thirumala Rao Talluri (Equine Production Campus, ICAR-NRC on Equines, Bikaner, Rajasthan) for providing the seminal plasma samples. I also thank Prof. Appa Rao Padile (Promer V.C. and Professor, Dept. of Plant Science, University of Hyderabad) and his student Dr. B. Bhuvanachandra; and Dr. Amit Nag and his student Dr. Deepthi P. Damera for the fruitful collaborative work, I am also grateful to Prof. Anunay Samanta of our school for giving me access to a time-correlated single-photon counting instrument and to his student Mr Somnath Das for their help with the TCSPC measurements.

Financial support from the Department of Science and Technology (DST), IoE program of the UGC (India) and research fellowship (IRF & SRF) from Maulana Azad National Fellowship (UGC and Ministry of Minority Affairs, India) is greatly acknowledged. I also want to acknowledge the Biocenter Finland/FINStrust, Biocenter Kuopio for the FT-ICR MS facility.

My life inside the lab has always been a memorable journey with colleagues who have made the lab atmosphere friendly and enjoyable. I am grateful to my senior, Dr. Sudheer Kumar Cheppali, for introducing me to biophysical chemistry techniques and for his timely suggestions on various things. I would also like to acknowledge Dr. Debparna Datta, Dr. Debashree Das, Dr. D. Sivaramakrishna, Dr. Kishore K. Bobbili and Dr. Pavan K. Nareddy for their fruitful suggestions and discussions. I have

enjoyed working with Dr. Saradamoni Mondal, with whom I have associated from the very first day of my Ph.D. journey, and we have discussed various aspects. I also have spent a good quality time and unforgettable memory with Ch. Ravinder. I appreciate Suman Kumar Chowdhury for being a most organized person and maintaining a cheerful enjoyment in the lab. I also would like to thank Sonali S. Pawar for being a responsible junior who always cooperates during our work, including making tea and black coffee in the lab. I am very thankful to my present other labmates Sneha Banerjee, Konga Manasa and Tejaswini for providing a friendly, cheerful and cooperative atmosphere in the lab. I would also like to thank my project students, Shruti Nambiar, Itishree Mishra and Anindya Das, for asking many interesting questions and discussions, which helped my research.

I thank all the research scholars and my seniors at the School of Chemistry, especially Sugata da, Rudra da, Navendu da, Suman da, Kallol da, Sudipta da, Subhobrata da, Tanmay da, Senthil Anna, Sathis Anna, Arun anna, Anupam da, Suriya anna, Anil anna, Ramesh Anna, Samita di, Shipra di, Mou di, Sneha di, Sabari di, Moumita di, Apurba, Tasnim, and my junior colleagues, especially, Noorul, Ashfaque, Somnath, Sumanta, Sabir, Asif, Suraj, Alamgir, Sashi, Debu, Somratan, Arunava, Somdatta, who have always been there to help me during my research journey.

I cherish bonding with all my Ph.D. batchmates (2016-batch): Akram, Irfan, Istiyak, Gorachand, Shubham, Soutick, Suman, Pritam, Nilanjan, Ravi, Shubham (Datta), Laxman. Jyotsna, Mamina, Prachi, Soumya, Jayakrushna and Santi for their support and encouragement.

Since the first day of joining VoH, I have been blessed with many Bangali friends and seniors. I thank them, especially Dr. Abu da, Dr. Intaj da, Hasan da, Arif da, Rahmat da, Mahmud da, Subrata da (Physis), Bappa, Arijit, Salman, Shamsurjjamman, Mahi, Dr. Abu Taher. I am also thankful for my juniors Nasir, Nurul, Mainul, Dr. Nazir, Chandan, Hanjala, Alam, Salam, Sohel and many more, who have always been there to help me and made my stay in Hyderabad a memorable one.

I want to cherish my friendship with NRS-Hostelmates Basha, Akram, Pravinder, Anupam da, Saddam, Hafijur, Ankit, Intejar, Irfan, Shubham, Soutrick, Suman, Pritam, Somnath, Anupam, Sumanta, Alamgir, Mujahid, Nasir, Shamsujjaman, Rahmat da, Mahmud da, Bappa, Arijit, Kuntal, Abhishek, Mainul, Nurul, Arshad, Sadab and many more, with whom I have spent a lot of memorable times.

I am incredibly thankful to Dr. Saddam, Basha bhai, Hafijur, Mujahid, Liton and Nasir. Without their cheerful company, my VoH campus life would have been boring. Saddam is not only my friend but also like to be my brother, with whom I have spent my life journey for more than 12 years, and I will never forget his unlimited love and care for me. I am very fortunate that I have a friend like him. Very Special thanks to Basha bhai, who always offered me a helping hand in my ups and downs, along with for making delicious biriyani every Friday night, and I liked to bike ride with him in Hyderabad city, which is an unforgettable memory for me. My special thanks to Hafijur bhai for helping and standing with me in various difficult times and making delicious food every Sunday. I appreciate my junior friends Liton, Nasir and Mujahid, who always helped me with many ups and downs.

During my hostel life for more than 14 years, I stayed with some amazing people as my room-mate in different hostels: Dr. Sabir Ahmed da, Sajjad, Noor da, Laxman bhaiya (UP), Sharif bhaiya, Niyaz bhaiya, Saddam Bhaiya (UP), Nayeem, Asif bhaiya, Izhar bhai, Mudasir bhai, Hasan da and Hafijur bhai and I had spent a wonderful time with them.

Before coming to Hyderabad, I had a wonderful time at 'Aligarh Muslim University, which was my second home then. It is difficult to express my love and memory with AMU; it was and will always remain in my heart. I still enjoy the unforgettable memories and happy moments I had with my Aliq friends. I sincerely thank my batch-mates, Rabiul (Malda), Rabiul (MSD), Mefta, Aminul, Akhi, Kanchan, Sakil, Munna, Arif Choudhry, Aslam, Nirshad, Zulfikar, Wasikul, Bittu, Selim, Atiur, Salauddin, Sahid, Hasan, Ishtiyak, Talha, Yousuf, Arafat, Anisur, Alkariya, Babloo Khan, Anurag, Chirag Kumar, Hira Lal, Ishrat, Nazia, Nazlin, Sudha Rani, Tuba Husain, Mantasa, Zeenat, Azharul, Wadut, Firoj, Ashfaque, Akhtar, Atiur, along with my seniors, Dr. Samima di, Dr. Tahasin da, Dr. Mohin da, Dr. Shamim da, Ashraful da, Dr. Saigal da, Dr. Mutaleb da, Rauf da, Ismail da, and juniors Najrul, Javed, Wahid, Alam, Tousif, Mafizur, Atikur, Sahel, Nooh, Badsha, Saddam Seikh, Samiul Gazi, and many more for encouraging me to do better and better constantly. I also acknowledge my friends and seniors in M.M. Hall, especially Dr. Sabir Ahmed da, who always blessed and cared for me during my starting journey at AMU. Along with Dr. Sujon da, Dr. Yusuf da, Dr. Ikbal da, Dr. Ajmal da, Dr. Bellal da, Dr. Ariful da, Dr. Faiyaz da, Dr. Firoj da, Dr. Hasibul da, Dr. Rustam da, Adil da, Tasif da, Noor da, and my friends Sayedil (Remedy), Nayan, Sohel, Akib, Monirul, Kabirul, Ejajul, Rony, Nur Ali, Rafikul, Faroog, Katatah, Faiyaz, Kaosar, Sipan, Matin, Lotus, Amir, Faiyaz, Karim, and my juniors Hafijul, Horyra, Monin Ali, Ashekul, Rahaman, Abid, Samaun, Nayeem, Tipu, Rakibul, Nurul, Saiful, Yousuf, Asif, Salauddin, shahid, Mukhlesur, Abuzar, and many more. There I had my unique association with some seniors and friends, whose I must acknowledge; Dr. Sabir da, Dr. Samima di, Saddam, Riyaj, Sayeed, Rabiul, Tasirul, and Sajjad for the friendship they offered and still maintained. Samima di is always showing her helping hand to me and giving me her valuable suggestions for my academic as well as personal life. It was an unforgettable journey I spent there and will remember throughout my life.

I also acknowledge my friends from 'Al-Ameen Mission', Azhar Answary, Iqbal, Sabbir, Minaruddin, Imran, Sannan, Salman, Samirul, Azhar Mondal, Azhar Biswas, Sakib, Arif Nowyaj, Arif Sk, Shahjahan, Ibrahim, Hasanat, Maroof, Faruque, and others for their friendship and supports. Friends from 'Bhatakul Swarnamoyee High School', especially Moniruddin, Emarul, Kabirul, Sudip, Arka, Kausik, Amit, Jahar, Bappa, Moni, and many more, along with "Balgona Coaching Centre" friends, Rintu, Argha, Palu, Yousuf, Debaki, Suprova, Joynti, Sathy, Priya, Riya, Manusi, and many more for the golden days of enjoyment and stupidity. Thank you all, guys, for sharing very crucial years with me.

How can I forget my childhood buddies, with whom I went to school, played with them, and spent valuable time with them; Ashadulla (Bullet), Mustakim (Ripu), Hasibuddin (Bokul), Tausif (Rentu), Bappa, Monalisha, and Moli. I have a lot of unforgettable memories with them.

I am highly thankful to all my teachers who taught me at different stages of my life, and I must acknowledge the valuable contribution of all my teachers; Basiruddin (Milu) mama, Bhutu mama, Dhanu Babu, Sanjay sir, Debasis sir, Bamkim sir, Pijus sir, Swapan Kanti sir (Head Master), Nanda sir, Pradeep sir, Subhas sir, Pratima di, Rekha di, and my 'Balgona Coaching Centre' teachers: Pilot sir, Pintu sir, Uttam sir, Haradhan sir, and my teacher of 'Al-Ameen Mission': Nurul Islam sir (Secretary), Azijul sir, Hasibul sir, Asif sir, Sofikul sir, Rafikul sir, Monirul sir, Habibur sir, Manik Sir, Ashraf sir, and along with 'AMU' professors: Aminul sir, Suhail Sabir sir, Akram Sir, Riyajuddin sir, Shakir sir, Palashuddin sir, Musawwer sir, Rafiuddin sir, Rouf sir, Samsurjamman sir, Sartaj sir, Faruqe ma'am, and Azam bhai (for coaching classes) for their encouragement, dedication, lessons, and hard work which made my academic path easier over the years.

This journey in my life would be impossible without my family's unconditional support, love, and contributions. I will never be expressed in words what the tiredness, struggle, support and sacrifice have done by my mother, Sufia Bibi, and my father, Late Sk. Mannan; my brothers Sk Salem and Sk Dalim; and my sisters Suhagi and Seli, for me. My sincere gratitude to my brothers Salem and Dalim, who are taking care of me as their son, and today what I am, just because of them only, and I am proud to be their younger brother. My special thanks to my brothers-in-law, Khorsed and Rafik, and my sisters-in-law, Nasima and Ajmira, for their love, support, and encouragement. I am blessed with my nephews, Bishal, Swadhin, Roni, Suhan and Ahaan, and my niece, Rima (Rikhta), whom I love so much and spend my time at home. I want to thank all of my relatives, especially my brother-in-law, Nayan bhai and Saju bhai; my cousins, Bulti Bubu, Tumpa, Siraj bhai, Bullet, Sulet, Babar, Sabir, Rahul, for their endless love and supports. My heartfelt gratitude to my life partner Farha Khatun (very special to me), for her continuous unconditional support, love, encouragement, sacrifice and endless patience, which always push me forward. I am also highly grateful to her family members, Fajlur Rahaman and Reksona Bibi (parents), and Samim da, Tumpa di, Jahid, Noor, and Sarmin for their support, love and encouragement throughout my PhD journey.

My deepest apologies if I have forgotten your name, but I wish to express my heartful gratitude to everyone who has played a role in my life directly or indirectly.

Once more, thank you, everyone!

Alim

ABBREVIATION

ADH Alcohol dehydrogenase

AFM Atomic force microscopy

ATP Adenosine triphosphate

AR Acrosome reaction

BSP Bovine seminal plasma

 ΔCp Change in excess heat capacity

CA Carbonic anhydrase

CD Circular dichroism

Chol Cholesterol

CLA Chaperone-like activity

Da Dalton

DNA Deoxyribonucleic acid

DMPC 1, 2-dimyristoyl-sn-glycero-3

phosphocholine

DMPG 1, 2-dimyristoyl-sn-glycero-3-(phospho-

rac-1-glycerol

DOPC 1, 2-Dioleoyl-sn-glycero-3-phosphocholine

DSC Differential scanning calorimetry

DVPC 1, 2-divaleyl-*sn*-glycero-3-phosphocholine

DTT Dihiothreitol

EDTA Ethylenediamine tetra acetic acid

ESR Electron spin resonance

Fn Fibronectin

 ΔG Change in free energy

GdmCl Guanidinium chloride

GdmSCN Guanidinium thiocyanate

GlcNAc N-acetylglucosamine

G6PD Glucose-6-phosphate dehydrogenase

 ΔH Change in enthalpy

HCl Hydrochloric acid

His Histidine

HPLC High performance liquid chromatography

Hsp Heat shock protein

I-TASSER Iterative Threading ASSEmbl Refinement

ITC Isothermal titration calorimetry

Ka Association constant

LDH Lactate dehydrogenase

 β -ME β -mercaptoethanol

MRE Mean residue ellipticity

MRW Mean residue weight

NaCl Sodium chloride

NADP Nicotinamide adenine dinucleotide

phosphate

NMR Nuclear magnetic resonance

OD Optical density

PAGE Polyacrylamide gel electrophoresis

PBS Phosphate buffered saline

PC Phosphatidylcholine

PD Parkinson's disease

PDB Protein data bank

PKA Protein Kinase A

PrC Phosphorylcholine

RBC Red blood cells

REES Red-edge excitation shift

ROS Reactive oxygen species

RNA Ribonucleic acid

 ΔS Change in entropy

SDS Sodium dodecyl sulfate

SPR Surface plasmon resonance

SUV Small unilamellar vesicles

TBS I Tris buffer containing 50mM Tris, 0.15M

NaCl, 5mM EDTA, pH=7.4

TFA Trifluoroacetic acid

 $T_{\rm m}$ Transition mid temperature

ThT Thioflavin T

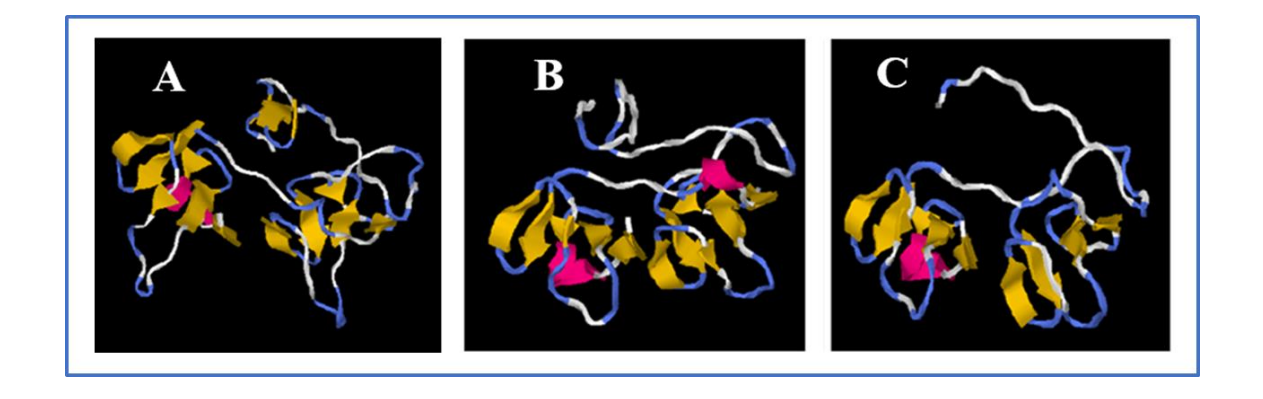
Trp Tryptophan

Tyr Tyrosine

ZP Zona pellucida

Chapter 1

Introduction



3-D modeling of (A) HSP-1, (B) HSP-2 and (C) PDC-109 (taken from Sankhala et al., 2012)

1.1. Mammalian reproduction system

Reproduction is a biological process in which the species are continued generation after generation. There are many ways to produce offspring, which are classified into two basic forms: sexual and asexual reproduction. In asexual reproduction, a single parent can produce new organisms which contain similar genetic materials like parent. Many plants, fungi, and single-celled organisms are reproduced through asexual reproduction. On the other hand, in sexual reproduction, male sperm and female egg interact and fuse each other and produce new offspring. Usually, higher organisms reproduce through sexual reproduction.

1.1.1. Sperm cell and its structure

The male gamete is called sperm cell or spermatozoon which is motile and fertilizes the female egg during fertilization. Initially, the immature sperm cells are produced in testis from male primordial germ cells which are present in the basal epithelium of testis and called spermatogonia. These spermatogonia become primary spermatocytes through mitotic cell division and each primary spermatocyte forms two secondary spermatocytes by first meiotic division. Single secondary spermatocytes divide into two spermatids through second meiotic cell division and these spermatids become mature spermatozoa (sperm) via the process known as spermiogenesis (Fig. 1.1). In this process the shape and size of spermatozoa undergo changes, which include acrosome formation, nuclear condensation and development of flagellum [Clermont et al., 1993].

Structure of sperm: Sperm cells carry genetic materials and have different sizes, shapes and forms among different animals. But their structure is uniform and highly conserved in the case of mammalian species. Through the female reproductive tract, the sperm are propelled with their flagellum by bending waveforms such as symmetric waveform (straight swimming path) as well as asymmetric waveform (curved path). [Gadêlha et al., 2020; Saggiorato et al., 2017]. A mature sperm cell contains four different parts, such as head, neck, middle piece and tail (Fig. 1.1).

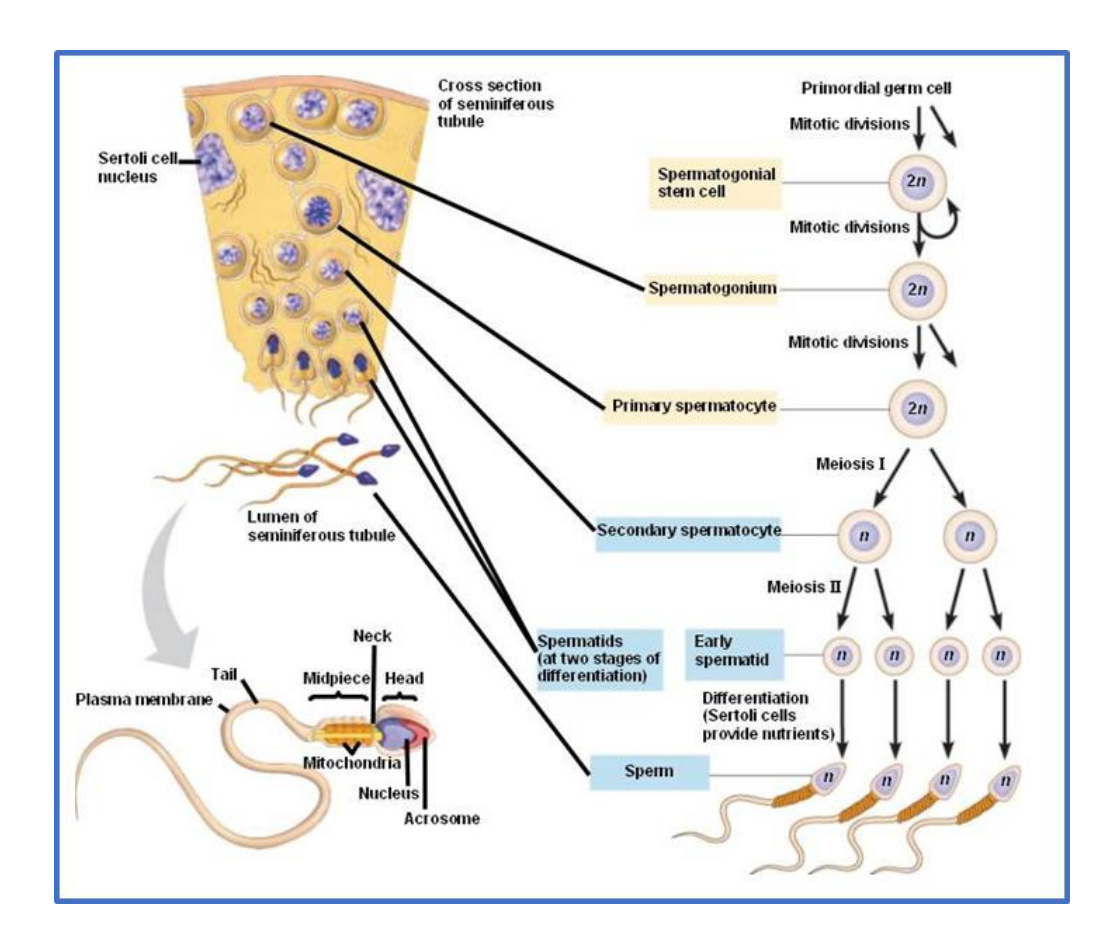


Fig. 1.1. Process of spermatogenesis. (Taken from bio1152.nicerweb.com).

Head contains a haploid nucleus and acrosome, a cap-like structure which is present on the anterior portion. Acrosome is protected by a membrane and contains various enzymes which help to lyse the egg membrane during fertilization. Most of the volume of the sperm head is occupied by a haploid nucleus which is covered by one nuclear membrane and contains nucleolus, DNA and a few basic proteins.

Neck is a small piece which separates the head and the midpiece and has two centrioles viz. distal centriole and proximal centriole. These two centrioles enter into female egg with the nucleus and assist the primary division of zygote. Distal centriole is remodelled structurally and compositionally into an atypical centriole and functions as the zygote's second centriole, which is used in diagnostics and therapeutic strategies in male infertility [Fishman et al., 2018].

Midpiece is essentially the middle part of the sperm cell and contains of various mitochondria which provide energy for sperm motility. Mitochondria are located around two longitudinal fibers (beta fibers) which are surrounded by 9+9+2 cross sectional pattern fibers, called alpha fibers [Fawcett, 1975; Philips, 1975].

Tail consists of principal piece part and end piece part and made of axial filaments which are arranged three and four perpendicular to one another which assist in sperm motility. Recent studies showed that spermatozoa are propelled by bending wave (like second harmonic wave form) travelling with their flagellum and the velocity depends on second harmonic amplitude and phase [Saggiorato et al., 2017].

1.1.2. Ovum (female gamete)

Ovum or oocyte is the female gamete or female reproductive cell which is produced in the ovary by a process known as "oogenesis". The maturation of ovum is a complex process and involves various stages via diploid 'oogonium' develop into a diploid "primary oocyte" which later matures into a haploid "secondary oocyte" by first meiotic division. The secondary oocyte forms mature ovum which is released from ovary by the process known as 'ovulation'. This mature ovum fuses with the sperm and forms a zygote.

1.1.3. Sperm capacitation

Ejaculated mammalian sperm cells are motile and mature but are unable to fertilize the ovum cell initially. These sperm have to spend a definite period of time in female reproductive tract before acquiring the fertilizing capability. In this period many physiological and biochemical changes occur in the spermatozoa which enable them to fertilize the female egg. This series of steps is referred to as "sperm *capacitation*" (Fig. 1.2). [Austin, 1952; Chang, 1951; Yanagimachi, 1994]. This process includes various sophisticated physiological modification such as "*cholesterol efflux*" from the sperm plasma membrane which increase the membrane permeability and fluidity of the plasma membrane, plasma membrane hyperpolarization, changes in protein kinase activity and protein phosphorylation [Arcelay et al., 2008; Hernandez-G. al., 2006; Visconti, 2009; Visconti et al., 1995]. Also, this process is regulated by protein kinase A (PKA) and

depends on various signaling pathways [Morgan et al., 2008; Salicioni et al., 2007]. Capacitation is a combination of fast event (associated with activation of the asymmetric and vigorous movement of ejaculated sperm) and slow event (changes in movement pattern known as hyperactivation), rather than a single event [Ickowicz et al., 2012; Salicioni et al., 2007]. After discovery of sperm capacitation, *in vitro* fertilization is possible but the molecular level mechanism and various factors involved in capacitation are still not clear [Visconti, 2009; Visconti et al., 1995. Recent studies developed logical surface manipulation technique which stabilize the sperm membrane that are beneficial for reproductive technology and animal breeding industries [Gadella and Luna, 2014; Leahy and Gadella, 2011a &b].

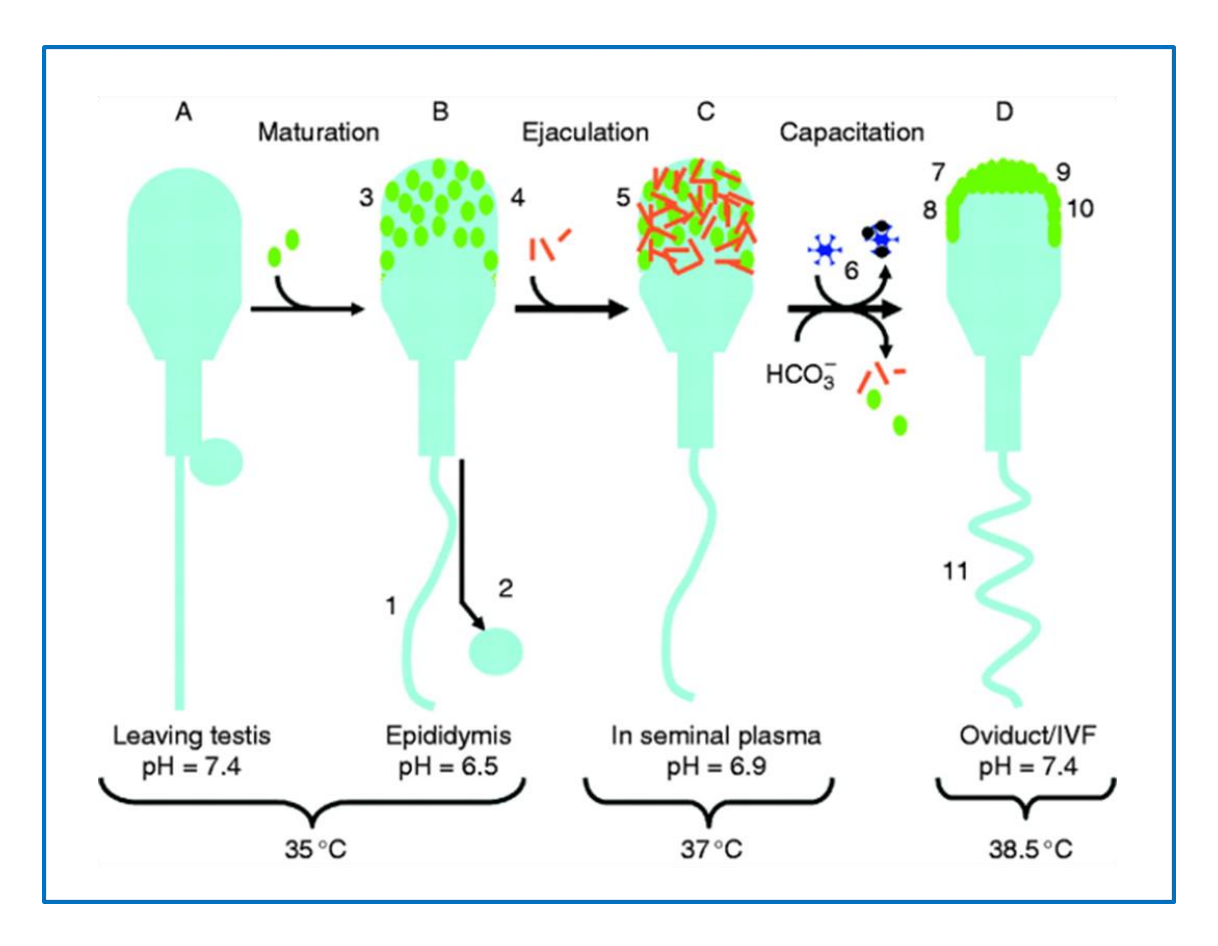


Fig. 1.2. Physiological sequence of sperm surface changes during capacitation. Taken from Leahy and Gadella, 2011.

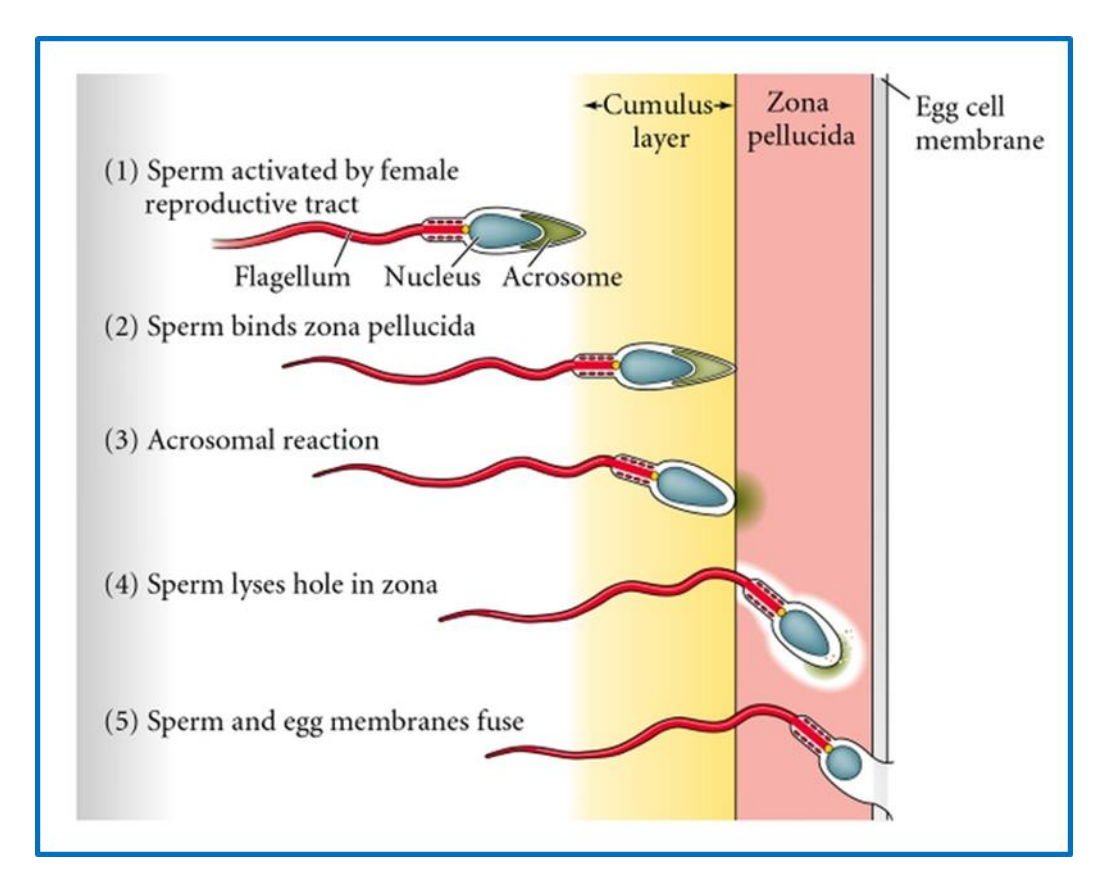


Fig. 1.3. Acrosome reaction in which sperm-egg fusion takes place and sperm nucleus enters into the ovum cell. (Reproduced from: https://commons.wikimedia.org/wiki/).

1.1.4. Acrosome reaction

Acrosome reaction (AR) is another very important event in mammalian fertilization, which is crucial for enabling the sperm to bind with and penetrate the zona pellucida, ZP [Yanagimachi, 1994]. The cap-like structure which is present on the sperm head is known as acrosome. While sperm comes in contact with the zona pellucida (egg membrane), the fusion of the acrosomal membranes and calcium influx occur, resulting in a release of the acrosomal hydrolytic enzyme which assist to dissolve the protective coat of the egg (Fig. 1.3). In case of mammalian fertilization, AR takes place in the fallopian tube of the female reproductive system. AR occurs through carbohydrate mediation Steroid hormones such as 17-estradiol (E2) and progesterone (P4) can also induce the AR through the receptor-mediator [Gimeno-Martos et al., 2021]. In the presence of tyrosine phosphorylation, the

percentage of AR increases which is associated with distribution of Concanavalin A (Con A) binding sites on the spermatozoa [Sáez-Espinosaa et al., 2021].

1.1.5. Fertilization

Fertilization is a complex process by which nucleus of spermatozoa (male gamete) and the nucleus of ovum (female gamete) are fused with each other and produce a zygote and this process occurs in fallopian tube of female mammals. During this process, various factors which are present on plasma membrane surface play important roles and also disrupt the plasma membrane. Initially, the interaction of capacitated sperm and zona pellucida is loose and reversible but after some time it becomes species specific, rigid and irreversible. As a result, nucleus is transferred from capacitated sperm to ovum and then both nuclei fuse with each other. [Wassermann, 1987; Yanagamachi, 1994].

1.2. Mammalian seminal plasma

Seminal plasma is released along with sperm during ejaculation, which is the liquid entity of semen and transports the spermatozoa in female reproductive system. Seminal plasma contains organic molecules along with some inorganic molecules such as sugar, metal ions, amino acids, basic amines such as spermidine, spermine and lipids. The only high molecular weight constituents present in seminal plasma are proteins; nucleic acids and polysaccharides and are absent [Shivaji et al., 1990]. A protective and healthy medium is provided for the sperm by seminal plasma during fertilization in the female reproductive system. Basically the environment of the vagina is viscous and acidic (due to lactic acid produced by microflora), and contains large number of immune cells and that is not suitable for sperm survival. Basic amines present in seminal plasma protect the spermatozoa from acidic denaturation. Various metal ions present in seminal plasma such as Mg²⁺ and Ca²⁺ also play a crucial role in maintaining basic pH during various stages of fertilization.

1.2.1. Fibronectin type II proteins

Fibronectin is a large glycoprotein, which contains multiple domains. It is soluble in plasma but exists in an insoluble form in the extracellular matrix. Fibronectin binds to

various compounds such as heparin, collagen, DNA, fibrin, actin and as well as bind with cell surface. Therefore, it performs some vital functions in cell migration, wound healing, maintenance of tissue integrity and blood coagulation. [Dean et al., 1987; Mosher, 1993]. The sequence of fibronectin consists of mainly three kinds of motifs, namely type I, type II and type III, which repeat multiple times. Among these, type II modules (FnII modules) are small, compact domains with two disulphide bonds and contain about 60 amino acid residues. Collagen was found to bind to the type II domain of fibronectin. The FnII modules are found in many other proteins with different functions, including proteins from "bovine seminal plasma", namely PDC-109, BSP A3 and BSP 30 kDa protein, mannose-6-phosphate receptors, members of the mannose receptor—phospholipase A2 receptor family, pancreas-specific sel-1 proteins of vertebrates, hepatocyte growth factor activator and blood coagulation factor XII [Skorstengaard et al., 1994].

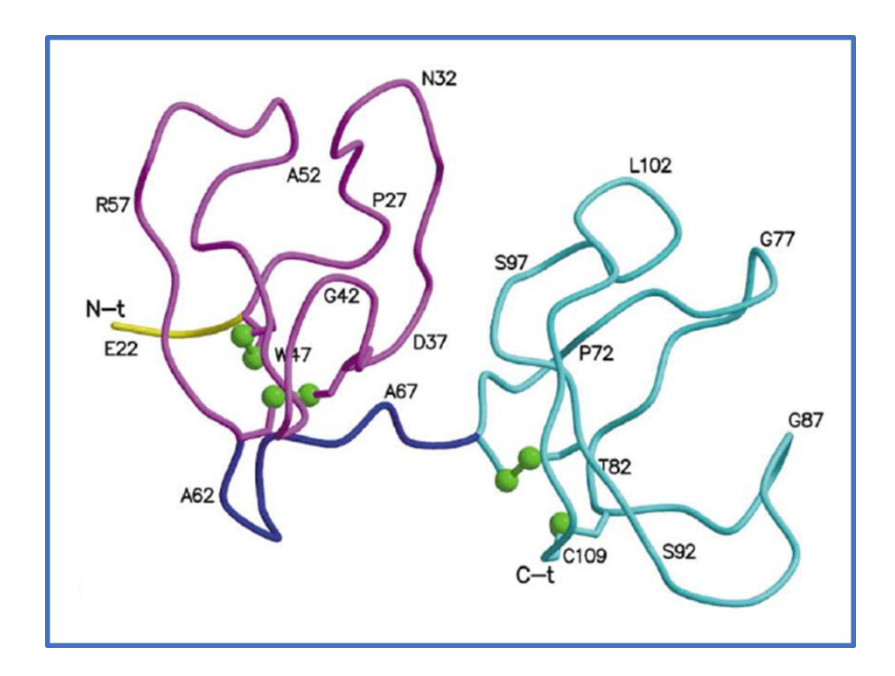


Fig. 1.4. Crystal structure of PDC-109, domain-I (violet colour) and domain-II (cyan colour). Taken from Wah et al., (2002).

PDC-109 was characterized using crystal structure (Fig. 1.4) and NMR and the results show that each FnII domain consists of around 40 amino acids with two antiparallel β-sheets, two disulfide bonds, formed between cysteines 1-3 and 2-4, and a conserved core tryptophan residue [Wah et al., 2002]. Phosphoryl choline was found to bind with Tyr and

Trp residues of PDC-109 via cation- π interactions as well as hydrogen bonds (Fig. 1.5) [Wah et al., 2002; Anbazhagan and Swamy, 2005].

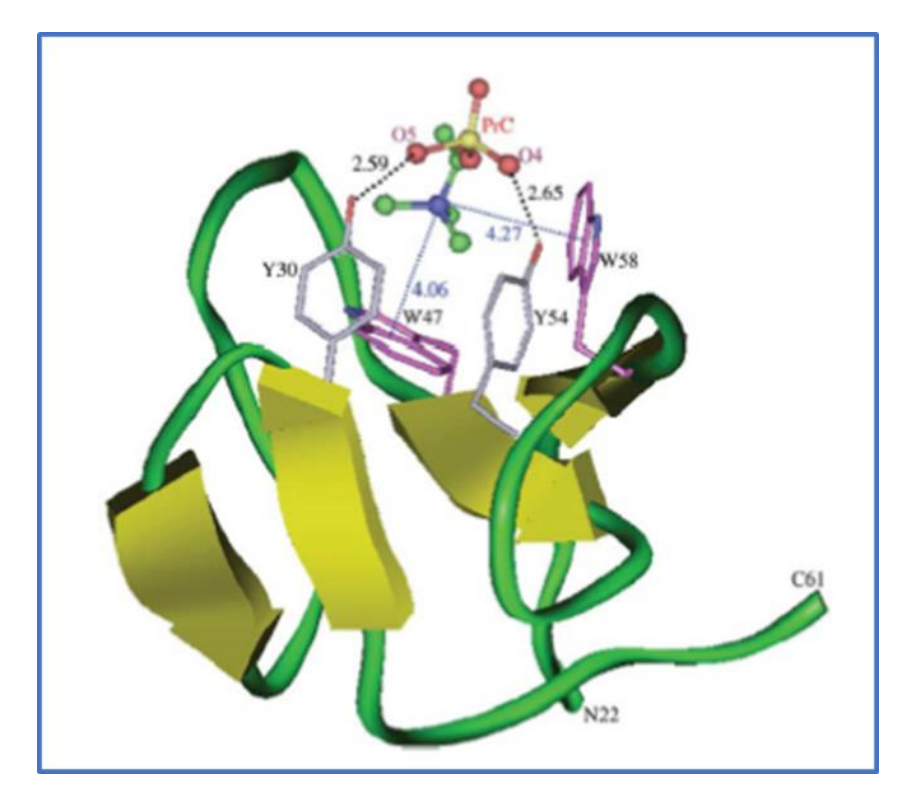


Fig. 1.5. Structure of a FnII domain of PDC-109 with bound PrC molecule. The structure was generated using the Insight II software. The backbone is shown as a ribbon and the side chains of Y30, Y54, W47 and W58, which interact with the ligand, are shown as sticks. Reproduced from Anbazhagan and Swamy (2005).

FnII domains are also present in various other mammalian seminal plasm proteins such as equine, porcine, goat etc. Among them, equine seminal plasma proteins (HSP-1 and HSP-2) are well characterized and they also show binding affinity towards choline containing phospholipids as well as phosphorylcholine via the tryptophan and tyrosine residues present on it (Fig. 1.6) [Kumar and Swamy, 2016a].

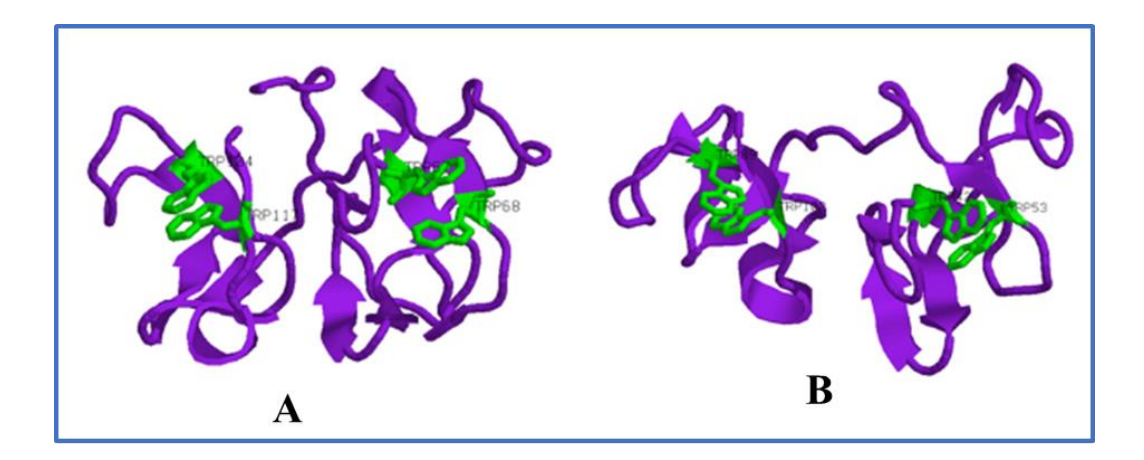


Fig. 1.6. Homology models of (A) HSP-1 (PDB code: P81121) and (B) HSP-2 (PDB code: CAA07074) generated using the I-TASSER server. Trp residues are shown in green color in the stick format. (Reproduced from Kumar and Swamy, 2016a).

Based on sequence similarity in kringle domain proteins and FnII domain proteins, it has been proposed that they are divergent members of a single family [Vali and Patthy, 1984]. Studies on those two domains reveals that FnII domain has many similarities with the protein-fold of protease kringles. Both FnII and kringle domains contain two short antiparallel β -sheets and ligand binding site that has several aromatic residues, besides two disulfide bonds [Ozhogina et al., 2001].

1.2.2. Bovine seminal plasma proteins

Bovine seminal plasma proteins are the acidic proteins released from the seminal vesicles and consist of four major proteins named as BSP-A1, BSP-A2, BSP-A3 and BSP-30 kDa [Manjunath et al., 1987a &b; Schiet et al., 1988]. The primary structure of these four proteins exhibits high homology [Calvete et al., 1996a; Seidah et al., 1987]. Among these proteins, BSP-A1, BSP-A2 and BSP -A3 are small proteins having molecular weights of 12-15 kDa, whereas BSP-30 kDa is a 30 kDa protein [Manjunath et al., 1987a]. The primary structure of BSP-A1 and BSP-A2 are identical but differ in the extent of glycosylation and the mixture of these two proteins is known as PDC-109 [Esch et al., 1983]. These proteins have two tandemly arranged repeating fibronectin type II (FnII) domains [Calvete et al., 1996a]. They exhibit affinity towards different ligands such as

choline phospholipids, heparin, sphingomyelin, gelatin, HDL, LDL etc [Desnoyers and Manjunath, 1992; Therien et al., 1995].

1.2.3. Structure and function of PDC-109

PDC-109 is present at a very high concentration (15-20 mg/mL) in "bovine seminal plasma" [Schiet et al., 1988]. PDC-109 has 109 amino acid residues and contains an N-terminal stretch of 23 residues followed by two tandemly repeating "fibronectin type" (FnII) domains [Baker, 1985; Esch et al., 1983] (Fig. 1.7). A large number of PDC-109 molecules (~9.5 million) bind to sperm surface during and upon ejaculation [Calvete et al., 1994]. This interaction is mediated through specific interaction between choline phospholipids and PDC-109 [Desnoyer and Manjunath, 1992]. This binding results in a release of cholesterol and choline phospholipids, which are present on the sperm plasma membrane together with PDC-109, and this process is termed "cholesterol efflux" and is an important step in "sperm capacitation" [Moraeu et al., 1998; Therien et al., 1998]. Single crystal X-ray diffraction study of PDC-109 complexed with PrC has revealed that both the PrC binding sites are on the same face of the protein and this binding occurs through cation-π interaction between tryptophan residue (indole ring) and the quaternary ammonium group of choline moiety [Wah et al., 2002].

Further PDC-109 shows binding affinity towards some other molecules such as gelatin, heparin, collagen, apolipoprotein A1, high- and low-density lipoproteins, casein, α -, β - lactalbulin and fibrinogen [Plante et al., 2015]. Spin-label electron spin resonance (ESR) studies show that the binding affinity of PDC-109 towards different phospholipids is different and it exhibits higher affinity towards choline phospholipids which is because of faster association and slower dissociation rate constant as compared to phospholipids having other head groups [Ramakrishnan et al., 2001; Thomas et al., 2003]. Absorption spectroscopic studies of the binding of Lyso-PC and PrC with PDC-109 revealed that the binding of Lyso-PC to PDC-109 is 250-fold stronger than that of PrC [Anbazhagan and Swamy, 2005]. The studies of interactions between PDC-109 and heparin using isothermal titration calorimetric (ITC) revealed that the binding affinity decrease with increasing pH or ionic strength [Sankhala et al., 2011], indicating the electrostatic forces play an

important role in the binding. PDC-109 exhibits "chaperone like activity" (CLA) by protecting different client proteins against thermal and other types of stress [Sankhala and Swamy, 2010].

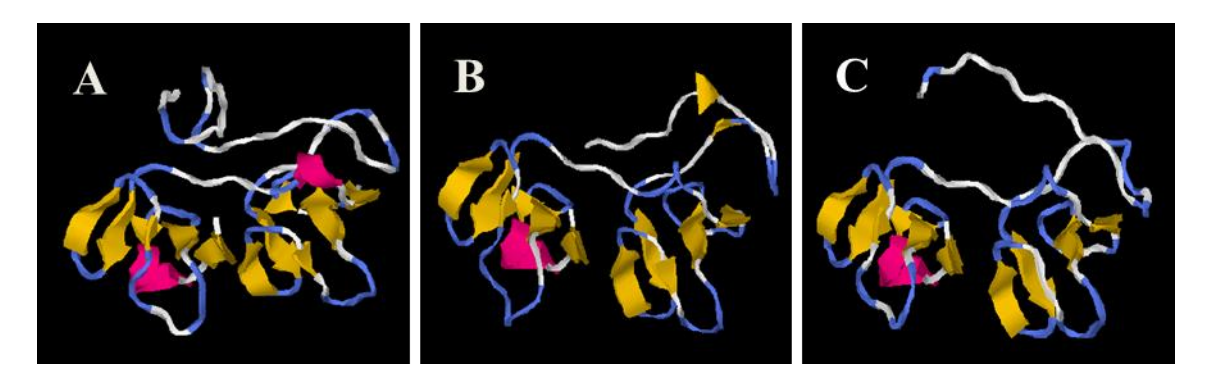


Fig. 1.7. 3-Dimensional structures of HSP-1 (A), HSP-2 (B) and PDC-109 (C) generated by I-TASSER server. Reproduced from Sankhala et al. (2012).

1.2.4. Equine (horse) seminal plasma proteins

Several proteins were isolated from horse (equine) seminal plasma using affinity chromatography and Reverse Phase-HPLC and these proteins have been named as Horse Seminal plasma Protein-1 (HSP-1) to HSP-8, based on their order of elution. Molecular weight of these proteins ranges between 14 and 30 kDa and all of them, except HSP-4, bind to the equine sperm [Calvete et al., 1994; Von Fellenberg et al., 1985]. Among these proteins only HSP-1 and HSP-2 belong to FnII type family proteins. HSP-3 belongs to cysteine-rich secretory protein (CRISP) type family protein whereas HSP-4 belongs to calcitonin gene like protein. But HSP-5 does not belong to any known protein family. HSP-6 and HSP-8 are homologous to human prostate specific antigen (PSA) and also isoforms of human kallikrein like proteins. HSP-7 is related to a family protein known as "Spermadhesins" which are the major proteins from porcine seminal plasma and have a single CUB domain. Among all these proteins only HSP-1, HSP-2 and HSP-7 exhibit lipid binding activity.

1.2.5. Equine seminal plasma protein-1 and -2 (HSP-1 and HSP-2)

Most of the seminal plasma proteins have a common characteristic structure that they contain an N-terminal flanking region, followed by two or four tandemly repeating

fibronectin type-II domains [Menard et al., 2003]. The major proteins from goat, bull, cattle and horse seminal plasma have only two FnII domains (short FnII proteins). Short FnII proteins are also present in ram, porcine, human and murine seminal plasma in less quantities [Fan et al., 2006]. Human and equine seminal plasma proteins which have four FnII domains belongs to long FnII proteins and named as SE-12 and EQ-12 [Saalmann et al., 2001].

1.2.6. HSP-1/2: Structure and functions

The amino acid sequence of HSP-1 consists of 121 amino acids which are organized into four domains in the pattern like AA'BB'. Unlike PDC-109 these proteins having two Fn-II domains designed as BB' and also contains an N-terminal flank with two repeated units of 16 amino acids, designated as A and A' (Fig. 1.7.A). HSP-1 and HSP-2 show a high degree of homology but HSP-2 has only one N-terminal 'A' domain (14 residues shorter in N-terminal region as compared to HSP-1) [Calvete et al., 1994; 1995]. These two proteins exhibit ~6% sequence similarity with PDC-109 [Sankhala and Swamy, 2010]. These two proteins could not be separated under non-denaturing conditions and their mixture is designed as HSP-1/2. Far- and near-UV CD spectroscopic studies revealed that the secondary structure of HSP-1/2 is very similar to PDC-109 [Anbazhagan and Swamy, 2005; Sankhala et al., 2012]. Thermal stability of HSP-1/2 increased in presence of PrC in a concentration-dependent manner, with unfolding temperature shifting from 49°C (HSP-1/2 alone) to 60°C (HSP-1/2 + 20 mM PrC) [Sankhala et al., 2012]. Normally, HSP-1/2 exists in polydisperse oligomeric form similar to PDC-109 but in the presence of PrC, it exists as a monomer or dimer [Calvete et al., 1997].

1.3. Molecular Chaperone

Chaperones proteins are molecules which assist the non-covalent folding or unfolding, and assembly or disassembly of other proteins or macromolecules [Laskey et al., 1978]. Normally proteins function as a molecular chaperone by protecting newly synthesized polypeptides from misfolding and aggregation under both normal and stressful conditions

[Ellis, 1987; Gething and Sambrook, 1992; Ullrich-Hartl, 1996; Horwitz, 1992; Kumar et al., 2005; Rajaraman et al., 1996].

1.3.1. Major families of molecular chaperones

The major classes of chaperone proteins are Hsp100, Hsp90, Hsp70, Hsp60, Hsp40 and the "small heat shock proteins" (*shsps*), which are present in cells and extra cellular region. Among these, Hsp100, Hsp90, Hsp70, Hsp60, Hsp40 are ATP-dependent chaperones and small heat shock proteins are ATP-independent. **Hsp100** (Clp) are present all most all organisms and these are highly conserved family proteins. They have a large hexameric structure and exhibit unfoldase activity in the presence of ATP. In this family some of the members like ClpA, ClpX etc. are associated with serine proteases and they target the misfolded proteins towards the degradation pathway, instead of refolding of that misfolded proteins (Fig. 1.8) [Glover et al., 1998].

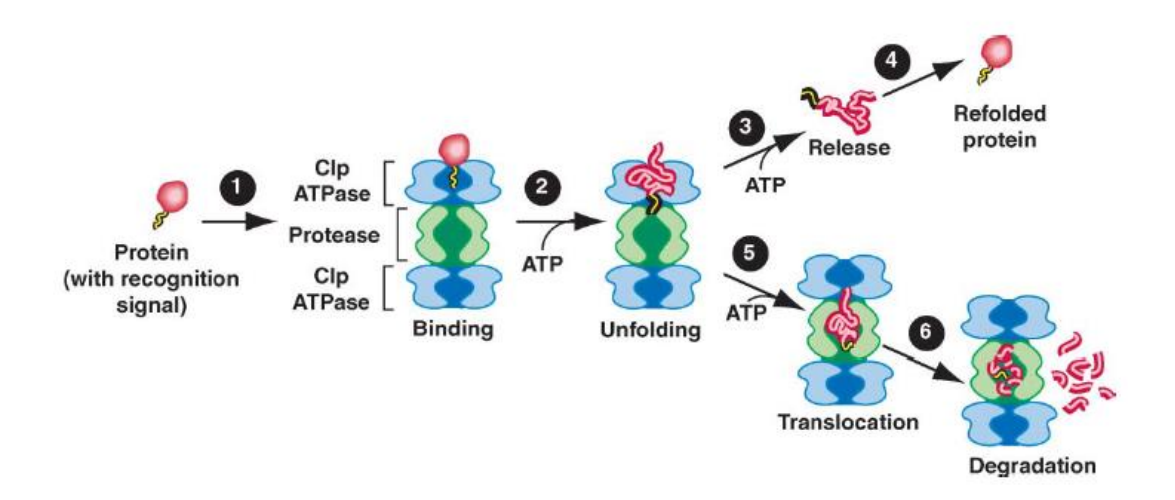


Fig. 1.8. Model of the mechanism of protein unfolding by Clp chaperones and degradation by Clp proteases. A lateral cross section of a Clp chaperone is shown in blue, associated with a proteolytic core shown in green. A substrate protein is shown in red, with a recognition signal shown in yellow. (Adopted from, Wickner and Hoskins, 2004).

Hsp90 and **Hsp70** families of proteins are also present in almost all organisms. Hsp90 exists as a dimer in mammals and functions with different co-chaperones [Prodromou et al., 1997; Wang et al., 2006]. Recent studies revealed that Hsp90 acts as an inhibitor in

cancer as 17-AAG which decreased cancer proliferation in head and neck cancer, breast cancer and colorectal cancer and binds to ATP binding site of Hsp90 [Zuo et al., 2020; Yang et al., 2021]. Hsp70 required a large set of co-chaperones (J-domain proteins) for regulating the ATPase cycle. Hsp70 and their cochaperones work together on the hydrophobic segments of the substrates and reduce the intermolecular interactions, thereby decreasing protein aggregation [Palleros et al., 1993; Goloubinoff et al., 1999; Rosenzweig et al., 2019]. **Hsp40** interacts with Hsp70 and functions as a co-chaperone for Hsp70 [Laufen et al., 1999] and DnaJ which belongs to Hsp40 family, can function as molecular chaperones independently [Hendershot et al., 1996] and can interact with Hsp70 protein [Hill et al., 1995; Qian et al., 1996]. One of the most famous proteins of **Hsp60** family is GroEL which regulates the assembly of bacteriophages [Ellis and van der Vies., 1991; Georgopoulos et al., 1973]. GroEL is also an ATP-dependent chaperone [Langer et al., 1992a; Martin et al., 1991; van der Vies et al., 1992].

"Small heat shock proteins" (*shsps*) and α-crystallin family proteins consist of extracellular heat shock proteins. They exhibit a large oligomeric structure of 300-1000 kDa with monomers of 12-43 kDa and this oligomeric nature is essential for their "chaperone-like activity" [Laufen et al., 1999; Sun and MacRae, 2005]. The major difference between this family and other Hsp family proteins is that these proteins are ATP-independent in nature [Horwitz, 1992]. They show a high affinity for partially folded intermediates but have no particular substrate specificity. The proposed mechanism of *shsps* is that under stress conditions they coated the target proteins through hydrophobic interactions and form stable complexes which gave protection from the unfavorable environment [Lee et al., 1997].

1.3.2. Spermatozoa-associated chaperone

In the male germline, several molecular chaperones have been identified such as DnaJB1, HspA1A, HspD1, HspE1, HspCA, HspH1, HspA5, Tra1 etc. which are somatic and germline specific [Mitchell et al., 2007]. Among these, DnaJB1, HspA1A, HspD1 and HspE1 are localized in the mid part and principal part of the sperm tail. HspA1A along with HspCA was detected in the equatorial region of the sperm. HspA1A along with

HspCA was present in the equatorial region of the spermatozoa. Tra1 is present in the sperm head and the localization of chaperones HspA5 and HspH1 are not clear so far. Though the actual role of these chaperones is not well characterized, studies on HspA1A indicate that it is very significant for fertilization as addition of anti-HspA1A antibody which reduced the rate of fertilization.

1.3.3. PDC-109 acts as a molecular chaperone

Experiments carried out *in vitro* demonstrated that PDC-109 acts as a molecular chaperone and protects a variety of proteins against various kinds of stress, indicating that it may also assist the proper unfolding or folding of proteins involved in the sperm "*capacitation*" *in vivo* [Sankhala and Swamy, 2010]. G6PD activity assay has shown that PDC-109 protected G6PD against inactivation at high temperature, whereas results of turbidimetric studies indicate that it is able to prevent thermally induced aggregation of various proteins such as LDH, ADH and aldose. Polydispersity is one the most important factor in chaperone-like activity of PDC-109. PDC-109 mainly exists as a polydisperse oligomer of high molecular weight of in bovine seminal plasma. This oligomeric form dissociates into dimer in the presence of PrC or high ionic strength and results in loss of CLA, indicating that polydispersity is important for the CLA of PDC-109 [Gasset et al., 1997]. PDC-109 complexed with lipid membranes exhibits more hydrophobicity than PDC-109 alone and the results show that PDC-109/lipid complex has higher CLA than PDC-109 alone [Sankhala et al., 2011]. The above results suggest that polydispersity and hydrophobicity are crucial factors for the CLA of PDC-109.

Recent studies have discovered that polyamines spermine and spermidine which are present in high concentrations in mammalian seminal plasma function as a chaperones and enhance the CLA of PDC-109 [Singh et al., 2017]. PDC-109 contains glycosylated (BSA-A1) and non-glycosylated (BSA-A2) forms and it has been shown that the non-glycosylated isoform of PDC-109 exhibits significantly lower CLA than PDC-109 [Singh et al., 2019]. In another study, it was demonstrated that conserved core tryptophans of FnII domains are crucial for the "chaperone-like activity" of PDC-109 [Singh et al., 2020].

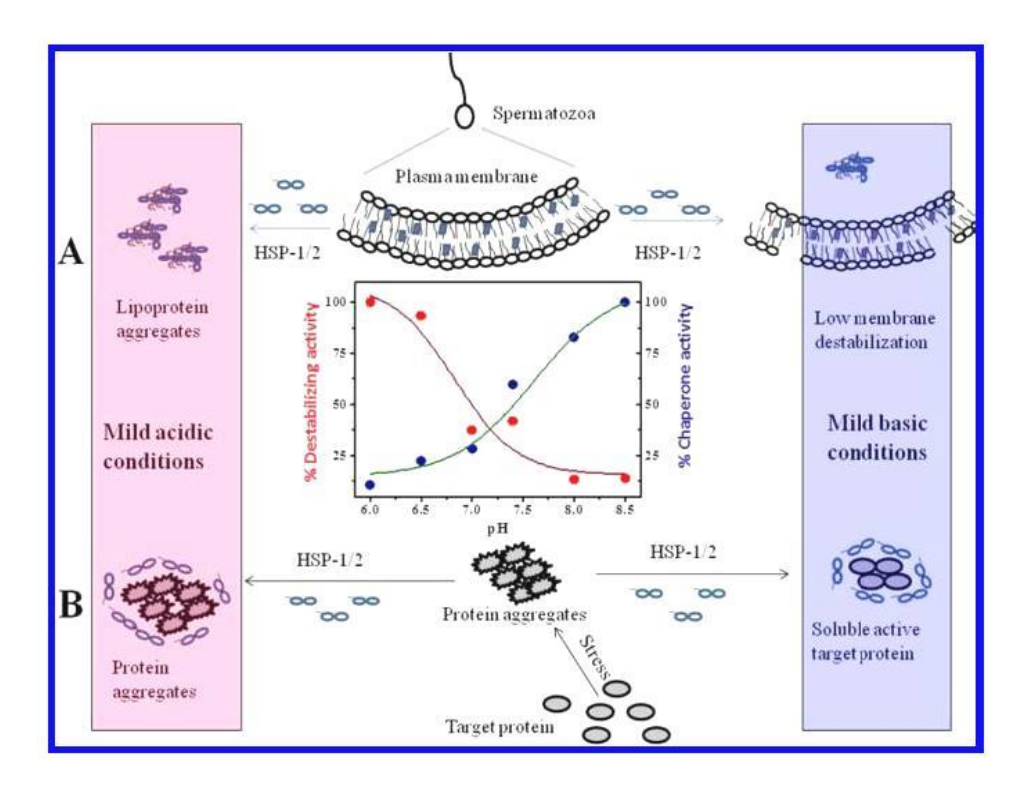


Fig. 1.9. Schematic representation of the dual functionality of HSP-1/2 regulated by a pH switch. (A) Cell membrane destabilization by HSP-1/2. (B) Chaperone-like activity of HSP-1/2 toward substrate proteins (Reproduced from Kumar and Swamy, 2016c).

1.3.4. HSP-1/2 acts as a molecular chaperone

The major protein from equine seminal plasma, HSP-1/2 exhibited chaperone-like activity *in vitro* and protected other proteins from misfolding/unfolding or aggregation against various thermal and oxidative stress conditions [Kumar and Swamy, 2016b; Sankhala et al., 2012]. Recent studies showed that the membranolytic activity of HSP-1/2 is low at basic pH and high at acidic pH whereas the CLA of HSP-1/2 is rather low at acidic pH but quite high at basic pH (Fig. 1.9). These results demonstrated that the chaperone-like and the membrane destabilizing activities of HSP-1/2 exhibit an inverse corelation with pH [Kumar and Swamy, 2016c].

Various other factors also modulate the CLA of HSP-1/2; these include surfactants, L-carnitine, ionic strength and membrane binding. Surfactants are molecules which can alter the properties of proteins such as change in the conformation, and surface hydrophobicity which are crucial for CLA of FnII type proteins. The results obtained in

one study by Kumar and Swamy (2017a) showed that neutral surfactants (e.g., triton X-100) and anionic surfactants (SDS) increase the CLA, whereas cationic surfactants (CTAB) decrease the CLA of HSP-1/2. L-carnitine, a metabolite presents at high concentration in various seminal plasma, interacts with HSP-1/2 and decreased both the chaperone-like and membrane destabilizing activities of it. Another report states that the chaperone-like activity of HSP-1/2 can be altered or modified by lipids and salinity of the medium and the results shows that high salt medium decrease the polydisperse nature of HSP-1/2 and correspondingly it exhibits lower chaperone activity [Kumar and Swamy, 2017b, 2018].

1.4. Lipids

Lipids are biomolecules which are soluble in organic solvents such as acetone, methanol, chloroform etc. and relatively insoluble in water and their solubility in organic solvents is due to their hydrophobic nature. Basically, lipids contain a hydrophilic head group which is connected to hydrophobic chains (alkyl or acyl chains). Lipids have a very important function in the living systems such as energy storage, signaling, acting as a structural component etc. Apart from this, lipids have applications in drug delivery, cosmetic and food industries and some lipids and their derivatives serve as hormones and vitamins. In general, lipids are two types: i) simple lipids, which cannot be hydrolyzed, such as cholesterol and other steroids and ii) complex lipids, which yield small molecules such as waxes and fats.

1.4.1. Classification of lipids

Membranes are important for the function and integrity of the cell and consists of lipids and proteins. Among the several model of membrane, the "Fluid-Mosaic model" proposed by Singer and Nicolson in 1972, is the most acceptable model. In this model, it was proposed that membrane has a bilayer structure, in which the hydrophobic tails are oriented towards each other and due to the presence of saturated and unsaturated fatty acids, those bilayers are fluid. The term mosaic comes from the presence of variety of molecules such as proteins, phospholipids, cholesterol etc [Singer and Nicolson, 1972; Singer, 1974]. Also,

this model indicates that membrane proteins diffuse through the surface of the membrane and lipid can 'flip-flop' (jumping of phospholipid from inner leaflet to outer leaflet). Mostly membrane contain three major types of lipids: glycolipids, phospholipids and sterols.

Basic phospholipid structu	re Su	bstituent (X)	Phospholi	pid/Characteristic
X	-н	hydrogen	PA	anionic
>	\nearrow NH ₂	ethanolamine	PE	zwitterionic
		choline	PC	zwitterionic
	→ NH ₂	serine	PS	anionic
\rangle	OH OH	glycerol	PG	anionic
	OH	P-O-O-O-O-O-O-O-O-O-O-O-O-O-O-O-O-O-O-O	CL	anionic
	но	phosphatidylglyce	rol Pl	anionic

Fig. 1.10. General structure of phospholipids and common head groups. Phospholipids contain two fatty acids ester-linked to glycerol which are attached at C-1 and C-2 and also a polar head group at C-3 through a phosphodiester bond. The different charges and common polar head groups are indicated. The lipids shown are: Phosphatidic acid (PA), phosphatidylethanolamine (PE), phosphatidylcholine (PC), phosphatidylserine (PS), phosphatidylglycerol (PG), cardiolipin (CL), phosphatidylinositol (PI) [Aktas et al., 2014].

Phospholipids: Phospholipids are amphiphilic in nature, containing a negatively charged phosphate moiety in the head group and two long hydrocarbon chains in the tail part which are hydrophobic. The hydrophobic tail part orient towards each other creating a non-polar environment in the membrane and hence the phosphate group facing out into the hydrophilic environment.

Glycerophospholipids: These phospholipids are naturally occurring and are found in biomembranes. Phosphatic acid (PA) is the simplest glycerophospholipid which is derived from glycerol and one primary hydroxyl attached with phosphate group and other two hydroxyls attached to fatty acyl long chains. Some other derivatives are found in the presence of different groups such as phosphatidylserine, phosphatidylcholine, phosphatidylethanolamine, phosphatidylglycerol etc (Fig. 1.10).

Sphingolipids: These consist of a sphingosine unit which acts as the backbone and contain polar head groups similar to those found in glycerophospholipids. Depending upon additional different groups linked to the backbone, these are classified into sphingomyelins, ceramides, phosphoethanolamine or phosphocholine which are linked to the hydroxyl group on C-1 of ceramide.

Sterols: These are mostly found in animal tissues and contain five or six-membered cyclic rings fused to one another, which makes them rigid hydrophobic molecules. with the only polar component in them is a single hydroxyl group. Sterols constitute about 30% of the plasma membrane lipids and also present in endosome, lysosome and Golgi complex. Sterols make gel phase more fluid-like and liquid-crystalline phase more rigid, and thus maintain the cell membranes at an intermediate level of rigidity.

1.4.2. Self-assembly of lipids

When the amphiphilic moieties like phospholipids are mixed with water, some specific structures are formed such as micelles, bilayers, liposomes or vesicles etc (Fig. 1.11), to minimize the interaction of hydrophobic part with water. The formation of these aggregated structures is modulated by specific external conditions such as pressure,

temperature, pH, ionic strength etc. This formation also depends on the size and shape of hydrophobic and hydrophilic parts of the lipid.

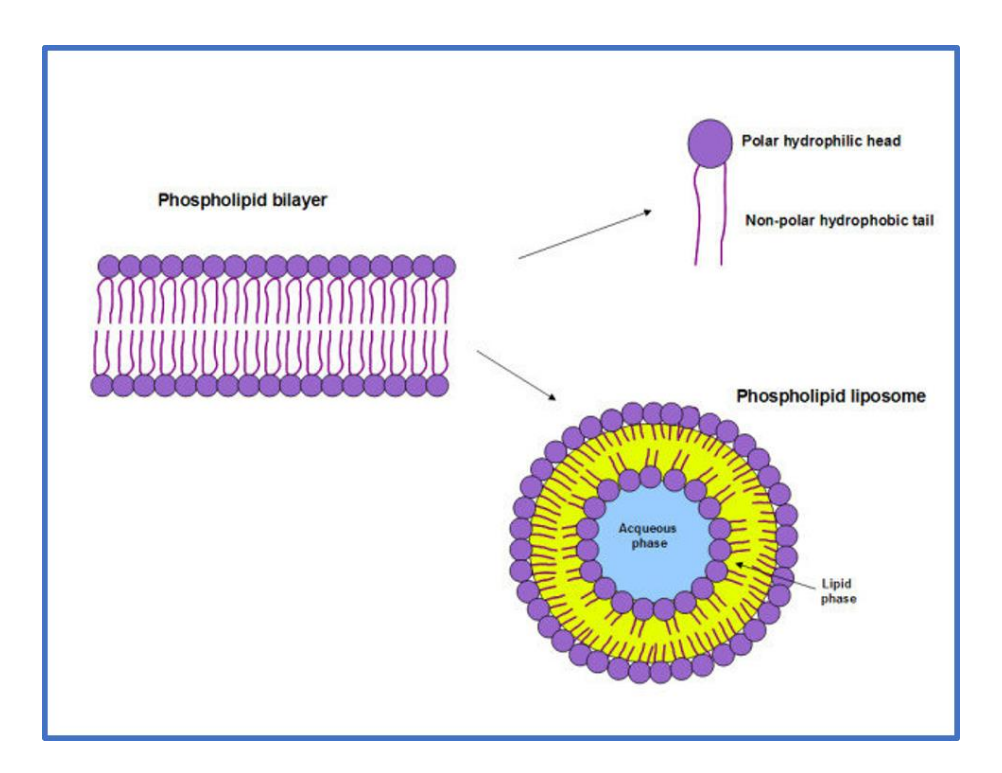


Fig. 1.11. Schematic representation of phospholipid, phospholipid bilayer and phospholipid liposome (Reproduced from Belhocine and Prato, 2011).

Micelles: This type of aggregates are formed in polar solvents in such a way that the hydrophilic part of the amphiphile is oriented towards the polar solvent whereas the hydrophobic part is oriented away from the polar solvent. Depending upon compositions and conditions, micelles may take several forms such as spheres, rods or disks etc. In nonpolar solvents such as benzene, reverse micelles are formed where the amphiphiles cluster around a drop of water in the system.

Monolayer: These are one layer thick and formed at the surface of aqueous solutions spontaneously when polar lipids are added. Here the hydrocarbon tails of polar lipids are exposed to air and the hydrophilic head groups extend into the aqueous phase.

Bilayer: This is very thin and formed spontaneously when phospholipids or amphiphiles are suspended in aqueous media and separate two aqueous compartments. In the bilayer, the hydrocarbon tails of the lipid moieties extend inwards from the two surfaces of the

aqueous compartments to form a continuous inner hydrocarbon core and the hydrophilic head groups towards the aqueous phase.

Liposomes: These are spherical vesicular structures (vesicles) made up of phospholipids or phospholipid-cholesterol mixtures or other lipids bilayer. Due to their special properties, liposomes are used in drug or enzyme delivery systems. Usually, liposomes are prepared by sonicating phospholipid suspensions in water.

1.4.3. Lipid-protein interaction

The plasma membrane consists of basically lipids and proteins, wherein the proteins perform different important cellular functions such as membrane reorganization, signaling and transportation of molecules/organelles [Tanguy et al., 2018]. Also, lipids in the membrane play a crucial role in the drug delivery system and to understand the mechanism of action of targeting drugs [Escriba, 2006; Escriba et al., 2008; Rask-Andersen et al., 2014].

Seminal plasma proteins - lipid membranes/vesicles interaction:

Interaction between seminal plasma proteins such as PDC-109 and HSP-1/2 with phospholipid membranes was investigated using various biophysical techniques such as ITC, ESR, AFM, fluoresce spectroscopy etc. [Anbazhagan et al., 2008, 2011; Damai et al., 2010, Kumar and Swamy 2016b &c; Gruebe et al., 2004]. The results obtained indicate that PDC-109 has a higher selectivity and stronger binding strength toward choline-containing phospholipids rather than other phospholipids such as phosphatidylglycerol, phosphatidylethanolamine etc. Interaction of PDC-109 with phosphatidylcholine was higher at higher pH which is physiologically significant. Fluorescence studies on HSP-1/2 showed a blue shift upon binding with choline phospholipids, indicating more hydrophobic microenvironment around the tryptophan residues. AFM studies indicated that destabilization of phosphatidylcholine membranes by HSP-1/2 binding is dependence on pH dependent with stronger destabilization being observed at acidic pH [Gruebe et al., 2004; Kumar and Swamy 2016b &c].

1.5. Motivations and major findings of the current study

As discussed in the beginning of this Chapter, mammalian fertilization proceeds via spermegg fusion. However, it is known that freshly ejaculated sperm is unable to fertilize the egg but requires to undergo activation and gain maturity through sperm "capacitation", which is a very important process during fertilization. This process is not clear at the molecular level, although it is known for several decades [Austin, 1952; Chang, 1951]. Various factors are involved in sperm capacitation and the steps of this process are different in different species and it is not possible to explain it using a single general mechanism. Therefore, it is important to investigate the complete picture of the sperm capacitation process and the different factors which are responsible for it in different species.

Studies with the major FnII proteins of bovine and equine seminal plasma as well as a few other species showed that their binding to sperm cells induce "cholesterol efflux", which is a key step in "capacitation" [Swamy et al., 2002; Desnoyers and Manjunath,1992; Thérien, 1997, 1998]. Hence, it is important to purify the major FnII proteins from the seminal plasma other mammals and characterize them in detail, in order to develop structure-function relationships in the FnII type proteins and to identify common features which are responsible for their functional activities. Therefore, we have chosen donkey seminal plasma for further investigation as the presence of FnII proteins in it was not investigated so far. The main objectives of present study are:

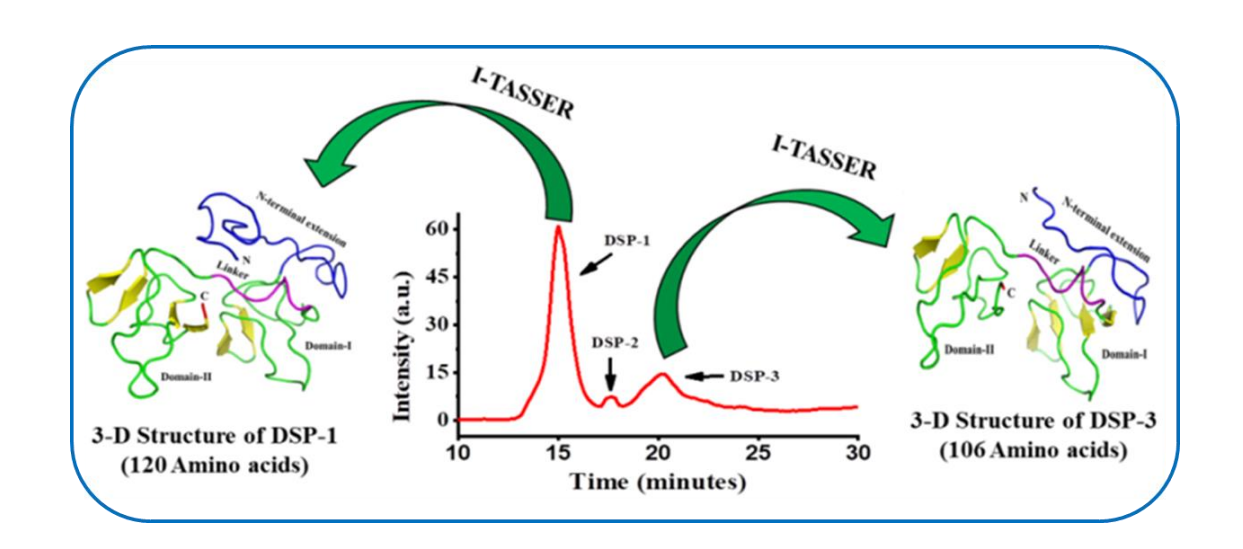
- To purify the major proteins from donkey seminal plasma, namely DSP-1, DSP-2 and DSP-3, and biochemical and biophysical characterization of DSP-1 using mass spectrometry, circular dichroism (CD) spectroscopy, differential scanning calorimetry (DSC), fluorescence spectroscopy, confocal microscopy and as well as computational studies.
- To investigate if DSP-1 exhibits chaperone-like activity and the effect of polydispersity, hydrophobicity and ligand binding on the CLA of DSP-1.
- To study the exposure and tryptophan accessibility of the native DSP-1 and in the presence of different soluble ligands using different quenchers such as, acrylamide,

iodide ion and cesium ion by fluorescence quenching and fluorescence life time measurements. In addition, to characterize the chemical unfolding of DSP-1 employing different chaotropic agents in the native state, in reduced condition and in the presence ligands.

 To determine the primary structure and to carry out studies to obtain a detailed biochemical and biophysical characterization and to investigate the effect of ligand binding on DSP-3 using biochemical and biophysical tools.

Chapter 2

Purification, Molecular Characterization and Ligand Binding Properties of the Major Donkey Seminal Plasma Protein, DSP-1



This work was published as

<u>Sk Alim</u>, Sudheer K. Cheppali, Mikko Laitaoja, Thirumala Rao Talluri, Janne Jänis, Musti J. Swamy*

Int. J. Biol. Macromol. 2022, 194, 213-222

2.1. Summary

Fibronectin type-II (FnII) family proteins are the major proteins in many mammalian species including bull, horse and pig. In the present study, a major FnII protein has been identified and isolated from donkey (Equus hemionus) seminal plasma, which we refer to as Donkey Seminal Plasma protein-1 (DSP-1). The amino acid sequence determined by mass spectrometry and computational modeling studies revealed that DSP-1 is homologous to other mammalian seminal plasma proteins, including bovine PDC-109 (also known as BSP-A1/A2) and equine HSP-1/2. High-resolution LC-MS analysis indicated that the protein is heterogeneously glycosylated and also contains multiple acetylations, occurring in the attached glycans. Structural and thermal stability studies on DSP-1 employing CD spectroscopy and differential scanning calorimetry showed that the protein unfolds at ~43°C and binding to phosphorylcholine (PrC) – the head group moiety of choline phospholipids – increases its thermal stability. Intrinsic fluorescence titrations revealed that DSP-1 recognizes lyso-phosphatidylcholine with over 100-fold higher affinity than PrC. Further, interaction of DSP-1 with erythrocytes, a model cell membrane, revealed that DSP-1 binding is mediated by a specific interaction with choline phospholipids and results in membrane perturbation, suggesting that binding of this protein to sperm plasma membrane could be physiologically significant.

2.2. Introduction

In mammals, fertilization occurs when spermatozoa from male fuse with the egg in the female uterus. Upon ejaculation, during their journey through the female genital tract, spermatozoa undergo a series of ultrastructural and biochemical changes, termed as capacitation, which is poorly understood at the molecular level [Visconti et al., 1998; Yanagimachi, 1994; Harrison, 1996]. In several mammals, a family of proteins present in the seminal plasma called seminal FnII or BSP (binder of sperm) proteins play a major and crucial role in sperm capacitation. All these proteins have a common characteristic structure comprising of an N-terminal flanking region, followed by two or four tandemly repeating fibronectin type-II (FnII) domains, and show greater binding specificity towards choline phospholipids [Desnoyers and Manjunath, 1992; Ramakrishnan et al, 2001; Greube, 2004]. Among the seminal FnII proteins, the major proteins from bovine seminal plasma, PDC-109 and equine seminal plasma, HSP-1/2 have been studied in great detail. Studies on its interaction with phospholipids indicate that PDC-109 exhibits high specificity for choline phospholipids such as phosphatidylcholine (PC) and sphingomyelin, as compared to other phospholipids such as phosphatidylglycerol, phosphatidylserine, phosphatidylethanolamine etc [Desnoyers and Manjunath, 1992; Ramakrishnan et al, 2001]. In addition, presence of cholesterol in the membranes was found to potentiate the interaction of PDC-109 with different phospholipids, suggesting that PC might mediate the interaction between PDC-109 and cholesterol [Swamy et al., 2002]. Single crystal X-ray diffraction studies on PDC-109/O-phosphorylcholine (PrC) complex revealed that each PDC-109 molecule has two PC binding sites and both of them are on the same face of the protein [Wah et al., 2002]. HSP-1/2, the major protein from horse seminal plasma and a homologue of PDC-109, is a non-separable mixture of HSP-1 and HSP-2 [Calvete et al., 1995]. The primary structure of these two proteins is nearly identical but differ in the number of residues in the N-terminal segment and in the extent of glycosylation [Calvete et al., 1994, 1995a &b].

The interaction of PDC-109 with different phospholipids, especially choline phospholipids, has been investigated in detail along with its interaction with other small molecules. Binding of PrC is shown to result in a more closed conformation along with

reducing the polydisperse nature of these seminal FnII proteins [Wah et al., 2002; Gasset, 1997]. Interaction of PDC-109 and HSP-1/2 with choline-containing ligands, model membranes and sperm plasma membranes has been greatly characterized in view of their physiological significance [Swamy, 2004; Anbazhagan and Swamy, 2005; Tannert et al., 2007]. Studies have shown that both these proteins are able to intercalate into lipid membranes and perturb the lipid chain dynamics [Ramakrishnan et al, 2001; Greube, 2004; Anbazhagan et al., 2011]. Studies on membrane perturbation by PDC-109 and HSP-1/2 using supported and model cell membranes show that these proteins cause membrane destabilization, which mimic their activity *in vivo* [Damai et al., 2010; Kumar and Swamy, 2016c].

Recent studies have shown that PDC-109 and HSP-1/2 can also act as small heat shock proteins (*shsps*), by exhibiting chaperone-like activity (CLA) by protecting various target proteins against thermal, chemical and oxidative stress [Kumar and Swamy, 2016b &c; Sankhala and Swamy, 2010; Sankhala et al., 2012]. This CLA was found to be modulated by various factors such as membrane binding, pH, presence of surfactants etc. [Damai et al., 2010; Sankhala et al., 2011; Kumar and Swamy, 2017a &b; Kumar et al., 2018]. Further, it was found that the CLA and membrane destabilizing activity of these proteins are inversely correlated to each other and are regulated by a 'pH switch' [Kumar and Swamy, 2016c; Kumar et al., 2018]. In addition, it has been shown that glycosylation differentially modulates the membrane-perturbing and chaperone-like activities of PDC-109, with the glycosylated protein exhibiting higher CLA whereas the non-glycosylated protein exhibited higher membrane perturbing activity [Singh et al., 2018]. Importantly, mutational studies have shown that conserved core tryptophan residues of FnII domains are essential for the membrane-perturbing and chaperone-like activities of this protein [Singh et al., 2020].

From the foregoing it is quite clear that the major FnII proteins of mammalian seminal plasma play crucial roles not only in priming spermatozoa for fertilization, but also in protecting other seminal plasma proteins from misfolding/inactivation as exemplified by the bovine protein, PDC-109 and the equine protein, HSP-1/2. Therefore, it is important to

purify the major FnII proteins from the seminal plasma of other mammals and characterize them in detail, in order to develop structure-function relationships in this class of proteins and to identify common features that are critical for their functional activities. With this objective, in the present study, we have purified the major protein from donkey seminal plasma, DSP-1 and characterized its biochemical and ligand binding properties. The primary structure of DSP-1, derived from mass spectrometric studies revealed that this protein belongs to the seminal FnII protein family. Furthermore, the protein was post-translationally modified by multiple *O*-glycosylations with acetylated sialic acid residues. By employing various biophysical techniques we studied the secondary and tertiary structures of DSP-1, investigated its thermal stability and characterized the binding of PrC and lyso-phosphatidylcholine (Lyso-PC). These studies revealed that DSP-1 recognizes the choline head group of phospholipids and exhibits membrane destabilizing activity against model cell membranes. Ligand binding results in a significant increase in the thermal unfolding temperature of DSP-1 and also leads to an increase in its resistance to chemical denaturation.

2.3. Materials and Methods

2.3.1. Materials

Choline chloride, phosphorylcholine chloride (calcium salt) and heparin-Agarose type-I affinity matrix were obtained from Sigma (St. Louis, MO, USA) and *p*-aminophenyl phosphorylcholine-Agarose column was purchased from Pierce Chemicals (Oakville, Ontario, Canada). Lyso-PC from egg yolk was obtained from Avanti Polar Lipids (Alabaster, AL, USA). All other chemicals were purchased from local suppliers and were of the highest purity available.

2.3.2. Purification of DSP-1

DSP-1 was purified from donkey seminal plasma using a procedure reported previously for HSP-1/2 with slight modifications [Sankhala et al., 2012]. Freshly ejaculated semen from healthy donkeys was obtained from the Equine Production Campus, ICAR-National Research Centre on Equines (Bikaner, India). Seminal plasma was separated from

spermatozoa by centrifugation of the semen at 1500 rpm in an Eppendorf 5810R centrifuge for 20 min at 4°C. The supernatant was collected and then seminal plasma was further clarified by centrifugation again at 6000 rpm for 15 min at 4°C. The collected seminal plasma was frozen in liquid nitrogen and stored at -80 °C until further use.

2.3.2.1. Affinity chromatography on heparin-Agarose

About 15 mL of clear donkey seminal plasma was diluted to 50 mL with 50 mM Tris/HCl, pH 7.4, containing 150 mM NaCl, 5 mM EDTA and 0.025% sodium azide (TBS) and double loaded on to a heparin-Agarose column which was pre-equilibrated with TBS buffer. The column was washed with the same buffer till absorbance of the column effluent at 280 nm was \leq 0.05, following which the bound proteins were eluted with TBS containing 20 mM PrC. The fractions with high protein content were pooled and dialyzed against TBS to remove PrC.

2.3.2.2. Affinity chromatography on *p*-aminophenyl phosphorylcholine-Agarose (PPC-Agarose)

The heparin bound-fraction obtained in the previous step was applied to a p-aminophenyl phosphorylcholine Agarose column pre-equilibrated with TBS. After extensive washing with TBS till the unbound proteins are completely removed (A_{280nm} of the column effluent ≤ 0.05), the bound protein fraction was eluted with 20 mM PrC in TBS. The eluted proteins were dialyzed against TBS to remove PrC and concentrated using an Amicon filter (3 kDa cutoff).

2.3.2.3. Reverse-phase high-performance liquid chromatography

The proteins bound to PPC-Agarose affinity matrix were further purified using reverse-phase high-performance liquid chromatography (RP-HPLC) on a Shimadzu LC 1080 (Shimadzu corporation, Tokyo, Japan) as described earlier for HSP-1/2 purification [Calvete et al., 1994; Sankhala et al., 2012]. PPC-Agarose bound, concentrated protein mixture was dialyzed extensively against double distilled water containing 0.1% trifluoroacetic acid (TFA) and RP-HPLC was performed using a Luna RP-100C-18 column (250 \times 4.6 mm, 5 μ M particle size) from Phenomenex (California, USA). The

column was pre-equilibrated with 0.1% TFA in milli-Q water (solution A, 75%) and acetonitrile (solution B, 25%). A flow rate of 1.0 mL/min was maintained throughout. A gradient of 25–60% acetonitrile containing 0.1% TFA was used as the mobile phase. After sample loading, the column was run using the following program: 25% B for 5 min, followed by a gradient of 25–30% B over 5 min and 30–35% B over another 25 min and a gradient of 35–60% B over 10 min. Three individual peaks obtained were collected manually, dialyzed against TBS and concentrated using an Amicon concentrator (3 kDa cutoff filter) and stored at 4 °C. Finally, purity of the proteins was checked using 15% sodium dodecyl sulfate-polyacrylamide gel electrophoresis (SDS-PAGE) [Laemmli, 1970].

2.3.3. Mass spectrometry

For mass spectrometry experiments, the protein samples were first buffer exchanged to 20 mM ammonium acetate (pH 7.4) using PD-10 desalting columns (Cytiva Europe GmbH). Further purification was performed by using size exclusion chromatography (SEC) on an Äktapurifier 100 instrument (Amersham Pharmacia Biotech AB, Uppsala, Sweden), using a Superdex 75 column (GE Life Sciences, Sweden). The proteins were eluted at a flow rate of 1.0 mL/min using 20 mM ammonium acetate solution (pH 7.4) as the elution buffer. The samples were further concentrated using Vivaspin2 concentrators (Sartorius Stedim Biotech GmbH, Germany). Trypsin digestion was performed by incubating the protein samples overnight with sequencing grade trypsin (Sigma Aldrich, USA) at a 1:50 (w/w) trypsin-to-protein ratio using an acetonitrile (MeCN)/water (1:1, v/v) solvent containing 10 mM dithiothreitol (DTT). The intact protein samples and the tryptic digests were analysed using an HPLC system (UltiMate 3000; Thermo Scientific) connected to a 12-tesla FT-ICR Daltonics, spectrometer (Bruker solariX-XR; Bruker The mass Germany). proteins/peptides were eluted over an Acclaim Pepmap100 C18 (0.075 × 150 mm, 3 μm) column (Thermo Scientific) at a flow rate of 0.5 μL/min, using a solvent gradient of 1-40% acetonitrile with 0.2% formic acid. For the direct infusion measurements, a standard Apollo-II electrospray (ESI) ion source was used, operating at a flow rate of 2 µL/min. In the LC-MS/MS, experiments, a Bruker nano-ESI nebulizer was connected to the ion source. The drying gas temperature was set at 200 °C and a flow rate to 4 L/min.

Additional top-down MS (i.e., intact protein MS/MS) experiments were performed on a QTOF mass spectrometer (Bruker timsTOF; Bruker Daltonics, Germany). The peptide or protein ions were fragmented by collision-induced dissociation (CID), using previously optimized fragmentation voltages. The instruments were controlled and the data were acquired using Chromeleon 6.80 (Ultimate 3000), ftmsControl 2.0 (solariX) or otofControl 5.1 (timsTOF) software, respectively. The data post-processing and further analysis was accomplished by using Bruker DataAnalysis 4.4/5.1 software. The NCBI database was searched for the sequences similar to PDC- 109, while limiting a species to donkey. Four possible predicted sequences were found, belonging to *Equus asinus* (accession codes 014723761.1, 014723758.1, 014723760.1, and 014723757.1). The signal peptide prediction was done with SignalP 5.1 (http://www.cbs. dtu.dk/services/SignalP/) [Armenteros, 2019].

2.3.4. Circular dichroism spectroscopy

CD spectroscopic studies were performed using a Jasco 810 spectropolarimeter (Jasco Corporation, Tokyo, Japan) fitted with a thermostatted cell holder and a thermostatic water bath at a scan speed of 30 nm/min. Far- and near-UV CD spectra were recorded using a 0.2 cm path length quartz cell with samples containing DSP-1 at a concentration of 0.1 mg/mL and 0.5 mg/mL, respectively in 10 mM Tris/HCl buffer, pH 7.4. Each spectrum recorded was the average of 8 consecutive scans from which buffer scans were subtracted. Spectra were also obtained in the presence of up to 50 mM PrC.

Thermal unfolding of DSP-1 was investigated by monitoring the CD spectral intensity of the protein (0.1 mg/mL) at 225 nm, while the temperature was increased from 25 to 80°C at a scan speed of 1°C /min. Effect of PrC binding on the thermal stability of DSP-1 was investigated by incubating a fixed concentration protein (0.1 mg/mL) for ~30 min with varying concentrations of PrC (10–50 mM) before the temperature scans were performed.

2.3.5. Computational modelling

The amino acid sequence of DSP-1 determined by the mass spectrometric studies was submitted to I-TASSER server (http://zhanglab. dcmb.med.umich.edu/I-TASSER) to build a 3-dimensional structural model of the protein. The crystal structure of PDC-109 (pdb code: 1H8P) was used as a scaffold template. In addition, binding of PrC to the two FnII domains of DSP-1 was also studied in silico using the I-TASSER server.

2.3.6. Differential scanning calorimetry

Differential scanning calorimetric (DSC) measurements were performed using a Nano DSC from TA instruments (New Castle, Delaware, USA) described earlier [Mondal and Swamy, 2020]. DSP-1 (1 mg/mL) in TBS was heated from 20 to 80°C at a scan rate of 1°C /min under a constant pressure of 3.0 atm. Buffer base line scan was subtracted from all the sample data to eliminate the contribution from buffer to the calorimetrically measured heat capacity of the protein. To investigate the effect of PrC binding, DSP-1 was pre-incubated with different concentrations of PrC and experiments were carried out under similar conditions and the thermograms were analysed using the 'Gaussian Model' in the DSC data analysis software provided by the manufacturer.

2.3.7. Steady-state fluorescence studies

Steady state fluorescence measurements were performed using a Spex model Fluoromax-4 fluorescence spectrometer at room temperature, with excitation and emission band pass filters set at 2 and 3 nm, respectively. All experiments were carried out with samples taken in a $1 \times 1 \times 4.5$ cm quartz fluorescence cuvette. DSP-1 (0.05 mg/mL) in TBS was excited at 280 nm and emission spectra were recorded between 310 and 400 nm. Titrations to determine the association constants for the binding of ligands were carried out by adding small aliquots of 100 μ M Lyso-PC and 20 mM PrC in TBS to DSP-1 solution in the same buffer. Fluorescence spectra were recorded after a 3-minute incubation period.

2.3.8. Erythrocyte lysis assay

Effect of DSP-1 binding on the erythrocyte membranes (lysis) was investigated by absorption spectroscopy as described earlier [Damai et al., 2010, Kumar and Swamy, 2016c]. A 4% suspension of human erythrocytes in TBS was incubated with varying concentrations of DSP-1 and the final volume was adjusted to 0.5 mL with TBS. After incubating the mixture for 90 min, the sample was centrifuged at 3000 rpm for 10 min. The supernatant was collected and its absorbance at 415 nm, corresponding to haem moiety was measured using an Agilent Cary 100 spectrophotometer equipped with a Peltier device for temperature control. For investigating the kinetics of erythrocyte membrane disruption, 150 μg/mL of DSP-1 was incubated with 0.04% RBC suspension in different vials and incubated for different time intervals (5–300 min) before measuring absorbance as described above. To investigate the effect of ligands on erythrocyte lysis, DSP-1 was preincubated with PrC, Lyso-PC and choline chloride prior to its addition to the erythrocyte suspension, and the experiment was carried out as described above. Results from a minimum of three independent experiments have been presented along with standard deviations.

2.3.9. Microscopy

Images of human erythrocytes in the presence of DSP-1 were obtained using a Leica TCS SP2 confocal microscope (Heidelberg, Germany) as described earlier [Kumar and Swamy, 2016b]. To investigate the effect of DSP-1, a 0.04% suspension of human erythrocytes in TBS was incubated with 150 µg/mL of protein. After incubation, 50 µL aliquots of the mixture were taken at 45 min and 90 min, spotted on a clean glass slip (Thermo Fisher) and shifted to confocal stage for imaging. The erythrocyte suspension in TBS alone was used as the control. To investigate the effect of ligand binding, DSP-1 was pre-incubated with 20 mM PrC for 10 min before its addition to the erythrocyte suspension.

2.4. Results and Discussion

2.4.1. Purification of DSP-1

DSP-1 was purified from donkey seminal plasma by a procedure similar to that used for the purification of HSP-1/2, using affinity chromatography on heparin-Agarose and *p*-aminophenyl phosphorylcholine-Agarose (PPC-agarose), followed by RP-HPLC (Fig. 2.1, Fig. 2.2A). Heparin-bound and PPC-Agarose-bound fractions gave three major peaks when subjected to RP-HPLC. Among the three peaks, the first peak showed highest intensity (Fig. 2.2A), and migrated as a single band in SDS-PAGE corresponding to a molecular weight of ~20 kDa (Fig. 2.2B). Hence we named this as Donkey Seminal Plasma protein-1 (DSP-1). The second and third peaks also migrated as single bands with approximate molecular masses of 16 kDa and 18 kDa, respectively and we refer to them as DSP-2 and DSP-3, respectively (Fig. 2.2B).

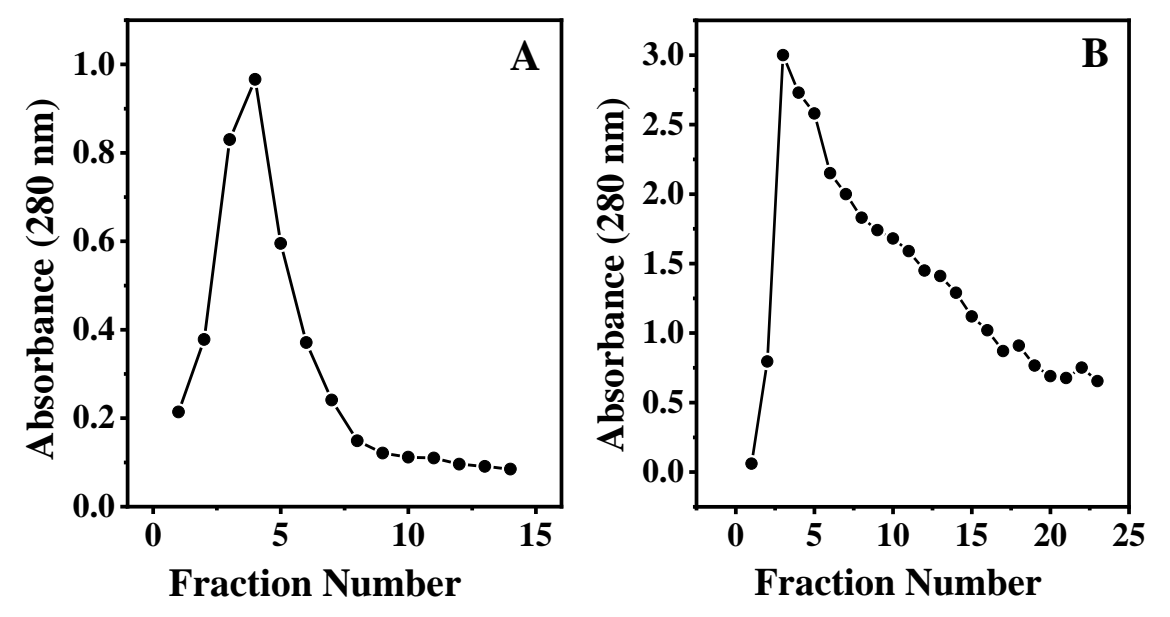


Fig. 2.1. Affinity chromatography of donkey seminal plasma proteins. Elution profiles of bound proteins eluted from heparin-Agarose column (A) and PPC-Agarose column (B). See methods for more details.

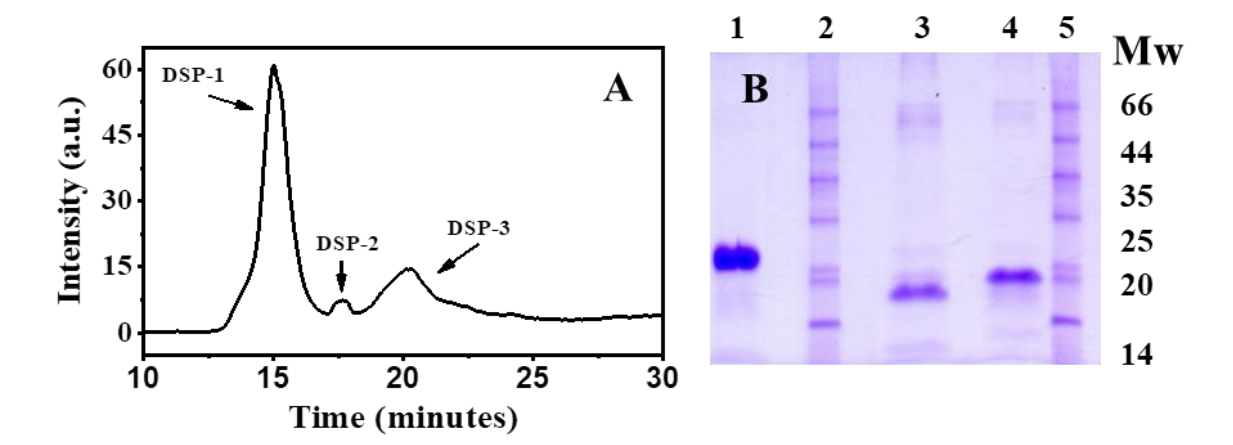


Fig. 2.2. (**A**) RP-HPLC chromatogram of heparin-Agarose-bound and PPC-Agarose-bound fraction showing three major peaks. (**B**) SDS-PAGE of purified donkey seminal plasma proteins: lane 1, DSP-1; lanes 2 & 5, molecular weight markers; lane 3, DSP-2; lane 4, DSP-3.

2.4.2. Mass spectrometric studies

2.4.2.1. LC-MS

Our previous studies on PDC-109 employing top-down mass spectrometry revealed the presence of several sequence variants [Laitaoja et al., 2012]. Since DSP-1 exhibited similar characteristics, we expected it to be homologous to PDC-109 and also contain several different proteoforms. Hence, we chose to characterize the primary structure of the protein by employing a combination of database search for proteins similar to PDC-109 in the donkey, and sequence analysis of peptides derived by enzymatic fragmentation of DSP-1. The direct infusion ESI FT-ICR MS measurements with DSP-1 showed that the protein is expressed as a highly heterogeneous mixture of different proteoforms (Fig. 2.3). Furthermore, additional peak patterns with 42 Da spacing were observed in the mass spectra, suggesting heterogeneous acetylation of the peptide chain or the attached glycans. For DSP-1, the observed protein masses were around 18.1–20.4 kDa, consistent with the SDS-PAGE analyses. In addition, unidentified polymeric substances, with a repeating unit of 44 Da (indicative of PEG-like compounds), were observed in the samples, which complicated the analysis. Therefore, further LC-MS experiments were performed with intact DSP-1, which confirmed the presence of different glycoforms with multiple acetylations (Fig. 2.4). Protein deglycosylation experiments using PNGase-F did not

change the appearance of the mass spectra, suggesting *O*-glycosylation, similar to that observed with PDC-109 and HSP-1 [Calvete et al., 1994 & 1995]. The mass spectra also indicated that each DSP-1 glycoform was similarly acetylated.

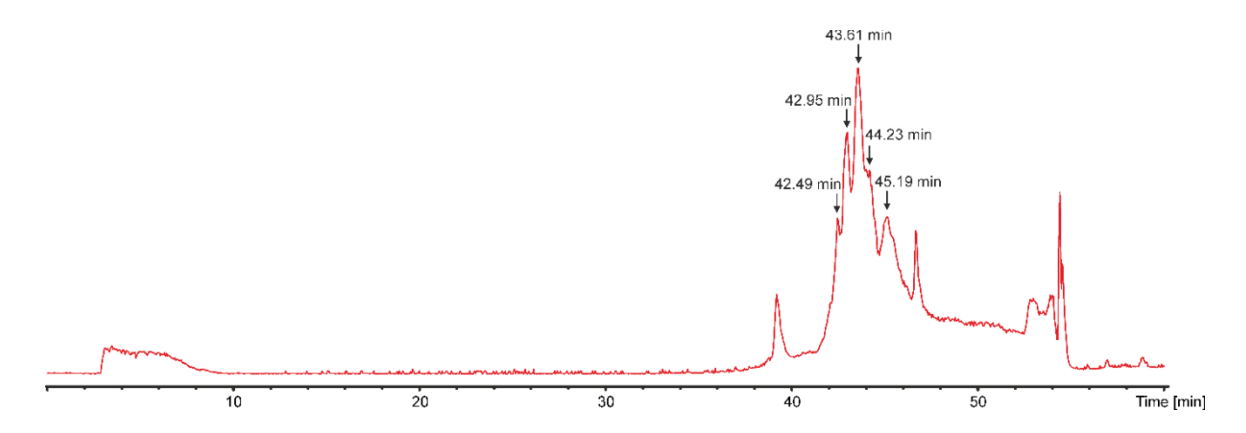


Fig. 2.3. Total ion chromatogram of the LC ESI FT-ICR MS/MS analysis of intact DSP-1. Different glycoforms of DSP-1 have been marked with arrows with retention times indicated. The other chromatographic peaks are small molecule impurities.

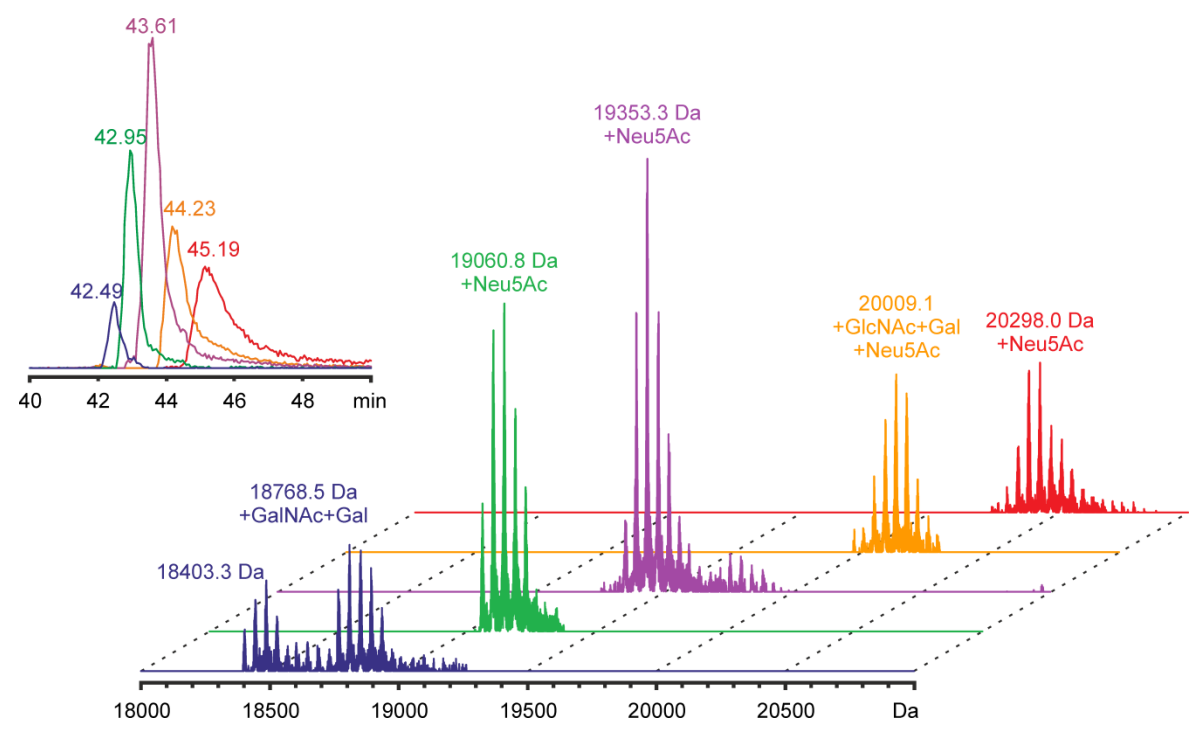


Fig. 2.4. LC ESI FT-ICR mass analysis of DSP-1. Deconvoluted mass spectra of different glycoforms of DSP-1, eluting at 42.49, 42.95, 43.61, 44.23, and 45.19 min are shown. The inset shows the corresponding extracted ion chromatograms (Fig. 2.3). The peak patterns observed for different glycoforms are due to multiple protein acetylations (+42 Da). The

most abundant isotopic masses are given for the lowest mass species for each glycoform (i.e., the non-acetylated forms).

Table 2.1. Peptides identified from trypsin digestion of DSP-1 by mass spectrometry.

m/z	charge	Experimental mass (Da)	Calculated mass (Da)	Error (ppm)	Sequence	MS/MS fragments
399.5099	3	1195.5079	1195.5080	-0.12	GYRYYDCTR	276.166 (y2), 377.193 (b3), 379.176 (y3), 488.179 (y7++), 494.202 (y4), 540.256 (b4), 657.265 (y5), 703.391 (b5), 818.347 (b6)
573.9297	3	1718.7673	1718.7682	-0.55	GQTYDRCTTDGSLFR	435.271 (y3), 522.303 (y4), 579.324 (y5), 635.795 (y11++), 694.351 (y6), 717.327 (y12), 767.851 (y13), 795.399 (y7)
530.5610	3	1588.6612	1588.6616	-0.28	YYDCTRTDSFYR	523.256 (y8++), 574.761 (y9++), 632.274 (y10++), 713.806 (y11++)
492.2190	4	1964.8469	1964.8475	-0.34	GYRYYDCTRTDSFYR	377.193 (b3), 472.733 (y7++), 523.256 (y8++), 540.256 (b4), 574.761 (y9), 632.274 (y10++), 703.319 (b5), 713.806 (y11++), 818.346 (b6)
500.9821	4	1999.8993	1999.8999	-0.31	ISWCSVTPNYDHHGA WK	612.781 (y10++), 663.304 (y11++), 712.839 (y12++), 735.368 (y6), 756.354 (y18++), 807.859 (y14++), 850.394 (y7), 1013.458 (y8)
606.5254	4	2422.0725	2422.0735	-0.42	RISWCSVTPNYDHHGA WKYC	646.312 (b5), 733.344 (b6), 832.412 (b7), 933.460 (b8)
566.9965	4	2263.9569	2263.9579	-0.45	ISWCSVTPNYDHHGA WKYC (ox)	490.193 (y3), 864.312 (y7), 1001.441 (y8), 1116.468 (y9)
523.2498	2	1044.4850	1044.4851	-0.06	CVFPFNYR	599.294 (y4), 696.346 (y5), 843.414 (y6)
515.7626	2	1029.5106	1029.5106	+0.04	CVFPFVYR	584.319 (y4), 681.371 (y5), 828.439 (y6)
683.0707	4	2728.2537	2728.2537	-0.01	CVFPFVYRGQTYDRCT TDGSLFR (ox)	522.303 (y4), 579.32447 (y5), 694.351 (y6), 795.401 (y7)
808.1064	4	3228.3965	3228.3968	-0.10	TDSFYRWCSLTGTYSG SWKYCAATDYAK (ox)	381.213 (y3), 496.240 (y4), 597.288 (y5), 688.325 (y6), 739.361 (y7)
749.0054	3	2243.9944	2243.9946	-0.11	TDSFYRWCSLTGTYSG SWK	477.245 (y4), 564.277 (y5), 727.341 (y6), 828.388 (y7), 885.409 (y8), 986.456 (y9)

Peptides marked with (ox) were found to contain a disulfide bridge.

Since the protein sequences for donkey are very limited and the databases contain mostly predicted sequences based on mRNA, trypsin digestion, and subsequent LC-MS/MS analysis enabled only a partial sequencing and preliminary protein identification. Only peptides from the two FnII domains and the linker between them were found in the mass spectra, possibly due to the presence of a detergent and/or heterogeneous glycosylation suppressing the signals of the *N*-terminal peptides. The eluted peptides did

not show typical glycan fragmentation patterns, indicating that *N*-terminal part of the protein was the likely location of the attached glycans, similar to the homologous proteins from other species. Fig. 2.5 shows the MS/MS sequencing of a peptide obtained from the tryptic digest of DSP-1. The identified peptide, along with other peptides sequenced (Table 2.1), matched the predicted sequence of 014723758.1 (Fig. 2.6), thus confirming similarity of these proteins to those from different species. Based on the expected sequence, the mass of the intact peptide chain of DSP-1 would be 13,954.28 Da, and thus the observed post-translational modifications (glycans, acetylations) covers about 4.0–6.4 kDa of the mass of the native protein.

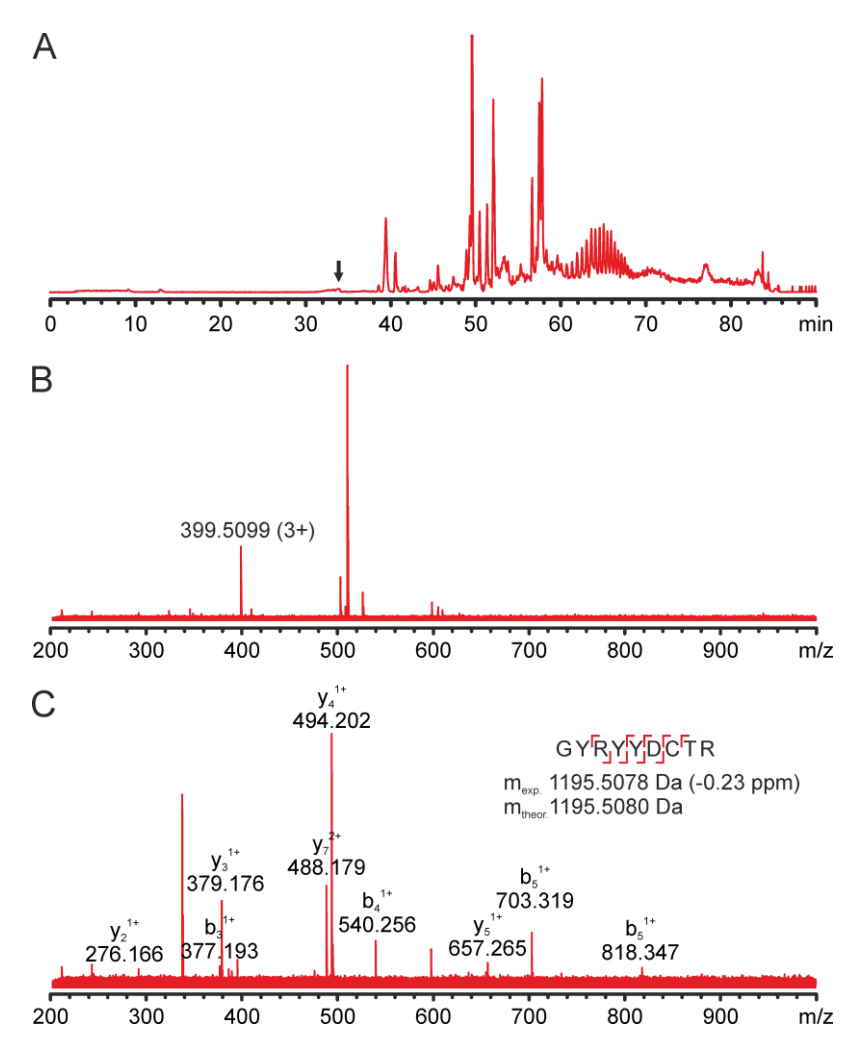


Fig. 2.5. LC ESI FT-ICR analysis of the tryptic digest of DSP-1. (A) Total ion chromatogram (polymeric impurities are seen at 60–70 min), (B) isolation of a triply

charged peptide eluting at 34 min (m/z 399.5099) and (C) MS/MS fragmentation of the peptide with the identified b and y fragments.

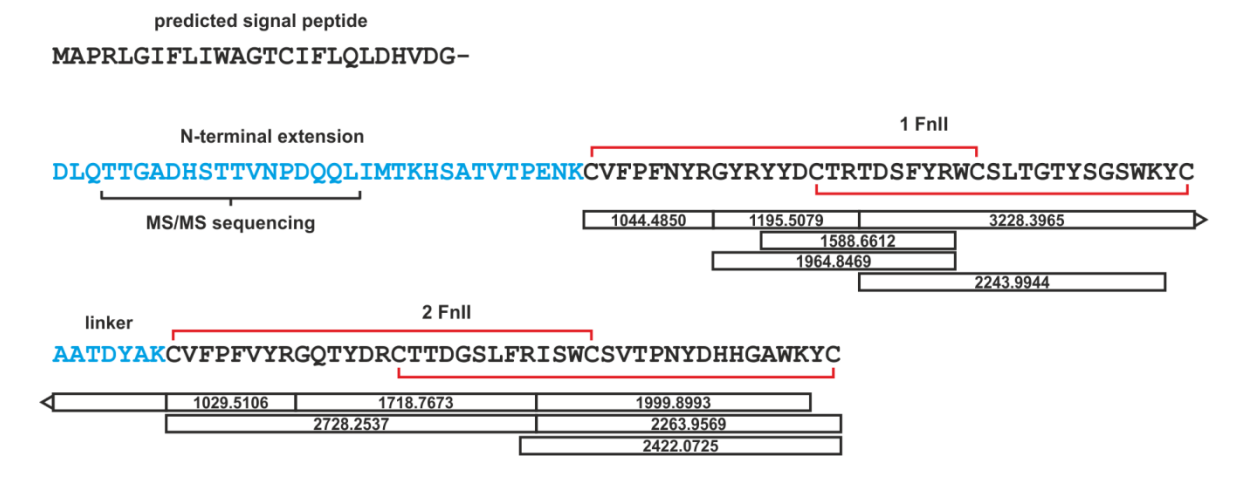


Fig. 2.6. Putative amino acid sequence of DSP-1 with the identified tryptic peptides and their monoisotopic masses indicated. The disulfide linkages shown are based on similarity with those observed in other homologous mammalian seminal FnII proteins PDC-109 and HSP-1/2. The *N*-terminal extension part is most likely missing due to the observed protein modifications (glycosylation/acetylations), and was characterized by additional top-down MS experiments.

2.4.2.2. Top-down MS

To determine the *N*-terminal sequence of the protein, top-down MS experiments were performed. In top-down MS, intact protein ions are isolated and further subjected to MS/MS experiments for sequencing and identifying post-translational modifications. As the fragmentation preferentially occurs in disordered or loop regions, disulfides in DSP-1 were not reduced in order to limit the fragmentation to the mobile linker region and the *N*-terminal part (see Section 3.4 for protein models). All top-down MS experiments were performed on a high-resolution QTOF mass spectrometer to obtain high fragmentation efficiency for intact protein ions. To maximize the fragment ion intensity, top-down experiments were performed without a precursor ion isolation.

In low-energy conditions, (collision energy ~ 50 eV) the mass spectra showed mainly small fragment ions with m/z values corresponding to different glycan fragments (Fig. 2.7A). The fragmentation of glycopeptides typically results in the cleavage of glycosidic bonds, and the subsequent formation of different oligosaccharides depending on

the glycan structures. These fragments can be used for the glycan structure annotations; however, information on the glycan locations within the polypeptide chain are lost. Although there is also a plausible *N*-glycosylation site (NKC) in DSP-1, based on the sequence and type of glycosylations observed in other homologous proteins, it is highly likely that the protein contains *O*-glycosylation. Since the *O*-glycans are typically small, containing only a few carbohydrate residues, it is assumed that there are multiple sites in DSP-1 where the glycans are attached, most likely threonine and serine residues as observed in PDC-109, HSP-1 and BSP- 30-kDa protein [Calvete et al., 1994, 1995 & 1996]. Similar to BSP-30k, we observed several *N*-acetylgalactosamine (GalNAc) and galactose (Gal) containing di- and trisaccharides which are further modified by attachment of sialic acid or acetylated sialic acid residues (Neu5Ac/Neu5, xAc2) residues. This further proves that glycosylation in DSP-1 occurs in the solvent-exposed serine or threonine residues within the *N*-terminal region, similar to the other homologous proteins. In addition, heterogeneous acetylation occurs in the attached sialic acid residues, observed only in top-down MS/ MS experiments [Muthana et al., 2012].

Moreover, large (\sim 14 kDa) fragment ions were also observed at $m/z \sim 2000$, corresponding to the protein fragments resulting from the complete glycan removals from the polypeptide chain. Among these ions, a fragment ion with a mass of 13,954.33 Da was observed, matching to the proposed amino acid sequence of DSP-1. In high-energy conditions (collision energy \sim 170 eV), additional fragments corresponding to the *N*-terminal region were detected in the mass spectra (Fig. 2.7B), further verifying the proposed sequence of DSP-1. The MS/ MS spectra also proved that the observed acetylations occur only in the sialic acid residues attached to glycans and no fragment ions corresponding to the acetylation occurring in the peptide chain were observed. In addition, the MS/MS experiments suggest that there are no major sequence variants of DSP-1 present in the sample, and the observed heterogeneity is solely a result of the heterogeneous *O*-glycosylation with multiple acetylations.

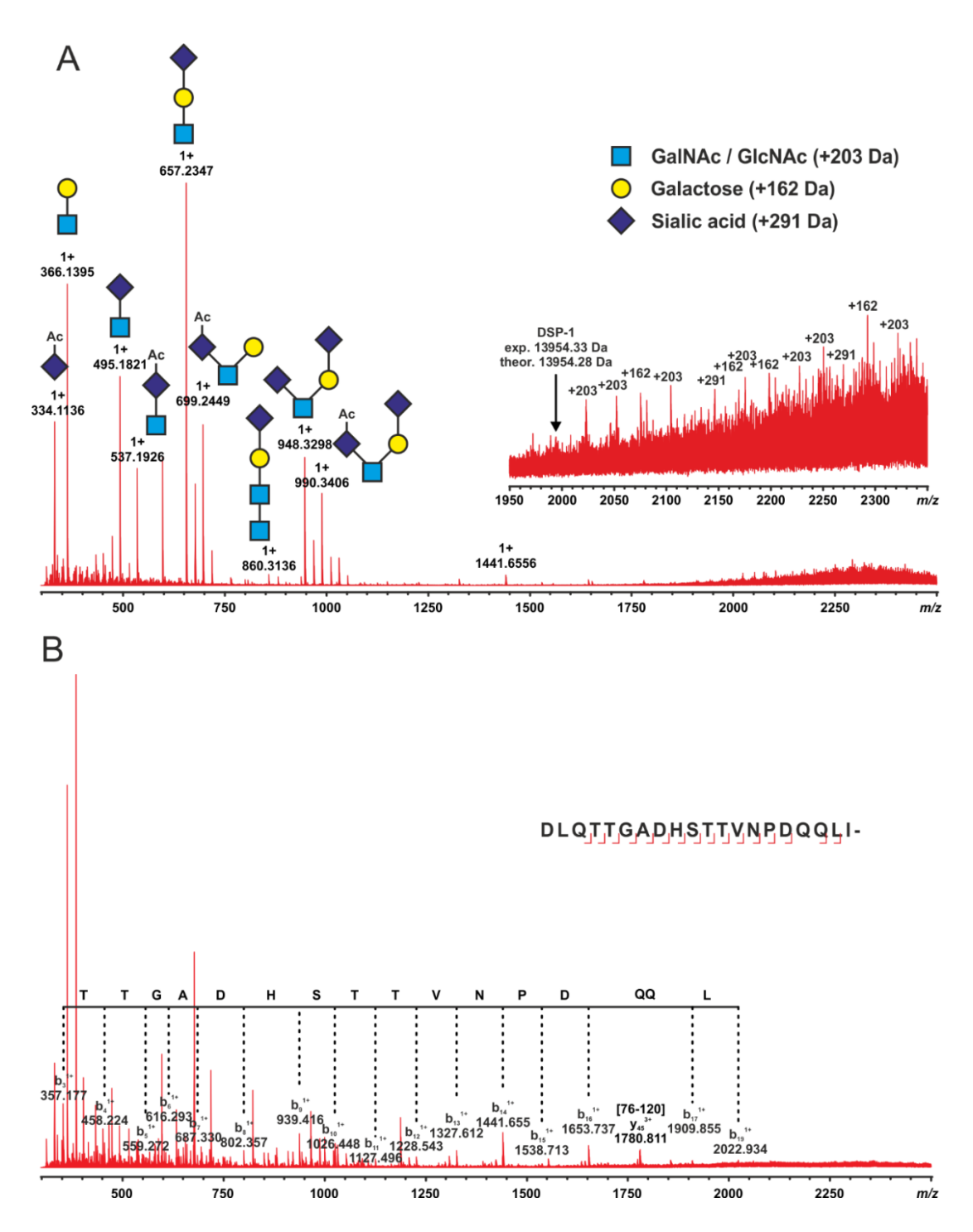


Fig. 2.7. Top-down MS/MS spectra of DSP-1. (A) Low energy CID shows mainly the fragmentation of the O-glycan structures. Additionally, high mass ions are observed in $m/z \sim 2000$, resulting from the sequential removal of glycosylations, up to the bare amino acid chain of DSP-1 (Ac=acetylation). (B) High energy CID shows the fragmentation of the N-terminal part of the protein, confirming the N-terminal residues of DSP-1. In

addition, cleavage in the linker region is observed, resulting in the peptide y_{45} (residues 76-120).

Multiple sequence alignment of the primary structure of DSP-1 with the seminal plasma FnII proteins from other mammals, viz., bull, horse, pig, mouse and human is given in Fig. 2.8. From this alignment it can be seen that the primary structure of DSP-1 exhibits highest homology to the amino acid sequence of HSP-1, with only two residues differing between the two proteins, wherein Ala-11 and Ala-80 in HSP-1 are replaced by Thr residues in DSP-1. Extensive homology is also seen among all these proteins, with all the 8 Cys residues involved in disulfide bond formation in the FnII domains as well as the 4 core Trp residues that have been shown to be crucial for ligand binding and chaperone-like activity of PDC-109 [Singh et al., 2020] being conserved among all these proteins.

```
DSP-1 (donkey)
              -----DLQTTGADHSTTVNPDQQLIMT
                                                                  22
HSP-1 (horse)
              -----DLQTTGADHSATVNPDQQLIMT
PDC-109 (bovine) -----DQDEGVSTEPTQ
                                                                  12
              -----DEQLSEDNVILPKEKKD
BSP-A3 (bovine)
                                                                  17
BSP-30k (bovine) GDIPDPGSKPTPPGMADELPTETYDLPPEIYTTTFLPRTIYPQEEMPYDDKPFPSLLSKA
PB1 (pig)
              -----DOHLPGR
                                                                  7
BSPH1 (human)
              -----CIFPVILNELSSTVET
                                                                  16
BSPH1 (mouse)
              -----FOVEDYYAPTIES
                                                                  13
BSPH2 (mouse)
              -----ELISHL
DSP-1 (donkey)
              KHSATVTPENKCVFPFNYRGYRYYDCTRTDSFYRWCSLTGTYSGSWKYCAATDYAKCVFP
                                                                  82
HSP-1 (horse)
              KHSATVTPENKCVFPFNYRGYRYYDCTRTDSFYRWCSLTGTYSGSWKYCAATDYAKCAFP
                                                                  77
PDC-109 (bovine) DGPAELPEDEECVFPFVYRNRKHFDCTVHGSLFPWCSLDADYVGRWKYCAQRDYAKCVFP
                                                                  72
BSP-A3 (bovine)
              PASGAETKDNKCVFPFIYGNKKYFDCTLHGSLFLWCSLDADYTGRWKYCTKNDYAKCVFP
                                                                  77
BSP-30k (bovine)
              NDLNAVFEGPACAFPFTYKGKKYYMCTRKNSVLLWCSLDTEYOGNWKFCTERDEPECVFP
                                                                  120
PB1 (pig)
              FLTPAITSDDKCVFPFIYKGNLYFDCTLHDSTYYWCSVTTYYMKRWRYCRSTDYARCALP
BSPH1 (human)
              ITHFPEVTDGECVFPFHYKNGTYYDCIKSKARHKWCSLNKTYEGYWKFCSAEDFANCVFP
                                                                  76
BSPH1
     (mouse)
              LIRNPETEDGACVFPFLYRSEIFYDCVNFNLKHKWCSLNKTYQGYWKYCALSDYAPCAFP
                                                                  73
              HPPEQEISTDSCVFPFVYADGFHYSCISLHSDYDWCSLDFQFQGRWRYCTAQDPPKCIFP
BSPH2 (mouse)
                                .: *
                        * *** * .
                                                    *::*
DSP-1 (donkey)
              FVYRGQTYDRCTTDGSLFRISWCSVTPNYDHHGAWKYC----
                                                    120
              FVYRGQTYDRCTTDGSLFRISWCSVTPNYDHHGAWKYC----
HSP-1 (horse)
                                                    120
PDC-109 (bovine) FIYGGKKYETCTKIGSMWMS-WCSLSPNYDKDRAWKYC----
              FIYEGKSYDTCIIIGSTFMNYWCSLSSNYDEDGVWKYC----
BSP-A3 (bovine)
              FIYRKKSYESCTRVHSFFWRRWCSLTSNYDRDKAWKYC----
BSP-30k (bovine)
              FIFRGKEYDSCIKEGSVFSKYWCPVTPNYDQDRAWRYC----
PB1 (pig)
              FWYRRLIYWECTDDGEAFGKKWCSLTKNFNKDRIWKYCE----
BSPH1 (human)
              FWYRHMIYWDCTEDGEVFGKKWCSLTPNYNKDQVWKYCIE---
BSPH1 (mouse)
                                                    113
BSPH2 (mouse)
              FQFKQKLIKKCTKEGYILNRSWCSLTENYNQDGKWKQCSPNNF 109
                                **.:: **:.. *: *
```

Fig. 2.8. Multiple sequence alignment of the primary structure of DSP-1 with the seminal plasma FnII proteins from different mammalian species. Only proteins containing 2 FnII domains have been selected. All sequences were taken from EMBL-EBI database and aligned using Clustal Omega program (https://www.ebi.ac.uk/Tools/msa/clustalo/) without the signal sequences. The different proteins used in the alignment (with database IDs in

brackets) are: horse seminal plasma protein, HSP-1 (SP:P81121); porcine (pig) seminal plasma protein, PB1 (SP:P80964); bovine seminal plasma proteins PDC-109 (SP: P02784), BSP-A3 (SP:P04557) and BSP-30k (SP:P81019); human seminal plasma protein, BSPH1 (SP:Q075Z2); mouse seminal plasma proteins, BSPH1 (SP:Q3UW26) and BSPH2 (SP:Q0Q236). Conserved cysteine residues involved in disulfide bonds are shown in bold cyan, conserved core tryptophans are shown in bold red. Residues that are fully conserved across all species (*) and residues that are similar (: and .) are indicated.

2.4.3. Secondary and tertiary structure of DSP-1

The secondary and tertiary structures of DSP-1 were characterized by CD spectroscopy. Far-UV CD spectra of DSP-1 alone and in the presence of 50 mM PrC, the head group moiety of its physiological ligand, phosphatidylcholine are shown in Fig. 2.9A. The spectrum of DSP-1 alone (black) is characterized by a broad positive asymmetric band with maxima at 226 nm and 220 nm and two shoulders at ~212 nm and 209 nm. In the presence of PrC (red), these bands shift to 225, 217 and 207 nm without major changes in the spectral intensity. The near-UV CD spectrum of DSP-1 contains three overlapping positive bands with maxima at ~260 nm, ~274 nm and ~288 nm (Fig. 2.9B). The positive band in far-UV CD spectrum of DSP-1 could not be analysed to obtain the secondary structural elements of the protein, due to lack of suitable reference dataset, as was the case with PDC-109 [Gasset et al., 1997].

Far-UV CD spectra of DSP-1 recorded at various temperatures between 25 and 55°C show that the spectral intensity decreases steadily with increase in temperature suggesting a gradual loss of the secondary structure of the protein (Fig. 2.9C). Broadly similar changes were seen in the near UV CD spectra (Fig. 2.10A). In contrast, in the presence of 50 mM PrC, only moderate changes were seen in the far- as well as near-UV CD spectra between 25 and 55°C, whereas significant decrease in signal intensity was observed with further increase in temperature with large decrease being seen between 60 and 70°C (Figs. 2.9D & 2.10B). The thermal stability of DSP-1 and the effect of ligand binding on it was also investigated by monitoring the CD signal intensity of the protein at 225 nm as a function of temperature in the absence and presence of different concentrations of PrC (Fig. 2.9E). The signal intensity of native DSP-1 decreases with the steepest decline being seen at ~43°C (black line), which is taken as the midpoint of thermal

unfolding of the protein. In the presence of 10 mM PrC the unfolding shifted to ~58°C (red line) and upon further increase in the concentration of PrC to 20 and 50 mM, the unfolding temperature further shifted to ~62°C (green) and 64°C (violet), respectively.

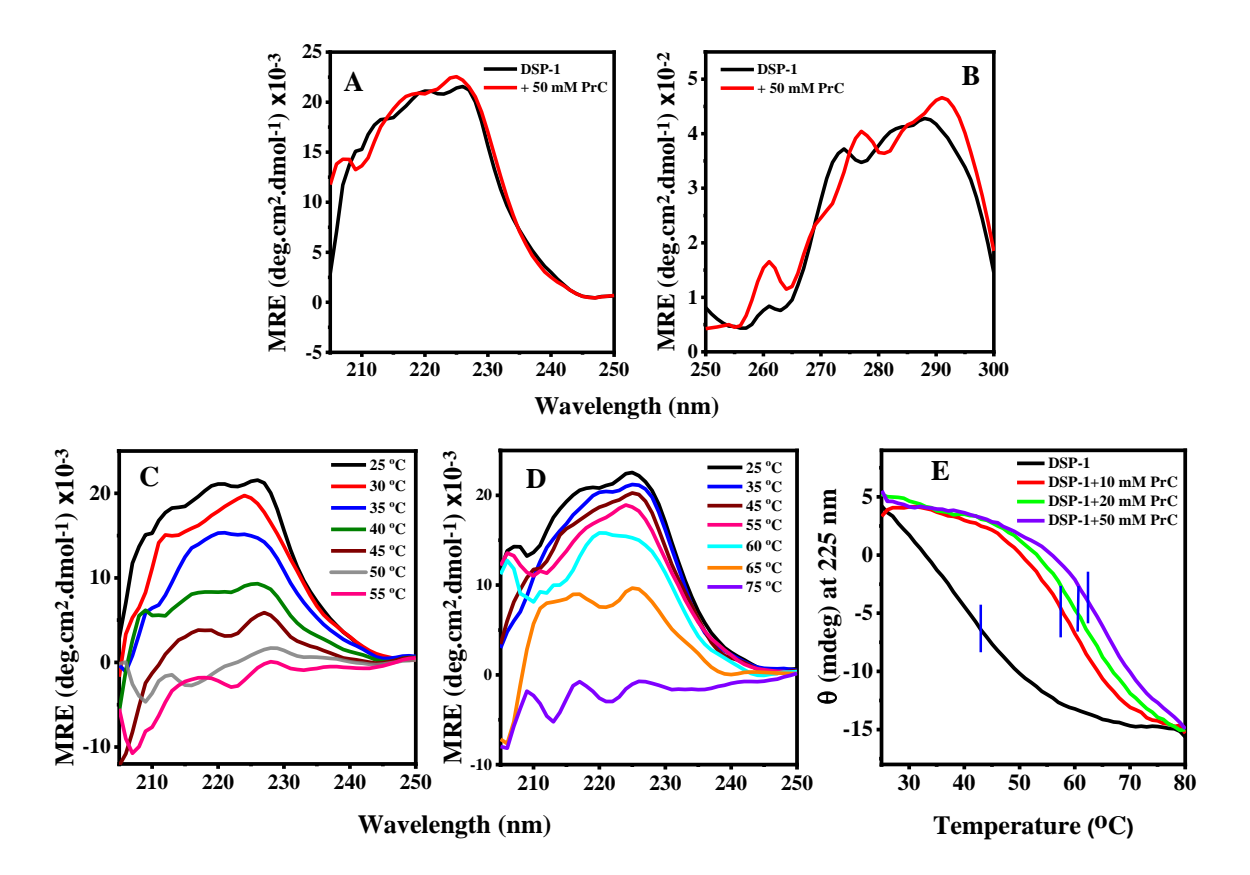


Fig. 2.9. CD spectroscopic studies of DSP-1. (A, B) Far- and near-UV CD spectra of DSP-1 alone (black) and in the presence of 50 mM PrC (red). Far-UV CD spectra of DSP-1 at various temperatures in absence (C) and presence (D) of 50 mM PrC. (E) Effect of PrC on the thermal stability of DSP-1. The CD signal intensity of the protein at 225 nm was recorded as the temperature was increased at a scan rate of 1°/min. Protein concentration was 0.1 mg/mL in all samples. Concentration of PrC in different samples is: black, 0 mM; red, 10 mM; green, 20 mM; violet, 50 mM.

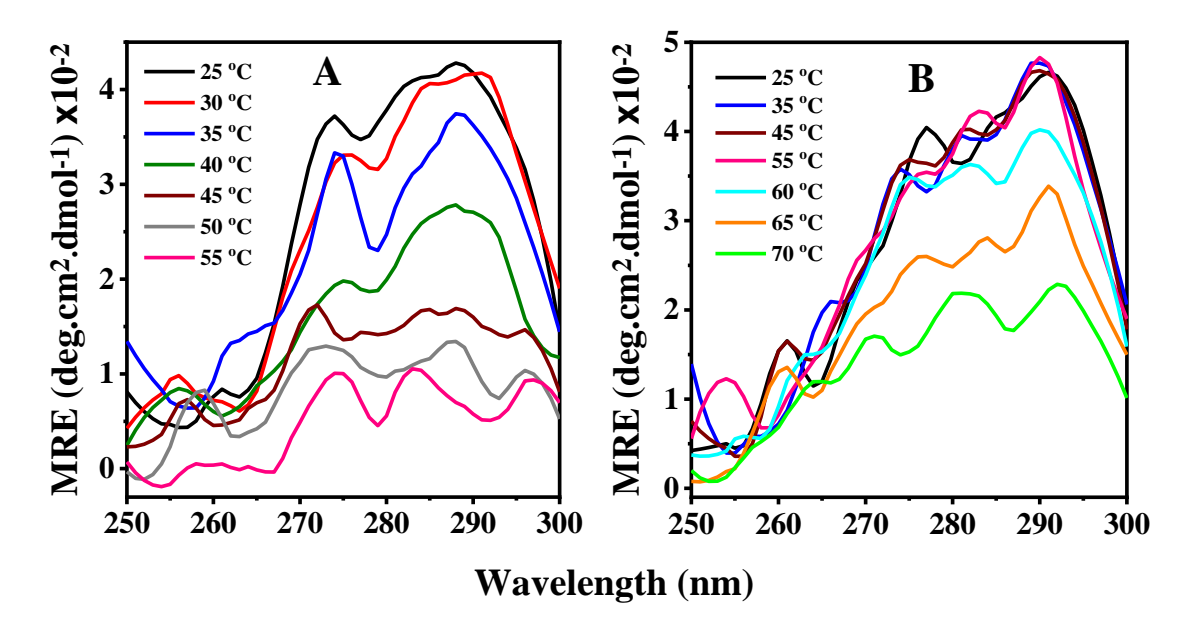


Fig. 2.10. Near-UV CD spectra of DSP-1 at various temperatures. (A) DSP-1 alone; (B) DSP-1 + 50 mM PrC.

2.4.4. Computational modeling of DSP-1 structure and binding of PrC

As the secondary structure of DSP-1 could not be determined from the near-UV CD spectra, we used computational methods to obtain a 3-dimensional structural model of DSP-1 using Iterative Threading ASSEmbly Refinement (I-TASSER) server (http://zhanglab.dcmb.med. umich.edu/I-TASSER) using the reported crystal structure of PDC-109 (pdb code: 1h8p) as the template. The modeled structure of DSP-1 is shown in Fig. 2.11 together with the modeled structures of PDC-109 and HSP-1, taken from our earlier study on HSP-1/2 [Sankhala et al., 2012]. A careful observation of the models indicates that the overall structure of DSP-1 is very similar to those of HSP-1 and PDC-109. Further, the relative content of various secondary structures of the three proteins, deduced from the computational models are rather similar, with all three proteins containing very little α -helix and about 25% β -sheet, whereas ~70% of the residues are present in β -turns and unordered structures (Table 2.2). In addition, comparison of the relative content of various secondary structural elements of PDC-109, deduced from its crystal structure with the results obtained in the present modeling studies shows a very good correlation (Table 2.2).

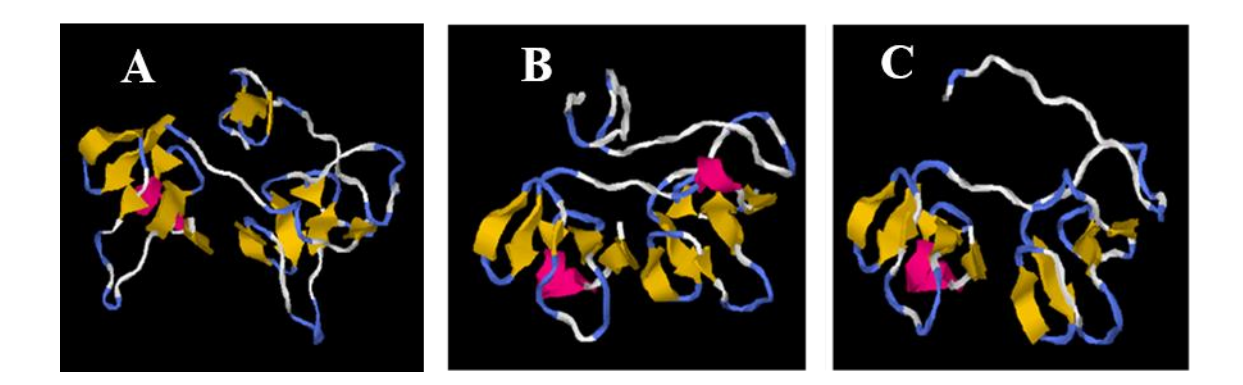


Fig. 2.11. Three-dimensional structures of DSP-1 (A), HSP-1 (B) and PDC-109 (C) generated by I-TASSER server.

Table 2.2. Secondary structure of DSP-1, HSP-1 and PDC-109 estimated from computational modeling using the I-TASSER server. Secondary structure of PDC-109 determined from the crystal structure (pdb code: 1h8p) is also given for comparison.

Protein	α-helix	β-sheet	β-turns +	
			unordered	
			structures	
DSP-1	3.3	25.0	71.7	
HSP-1	5.8	25.0	69.1	
PDC-109 (from	3.7	23.8	72.4	
modeling)				
PDC-109 (from	9.2	22.9	67.8	
crystal structure)				

Along with building a 3-D model of DSP-1 we also investigated the binding of PrC to its FnII domains using the I-TASSER server. The structures of the first and second FnII domains of DSP-1 with bound PrC molecules are shown in Fig. 2.12A and D, respectively. The binding of PrC is mediated by multiple weak interactions including cation- π , O-H···O and C-H···O hydrogen bonds as well as C-H··· π interactions. The cation- π interactions in the two FnII domains are shown in Fig. 2.12B and E, whereas the H-bonding and C-H··· π interactions are shown in Fig. 2.12C and F. It is noteworthy that in the first FnII domain of

DSP-1, 4 out of the 5 residues that interact with PrC, namely Y40, Y64, W57 and W68 are fully conserved, whereas D52 is highly conserved among the FnII proteins whose sequences are used for comparison in the multiple sequence alignment shown in Fig. 2.8. Similarly, in the second FnII domain, W104, Y111 and W117, which interact with PrC are fully conserved whereas S98 which forms an important O–H···O hydrogen bond with PrC is conserved in 6 out of 9 sequences.

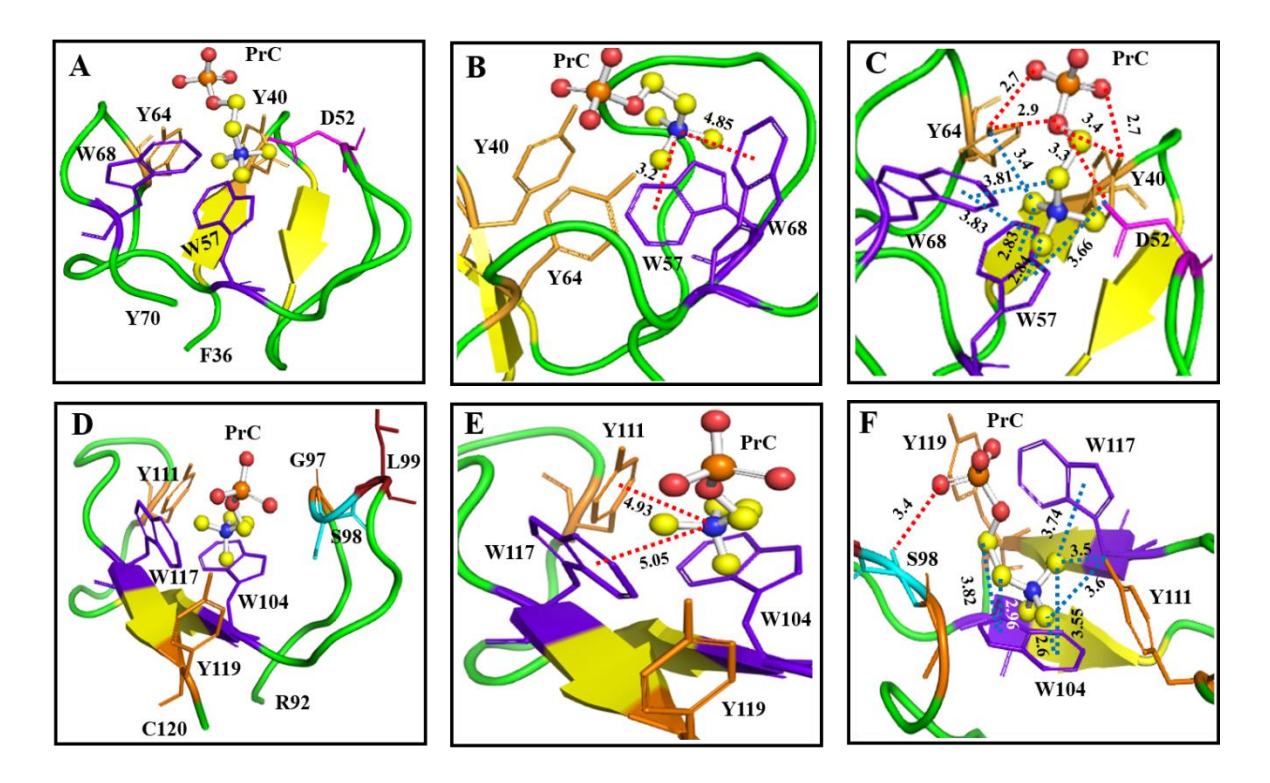


Fig. 2.12. Structure of the FnII domains of DSP-1 with bound PrC, generated using I-TASSER. The structures have been visualized using PyMOL. (A) The side chains of residues involved in ligand binding (domain-I) Y40, Y64, D52, W57 and W68 are shown in stick format; (B) the cation- π interaction of the quaternary ammonium group with W57 and W68 are indicated by red dotted lines; (C) hydrogen bonds between the hydroxyls of Y40 and Y64 and the phosphate oxygens are shown in red dotted lines and the possible CH- π and CH-O interactions are in blue dotted line; (D) the site chains of residues involved in ligand binding (domain-II) G97, S98, L99, W104, W117, Y111 and Y119 are shown in stick format; (E) the cation- π interaction of the quaternary ammonium group with Y111 and W117 are indicated by red dotted lines and (F) hydrogen bonds between the hydroxyls of S98 and the phosphate oxygen is shown in red dotted line and the possible CH- π and CH-O interactions are in blue dotted line.

2.4.5. Thermal denaturation of DSP-1 and the effect of ligand binding

To investigate the thermal unfolding of DSP-1 in more detail, especially to obtain the thermodynamic parameters associated with it, differential scanning calorimetric studies were performed. Thermograms of DSP-1 alone and in the presence of different concentrations of PrC are shown in Fig. 2.13. The thermogram of native DSP-1 exhibits two thermotropic transitions centred at ~32.4 (±0.2) and 43.1 (±0.3) °C (Fig. 2.13A). The transition occurring at the lower temperature could be attributed to the dissociation of the oligomeric form of DSP-1 to monomers whereas the higher temperature transition can be attributed to the complete unfolding of the monomer. This suggests that the thermal unfolding of DSP-1 is a three-state transition with two partially overlapping, yet distinct transitions. That the higher temperature transition corresponds to the protein unfolding is supported by the results of CD spectroscopic studies which showed a steep decrease in the spectral intensity at 225 nm at 43°C.

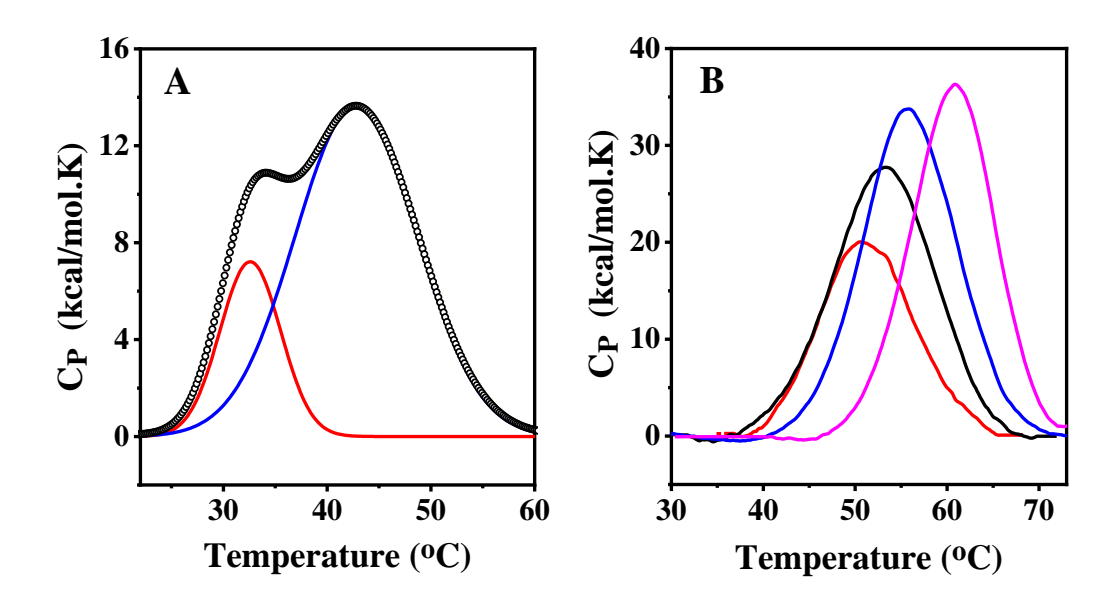


Fig. 2.13. Differential scanning calorimetry of DSP-1. (A) DSC thermogram of native DSP-1. Open circles correspond to the experimental data and the red and blue lines correspond to the deconvoluted components. (B) Thermograms of DSP-1 in presence of different concentration of PrC: 5 mM (red), 10 mM (black), 20 mM (blue) and 50 mM (magenta). The thermogram of DSP-1 alone could be best fitted to two thermotropic transitions centred at about 32°C (red line) and 43°C (blue line). Thermograms obtained in the presence of PrC could be fitted satisfactorily to a single transition.

Importantly, in the presence of PrC, the thermogram of DSP-1 exhibits only a single transition. These observations are similar to those made with PDC-109 and indicate that binding of PrC decreases the polydisperse nature of DSP-1 [Gasset et al., 1997]. In the presence of different concentrations of PrC, the transition temperature and transition enthalpy increased with increasing concentrations of the ligand (Fig. 2.13B, Table 2.3). The temperature corresponding to the major thermotropic transition of DSP-1 shifted from 43.1 (±0.3) °C in the absence of PrC to ~60.6 (±0.3) °C in the presence of 50 mM PrC, with a concomitant increase in the transition enthalpy from 258 kJ/mol to 411 kJ/mol. These observations strongly suggest that PrC binding stabilizes the structure of DSP-1 and increases its unfolding temperature.

Table 2.3. Thermodynamic parameters associated with the thermal unfolding of DSP-1 derived from DSC studies. Protein (1 mg/mL) in the absence and presence of PrC was used to obtain the thermodynamic parameters such as T_m and ΔH from the DSC studies. Values given are averages from 2 or 3 independent scans with standard deviations given in parentheses.

Sample/Condition	T _{m1} (°C)	T _{m2} (°C)	ΔH_1 (kJ/mol)	ΔH_2 (kJ/mol)
DSP-1	32.4 (±0.2)	43.1 (±0.3)	61 (±8)	217 (±15)
DSP-1 + 5mM PrC	-	51.3 (±0.3)	-	258 (±11)
DSP-1 + 10mM PrC	-	53.1 (±0.2)	-	383 (±14)
DSP-1 + 20mM PrC	-	55.9 (±0.4)	-	429 (±18)
DSP-1 + 50mM PrC	-	60.6 (±0.3)	-	411 (±23)

2.4.6. Fluorescence studies on the binding of PrC and Lyso-PC to DSP-1

To obtain quantitative information on ligand binding to DSP-1, we performed fluorescence spectroscopic studies in which DSP-1 was titrated with PrC and Lyso-PC in separate experiments and changes in the protein intrinsic fluorescence properties have been monitored. Fluorescence spectra corresponding to the titration with PrC are given in Fig.

2.14 and plots reporting the analysis of the titration data are given in Fig. 2.15 and the corresponding plots for the binding of Lyso-PC are given in Fig. 2.16. It was observed that addition of each aliquot of PrC resulted in a small decrease in the emission intensity of the protein (Fig. 2.14) with a concomitant blue shift in the emission maximum, and a plot of change in fluorescence emission intensity at 360 nm (ΔF) versus the ligand concentration showed saturation behaviour (Fig. 2.15B). For Lyso-PC binding, due to a larger blue shift in the emission maximum, the difference spectra showed a maximum centred around 317 nm and a minimum centred around 365 nm (Fig. 2.16A). Therefore, the change in fluorescence intensity at 317 nm was used to obtain the binding curve (Fig. 2.16B).

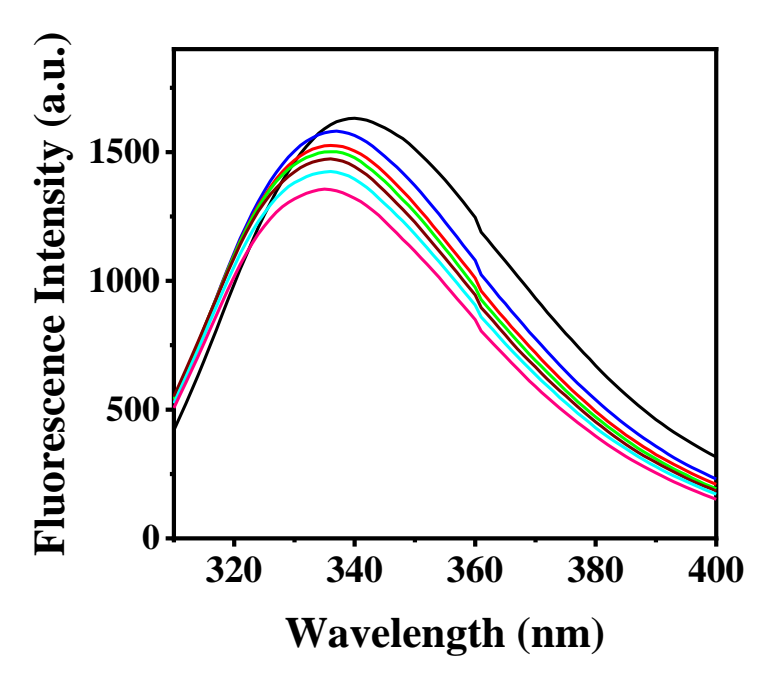


Fig. 2.14. Fluorescence titration of DSP-1 with 20 mM PrC. Fluorescence emission spectra of DSP-1 alone (black) and in presence of different concentration of PrC: 0.3 mM (blue), 0.6 mM (red), 0.9 mM (green), 1.25 mM (wine), 1.75 mM (cyan) and 2.5 mM (pink). The highest concentration of PrC in the titration mixture was 2.5 mM. Although more aliquots were added (at intermediate concentrations of PrC), only selected spectra are shown for the sake of clarity.

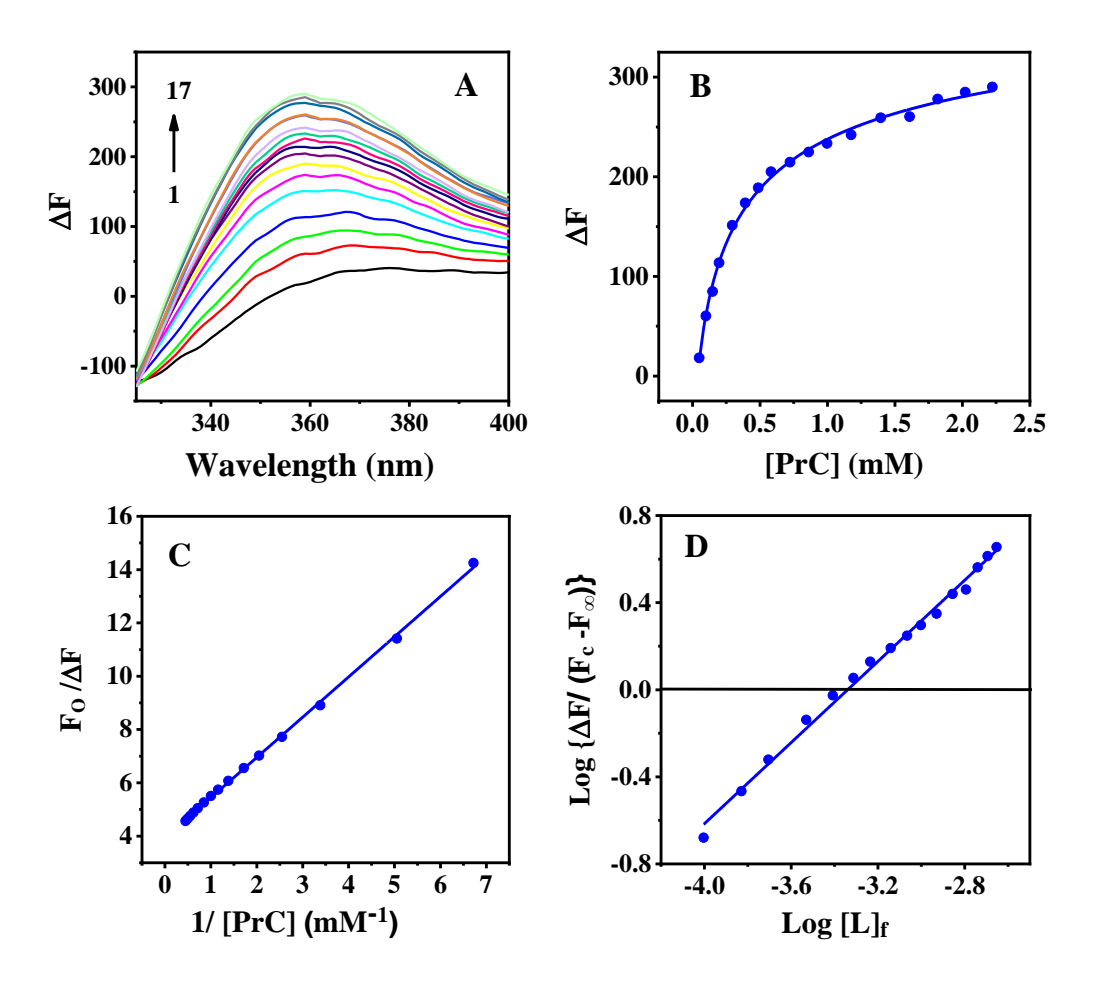


Fig. 2.15. Fluorescence titration to determine the association constant, K_a for PrC binding to DSP-1. (A) Fluorescence difference spectra of DSP-1 obtained in the presence of various concentrations of PrC. (B) Binding curve obtained by plotting ΔF versus [PrC]. (C) A double reciprocal plot of $F_o/\Delta F$ versus 1/[PrC]. From the Y-intercept of the plot F_∞ , the fluorescence intensity of the protein at saturation binding is obtained. (D) A double log plot of [log { $\Delta F/(F_c - F_\infty)$ }] versus log [L]_f. From the X-intercept of the plot the association constant, K_a for PrC binding to DSP-1 is obtained. See text for details.

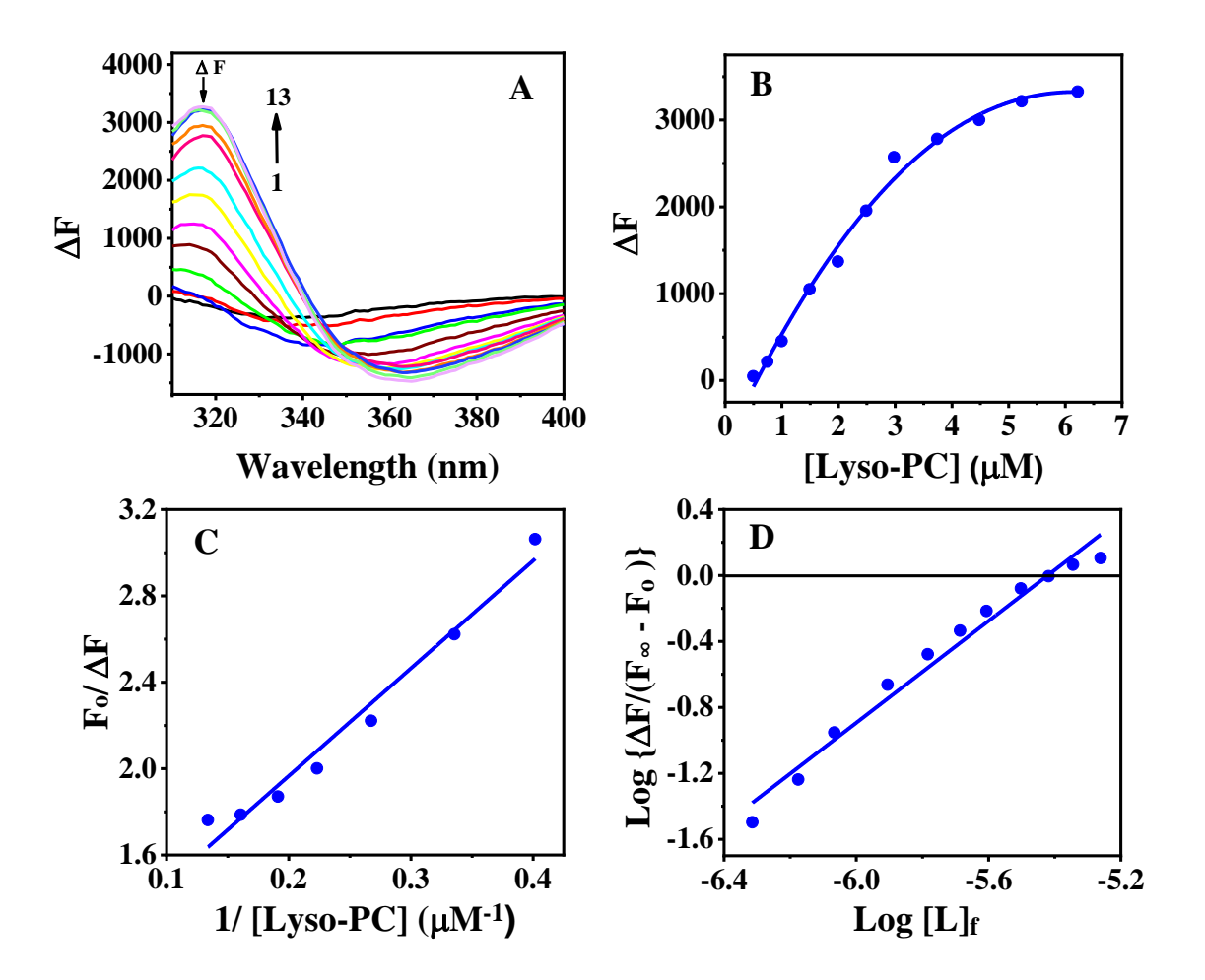


Fig. 2.16. Fluorescence titration for the binding of DSP-1 with Lyso-PC. (A) Fluorescence difference spectra for the titration of DSP-1with Lyso-PC at room temperature. 1-13 correspond to difference spectra obtained in presence of increasing concentration of Lyso-PC. (B) Binding curve for the interaction of DSP-1 with Lyso-PC. The change in fluorescence intensity (ΔF) at 317 nm was plotted as a function of Lyso-PC concentration. The solid line corresponds to a 'hyperbolaGen' fit of experimental data. (C) A double reciprocal plot of $F_o/\Delta F$ versus 1/[Lyso-PC]. From the Y-intercept of the plot, the fluorescence change at saturation binding (ΔF_∞) is obtained. (D) A double log plot of log { $\Delta F/(F_c-F_\infty)$ } versus log [L]_f for the binding of Lyso-PC to DSP-1. X-intercept of the plot gives pK_a (-5.42) value for the titration, from which association constant, K_a was estimated as $2.63 \times 10^5 \,\mathrm{M}^{-1}$.

The titration data was further analysed using the Chipman plot in order to obtain the association constant, K_a as described earlier for the interaction of these ligands to PDC-109 [Anbazhagan and Swamy, 2005; Chipman et al., 1967]. In brief, a plot of $1/\Delta F$ versus $1/[L]_t$ where ΔF (= $|F_o - F_c|$) refers to the change in fluorescence intensity at any point of in

the titration and F_o and F_c correspond to the fluorescence intensity of DSP-1 alone and in the presence of ligand (PrC or Lyso-PC), respectively, and [L]_t is the corresponding total ligand concentration (Figs. 2.15C, 2.16C). From the ordinate intercept of the plot, F_{∞} , fluorescence intensity of the sample at infinite concentration, was calculated. The titration data was further analysed according to the following expression [Anbazhagan and Swamy, 2005; Chipman et al., 1967]:

$$Log \{\Delta F/(F_c - F_\infty)\} = log K_a + log [L]_f$$
(2.1)

where [L]_f, the free ligand concentration, is given by:

$$[L]_{f} = [L]_{t} - \{(\Delta F/\Delta F_{\infty})[P]_{t}\}$$

$$(2.2)$$

where [L]t and [P]t are total ligand concentration and total protein concentration, respectively, and ΔF_{∞} (= $|F_0 - F_{\infty}|$) is the change in fluorescence intensity at infinite concentration (saturation). From the X-intercepts of plots of log $\{\Delta F / (F_c - F_{\infty})\}$ versus log [L]_f the association constant, K_a for the binding of PrC and Lyso-PC to DSP-1 were determined (Figs. 2.15D, 2.16D). The association constants thus obtained were 2.16 $(\pm 0.03) \times 10^3$ M⁻¹ for PrC and 2.72 $(\pm 0.09) \times 10^5$ M⁻¹ for Lyso-PC (averages of two independent titrations). These results show that DSP-1 binding of Lyso-PC is two orders of magnitude stronger than its association with PrC.

2.4.7. Spectrophotometric and microscopic studies on DSP-1 binding to erythrocytes

To investigate the effect of DSP-1 binding on the cell membrane, human erythrocytes were taken as a model cell system since both erythrocytes and spermatozoa of different mammalian species contain a high proportion of choline phospholipids [Mann and Lutwak-Mann (Eds), 1981; Holt and North, 1985; Parks et al., 1987; Martínez and Morros, 1996]. Binding of DSP-1 to erythrocytes disrupted their membrane structure and led to cell lysis and release of haemoglobin into the solution. This process was monitored by measuring absorption at 415 nm corresponding to the haem bound to haemoglobin [Damai et al., 2010]. When erythrocytes were incubated with DSP-1, the amount of haemoglobin released increased with increasing concentration of DSP-1, indicating concentration-

dependent membrane destabilization, and reached saturation at \sim 250 µg/mL (Fig. 2.17A). Kinetics of DSP-1 induced erythrocyte destabilization, monitored over time periods of 5–300 min showed that the release of haemoglobin increased with increasing incubation time up to 240 min and then remained constant (Fig. 2.17B). These results show that DSP-1 can destabilize the erythrocyte membrane in a time- and concentration-dependent manner.

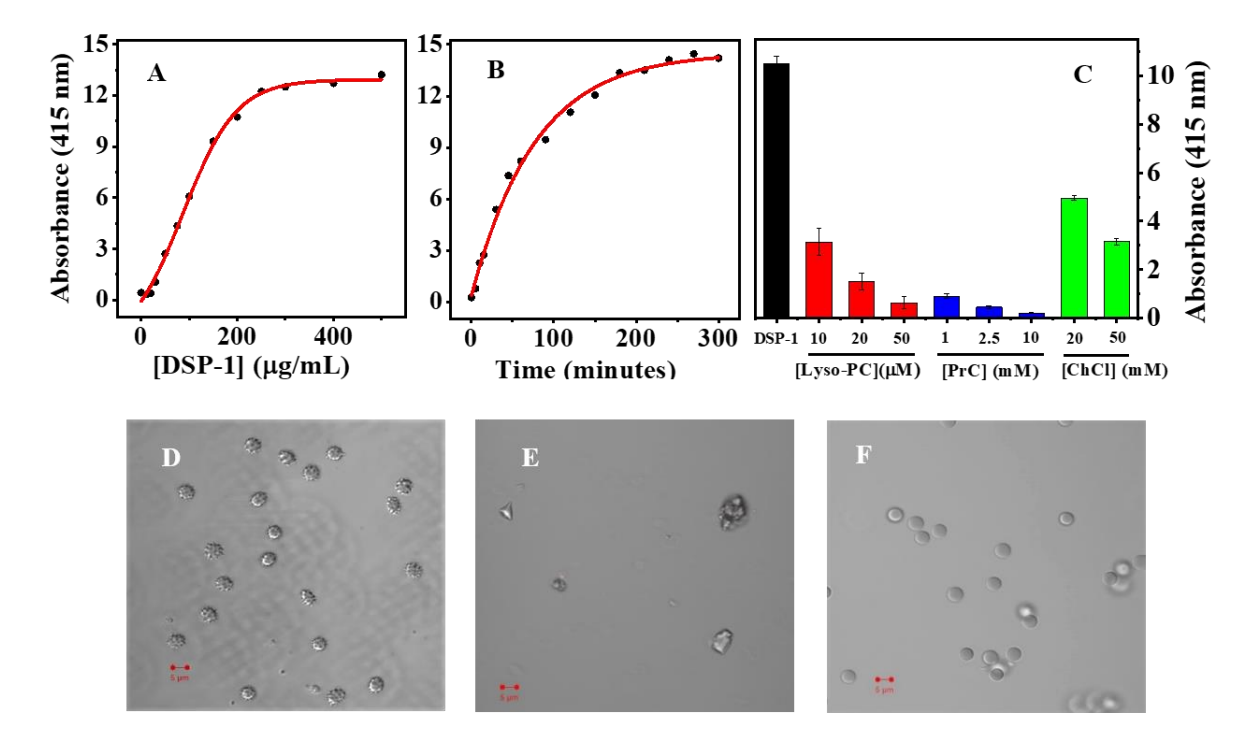


Fig. 2.17. Effect of DSP-1 on human erythrocyte membrane. (A) Effect of increasing the concentration of DSP-1 on erythrocyte lysis. (B) Kinetics of erythrocyte lysis induced by DSP-1. The protein concentration in each sample was 100 μg/mL. (C) Erythrocyte lysis induced by DSP-1 alone and upon pre-incubation with different concentrations of Lyso-PC, PrC and choline chloride. Absorbance at 415 nm was measured to detect the haemoglobin released upon cell lysis. (D-F) Confocal images of human erythrocytes under different conditions: (D) in TBS buffer alone, (E) upon incubation for 90 min with 200 μg/mL DSP-1 and (F) upon incubation with 200 μg/mL DSP-1 and 20 mM PrC for 60 min. Scale bar = 5 μm.

Further, to examine the specificity of erythrocyte lysis induced by DSP-1, the protein was pre-incubated with different concentrations of Lyso-PC, PrC and choline chloride, which can block its phospholipid binding site, thus hindering its binding to the erythrocyte membrane. In these experiments a decrease in the erythrocyte lysis was

observed (Fig. 2.17C), clearly establishing that DSP-1 induced erythrocyte lysis is due to membrane perturbation by this protein, which is mediated by its binding to choline phospholipids present on the erythrocyte membrane. While 50 μ M Lyso-PC could inhibit the cell lysis by >90%, similar inhibition was achieved only at 1–2 mM concentrations of PrC, whereas inhibition by choline chloride was considerably weaker even at 50 mM concentration (Fig. 2.17C). These observations are consistent with the significantly higher association constant estimated for the binding of Lyso-PC to DSP-1 than PrC. Interestingly, incubation with \geq 200 μ M Lyso-PC resulted in strong lysis of the erythrocytes (not shown). This is most likely due to the detergent-like activity of this amphiphile.

Erythrocyte membrane lysis induced by DSP-1 was also investigated by confocal microscopy. In these studies, human erythrocytes were imaged in buffer and upon preincubation with DSP-1 at different time intervals. Images of erythrocytes alone in buffer showed well-defined morphology (Fig. 2.17D), whereas upon incubation with DSP-1 for 90 min, no erythrocytes were observed and only few membrane fragments membranes were broken down to smaller fragments (Fig. 2.17E). Pre-incubation of DSP-1 with 20 mM PrC prevented the erythrocyte lysis (Fig. 2.17F), clearly establishing that binding of DSP-1 to choline phospholipids on the erythrocyte membrane is obligatory for its membrane perturbing activity.

Seminal FnII proteins constitute the major protein fraction in the seminal plasma of various mammals. The seminal FnII proteins from a number of mammals have been isolated, purified and characterized, both structurally and functionally using various biochemical and biophysical methods [Swamy, 2004; Plante et al., 2016]. Extensive studies were carried out to investigate their interaction with choline phospholipids, their physiological ligands. Their role in *cholesterol efflux* and 'sperm capacitation' has been the main focus of investigation in a majority of these studies [Desnoyers and Manjunath, 1992; Ramakrishnan et al, 2001; Swamy et al., 2002; Greube, 2004; Wah et al., 2002; Anbazhagan and Swamy, 2005; Anbazhagan et al., 2011; Tannert et al., 2007; Damai et al., 2010; Kumar and Swamy, 2016c]. The recent discovery of chaperone-like activity (CLA) of these seminal FnII proteins has grouped them into small heat shock protein (*shsp*) family

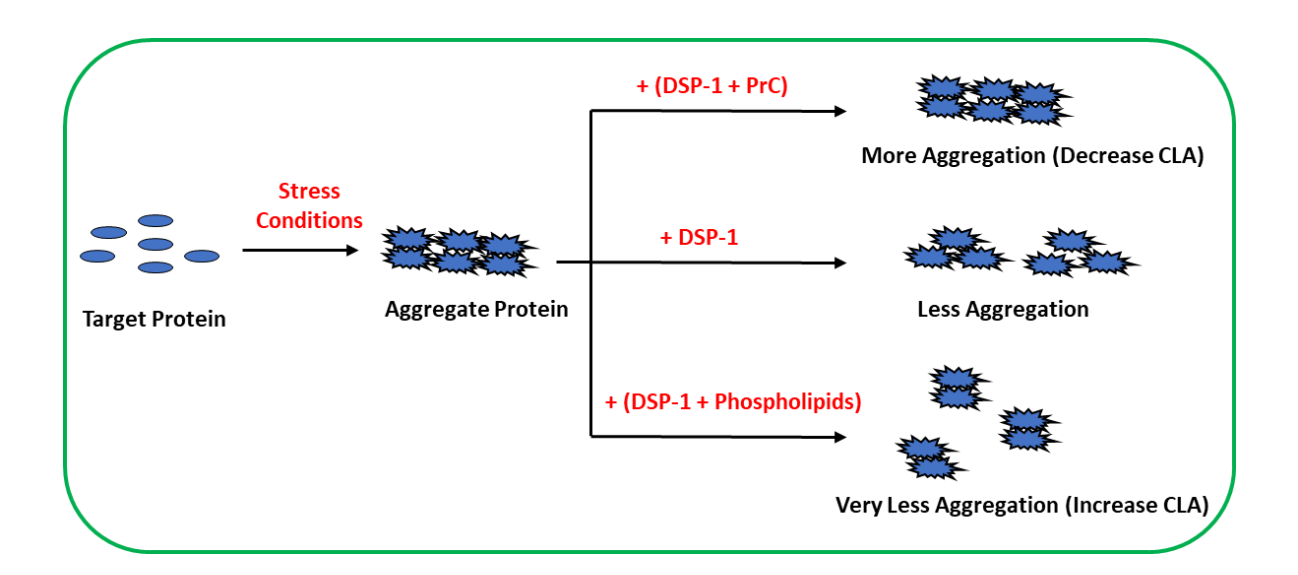
and a more significant role/function of these proteins has been postulated as they are the only proteins that exhibit protection towards other proteins against various stress conditions in the seminal plasma [Sankhala and Swamy, 2010; Sankhala et al., 2012; Kumar and Swamy, 2016b]. In this context, the present study reporting the purification and characterization of a major seminal FnII protein present in the donkey seminal plasma assumes relevance. Further work to characterize the chaperone-like activity of DSP-1 is currently underway in our laboratory.

2.5. Conclusion

In summary, we successfully purified DSP-1, a major protein from donkey seminal plasma that belongs to seminal FnII protein family and carried out primary, secondary, tertiary and quaternary structural characterization of this protein. The protein was found to be heterogeneously modified by O-glycosylation with acetylated sialic acid residues. Thermal unfolding studies have shown that DSP-1 exhibits polydispersity along with structural flexibility that is intrinsic in nature and plays a major role in its structural stability. Binding of PrC and Lyso- PC to DSP-1 has been characterized by fluorescence titrations and it was found that DSP-1 exhibits higher binding strength towards PrC and Lyso- PC as compared to PDC-109. Binding of PrC to DSP-1 not only results in a thermal stabilization of the protein but also reduces its polydisperse nature. Furthermore, membrane perturbing activity of DSP-1 was investigated under in vivo-mimicking conditions with model cell membranes (erythrocytes) and it was found that DSP-1 induces membrane destabilization and causes cell lysis. This could be of considerable physiological significance since similar activity of FnII proteins on sperm cell membrane has been reported to be important for inducing acrosome reaction in spermatozoa and subsequent sperm 'capacitation' in various mammals [Plante et al., 2016]. Since the role of seminal FnII proteins is expanding beyond their role in sperm capacitation as shsps and other regulatory activities, DSP-1 functions and activities will be explored in that direction. Studies on the CLA of DSP-1 established that acts as a *shsp*, and exhibits chaperone activity against various client proteins. These results are presented in Chapter 3.

Chapter 3

Chaperone-like Activity of the Major Donkey Seminal Plasma Protein DSP-1 is Modulated by Ligand Binding, Polydispersity and Hydrophobicity



Sk Alim^{\$}, Sudheer K. Cheppali^{\$}, Musti J. Swamy^{*}

(Manuscript under preparation)

^{\$} These two authors has contribute equally to this study

3.1. Summary

Fibronectin type-II (FnII) proteins are the major constituents in the seminal plasma of many mammals and play a very important role during "sperm capacitation". Recent studies have indicated that these seminal FnII proteins also exhibits "chaperone-like activity" (CLA) thereby acting as "small heat shock proteins" (*shsps*). The present work demonstrates that the major protein of donkey (*Equus hemionus*) seminal plasma, DSP-1 exhibits CLA by protecting various client proteins such as alcohol dehydrogenase, lactate dehydrogenase etc against thermal and oxidative stress. Binding of phosphoryl choline (PrC), the head group moiety of choline phospholipids, which are the physiological ligands of DSP-1, decreased the CLA whereas binding to choline phospholipids increased the CLA. This peculiar behavior of modulation of CLA by lipids containing similar head group but different hydrophobic chains is attributed to the changes in the surface hydrophobicity of DSP-1. Further, these changes in the surface hydrophobicity has been correlated to the polydisperse nature of DSP-1. The present studies expand the family of mammalian seminal FnII protein family that can act as *shsps*.

3.2. Introduction

In mammals, seminal plasma – a complex fluid containing a variety of low and high molecular weight molecules and inorganic ions – functions as a carrier for spermatozoa from male testes to female uterus, where fertilization takes place. Proteins are the only high molecular weight biopolymers present in the seminal plasma [Wassarman, 1987; Yanagimachi, 1994]. The major proteins present in the seminal plasma of most mammals contain two or four fibronectin type-II (FnII) domains and are therefore referred to as FnII proteins [Töpfer-Petersen et al., 2005; Greube et al., 2004]. PDC-109 and HSP-1/2 are the FnII proteins present in the bovine and equine seminal plasma, respectively. Among the FnII family proteins, PDC-109 contains 109 amino acid residues, which can be divided into an N-terminal segment followed by two FnII domains. It is the most well characterized seminal FnII protein, and exists as a polydisperse aggregate in solution [Esch et al., 1983; Baker, 1985; Swamy, 2004]. The interaction between PDC-109 and choline phospholipids and various factors affecting it have been extensively characterized using various biophysical and biochemical methods, as this interaction lays the foundation for the sperm capacitation to occur [Desnoyers and Manjunath, 1992; Ramakrishnan et al., 2001; Swamy et al., 2002]. Horse seminal plasma protein, HSP-1/2 is an homologue of PDC-109 in the equine seminal plasma. It is a mixture of two proteins HSP-1 and HSP-2, which are nearly identical in amino acid sequence, with some differences in the N-terminal flanking region and extent of glycosylation; HSP-2 contains 14 amino acids less in its Nterminal end and fewer glycosylation sites [Calvete et al., 1994, 1995a &b]. Studies on the interaction of HSP-1/2 with choline phospholipid membranes have shown that the binding involves tryptophan residues of the proteins, with the protein partially penetrating into the membrane hydrophobic core and disrupting the membrane, resulting in the formation of lipoprotein aggregates/particles in vitro [Greube et al., 2004; Sankhala and Swamy, 2010; Kumar and Swamy, 2016a &c].

Another important characteristic functionality of HSP-1/2 and PDC-109 is their role as a "small heat shock protein" (*shsp*) by exhibiting chaperone-like activity (CLA). Studies carried out on the CLA of HSP-1/2 and PDC-109 have shown that they can protect various proteins/enzymes against thermal, chemical and oxidative stress [Sankhala and

Swamy, 2010; Sankhala et al., 2012, Kumar and Swamy, 2016b]. Various factors such as pH, surfactants and small molecules such as carnitine were found to modulate the CLA of HSP-1/2. The CLA of HSP-1/2 was found to be inversely correlated to its membrane destabilizing activity and both activities were regulated by a 'pH switch' [Kumar and Swamy, 2016c, 2017a &b, 2018].

In recent work, we have purified the major protein from donkey seminal plasma, DSP-1 and carried out biochemical and biophysical investigations on it. These studies showed that DSP-1 is homologous to PDC-109 and HSP-1/2 and binds phosphorylcholine and choline phospholipids [See Chapter 2; Alim et al., 2022]. The main objective of the present work is to investigate if the similarity between DSP-1 and its well characterized homologues also includes CLA. In this direction, we have carried out various biophysical and biochemical studies/assays to explore this possibility. The results of those studies revealed that DSP-1 exhibits "chaperone-like activity" against thermal and oxidative stress. Further we have investigated the polydispersity and hydrophobicity induced chaperonelike activity of DSP-1 in the absence and presence of PrC and different phospholipids through aggregation assays, differential scanning calorimetry (DSC) and studies on the surface hydrophobicity using bis-ANS as a hydrophobic probe. These observations indicate that the polydispersity and surface hydrophobicity both decreased in presence of PrC, hence decreased the CLA of DSP-1, whereas in the presence of choline phospholipids, the polydispersity and surface hydrophobicity both increased and therefore increased the CLA.

3.3. Materials and methods

3.3.1. Materials

Alcohol dehydrogenase (ADH) and carbonic anhydrase (CA) were purchased from Sigma (St. Louis, MO, USA). 1,2-Dioleoyl-sn-glycero-3-phospholcholine (DOPC) and 1,2-dimyristoyl-sn-glycero-3-phospho-1-glycerol sodium salt (DMPG) were obtained from Avanti Polar Lipids (Alabaster, AL, USA). 4,4′-Dianilino-1,1′-binaphthyl-5,5′-disulphonic acid (bis-ANS), phosphorylcholine chloride calcium salt, glucose-6-phosphate dehydrogenase (G6PD) (from *Leuconostoc mesenteroides*), glucose-6-phosphate (G6P),

heparin-agarose type I beads and phosphorylcholine (PrC) were from Sigma. *p*-Aminophenyl phosphorylcholine-Agarose column was obtained from Pierce Chemical Co. (Oakville, Ontario, Canada). Enolase (ENL), lactate dehydrogenase (LDH), nicotinamide adenine dinucleotide (NAD), nicotinamide adenine dinucleotide phosphate (NADP), Tris base and other chemicals were purchased from local suppliers and were of the highest purity available.

3.3.2. Purification of DSP-1

DSP-1 was purified from the donkey seminal plasma as described earlier [See Chapter 2; Alim et al., 2022]. Purity of the protein was checked with 15% SDS-PAGE and the results were consistent with the previous report [see Chapter 2; Alim et al., 2022]. The purified protein was dialyzed extensively against 50 mM tris buffer, pH 7.4, containing 0.15 M NaCl and 5 mM EDTA (TBS) and stored at 4°C.

3.3.3. Aggregation assays

The chaperone-like activity (CLA) of DSP-1 was assayed as described previously for studies on PDC-109 and HSP-1/2 by monitoring the ability of DSP-1 to prevent heat-induced aggregation of ADH, LDH and enolase [Sankhala and Swamy, 2010; Sankhala et al., 2012]. A fixed concentration of each protein (0.05 – 0.1 mg/mL) was pre-incubated with different concentrations of DSP-1 (0.01 – 0.05 mg/mL) at 48°C and the sample aggregation was monitored by recording optical density at 360 nm as a function of time in a Cary 100 UV/visible spectrophotometer. Aggregation profile for each protein in buffer alone was taken as 100% and percent aggregation of other samples was calculated with respect to native enzyme.

3.3.4. G6PD activity assay

G6PD activity was assayed by a spectrophotometric method according to the earlier protocol [Sankhala and Swamy, 2010; Kumar et al., 2005]. Briefly, in this assay G6P gets oxidized to 6-phospho-D-gluconate by G6PD with simultaneous reduction of NADP to NADPH. The reaction was initiated by addition of NADP to a mixture containing G6PD (0.3 μM), NADP (0.1 mM), G6P (5 mM) and 12 mM each of MgCl₂ and KCl, and increase

in absorbance at 340 nm due to the reduction of NADP was monitored. To investigate the effect of DSP-1 on the thermal inactivation of the enzyme, $0.3~\mu M$ G6PD was incubated for 40 minutes in the absence or presence of $0.5~\mu M$ DSP-1 at $45^{\circ}C$. Relative activities of various treated samples were normalized with respect to that of the native enzyme activity at room temperature.

3.3.5. Assays of G6PD and ADH activity under oxidative condition

In order to investigate the ability of DSP-1 to protect client proteins against oxidative stress, activity of two enzymes, G6PD and ADH, was assayed under oxidative conditions as described earlier [Kumar and Swamy, 2016b]. The assay was performed essentially as described in the above manuscript with minor modifications as indicated below. Samples of G6PD (0.3 µM) was pre-incubated for 5 min with different concentrations of DSP-1, followed by addition of small aliquots of H₂O₂ from a 1 M stock solution before carrying out the assay. Relative activities of various treated samples were normalized with respect to that of native enzyme. Average values of three independent experiments are reported.

ADH activity under oxidative stress was assayed as described earlier [Kumar and Swamy, 2016; Men and Wang, 2007] with slight modification. The assay was performed by adding ethanol (400 mM) to the reaction mixture containing ADH (0.5 μ g/mL) and NAD⁺ (2.5 mM). Increase in absorbance at 340 nm (due to formation of NADH) was monitored using a Cary 100 UV-Vis spectrophotometer. To investigate the effect of oxidative stress, ADH was pre-incubated with 50 mM H_2O_2 for 10 min. To investigate the ability of DSP-1 to prevent the oxidation of ADH, samples were pre-incubated with DSP-1 for 5 min before the addition of H_2O_2 . The relative activities of different treated samples were normalized with respect to that of the native enzyme. All the results reported are averages of three independent experiments.

3.3.6. Fluorescein assay for hydroxyl radical ('OH) detection

Fluorescein assay for monitoring the production of hydroxyl radicals was performed as described earlier [Kumar and Swamy, 2016b; Ou et al., 2002]. Briefly, 50 mM H_2O_2 was added to the reaction mixture containing 0.2 μ M fluorescein and reactive oxygen species

(ROS) was generated by the addition of 10 μ L of Co²⁺ (100 μ M). The same reaction was carried out in the presence of various additives as indicated. Fluorescence decay profile of fluorescein was monitored at 515 nm in an ISS PC1 fluorescence spectrometer (Champaign, IL) by exciting at 493 nm and 5 nm slits on both excitation and emission monochromators. The percent inhibition of hydroxyl radical was calculated using the formula (100 - (F_c / F_o) x 100), where F_o and F_c are the normalized fluorescence intensities in the absence and in the presence of various additives at 60 minutes. All reported results are averages of at least two independent experiments.

3.3.7. Preparation of liposomes

Lipids taken in a glass tube were dissolved in chloroform or chloroform/methanol (3:1, v/v) mixtures were dried under a gentle stream of nitrogen gas followed by vacuum desiccation for 3-4 h. The lipid film was hydrated with buffer to give the desired lipid stock concentration. Small unilamellar vesicles (SUVs) were prepared by homogenizing the lipid mixture with 3-4 freeze-thaw cycles followed by sonication of the lipid suspension for 30 min in a bath sonicator above its transition temperature.

3.3.8. Effect of ligand (PrC) binding on CLA of DSP-1

The effect of ligand binding on the CLA of DSP-1 was investigated by performing the thermal aggregation assays using ADH and enolase as client proteins as described above (see Section 3.3.3). ADH/enolase was incubated at 48°C and its aggregation was monitored by recording light scattering at 360 nm as a function of time in a Cary 100 UV/Visible Spectrophotometer. A fixed concentration of DSP-1 was pre-incubated with ADH for 5 minutes at room temperature and then experiments were performed as described above. To investigate the effect of PrC binding on the CLA of DSP-1, varying concentrations of PrC (0.05-1 mM) were mixed with a fixed concentration of DSP-1 (0.02 mg/mL) and incubated for about 10 min and then experiments were performed as described above. Aggregation profile for the native enzyme was taken as 100% and percent aggregation of other samples was calculated with respect to that of the native enzyme.

3.3.9. Investigating the effect of phospholipids on CLA of DSP-1

The effect of phospholipids on the CLA of DSP-1 was investigated by carrying out thermal aggregation assays employing enolase and LDH as client proteins and using DSP-1 that was pre-incubated with DOPC or DMPG as reported previously [Sankhala et al., 2012; Kumar et al., 2018]. Different concentrations of each lipid were mixed with a fixed concentration of DSP-1 and incubated for 5-10 min, followed by the addition of the client protein (enolase/LDH) and further incubation for 5 min. Then the aggregation assay was performed as described above. Concentration of DSP-1, LDH, enolase and the lipids used are given in the figure legends.

3.3.10. Fluorescence spectroscopic studies of Bis-ANS

Interaction of bis-ANS with native DSP-1, phospholipid vesicles (DOPC or DMPG) and DSP-1/phospholipid mixtures was investigated at room temperature by steady-state fluorescence spectroscopy [Kumar et al., 2018; Sankhala et al., 2011a]. Fluorescence spectra were recorded on a JASCO FP-8500 fluorescence spectrometer using 2.5 nm slits on both excitation and emission monochromators. Samples taken in a $1 \times 1 \times 4.5$ cm quartz cuvette were excited at 385 nm, and emission spectra were recorded between 400 and 600 nm. Samples containing DSP-1, phospholipids and their mixtures were used in these studies. The final concentrations used were: DSP-1 (0.022 mg/mL), bis-ANS (~15 μ M) and phospholipids (~1 - 2.5 μ M). Studies were also done in the absence and presence of DSP-1 and different concentration of PrC (0.5 and 1 mM). All results reported are average values from two independent experiments (with standard deviations <5%).

3.4. Results and Discussion

We carried out various assays/studies to investigate the "chaperone-like activity" of DSP-1 against heat stress as well as oxidative stress and the factors that can modulate it. The observations of these studies are discussed below.

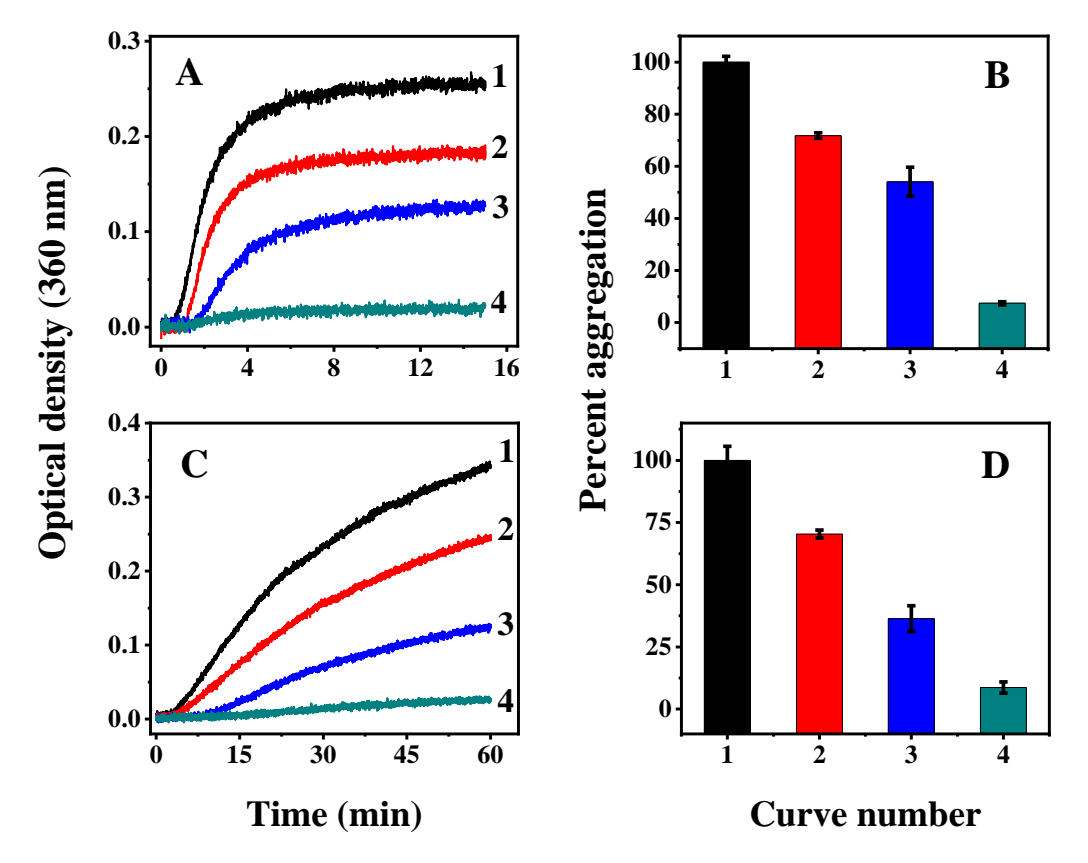


Fig. 3.1. Chaperone-like activity of DSP-1. (**A**) Prevention of aggregation of ADH (0.05 mg/mL) by DSP-1. Aggregation profiles of: (1) ADH at 48°C, (2) ADH + 10 μg/mL DSP-1, (3) ADH + 20 μg/mL DSP-1 and (4) ADH + 35 μg/mL DSP-1. (**B**) Bar diagram of results shown in **A**. (**C**) LDH (75 μg/mL) aggregation assays of: (1) LDH at 49°C, (2) LDH + 10 μg/mL DSP-1, (3) LDH + 25 μg/mL DSP-1 and (4) LDH + 50 μg/mL DSP-1. (**D**) Bar diagram representation of results shown in **C**.

3.4.1. DSP-1 inhibits thermal aggregation of target proteins

Assays aimed at investigating the effect of DSP-1 on the thermal aggregation of ADH, upon incubation at high temperature such as 48°C, are shown in Fig. 3.1A. ADH, similar to many other proteins, aggregates and precipitates upon incubation at high temperatures, which can be measured by monitoring the turbidity of the solution (see Fig. 3.1A, curve 1). In the presence of DSP-1, this aggregation decreased in a concentration dependent manner. In the presence of 10 μ g/mL DSP-1, ~71% aggregation was observed as compared to native enzyme alone (curve 2). When the concentration of DSP-1 was doubled to 20 μ g/mL the relative aggregation decreased to ~54% and when it was further increased to 35

μg/ml, very little aggregation was observed (curves 3, 4). DSP-1 alone did not show any aggregation when incubated at 48°C. A bar diagram representing these results is shown in Fig. 3.1B. Similar results were obtained when lactose dehydrogenase (LDH) (Fig. 3.1C, 1D), enolase (Fig. 3.2A, B) and carbonic anhydrase (CA) (Fig. 3.2C, D) were used as client proteins, showing that DSP-1 was capable of suppressing/inhibiting the heat induced aggregation of all the above client proteins. These results show that DSP-1 functions like a small heat shock protein (*shsp*) by protecting a variety of client proteins against thermal stress.

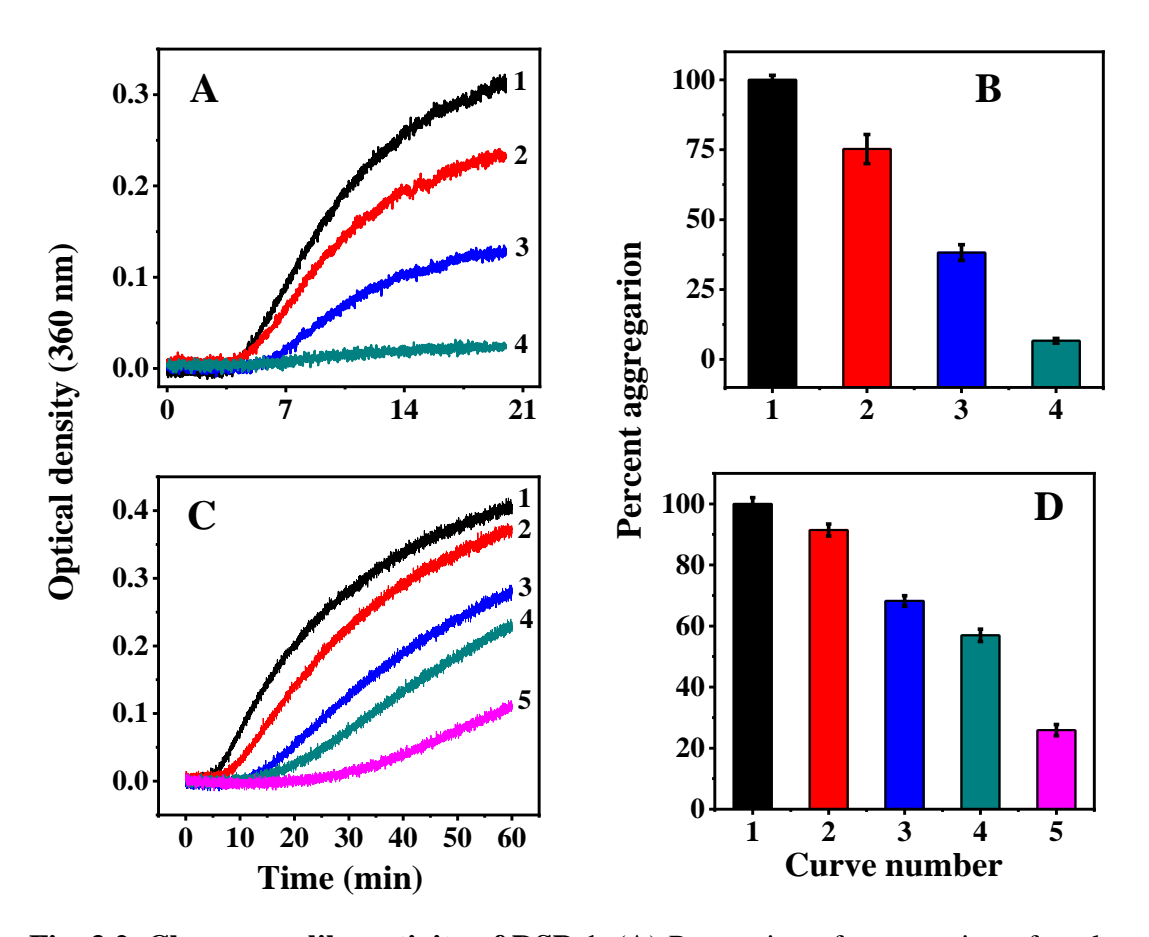


Fig. 3.2. Chaperone-like activity of DSP-1. (**A**) Prevention of aggregation of enolase (0.1 mg/mL) by DSP-1. Aggregation profiles of: (1) enolase at 48 °C, (2) enolase + 10 μ g/mL DSP-1, (3) enolase + 25 μ g/mL DSP-1 and (4) enolase + 50 μ g/mL DSP-1. (**B**) Bar diagram representation of results presented in **A**. (**C**) Aggregation profiles of Carbonic anhydrase (CA) (0.075 mg/mL) at 48°C under different conitions: (1) CA alone, (2) CA + 0.025 mg/mL DSP-1, (3) CA + 0.05 mg/mL DSP-1, (4) CA + 0.075 mg/mL DSP-1 and (5) CA + 0.1 mg/mL DSP-1. (**D**) Bar diagram representation of results presented in C.

3.4.2. DSP-1 protects G6PD against thermal and oxidative stress

After establishing that DSP-1 can inhibit thermal aggregation of other proteins, we carried out further studies to investigate whether DSP-1 can protect the catalytic activity of an enzyme under stress conditions. G6PD, a very vital enzyme involved in the pentose phosphate pathway, is present in most of the organisms and cells, including mammalian spermatozoa. Diseases such as neonatal hyperbilirubinemia and chronic hemolytic anemia are caused due to deficiency of G6PD [Nkhoma et al., 2009]. G6PD is highly susceptible to thermal stress and incubation of the enzyme at the moderately high temperatures of 45°C for 30 min led to ~64% loss of activity (Fig. 3.3A, curve 2) as compared to the activity at room temperature (~25°C, curve 1). Preincubation with DSP-1 decreased the inactivation significantly, with 63% and 92% of activity being retained when the concentration of DSP-1 was 25 and 50 μg/mL, respectively and revealed that DSP-1 can protect G6PD against thermal deactivation. Incubation with DSP-1 at room temperature did not lead to any significant changes in the G6PD activity. These studies indicate that DSP-1 is able to protect G6PD from heat-induced inactivation and help maintain its activity even at higher temperatures.

G6PD has a binding pocket for G6P which is susceptible to oxidation. Radical generating systems such as Fe^{3+} /citrate, Fe^{3+} /EDTA, Fe^{3+} /ascorbate, Fe^{3+} /H₂O₂, or H₂O₂ alone can oxidize the active site residue(s), which results in loss of G6PD activity [Szweda and Stadtman, 1992]. In further studies aimed at exploring the CLA of DSP-1, we investigated the decrease in the activity of G6PD induced by oxidative stress. G6PD showed ~20% activity under oxidative stress as compared to that observed under native conditions (Fig. 3.3C, curve 2). In presence of DSP-1 (20 μ g/mL and 50 μ g/mL) the activity increased to 50% and 68%, respectively, and indicate that DSP-1 can protect the enzyme from oxidative stress induced inactivation (Fig. 3.3C, curves 3, 4). When, the experiment was carried out after pre-incubation of G6PD with DSP-1 but without H₂O₂, a slight increase (~2%) in the activity was observed (Fig. 3.3C, curve 5) which is similar to observations for PDC-109 and HSP-1/2 [Sankhala and Swamy, 2010; Kumar and Swamy, 2016c].

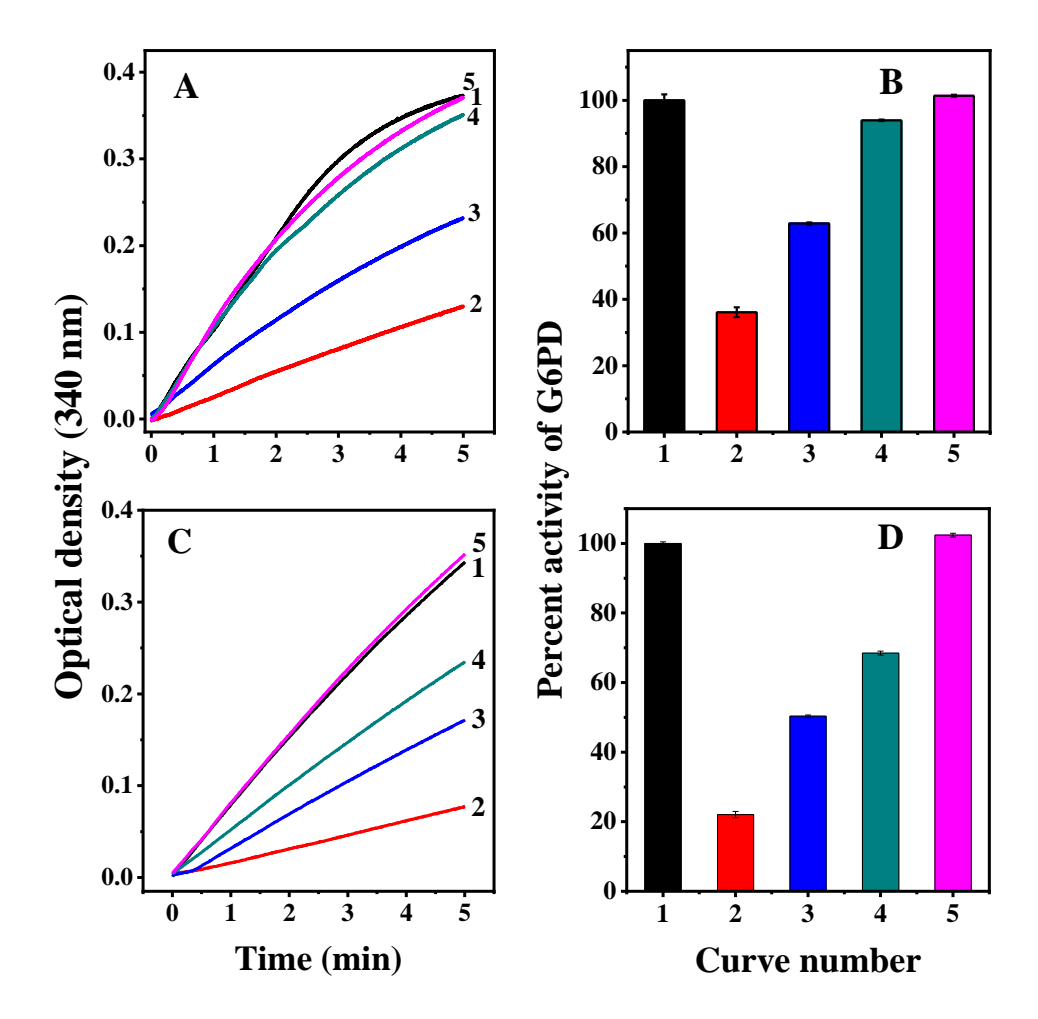


Fig. 3.3. G6PD activity assays under thermal and oxidative stress. Activity of the enzyme was assessed by monitoring absorption as 340 nm. (**A**) Activity at room temperature under native conditions (1), after incubation at 45°C for 30 min (2), upon incubation at 45°C in the presence of 25 μg/mL, 50 μg/mL of DSP-1 (3,4) and after incubation at 4°C in the presence of 50 μg/mL DSP-1 (5). (**B**) Bar diagram representation of the activity at 5 min (from **A**). (**C**) G6PD activity assay under oxidative stress. Activity was measured at room temperature under native conditions (1), after incubation with 10 mM $_{2}O_{2}$ for 5 min (2), upon incubation with 10 mM $_{2}O_{2}$ in the presence of 20 μg/mL DSP-1 and 50 μg/mL DSP-1 (3, 4) and after incubation in the presence of 50 μg/mL DSP-1 alone (5). (**D**) Bar diagram representation of the activity at 5 min (from **C**).

3.4.3. ADH activity assay under oxidative stress

In further studies, we investigated if DSP-1 can exhibit CLA by protecting client proteins against loss of activity due to oxidative stress. For this studies, ADH was chosen as the

client protein. ADH is a zinc-containing enzyme and has multiple disulfide linkages. It loses its activity under oxidative stress due to conversion of Cys^{43} and Cys^{153} to $Cys\text{-}SO_2H$ and $Cys\text{-}SO_3H$, respectively, which results in the loss of Zn^{2+} from the active site [Men and Wang, 2007]. This is shown in Fig. 3.4A (curve 3), where ADH activity was reduced ~43%, when pre-incubated with H_2O_2 compared to the activity seen under native condition (curve 1). In presence of 25 and 50 μ g/mL of DSP-1, ~70% and ~79% activity was retained (curves 4, 5), which indicates that DSP-1 is capable of protecting ADH against oxidative stress induced inactivation, in a concentration dependent manner. Under native conditions addition of DSP-1 did not significantly affect the ADH activity (curve 2). A bar diagram representing percent of ADH activity under various conditions is shown in Fig. 3.4B.

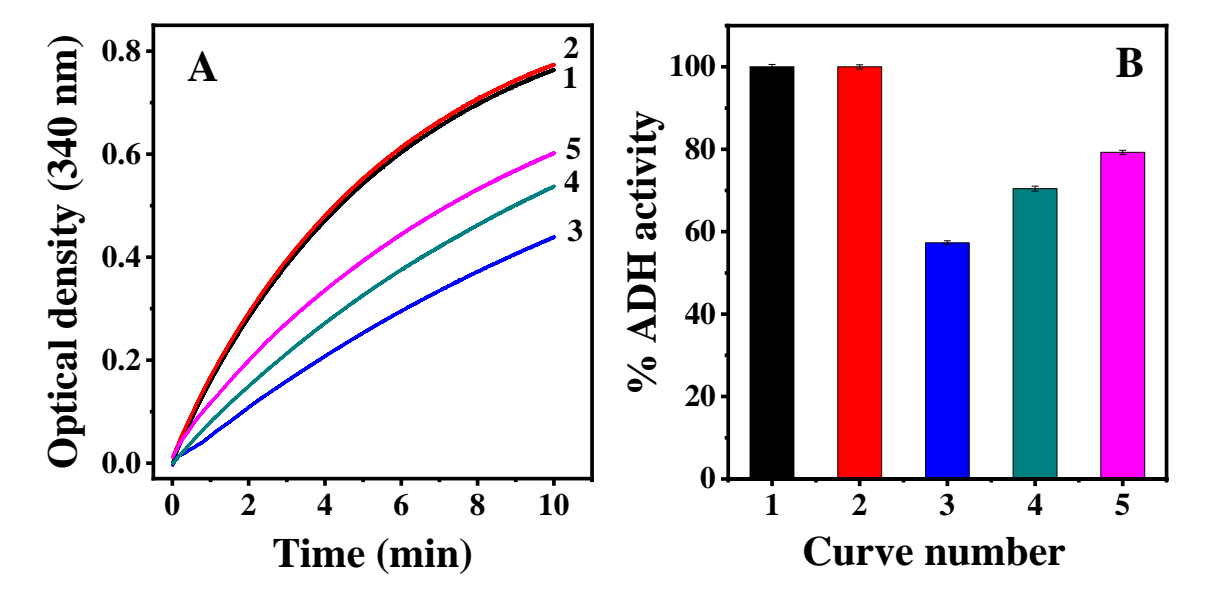


Fig. 3.4. ADH activity assay against oxidative stress. A) Activity of ADH alone under native conditions (1); ADH + 50 μ g/mL DSP-1 (2); ADH + H_2O_2 (3); ADH + H_2O_2 + 25 μ g/mL DSP-1 (4) and ADH + H_2O_2 + 50 μ g/mL DSP-1 (5). B) Bar diagram representation of the results presented in A. H_2O_2 concentration was 50 mM in all samples where it was used. See text for details.

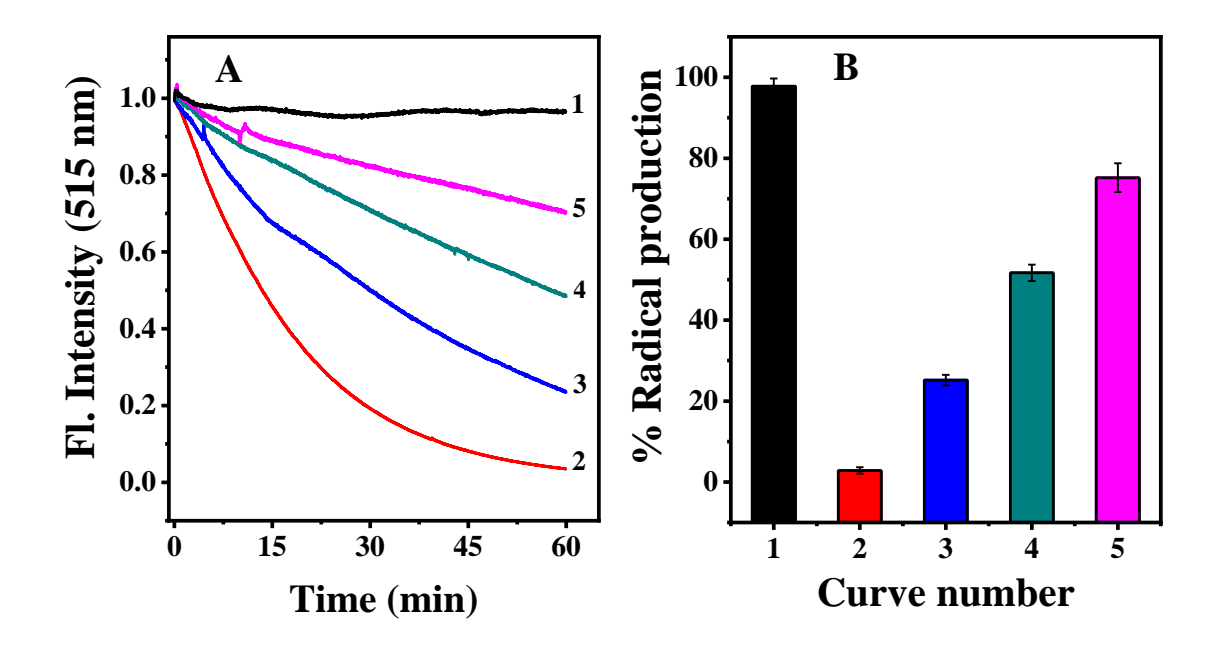


Fig. 3.5. Fluorescein assay to assess the CLA of DSP-1 against oxidative stress. (A) Fluorescence of fluorescein was monitored as a function of time under different conditions as indicated: In the presence of DSP-1 alone (curve 1); in the presence of $\text{Co}^{2+}/\text{H}_2\text{O}_2$ system (curve 2); in the presence of $\text{Co}^{2+}/\text{H}_2\text{O}_2$ system and different concentrations of DSP-1: 50 µg/mL (3), 100 µg/mL (4) and 200 µg/mL (5). (B) Bar diagram representation of the results presented in A.

3.4.4. DSP-1 inhibits the production of hydroxyl radicals

In further studies, we investigated the ability of DSP-1 to protect G6PD and ADH under oxidative stress conditions. As the hydroxyl radicals decreased the activity of G6PD and ADH, we investigated how DSP-1 affects hydroxyl radical production *in vitro*. It is well known that hydroxyl radicals produced during glycolysis are the main cause for the oxidative stress in the spermatozoa in mammals due to their ability to permeate across the sperm plasma membrane effectively [Baumber et al., 2001]. Here, we employed conventional fluorescein dye assay for the detection of hydroxyl radicals and the effect of DSP-1 on their production. In the presence of a hydroxyl radical generating system (Co²⁺+H₂O₂), fluorescein undergoes oxidation resulting in loss of fluorescence (Fig. 3.5A, curve 2). However, when the assay was conducted in the presence of DSP-1 (50 and 100 μg/mL), more than 25% and 51% of the initial fluorescence is retained. In the presence of 200 μg/mL of DSP-1, ~75% fluorescence is observed compared to the control (fluorescein

alone). These studies indicate that DSP-1 can inhibit the production of hydroxyl radicals in a concentration dependent manner. These results together with those of the aggregation assays presented above (sections 3.4.1- 3.4.3) indicate that DSP-1 can exhibit chaperone-like activity (CLA) and protect various client proteins/enzymes from heat stress and oxidative stress.

3.4.5. Effect of PrC binding on CLA of the DSP-1

CLA of many "small heat shock proteins" is known to be dependent on hydrophobicity as well as polydisperse nature of these proteins [Kumar and Swamy, 2017a; Kumar et al., 2018; Sankhala et al., 2011; Voellmy and Boellmann, 2007; Lee et al., 1997; Bakthisaran et al., 2015; Sheluho and Ackerman, 2001]. As these two factors have been shown to modulate the CLA, we sought to investigate the effect of varying hydrophobicity and polydispersity of DSP-1 on its CLA.

3.4.5.1. Effect of PrC binding on the CLA of DSP-1 by ADH aggregation assay

In a recent study, we observed that DSP-1 exhibits polydispersity and exists in a higher order oligomeric form as well as a monomer and binding to PrC reduces the polydisperse protein to a predominantly monomeric form [see Chapter 2; Alim et al., 2022]. In view of this, in order to investigate the effect of polydispersity of DSP-1 on its CLA, we performed chaperone activity assays in the presence of PrC. PrC binding effect on the CLA of DSP-1 was assessed by turbidimetry and the observations are presented in Fig. 5A. When incubated at 48°C, "ADH" showed a rapid increase in the turbidity, which reached a maximum and then remained constant (Fig. 3.6A, curve 1). When the experiment was performed in the same manner, but in the presence of DSP-1 (20 μg/mL) the aggregation of ADH decreased significantly (~90% reduction, curve 2). However, pre-incubation of DSP-1 with PrC reversed this in a concentration dependent manner (Fig. 3.6A, curves 3–6). From the curves it is clear the even at sub-millmolar concentration PrC was able to reduce the CLA of DSP-1 and pre-incubation with 1 mM PrC has reduced the CLA of DSP-1 to <20%. A similar decrease in the ability of DSP-1 to protect the aggregation of enolase was observed in the presence of PrC (Fig. 3.7).

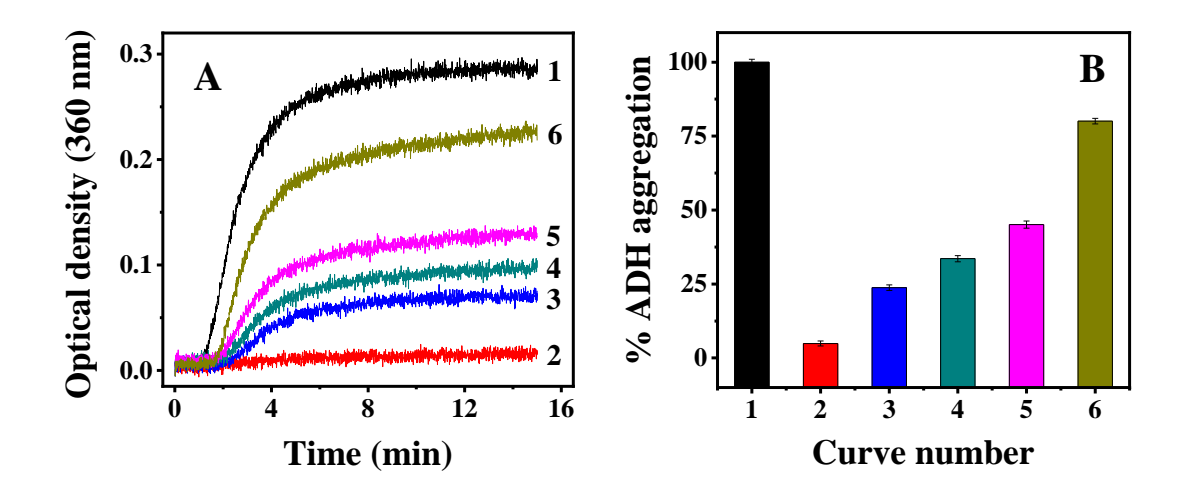


Fig. 3.6. Effect of phosphorylcholine binding on the CLA of DSP-1. (A) Aggregation profiles of ADH (0.05 mg/mL): (1) ADH at 48 °C, (2) ADH + 20 μ g/mL DSP-1, (3) ADH + DSP-1 + 50 μ M PrC, (4) ADH + DSP-1 + 0.1 mM PrC, (5) ADH + DSP-1 + 0.5 mM PrC and (6) ADH + DSP-1 + 1 mM PrC. (B) Bar diagram representation of the aggregation of ADH in various samples at 15 min.

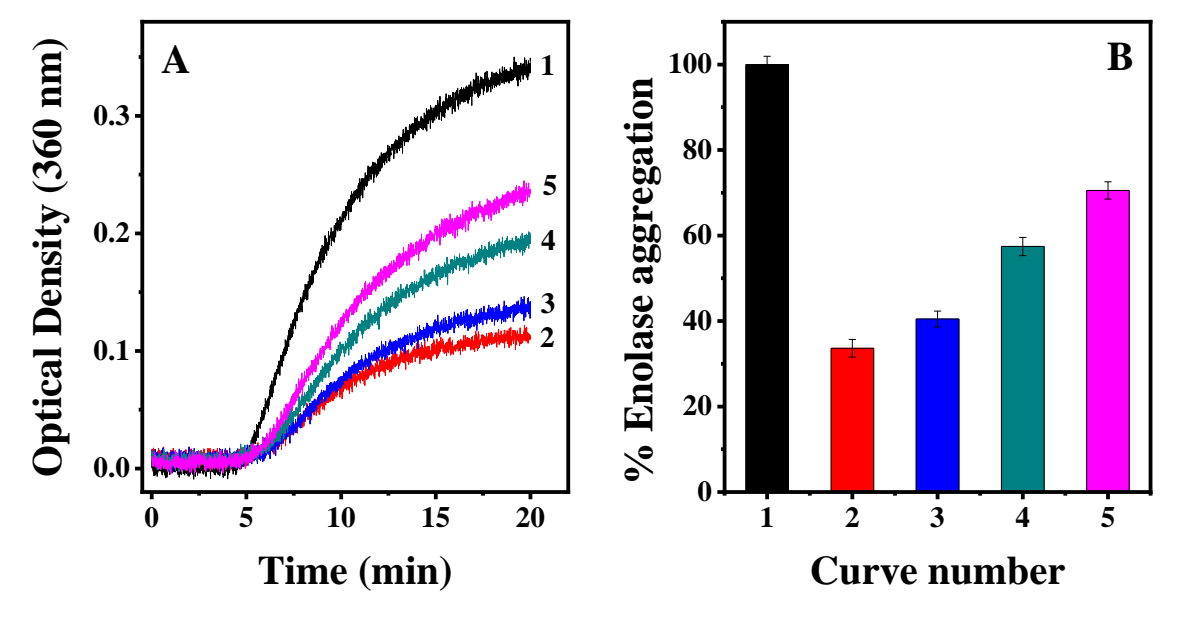


Fig. 3.7. Effect of phosphorylcholine binding on the CLA of DSP-1. A) Aggregation profiles of enolase (0.1 mg/mL) correspond to: (1) enolase at 48°C, (2) enolase + 0.01 mg/mL DSP-1 at 48°C, (3) enolase+ 0.01 mg/mL DSP-1 + 0.1mM PrC at 48°C, (4) enolase + 0.01 mg/mL DSP-1 + 0.5 mM PrC at 48°C and (5) enolase+ 0.01 mg/mL DSP-1 + 1 mM PrC at 48°C. **B)** Bar diagram representing the aggregation of enolase in various samples corresponding to curves in panel A.

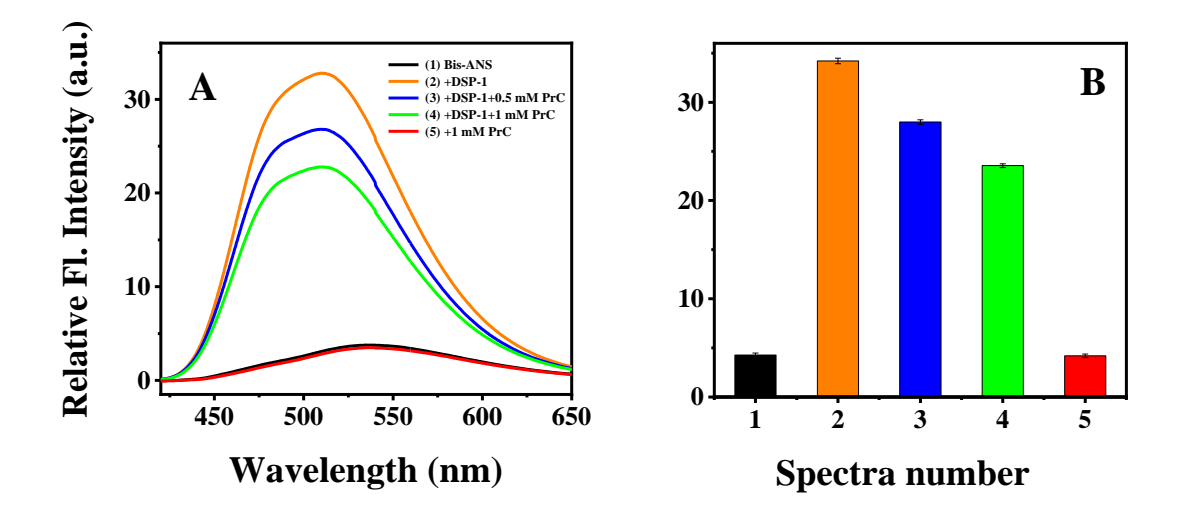


Fig. 3.8. (**A**) Changes in the surface hydrophobicity of DSP-1 upon binding with PrC: Fluorescence spectra shown correspond to bis-ANS in buffer (black), DSP-1 (orange), DSP-1 + 0.5 mM PrC (blue), DSP-1 + 1 mM PrC (green) and 1 mM PrC (red). (**B**) Relative fluorescence intensity of various samples in panel (**A**) shown in a bar diagram format. The final concentration of Bis-ANS and DSP-1 were 10 μ M and 22 μ g/mL respectively.

3.4.5.2. Surface hydrophobicity upon binding of PrC to DSP-1

CLA of many extracellular chaperones and small heat shock proteins such as murine Hsp25, human Hsp27, bovine α B-crystallin and Atp11p has been directly correlated to their surface hydrophobicity [Bakthisaran et al., 2015; Sheluho and Ackerman, 2001; Voellmy and Boellmann, 2007; Lee et al., 1997]. It was postulated that through hydrophobic patches present on the protein surface the *shsps* were able to interact with the target/client proteins and exhibit CLA against various stress conditions. Therefore, we have investigated changes in the surface hydrophobicity of DSP-1 in the presence of PrC using bis-ANS as a fluorescence probe. It is known that bis-ANS binds to hydrophobic regions of proteins, which results in a significant increase in its fluorescence emission along with a blue shift in the emission λ_{max} [Manček-Keber Jerala, 2006]. Therefore, the enhancement in bis-ANS fluorescence intensity could be correlated to increased exposure of hydrophobic regions or residues on the protein surface. Fluorescence spectra and relative fluorescence intensities of bis-ANS alone and in the presence of DSP-1, PrC and their combinations are shown in Fig. 3.8A. Fluorescence intensity of bis-ANS increased

Table 3.1. Emission maxima (λ_{max}) and relative fluorescence intensity of bis-ANS in the presence of DSP-1 under various conditions. Fluorescence intensity of bis-ANS in the presence of DSP-1 was considered as 100%. All the values given are averages from 2 or 3 independent experiments. Fluorescence intensities of all samples were normalized against DSP-1 in the presence of bis-ANS.

Samples/ Conditions	Relative Fluorescence	$\lambda_{max}(nm)$	Fold Enhancement
	Intensity (%)		
Bis-ANS in buffer	12.42 (±2.5)	545	-
+ DSP-1	100.00 (±3.0)	515	8.0
+ DSP-1 + 0.5 mM PrC	81.93 (±3.4)	516	6.5
+ DSP-1 + 1 mM PrC	68.15 (±2.3)	516	5.5
+ 1 mM PrC	12.07 (±2.7)	546	-
+ DMPG	12.93 (±3.1)	543	-
+ DMPG + DSP-1	175.02 (±4.2)	510	13.3
+ DOPC	109.36 (±3.7)	513	8.3
+ DOPC + DSP-1	237.83 (±4.5)	512	18.0

8-fold in the presence of DSP-1 together with a 30 nm blue shift in the emission λ_{max} from 545 nm to 515 nm, suggesting the presence of hydrophobic patches on the surface of the protein, which was also proposed from the predicted 3D structure of DSP-1 obtained by homology modeling [see Chapter 2; Alim et al., 2022]. Binding of PrC to DSP-1 led to smaller changes in the fluorescence intensity of bis-ANS, with about 6.5-fold and 5.5-fold increase being observed in the presence 0.5 and 1 mM PrC, respectively. This corresponds to about 18 and 31% decrease in the fluorescence intensity, respectively, as compared to bis-ANS in presence of DSP-1 alone (Table 3.1). This decrease in fluorescence intensity of bis-ANS-DSP-1 in the presence of PrC indicates decreased hydrophobicity of the protein surface. This observation is consistent with decreased CLA of DSP-1 in the presence of PrC (0.5-1 mM) as compared to DSP-1 alone (Fig. 3.6A). Addition of 1 mM PrC alone had little or no effect on the fluorescence intensity of bis-ANS. These observations indicate that binding decreases the surface hydrophobicity of DSP-1. This could be due to

conformational changes in the protein structure induced by the binding or due to the direct interaction of PrC with the aromatic aminoacids in the binding pocket of the DSP-1 [Alim et al., 2022] that can mask the surface hydrophobic amino acids, which results in a decrease in the surface hydrophobicity.

3.4.5.3. Effect of oligomerization on the CLA of DSP-1 upon binding with PrC

Another important factor that affects the CLA of many *shsps* is their polydisperse nature. Polydispersity was found to modulate the surface hydrophobicity of the seminal plasma FnII proteins from other mammals, which in turn affects their interaction with client proteins, thus modulating their CLA. As DSC studies revealed that the first thermotropic transition centered around 32°C, indicating dissociation of the oligomers to monomer was absent in the DSC thermograms obtained in the presence of PrC [see Chapter 2; Alim et al., 2022], the decrease in the hydrophobicity and CLA is likely due to the conversion of the polydisperse oligomers of DSP-1 to monomers. This is similar to the observations made with PDC-109, the major protein of "bovine seminal plasma" which converts from polydisperse oligomers to monomers upon PrC binding, and also showed drastically decreased CLA and surface hydrophobicity [Gasset et al., 1997; Sankhala et al., 2011b]. Thus, the polydispersity of DSP-1 seems to be crucial for the CLA of DSP-1 as it confers considerable surface hydrophobicity to the protein and binding of PrC seems to abrogate the CLA by altering its oligomeric nature, which reduces its surface hydrophobicity.

Fluorescence intensity of bis-ANS increased in the presence of oligomeric form of DSP-1 due to the dynamic and flexible movements of the oligomeric species, whereas interaction with monomer blocked this movement reducing fluorescence intensity, hence decreased surface hydrophobicity [Smoot et al., 2001]. DSC studies suggested that only the monomeric form of DSP-1 exists in solution in the presence of PrC, with complete absence of the oligomers. These results correlate well with decreased surface hydrophobicity of DSP-1 in the PrC-bound state as compared to the native form of DSP-1. This decrease in intensity could be because of shielding of the aromatic amino acids Y40, Y64, Y111, W57, W68, W104 and W117 by the bound PrC [see Chapter 2; Alim et al., 2022].

3.4.6. Effect of phospholipids on the CLA of DSP-1

3.4.6.1. Phospholipid binding affects the CLA of DSP-1

Since decrease in the surface hydrophobicity and oligomerization of DSP-1 led to decrease in its CLA, we looked at the factors that can increase the surface hydrophobicity to investigate if a correlation can be established between the hydrophobicity and CLA. Previous studies have shown that phospholipid binding increases the surface hydrophobicity of both PDC-109 and HSP-1/2 [Sankhala et al., 2011a; Kumar and Swamy, 2016c]. As DSP-1 is homologous to these two proteins, we investigated the effect of phospholipids on the CLA of DSP-1 using enolase and LDH as the client proteins. CLA of DSP-1 was assayed in presence of various phospholipids (Fig. 3.9A). Incubation of enolase at 48°C leads to aggregation of the protein, resulting in an increase in the turbidity of the sample (Fig.3.9A, curve 1). In the presence of 0.01 mg/mL DSP-1 alone, the aggregation reduced to ~68% when compared to the native enzyme. When DSP-1 was pre-incubated with 1 μM DOPC the aggregation of enolase decreased to ~54% and incubation with a higher concentration of DOPC (2.5 µM) decreased the aggregation further to ~40%. Incubation of DSP-1 with 2 µM DMPG did not show any significant effect on the CLA, with aggregation of enolase being ~67% (Fig.3.9A, curve 4). These results indicate that the presence of DOPC, a choline phospholipid which is the physiological ligand of DSP-1, increases the CLA of DSP-1. Similar results were observed with LDH as well (Fig. 3.10).

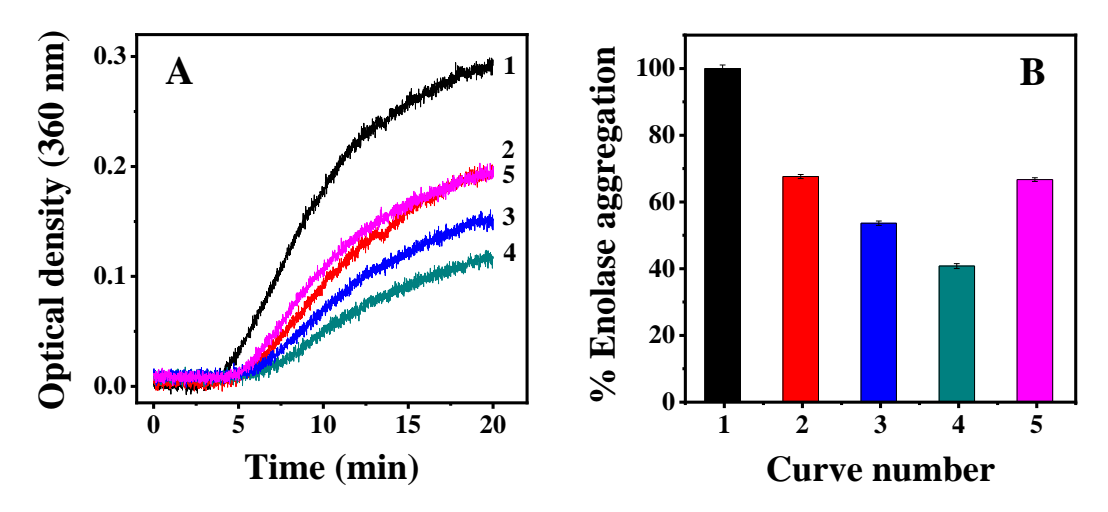


Fig. 3.9. Effect of phospholipid binding on the CLA of DSP-1. (**A**) Aggregation assay with enolase (0.05 mg/mL): (1) enolase at 48°C, (2) enolase + 0.01 mg/mL DSP-1, (3)

enolase + DSP-1 + 1 μ M DOPC, (4) enolase + DSP-1 + 2.5 μ M DOPC and (5) enolase + DSP-1 + 2 μ M DMPG. (**B**) Bar diagram representing the aggregation of enolase of various samples at 20 minutes (from panel **A**).

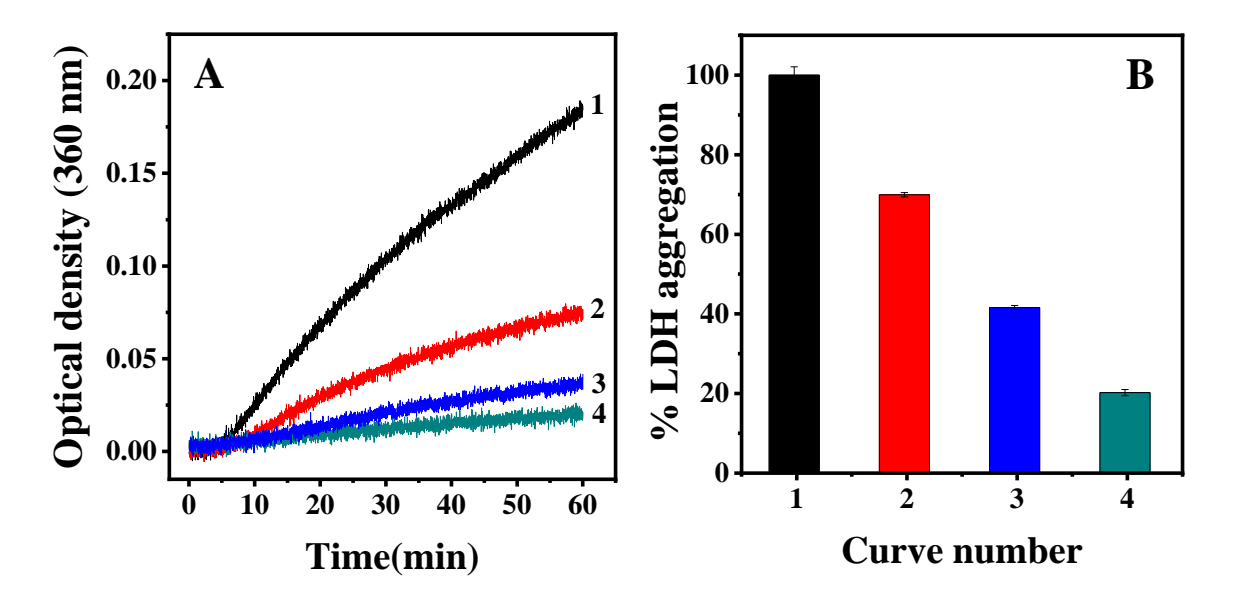


Fig. 3.10. Effect of phospholipids on CLA of DSP-1 with LDH (0.075 mg/mL). A) Aggregation profiles correspond to: (1) LDH at 48° C, (2) LDH + 0.01 mg/mL DSP-1 at 48° C, (3) LDH + 0.01 mg/mL DSP-1 + 1 μ M DOPC at 48° C and (4) LDH + 0.01 mg/mL DSP-1 + 2.5 μ M DOPC at 48° C. B) Bar diagram corresponding to percent aggregation of LDH alone and in presence of DSP-1 and various phospholipids corresponding to the curves in panel A.

3.4.6.2. Extent of hydrophobicity upon interaction of DSP-1 with phospholipids

The interaction between chaperones and their client proteins occurs mostly through the hydrophobic patches on the target protein and the hydrophobic regions present on their surface [Moparthi et al, 2010; Lee et al, 1997]. Fluorescence spectra and relative fluorescence intensities of bis-ANS alone and in presence of DSP-1, DMPG, DOPC, as well as DSP-1/DMPG and DSP-1/DOPC complexes are shown in Fig. 3.11 (panels A & B). Fluorescence intensity of bis-ANS in the presence of DMPG (green line), was comparable to that of bis-ANS in buffer (black line), whereas in the presence of DOPC vesicles (magenta line) the intensity increased by about 8.3-fold. The fluorescence intensity increased by ~7.8 fold in the presence of DSP-1 (blue line). The fluorescence enhancement was ~1.7 times higher in the presence of DSP-1/DMPG mixture (dark cyan

line) as compared to that observed in the presence of DSP-1 alone, and 13.3 time higher than that of bis-ANS in buffer. On the other hand, in presence of DSP-1/DOPC complex (red line), the increase of fluorescence intensity was observed to be 2.4 folds higher than that observed in presence of native DSP-1 and 18-folds higher as compared to that of bis-ANS in buffer. These results show that DSP-1/DOPC mixture shows higher surface hydrophobicity than the individual components or their cumulative effect, indicating a synergistic effect of DSP-1/DOPC mixture. This increase in surface hydrophobicity correlates well with the increase in CLA of DSP-1 in the presence of DOPC.

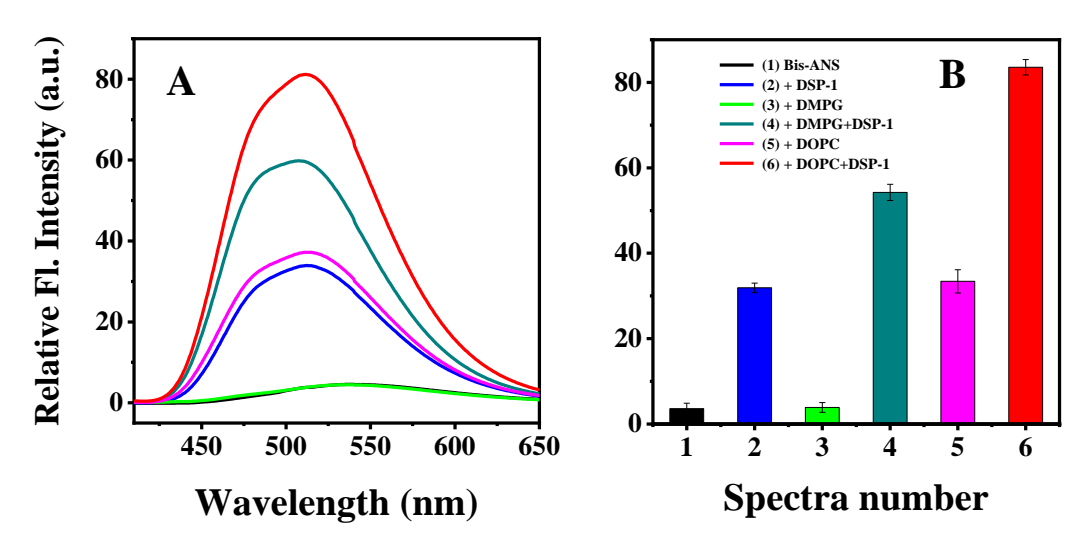


Fig. 3.11. (**A**) Fluorescence spectra of bis-ANS to phospholipids, DSP-1 and phospholipid/DSP-1 mixture spectra shown correspond to: bis-ANS in buffer (black), DMPG (green), DSP-1 (blue), DOPC (magenta), DMPG-DSP-1 mixture (dark cyan) and DOPC-DSP-1 mixture (red). (**B**) Bar diagram representation of the relative fluorescence intensity of various samples (data from panel **A**). The final concentration of Bis-ANS, DSP-1 and individual lipids were 15 μM, 0.022 mg/mL and 50 μM, respectively. See text for details.

3.4.6.3. Effect of oligomerization on the CLA of DSP-1 upon binding with phospholipids

The increase in the fluorescence intensity of the fluorescent probe, bis-ANS indicates greater exposure of hydrophobic surfaces. DSP-1 binds to choline phospholipids with high affinity which leads to membrane disruption and formation of lipid/protein complexes as was observed earlier with PDC-109 and HSP-1/2 [Ramakrishnan et al., 2001; Tannert et

al., 2007]. In this study, we observed a large increase in the fluorescence intensity of bis-ANS in the presence of DOPC/DSP-1 complex indicating that lipid/protein complexes have greater hydrophobicity as compared to DSP-1 aloneand this increase in hydrophobicity could facilitate the interaction of DSP-1 with client proteins, resulting in the suppression/partial inhibition of their aggregation (Fig. 3.9A, curves 3 and 4). Interaction of DSP-1 with DMPG is weaker as compared to that of DSP-1 with DOPC, due to which DSP-1 may not intercalate into the hydrophobic regions of DMPG membranes to the same extent as that of with DOPC membranes. Therefore, the exposure of hydrophobic core of DMPG may not be the same as DOPC, resulting in a smaller change in the fluorescence intensity of DSP-1/DMPG complex compared to that of DSP-1/DOPC complex (Fig. 3.11A, dark cyan line), which are correlated with the smaller change seen in the presence of DMPG on the CLA of DSP-1 (Fig. 3.9A, curve 5).

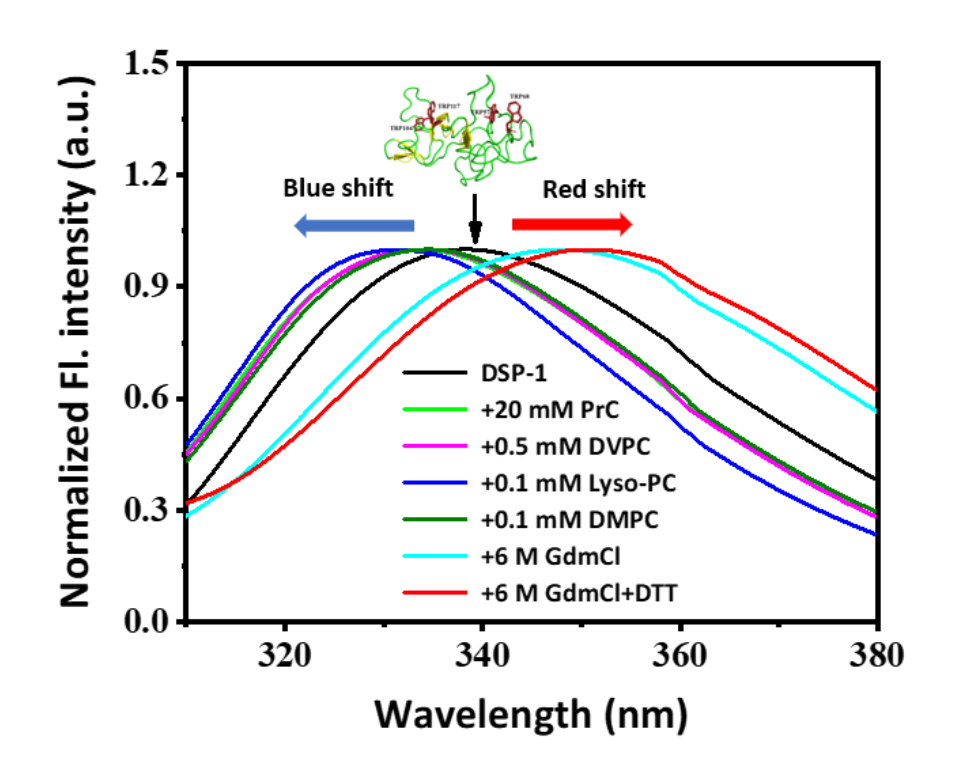
3.5. Conclusion

In summary, we have characterized the CLA of DSP-1, through various assays which show that DSP-1 is capable of protecting various client proteins against heat stress and oxidative stress conditions. These results establish the common role of seminal FnII proteins as the shsps in the reproductive tract. This is particularly significant as the seminal plasma doesn't have any ATP dependent chaperones and other factors that could protect the contents of seminal plasma in the hostile female reproductive tract. Our observations also indicate the role of polydispersity and hydrophobicity as key factors that can modulate the CLA of DSP-1. It is important to note that DSP-1/DOPC mixture which forms lipoprotein complexes and prevents the aggregation, increased CLA of DSP-1 and this mixture exists in vivo as it is the main byproduct of DSP-1 induced sperm capacitation and hence could play a crucial role as CLA under in vivo conditions. Our results show that choline phospholipids induce a different effect on the structure and function of DSP-1 than that observed upon PrC binding. Preincubation of DSP-1 with PrC shows a decrease in polydisperse nature as well as surface hydrophobicity because of the direct association of PrC with the aromatic amino acids in the binding pocket of DSP-1, which decreased CLA as compared to native DSP-1. Overall this study expands the functional characterization of

seminal FnII proteins and establishes their role not just as sperm capacitation inducing agents but also as *shsps*.

Chapter 4

Probing the chemical unfolding of and phospholipid binding to the major protein of donkey seminal plasma, DSP-1 by fluorescence spectroscopy



Sk Alim, Somnath Das, Musti J. Swamy

J. Photochem. Photobiol. A: Chemistry (Under review)

4.1. Summary

Fibronectin type-II (FnII) proteins which constitute the major fraction in the seminal plasma of many mammals, bind to choline phospholipids on the spermatozoa and play a crucial role in "sperm capacitation", which enables the sperm to fertilize the egg. In the current study, we have investigated the heterogeneity of microenvironment around the tryptophan residues in the major FnII protein of donkey seminal plasma, DSP-1, in the native state and upon ligand binding employing fluorescence methods. Steady-state and time-resolved fluorescence studies on the quenching of the protein intrinsic fluorescence employing neutral and ionic quenchers revealed that the tryptophan environment in DSP-1 is less heterogeneous than other homologous seminal plasma FnII proteins, PDC-109 (bovine) and HSP-1/2 (equine). The quenching was decreased by ligand binding with choline containing lipids, Lyso-PC and DMPC providing stronger shielding of the Trp residues than the soluble ligand, phosphorylcholine, which is most likely due to segment(s) of the protein penetrating into the hydrophobic interior of the lipid membrane/micelles. Studies on the chaotrope-induced unfolding of DSP-1 revealed that disulfide bonds in the FnII domains of the protein prevent its complete unfolding, and that cooperativity of unfolding is also modulated by polydispersity of the protein.

4.2. Introduction

In mammalian fertilization the sperm-egg interaction is the initial step, which results in the formation of the zygote. The freshly ejaculated spermatozoa are incapable of fertilizing the egg and acquire the ability to do so only after undergoing a series of biochemical and ultra-structural changes during their residence in the female reproductive tract. These sequence of steps are collectively termed "capacitation" [Shivaji et al., 1990; Yanagimachi, 1994]. Despite its discovery many decades ago [Chang, 1951; Austin, 1952], the molecular mechanism of capacitation is not fully understood [Harrison, 1996; Visconti et al., 1998; Gervasi and Visconti, 2016; Zigo et al., 2020]. During ejaculation, spermatozoa are released along with seminal plasma, a fluid medium which transports the sperm cells to ovum and plays an important role in the "capacitation" as well as in the fertilization. Capacitation occurs during the transit through and residence of the ejaculated spermatozoa in the female reproductive tract, which results in an increase in the membrane fluidity, ultimately making the sperm competent to fertilize the egg. [Austin, 1952; Manjunath and Thérien, 2002; Selvaraj et al., 2006].

Proteins belonging to the "fibronectin type-II" (FnII) family are present in the seminal plasma of several mammals which have some common characteristic features in their structure like an *N*-terminal flanking region and two or four tandemly repeating fibronectin type-II (FnII) domains, and exhibit an ability to specifically bind choline phospholipids among the membrane lipids [Desnoyers and Manjunath, 1992; Ramakrishnan et al., 2001; Greube et al., 2004; Swamy, 2004; Plante et al., 2016]. The major seminal FnII proteins from bull (PDC-109) and horse (HSP-1/2) are the most thoroughly characterized proteins of this family. The most important characteristic of FnII proteins is that they exhibit high specificity towards choline phospholipids, namely phosphatidylcholine (PC) and sphingomyelin and negligible or no binding to other phospholipids such as phosphatidylethanolamine, phosphatidylgylcerol, phosphatidylserine etc [Desnoyers and Manjunath, 1992; Ramakrishnan et al., 2001; Thomas et al., 2003; Anbazhagan et al., 2011]. Single crystal X-ray diffraction studies on PDC-109/O-phosphorylcholine complex showed that each PDC-109 molecule has two PC binding sites and those two binding sites are on the same face of the protein [Wah et al., 2002].

Interaction of PDC-109 with choline phospholipids was characterized using different methods such as SPR, EPR, ITC, absorption spectroscopy and fluorescence spectroscopy [Ramakrishnan et al., 2001; Thomas et al., 2003; Anbazhagan et al., 2011; Swamy et al., 2002; Anbazhagan and Swamy, 2005; Anbazhagan et al., 2008; Greube et al., 2001]. In addition to their binding to choline phospholipids, PDC-109 and HSP-1/2 act as molecular chaperones by protecting different target proteins against heat stress and oxidative stress [Sankhala and Swamy, 2010; Sankhala et al., 2012; Kumar and Swamy, 2016b]. Various factors such as pH, membrane binding, presence of surfactants, and components of seminal plasma such as carnitine, spermine and spermidine, have also been reported to modulate the "chaperone-like activity" (CLA) of those proteins [Sankhala et al., 2011 & 2012; Kumar and Swamy, 2016c & 2017a; Singh et al., 2017; Kumar et al., 2018; Kumar and Swamy, 2017b].

Recently we have purified and characterized the major FnII protein of donkey seminal plasma, DSP-1 [Alim et al., 2022]. These studies established that DSP-1 is highly homologous to PDC-109 and HSP-1/2 and contains two FnII domains. Also, similar to these two proteins, DSP-1 exhibits high specificity towards choline phospholipids. In the present work, we have carried out biophysical studies on DSP-1 employing steady-state and time-resolved fluorescence spectroscopy monitoring the Trp fluorescence properties of the protein in the native state and in the presence of different soluble ligands and various phospholipids. The quenching studies using a "neutral quencher" (acrylamide) and two "ionic quenchers", Γ and Cs⁺ in the absence and presence of soluble ligands and choline phospholipids have been carried out, to investigate the Trp accessibility of DSP-1. Further, chemical unfolding of DSP-1 has been investigated using various denaturants, viz., urea, guanidinium hydrochloride (GdmCl) and guanidinium thiocyanate (GdmSCN), following intrinsic fluorescence properties of DSP-1. Finally, "red-edge excitation shift" (REES) studies, where the effect of changing excitation wavelength on the emission λ_{max} is monitored, were carried out to get informations around Trp residues of DSP-1.

4.3. Materials and Methods

4.3.1. Materials

Acrylamide, cesium chloride, dithiothreitol (DTT), guanidinium thiocyanate (GdmSCN), guanidinium chloride (GdmCl), potassium iodide, urea, heparin-Agarose type-I beads, lyso-phosphatidylcholine (Lyso-PC) and phosphorylcholine chloride calcium salt (PrC) were purchased from Sigma (St. Louis, MO, USA). Dimyristoylphosphatidylcholine (DMPC) and divalaroylphosphatidylcholine (DVPC) were purchased from Avanti Polar Lipids (Alabaster, AL, USA). *p*-Aminophenyl phosphorylcholine-Agarose column was obtained from Pierce Chemical Co. (Oakville, Ontario, Canada). All other chemicals were obtained from local suppliers and were of the highest purity available.

4.3.2. Purification of DSP-1

DSP-1 was purified from seminal plasma collected from healthy donkeys by affinity chromatography on heparin-agarose and *p*-aminophenylphosphorylcholine-agarose, followed by reverse phase HPLC (RP-HPLC) as described in Chapter 2 [see also Alim et al., 2022]. The purified protein was dialyzed extensively against 50 mM tris buffer, pH 7.4, containing 150 mM NaCl and 5 mM EDTA (TBS) and stored at 4 °C. All experiments were carried out in the same buffer unless stated otherwise.

4.3.3. Preparation of liposomes

Liposomes were prepared essentially as reported in a previous study [Kumar et al., 2016a]. Phospholipids bearing various head groups (1-2 mg) were taken in clean glass test tubes and dissolved in chloroform or chloroform-methanol (2:1, v/v) mixture. The solvent was removed under a gentle stream of nitrogen gas, followed by vacuum desiccation for 3-4 hours. The lipids were hydrated with TBS to yield the desired concentration. Samples were warmed to ~30 °C, vortexed and then subjected to 10 freeze-thaw cycles, followed by bath sonication for 30 minutes at room temperature to obtain unilamellar vesicles (ULVs).

4.3.4. Steady-state fluorescence spectroscopy

Steady state fluorescence measurements were performed using a JASCO FP-8500 fluorescence spectrometer at room temperature, with both excitation and emission band pass filters set at 2.5 nm. All experiments were carried out with samples taken in a 1×1×4.5 cm quartz fluorescence cuvette. DSP-1 (OD_{280 nm} <0.1) in TBS was excited at 280 nm for ligand binding studies and at 295 nm for quenching studies and emission spectra were recorded between 310 and 400 nm. Ligand binding experiments were performed by adding various lipids at specific concentrations mentioned to the protein sample and the sample was carefully mixed. Fluorescence spectra were recorded after 3 minutes of incubation. For intrinsic fluorescence quenching experiments, small aliquots of the quenchers from 5 M stock solutions in TBS were added to the proteins. The stock solution of KI contained 0.2 mM sodium thiosulfate in order to prevent the formation of triiodide. All the emission spectra were corrected for inner filter effect as described in [Lakowicz, 1999]. In red edge excitation shift (REES) experiments samples were excited at various wavelength between 280 to 305 nm and emission spectra were recorded from 320 nm to 400 nm.

Fluorescence experiments to investigate chaotrope-induced unfolding were performed by mixing a fixed quantity of DSP-1 to yield \sim 5 μ M final concentration in TBS with different quantities of the chaotropic denaturants from a stock solution (10 M urea, 8 M GdmCl, or 6 M GdmSCN) and incubated overnight. The samples were excited at 280 nm and emission spectra were recorded in the wavelength range of 310 to 400 nm. Unfolding experiments were also carried out in the presence of 10 mM DTT or 20 mM PrC.

4.3.5. Fluorescence lifetime measurements

Time resolved fluorescence measurements were performed using a HORIBA Jobin Yvon IBH (Glasgow, UK) time correlated single photon counting (TCSPC) spectrofluorometer. A pulsed LED (NanoLED-01) with an excitation source of 284 nm with a pulse duration of <1.0 ns was used. The instrument response function of the setup was measured to be 877.6 ps obtained using a Ludox solution (in water) as a scatterer. Samples of $OD_{295 \text{ nm}} < 0.07$ ($\leq 5.0 \text{ } \mu\text{M}$) in a quartz cell (10 mm path length) were excited and emission decay profile

was monitored at 340 nm for DSP-1, 348 nm for denatured protein, 334 nm for DSP-1 + PrC and DSP-1 + DVPC, 333 nm for DSP-1 + DMPC vesicles and 331 nm for DSP-1 in presence of Lyso-PC micelles, which correspond to wavelengths of the maximum fluorescence of the respective samples. All experiments were performed using emission slits with a band pass of 4-6 nm. To optimize the signal-to-noise ratio, 5,000 photon counts were collected in the peak channel. The sample and the scatterers were alternated for every 10% acquisition to ensure compensation for timing and shape drifts occurring during the period of collection. The fluorescence intensity decay curves obtained were deconvoluted with the instrument response function and analyzed using IBH DAS6 (version 2.2) decay analysis software (Horiba Jobin Yvon). Further information about the setup can be found elsewhere [Das and Samanta, 2022].

4.4. Results and Discussion

Fluorescence spectroscopy is one of the most useful techniques for the investigation of protein conformation, ligand binding, structural dynamics, and unfolding. The intrinsic fluorescence characteristics of the protein can be monitored under native conditions, upon binding with different ligands and in the presence of additives such as external quenchers and "chaotropic agents" to get information about the microenvironment of tryptophan residues, determine thermodynamic parameters of ligand binding and to unravel the mechanism of protein unfolding by chemical denaturants.

The 3-D structure of PDC-109 complexed with phosphorylcholine revealed that the binding involves cation- π interaction between the phosphate moiety of the ligand and the indole side chain of a core tryptophan residue in each FnII domain. Fluorescence quenching studies on PDC-109 and equine HSP-1/2 revealed that binding of PrC shields the Trp residues of both proteins from quenching in a rather similar manner [Anbazhagan et al., 2008; Kumar et al., 2016a]. However, differences were observed in the results obtained upon binding to phosphatidylcholine liposomes, which suggested that the two proteins penetrate into the interior of the lipid bilayer to different extents [Kumar et al., 2016a]. In view of the high homology of DSP-1 with PDC-109 and HSP-1, with all the 4 Trp residues in the former being conserved among all the three proteins [Chapter 2; see

also Alim et al., 2022], we carried out studies employing various fluorescence approaches to investigate the tryptophan environment in DSP-1 and the effect of binding of soluble ligands and phospholipids to it. In addition, we investigated the mechanism of unfolding of the protein by chaotropic agents and the results obtained from these studies are discussed below.

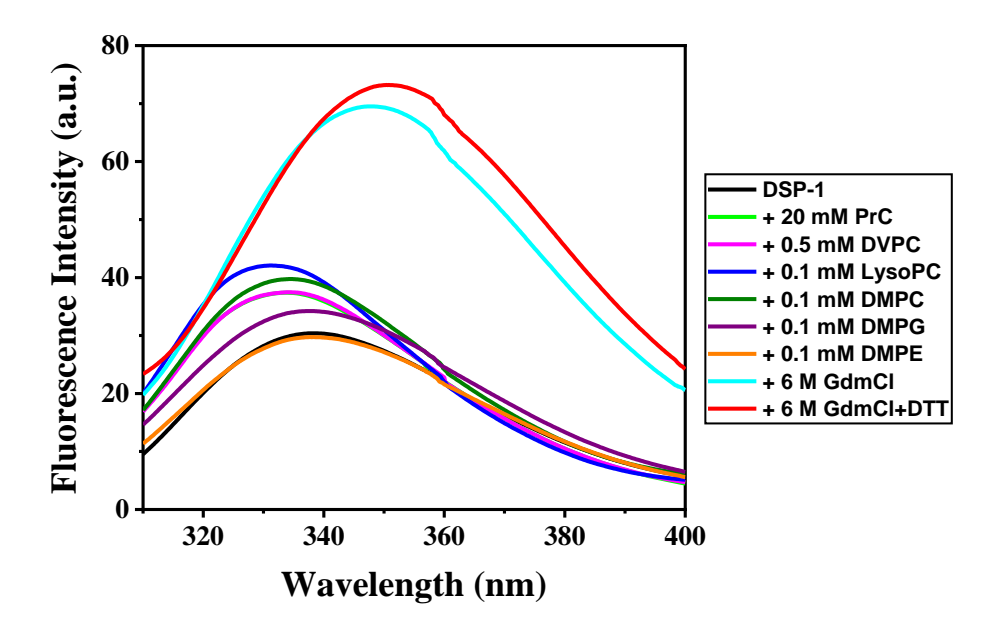


Fig. 4.1. Fluorescence emission spectra of DSP-1 obtained under different conditions. The samples investigated are indicated in the figure. Native DSP-1 (—), DSP-1+ 20 mM PrC (—), DSP-1 + 0.5 mM DVPC (—), DSP-1 + 0.1 mM Lyso-PC (—), DMPC (—), DSP-1 + 0.1 mM DMPG (—), DSP-1+ 0.1 mM DMPE (—), DSP-1+ 6 M GdmCl (—) and DSP-1+ 6 M GdmCl + 10 mM DTT (—).

4.4.1. Ligand binding to DSP-1: Effect on the fluorescence properties

Fluorescence emission spectra of native DSP-1 and in the presence of various soluble ligands, phospholipids and upon denaturation with 6 M GdmCl (in the presence and absence of 10 mM DTT), are shown in Fig. 4.1. The same spectra after normalization to the same intensity at the wavelength of maximum emission (λ_{max}) are shown in Fig. 4.2A. Changes in the fluorescence emission characteristics like, shift in emission λ_{max} and emission intensity are presented in Table 4.1. The emission λ_{max} of DSP-1 is observed at 340 nm, whereas in the presence of both 20 mM PrC and 0.5 mM DVPC it is shifted to 334 nm (blue shift). In the case of 0.1 mM Lyso-PC and DMPC the emission λ_{max} blue

shifted to 331 nm and 333 nm, respectively, whereas in the presence of 0.1 mM of DMPG and DMPE, only 2 nm blue shift was observed. Upon denaturation with 6 M GdmCl the emission maximum was red shifted to 348 nm, whereas denaturation with 6 M GdmCl in presence of 10 mM DTT the λ_{max} was further red shifted to 351 nm, indicating complete unfolding. The changes in the emission intensity are shown in Fig. 4.2B as a bar diagram.

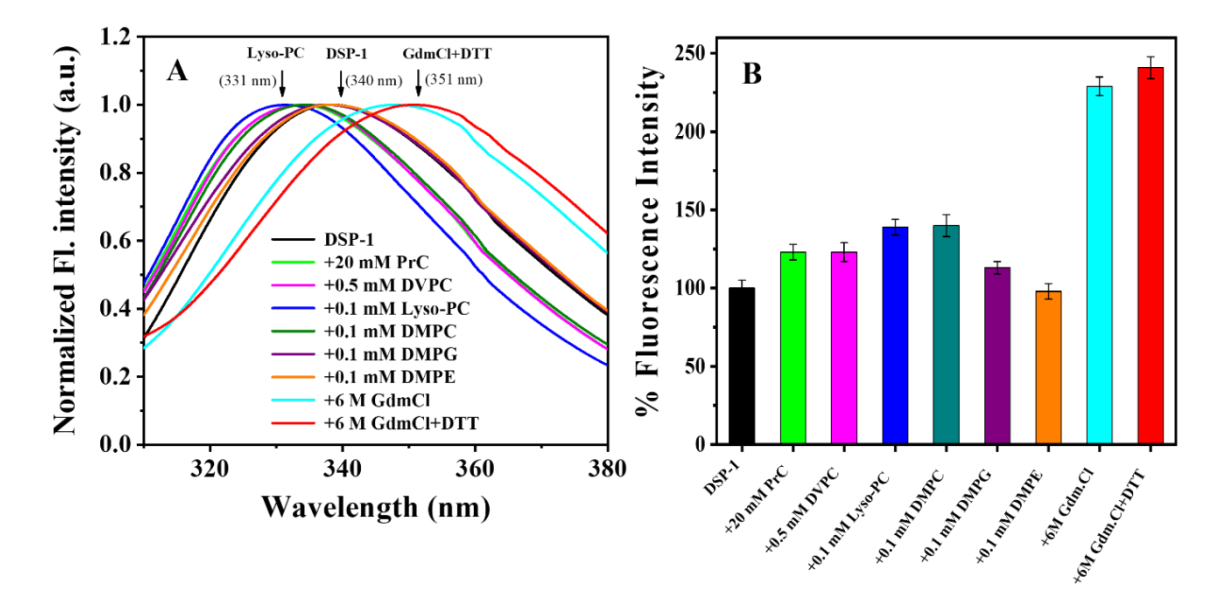


Fig. 4.2. (A) Fluorescence emission spectra of DSP-1 obtained under different conditions. The spectra were normalized to the same spectral intensity at the λ_{max} . The details of various samples investigated are indicated in the figure. (B) Bar diagram showing the relative intensities at the λ_{max} for various samples.

In addition to the changes seen in the emission λ_{max} , the fluorescence intensity of the protein is also affected in presence of different ligands/lipids and also upon treatment with "chaotropic agents". The emission intensity of DSP-1 increased by 23-39% in the presence of PrC and DVPC, lyso-PC and DMPC, all of which contain the choline moiety in the head group, whereas 13% increase was seen in the presence of DMPG, but DMPE induced a marginal decrease of 2% in the emission intensity. Large increase in the emission intensity was seen in the presence of chaotropic reagents urea (75%), GdmCl (129%) and GdmSCN (60%). Disulfide bond reduction by DTT increased the emission intensity of the GdmCl denatured protein to 141%.

Table 4.1. Fluorescence emission maxima (λ_{max}) and percentage change in emission intensity of DSP-1 in the presence of different ligands/conditions.

Samples/ Conditions	Fluorescence emission maximum (λ_{max}) (nm)	Change in the emission maximum compared to DSP-1 $(\Delta \lambda_{max})$ (nm)	Increase in the fluorescence intensity (%)
DSP-1	340.0	-	-
+ 20 mM PrC	334.0	6	23
+ 0.5 mM DVPC	334.0	6	23
+ 0.1 mM Lyso-PC	331.0	9	39
+ 0.1 mM DMPC	333.0	7	31
+ 0.1 mM DMPG	338.0	2	13
+ 0.1 mM DMPE	338.0	2	-2
+ 6 M GdmCl	348.0	8	129
+ 6 M GdmCl+ DTT	351.0	11	141
+ 8 M Urea	342.0	2	75
+ 5 M GdmSCN	344.0	4	60

The fluorescence spectra presented in Fig. 4.2A show that the emission λ_{max} of DSP-1 is blue shifted upon binding to PrC, DVPC, Lyso-PC and DMPC, but to different extent in each case. These observations are similar to those obtained with other seminal plasma proteins like PDC-109 and HSP-1/2 [Anbazhagan et al., 2008; Kumar et al., 2016a; Damai et al., 2009], and indicate that the microenvironment around Trp residues involved in lipid binding becomes more hydrophobic in nature upon binding of ligands containing the choline moiety. The highest blue shift is observed for Lyso-PC and DMPC indicating a role of the hydrocarbon chain in the interaction along with the choline moiety. This results are consist of our previous studies on the binding of PrC and Lyso-PC to DSP-1, which showed that binding of Lyso-PC to DSP-1 is an order of magnitude stronger than the binding of PrC [Chapter 2; Alim et al., 2022].

4.4.2. Fluorescence quenching studies of DSP-1

Fluorescence spectra corresponding to acrylamide quenching of native DSP-1 and in the presence of different ligands are shown in Fig. 4.3, whereas the spectra corresponding to the quenching studies using "ionic quenchers" I and Cs⁺ are shown in Figs. 4.4 and 4.5. The spectra obtained with native DSP-1 are shown in Fig. 4.3A, whereas those obtained with DSP-1 in the presence of PrC, DVPC, Lyso-PC and DMPC are shown in Fig. 4.3B, C, D and E, respectively.

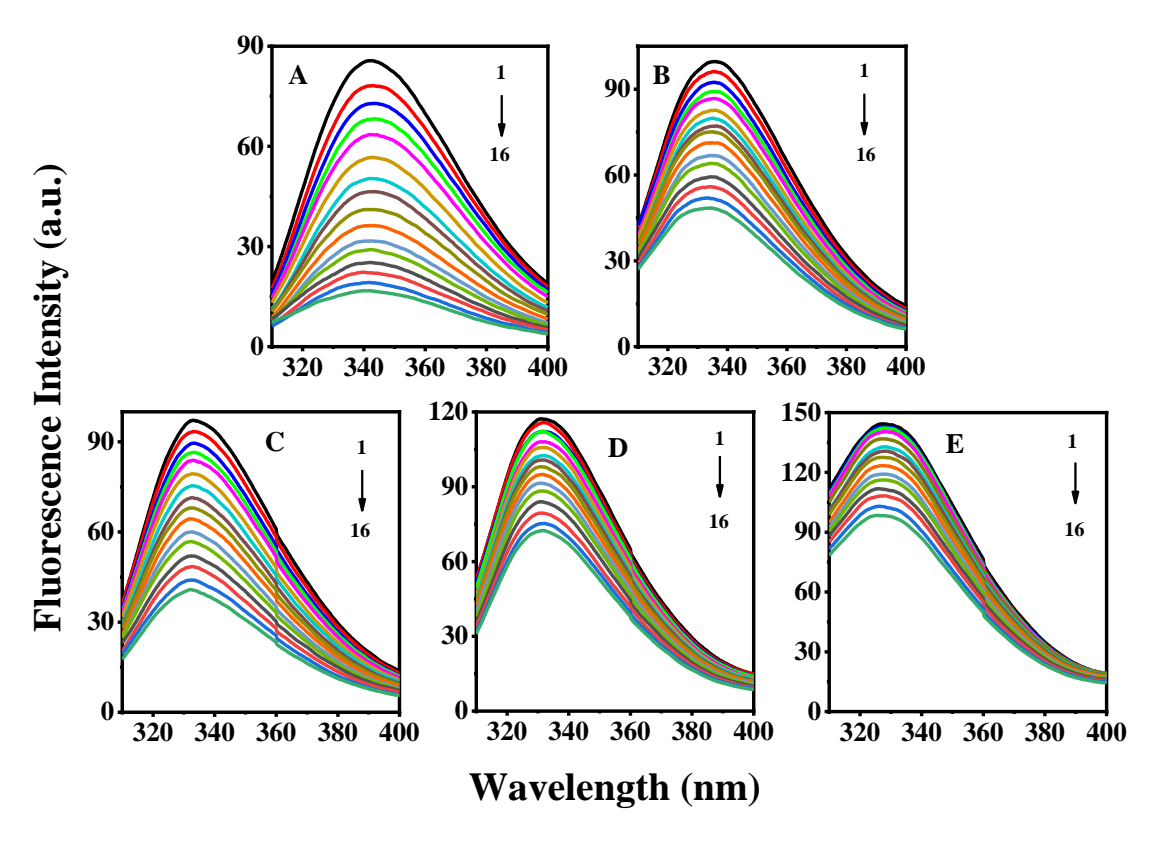


Fig. 4.3. Quenching of DSP-1 fluorescence by acrylamide in the native state and upon binding to different ligands. (A) Native DSP-1; (B) DSP-1 + 20 mM PrC; (C) DSP-1 + 0.5 mM DVPC; (D) DSP-1 + 0.1 mM Lyso-PC; (E) DSP-1 + 0.1 mM DMPC.

In each panel, the spectrum with the highest intensity corresponds to that obtained in the absence of the quencher and the lowest intensity spectrum corresponds to that recorded in the presence of 0.5 M quencher. All the other spectra were recorded in the presence of different concentrations of acrylamide and it was observed that in all cased increasing the quencher concentration led to a decrease of the fluorescence intensity (Fig.

4.3). While the fluorescence emission of native DSP-1 is quenched quite significantly by acrylamide (Fig. 4.3A), the quenching decreased to different extents in of different ligands mentioned above (Table 4.2).

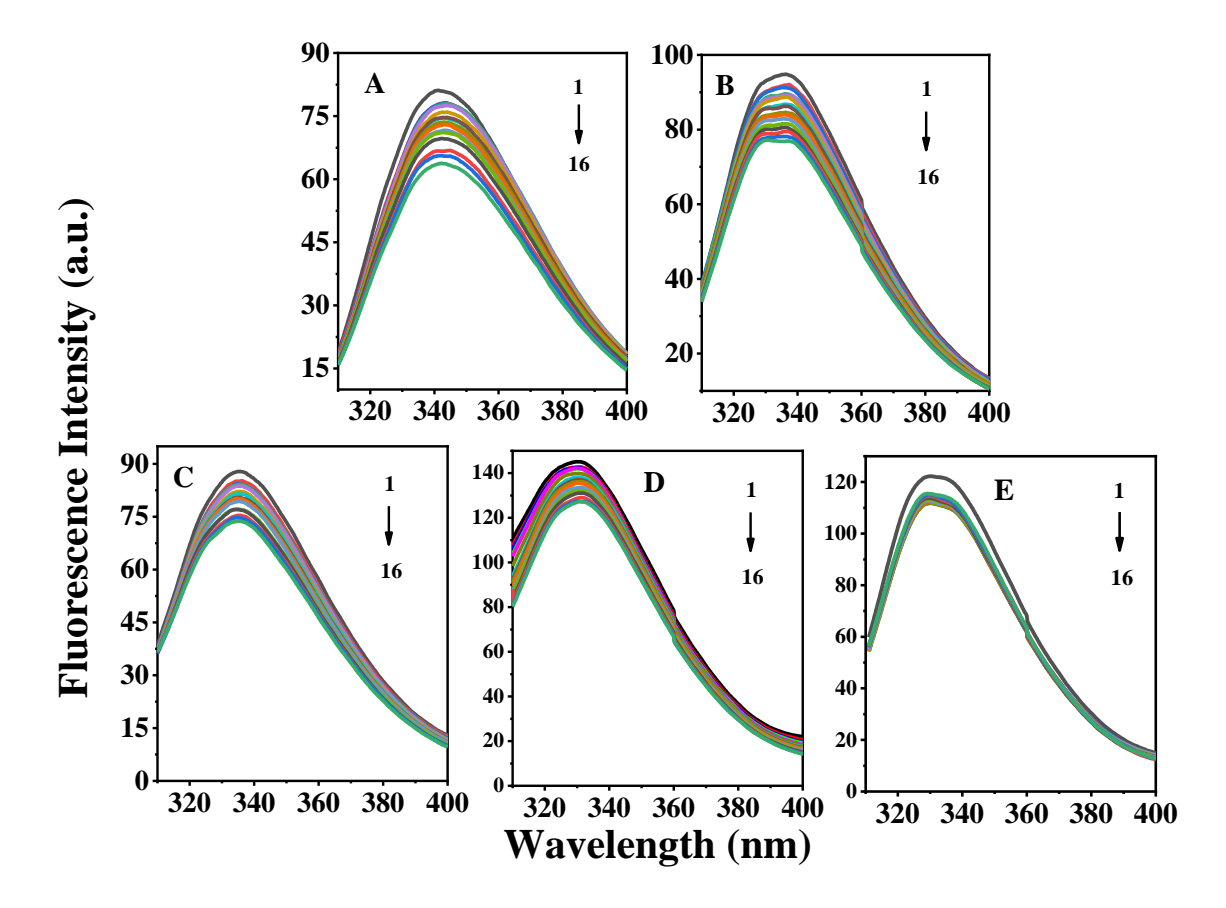


Fig. 4.4. Quenching of DSP-1 fluorescence by iodide in the native state and upon binding to different ligands. (A) Native DSP-1, (B) DSP-1 + 0.5 mM DVPC, (C) DSP-1 + 20 mM PrC, (D) DSP-1 + 0.1 mM Lyso-PC and (E) DSP-1 + 0.1 mM DMPC.

Among the three quenchers used in this study, acrylamide was the most efficient one and quenched the intrinsic fluorescence of DSP-1 by ~81% at 0.5 M concentration of the quencher, whereas the quenching observed with 0.5 M concentration of the ionic quenchers, Cs⁺ (25%) and Γ (21%) was considerably lower. Among the various ligands, DMPC provided the maximum shielding from quenching by acrylamide, with the quenching percentage decreasing to 58.2%, 51.4%, 38.1% and 31.8% in presence of 0.5 mM DVPC, 20 mM PrC, 0.1 mM Lyso-PC and 0.1 mM DMPC, respectively. In previous work with PDC-109 and HSP-1/2 the higher shielding observed in the presence of Lyso-

PC and DMPC was attributed to the penetration of one or more short segments of the protein into the DMPC and Lyso-PC. The present observations suggest that in the case of DSP-1 a similar explanation holds. Interestingly, for quenching by ionic quenchers maximum shielding was provided by Lyso-PC, with the extent of quenching decreasing from 25% to 2.1% for Cs⁺ and from 21.2% to 9.6% for Γ. The observations made from these studies are shown in Table 4.2.

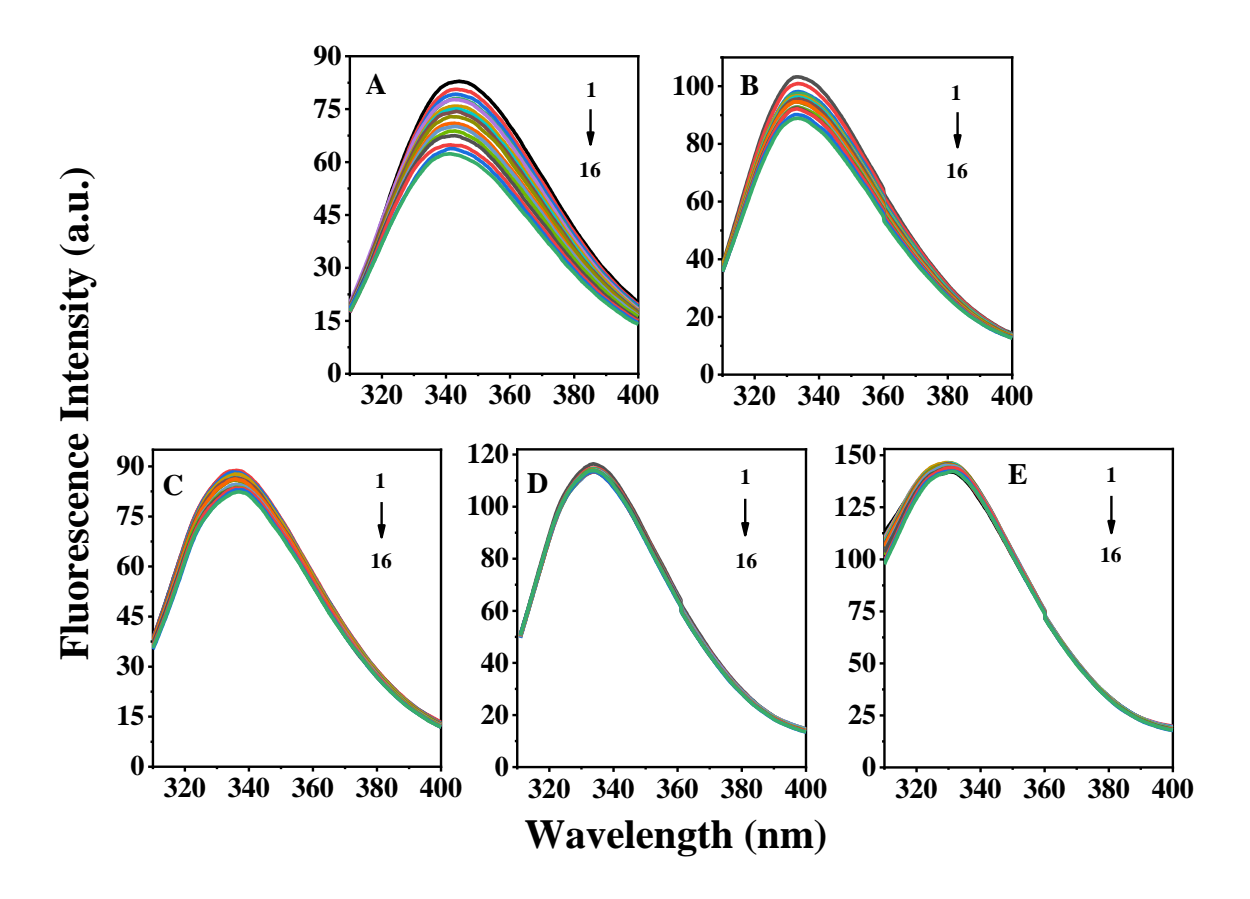


Fig. 4.5. Quenching of DSP-1 fluorescence by cesium ion in the native state and upon binding to different ligands. (A) Native DSP-1, (B) DSP-1 + 0.5 mM DVPC, (C) DSP-1 + 20 mM PrC, (D) DSP-1 + 0.1 mM Lyso-PC and (E) DSP-1 + 0.1 mM DMPC.

4.4.3. Stern-Volmer analysis of quenching data

Data obtained on the quenching of the intrinsic fluorescence of DSP-1 by different quenchers under different conditions were analyzed by the "Stern-Volmer equation" (Eq. (4.1)) and "modified Stern-Volmer equation" (Eq. (4.2)) given below [Lehrer, 1971]:

$$F_o/F_c = 1 + K_{SV}[Q]$$
 (4.1)

$$F_o/(F_o-F_c) = f_a^{-1} + 1/(K_a f_a [Q])$$
 (4.2)

where F_o and F_c are fluorescence intensities of the protein recorded in the absence and presence of the quencher, respectively. [Q] is the resultant quencher concentration, K_{SV} is the "Stern-Volmer constant", f_a is the fraction of total fluorophores accessible to the quencher and K_a is the corresponding "Stern-Volmer constant" for the accessible fraction of fluorophores.

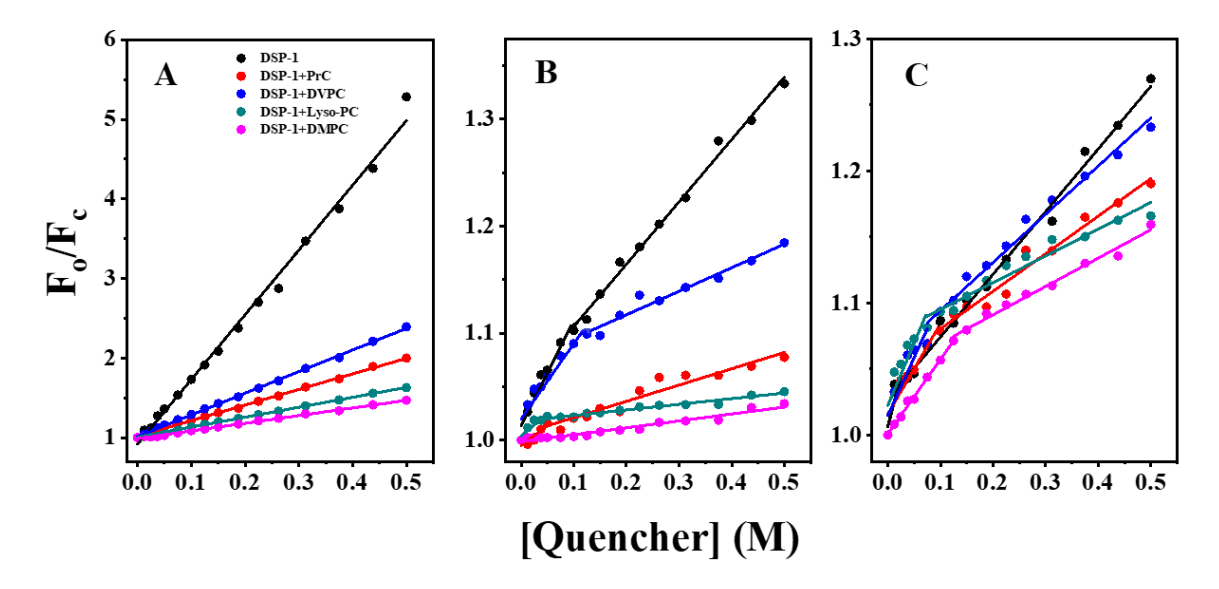


Fig. 4.6. Stern-Volmer plots for the quenching of the intrinsic fluorescence of DSP-1 by different quenchers in the absence and presence of various ligands. The quenchers used are: (A) acrylamide; (B) Cs⁺; (C) Γ. Color code for the different conditions: DSP-1 alone (•), and DSP-1 in presence of: 20 mM PrC (•); 0.5 mM DVPC (•); 0.1 mM Lyso-PC (•); 0.1 mM DMPC (•).

"Stern-Volmer plots" for the quenching of DSP-1 alone and in the presence of 20 mM PrC, 0.5 mM DVPC, 0.1 mM Lyso-PC and 0.1 mM DMPC vesicles with acrylamide, cesium ion and iodide ion are shown in Fig. 4.6A, B and C, respectively. Each panel shows the "Stern-Volmer plots" obtained with native DSP-1 and in the presence of the four different ligands. It was observed that the Stern-Volmer plot for acrylamide quenching of the native DSP-1 alone and as well as in presence the above ligands is linear. For quenching by Cs⁺, the "Stern-Volmer plots" for native DSP-1 and in the presence of all the ligands are biphasic, except for the sample containing DMPC, for which a linear plot was

obtained. However, for quenching by iodide ion all the "Stern-Volmer plots" are biphasic. The biphasic "Stern-Volmer plots" indicate that Trp residues become more heterogeneous and the Trp residues can be divided into two groups in which one group is more accessible to the "ionic quenchers" than the other group. From the slopes of the two linear components of the biphasic plots two "Stern-Volmer constants", K_{SV1} and K_{SV2} were determined and are listed in Table 4.2. In addition, f_a , the fraction of accessible fluorophores to the quenchers was estimated from the Y-intercepts of the modified Stern-Volmer plots (Fig. 4.7).

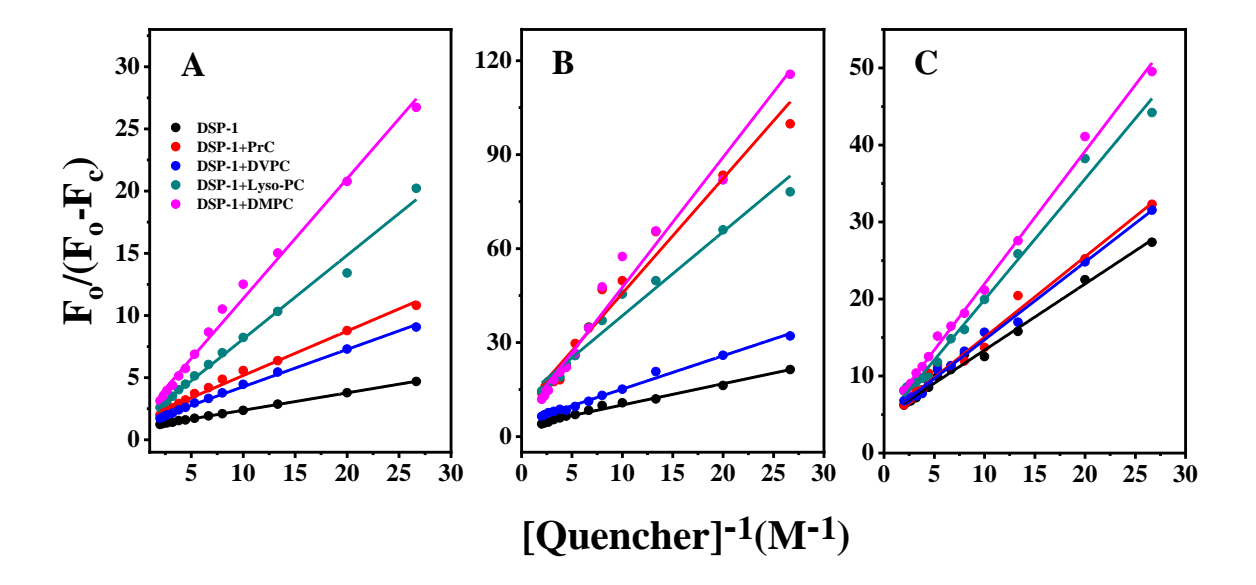


Fig. 4.7. Modified Stern-Volmer plots for the quenching of the intrinsic fluorescence of DSP-1 by different quenchers in the absence and in presence of various ligands. The quenchers used are: (A) acrylamide; (B) Cs⁺; (C) Γ. Color code for the different conditions: DSP-1 alone (•); DSP-1 in presence of: 20 mM PrC (•); 0.5 mM DVPC (•); 0.1 mM Lyso-PC (•); 0.1 mM DMPC (•).

Table 4.2. Quenching parameters obtained from steady-state fluorescence quenching of DSP-1. Percent quenching indicated corresponds to 0.5 M concentration of the quencher.

Quencher/ Sample	% Quenching	K _{SV1} (M ⁻¹)	K _{SV2} (M ⁻¹)	f _a (%)	K _a (M ⁻¹)		
Acrylamide							
Native DSP-1	81.1	8.13	-	93.2	6.97		
+20 mM PrC	51.4	1.96	-	62.8	4.46		
+0.5 mM DVPC	58.2	2.72	-	78.8	4.25		
+0.1 mM Lyso-PC	38.1	1.25	-	72.7	2.05		
+0.1 mM DMPC	31.8	0.92	-	58.3	1.78		
Cesium ion							
Native DSP-1	25.0	0.98	0.58	30.3	4.87		
+20 mM PrC	14.1	0.37	0.15	11.1	2.46		
+0.5 mM DVPC	23.3	0.71	0.22	22.3	2.46		
+0.1 mM Lyso-PC	2.1	0.41	0.05	8.5	4.31		
+0.1 mM DMPC	3.3	0.07	-	16.4	1.47		
Iodide							
Native DSP-1	21.2	1.56	0.48	22.1	5.45		
+20 mM PrC	16.7	0.68	0.29	21.8	4.09		
+0.5 mM DVPC	17.6	0.81	0.35	21.6	4.06		
+0.1 mM Lyso-PC	9.6	0.95	0.20	20.2	3.16		
+0.1 mM DMPC	13.7	0.57	0.22	21.0	2.77		

The observed results reveal that around 93% of the intrinsic fluorescence of DSP-1 is accessible to acrylamide, indicating that the Trp residues of the protein are almost completely accessible to this "neutral quencher", which can penetrate into the hydrophobic

interior of the protein matrix. In contrast, in the case of "ionic quenchers", Cs^+ and Γ , the accessible fraction of fluorophores was found to decrease significantly to 30.3% and 22.1%, respectively. Interestingly, while binding with the four choline-based ligands investigated, viz., PrC, DVPC, Lyso-PC and DMPC decreased the fraction of accessible Trp residues to different extents for quenching by the cationic Cs^+ , with f_a values ranging between 8.5% (DSP-1+Lyso-PC) and 30.3% (DSP-1 alone), the f_a values are nearly unaltered for quenching by iodide ion, and were found to be in the narrow range of 20.2 and 22.1 (Table 4.2).

4.4.4. Time-resolved fluorescence measurements

Time resolved fluorescence studies were carried out on DSP-1 alone under native conditions, in presence of various ligands and presence of DTT and complete denaturation by GdmCl. Fluorescence decay curves of native DSP-1, DMPC bound state and upon incubation with 10 mM DTT and 6 M GdmCl are given in Fig. 4.8, whereas those obtained in the presence of PrC, DVPC, Lyso-PC, 6 M GdmCl as well as in presence of different ligands and 0.5 M acrylamide are presented in Fig. 4.9. Since the decay curves could be fitted better with a triexponential function ($\chi^2 < 1.1$) than a biexponential function ($\chi^2 =$ 1.3-1.9), all decay profiles were fitted to a triexponential function. For example, for native DSP-1, triexponential fit was quite satisfactory and yielded three decay times τ_1 , τ_2 and τ_3 as 0.35, 1.12 and 4.04 ns, respectively with corresponding weighting factors of 0.73, 0.24 and 0.03, respectively ($\chi^2 = 1.00$). On the other hand, biexponential fitting was unsatisfactory ($\chi^2=1.65$). The results of time-resolved fluorescence studies, viz., decay times and corresponding weighting factors for measurements made at different conditions are listed in Table 4.3. It is interesting to note that while denaturation (without and upon reduction of disulfide bonds) led to an increase in the both shorter lifetimes (τ_1 and τ_2), the longer lifetime (τ_3) shows a modest increase in the absence of DTT but decreases when the disulfide bonds are broken. As expected, all three lifetimes decreased significantly in the presence of the neutral quencher acrylamide.

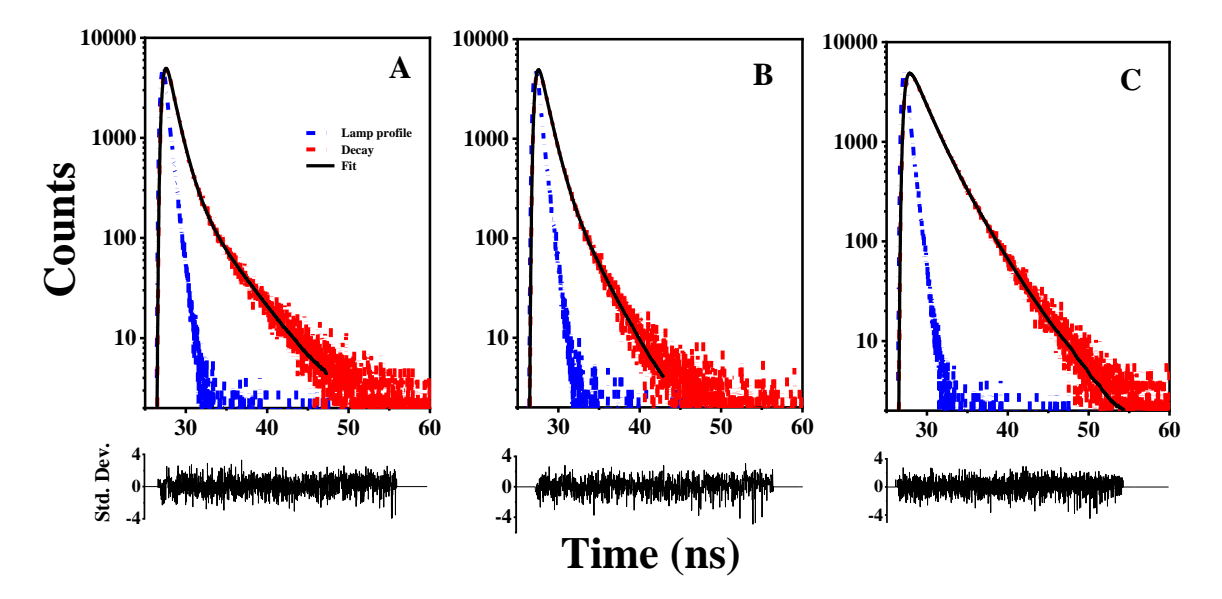


Fig. 4.8. Fluorescence decay profiles of DSP-1 under different conditions. (A) Native DSP-1; (B) in the presence of 0.1 mM DMPC; (C) upon denaturation with 6 M GdmCl + 10 mM DTT. Experimental data (•) and lamp profile (•) are shown. The solid black lines correspond to triexponential fits. Lower panels correspond to residuals.

The average lifetimes of native DSP-1 and under different conditions were calculated from lifetime values τ_i and the corresponding pre-exponential weighting factors, α_i using equations 4.3 and 4.4 given below [Lakowicz, 1999]:

$$\tau = \Sigma_i \; \alpha_i \tau_i / \Sigma_i \; \alpha_i \tag{4.3}$$

$$\langle \tau \rangle = \sum_{i} \alpha_{i} \tau_{i}^{2} / \sum_{i} \alpha_{i} \tau_{i} \tag{4.4}$$

where τ and $\langle \tau \rangle$ are the amplitude and intensity average fluorescence lifetimes, respectively. The values of τ and $\langle \tau \rangle$ for native DSP-1 were obtained as 0.646 and 1.364 ns. Values of τ and $\langle \tau \rangle$ corresponding to measurements obtained under various conditions are listed in Table 4.3.

In view of the high homology in the primary structure of DSP-1, PDC-109 and HSP-1/2 and due to the fact that of all 4 Trp residues of DSP-1 are conserved in the other two proteins, it is relevant to compare the results obtained from time-resolved fluorescence measurements with all the three proteins. A prominent difference observed from such a comparison is that while the decay profiles of PDC-109 could be fitted to a biexponential function under all conditions investigated, both DSP-1 and HSP-1/2 required a

triexponential function for satisfactory fits. This studies revealed that Trp residues in DSP-1 and HSP-1/2 have more heterogeneous microenvironment than those in PDC-109.

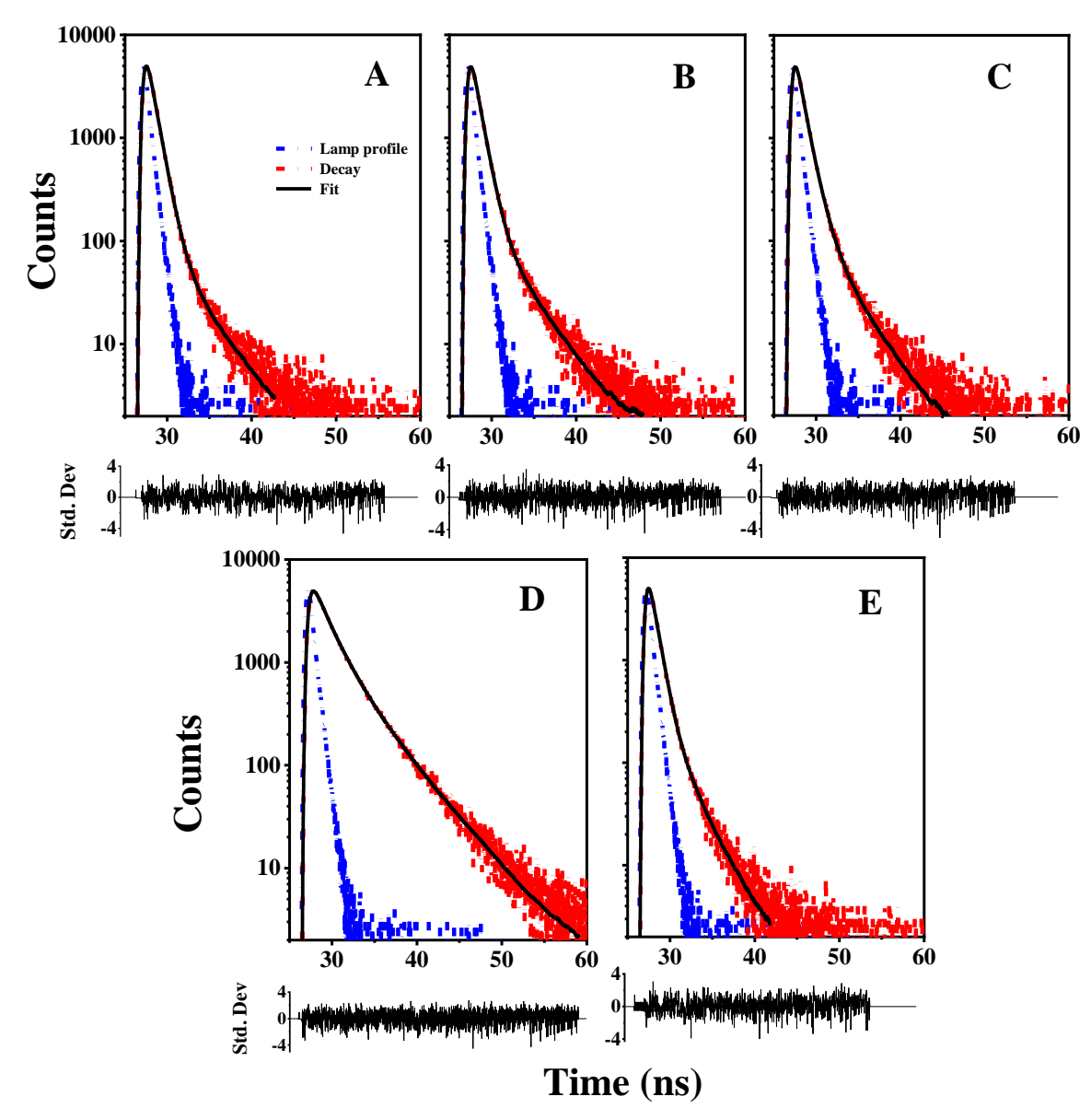


Fig. 4.9. Fluorescence decay profiles of DSP-1 obtained in different conditions. DSP-1+ 20 mM PrC (A); +0.5 mM DVPC (B); +0.1 mM Lyso-PC (C); upon denaturation with 6 M Gdm.Cl (D); +0.5 M acrylamde (E).

Table 4.3. Results of fluorescence decay measurements on DSP-1 under different conditions.

Sample	Type of fitting	α_1	α_2	α_3	τ_1	τ_2	τ_3	τ	<τ>	χ^2
DSP-1	triexp	0.73	0.24	0.03	0.35	1.12	4.04	0.646	1.364	1.00
+20 mM PrC	triexp	0.71	0.27	0.02	0.28	0.86	3.59	0.503	0.968	1.03
+DVPC	triexp	0.74	0.24	0.02	0.29	0.87	3.49	0.493	1.223	1.03
+Lyso-PC	triexp	0.80	0.18	0.02	0.32	1.02	3.34	0.506	0.973	1.05
+DMPC	triexp	0.69	0.26	0.05	0.26	0.96	2.76	0.567	1.177	1.12
+Gdm.Cl	triexp	0.45	0.40	0.15	0.51	1.90	4.35	1.640	2.683	1.02
+Gdm.Cl+DTT	triexp	0.30	0.49	0.21	0.51	1.80	3.49	1.770	2.386	1.01
+Acryl	triexp	0.70	0.28	0.02	0.18	0.67	2.41	0.362	0.731	1.03

4.4.5. Red-Edge Excitation Shift (REES) studies

We have plotted the fluorescence "emission maximum" of DSP-1 as a function of excitation wavelength of protein alone, in presence of various ligands and under denaturing conditions are presented in Fig. 4.10. For each sample, the excitation wavelength was varied from 280 to 305 nm. Upon shifting of excitation wavelength from 280 to 305 nm, the emission maximum of DSP-1 shifted from 340.5 nm to 343.5 nm, which corresponds to REES of 3 nm. For the sample denatured with 6 M GdmCl, the emission maximum shifted from 349 to 351.6 nm, which amounts to a REES of 2.6 nm. When DSP-1 was denatured and reduced with 10 mM DTT, the REES decreased to 1.7 nm, with the emission maximum shifting from 351.3 nm to 353 nm. Upon binding to Lyso-PC and DMPC vesicles the REES values were estimated as 0.4 and 1.3 nm respectively, whereas in the presence of PrC a REES of 0.3 nm was observed.

REES is generally observed when polar fluorophores are located in motionally restricted media where the dipolar relaxation time for the solvent molecules surrounding the fluorophore is similar to or more than the lifetime of its fluorescence decay [Demchenko, 2002; Mukherjee and Chattopadhyay, 1995]. In biological systems, very useful information can be obtained from REES studies on the relative rates of water

relaxation dynamics. Since hydration modulates a variety of important cellular events such as protein folding, protein-ligand interactions, lipid phase structure, structure and function of DNA etc [Meyer, 1992; Pal and Zewail, 2004; Cevc et al., 1986; Privalov and Crane-Robinson, 2017], the information deduced from REES measurements will be quite valuable.

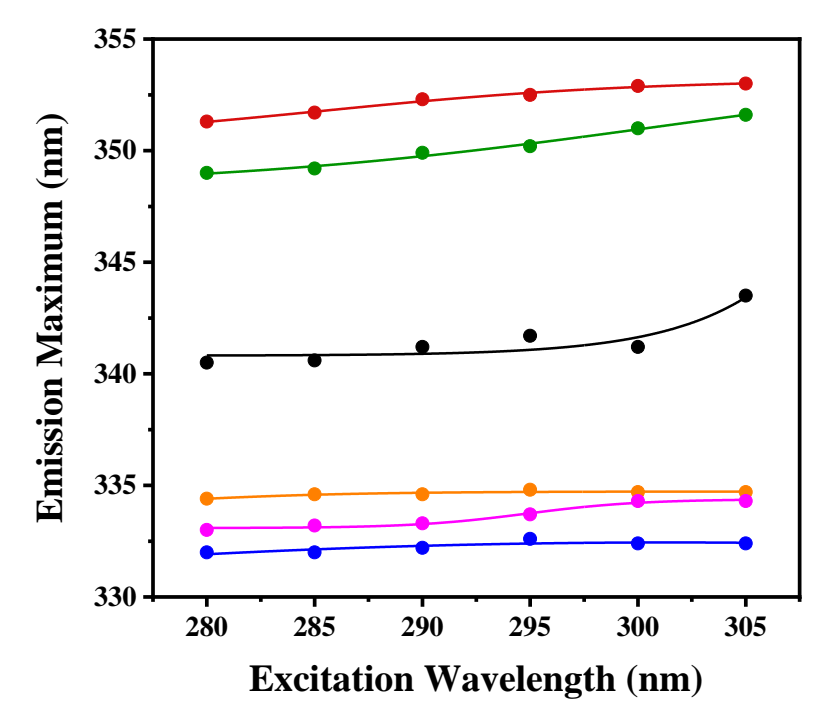


Fig. 4.10. Effect of changing excitation wavelength on the emission maximum of DSP-1 under various conditions. Native DSP-1 (●); DSP-1+ 20 mM PrC (●); DSP-1+ 0.1 mM DMPC (●); DSP-1+ 0.1 mM Lyso-PC (●); DSP-1 denatured with 6 M GdmCl (●); DSP-1 denatured with 6 M GdmCl + 10 mM DTT (●).

In view of the presence of 4 Trp residues in DSP-1, the REES value of 3 nm in this protein should be considered to be an average effect. Nevertheless, this suggests that at least some of the tryptophan side chains must be experiencing motional restriction. Binding of PrC and Lyso-PC lead to drastic decrease in the REES values to 0.4 nm, suggesting that the motional restriction is significantly reduced. This could possibly be due to the removal of water molecules from the ligand binding site of the FnII domains which makes the surroundings of the Trp residues involved in PrC binding less polar. This interpretation is consistent with the blue shift observed in the emission λ_{max} upon binding of these two ligands to DSP-1, as mentioned above (see Section 4.4.1). Interestingly,

however, the change in the REES upon binding to the diacyl phospholipid DMPC was marginal with DSP-1 bound to DMPC liposomes exhibiting a REES value of 1.3 nm, i.e. a decrease in REES by 1.7 nm. This could be attributed to a conformational change in the protein upon binding to the phosphatidylcholine bilayer membranes leading to a partial penetration of a protein segment into the bilayer, analogous to the observations made with bovine PDC-109 for which a REES value of 2.5 nm was observed in DMPC-bound state [Ramakrishnan et al., 2001; Anbazhagan et al., 2008].

Even upon treatment with the chaotropic denaturant GdmCl (6 M), DSP-1 shows a REES of 2.6 nm, which decreases to 1.7 nm upon reduction of disulfide bonds. This result shows that the Trp microenvironment of DSP-1 is retained such that even after denaturation due to which the reorientation of water molecules around them is restricted. Breaking the disulfide bonds by DTT treatment reduces the REES to 1.7 nm, clearly showing that the restriction imposed by the disulfide bonds is partially responsible for the higher REES observed in the GdmCl treated protein. These results are also similar to the observations made with PDC-109 and HSP-1/2 [Anbazhagan et al., 2008; Kumar et al., 2016a].

4.4.6. Chemical denaturation of DSP-1

Chemical unfolding of DSP-1 by "chaotropic agents" such as urea, GdmCl and GdmSCN was studied by monitoring changes observed in the intrinsic fluorescence properties of DSP-1 when the protein was treated with these chemical denaturants [Anbazhagan et al., 2008; Damai et al., 2009]. Plots representing the change in emission λ_{max} of DSP-1 as a function of denaturant concentration under different conditions are shown in Fig. 4.11. This figure indicates that with all three chaotropic agents in the absence of the reducing agent or the ligand (PrC) DSP-1 exhibits incomplete denaturation with low cooperativity, as the unfolding curves are non-sigmoidal with no clear midpoint. Also, the emission λ_{max} observed with the highest concentration of the chaotrope was 341, 344.8 and 346 nm, for urea, GdmCl and GdmSCN, respectively (Fig. 4.12), which are lower than ~350 nm expected for a fully denatured protein. Reduction of disulphide bonds makes chaotropic agents more effective in unfolding the FnII proteins as previously observed with PDC-109,

its domain B and HSP-1/2 [Anbazhagan et al., 2008; Kumar et al., 2016a; Damai et al., 2009].

Consistent with the above, chemical unfolding experiments on DSP-1 carried out in the presence of 10 mM DTT yielded sigmoidal unfolding curves with urea, GdmCl and GdmSCN with midpoints at 3.0 M, 1.7 M and 1.0 M, respectively, indicating cooperative unfolding of DSP-1. Additionally, the emission λ_{max} shifted to 346, 347.2 and 349.5 nm for urea, GdmCl and GdmSCN, respectively. These observations show that GdmSCN is the most efficient in unfolding DSP-1, followed by GdmCl, whereas urea is the least efficient. Unfolding experiments were also carried out with DSP-1 samples that were pre-incubated with 20 mM PrC to find out the ligand binding effect on the unfolding studies of DSP-1. Interestingly, unlike the native protein, DSP-1 that was pre-incubated with PrC gave cooperative unfolding curves with GdmSCN and GdmCl, whereas urea, being a weaker chaotrope, did not affect the unfolding of DSP-1. Further, binding of PrC seems to stabilize the protein against chemical denaturation, as seen from the shift in the midpoint of the sigmoidal curves towards higher concentrations of the denaturants.

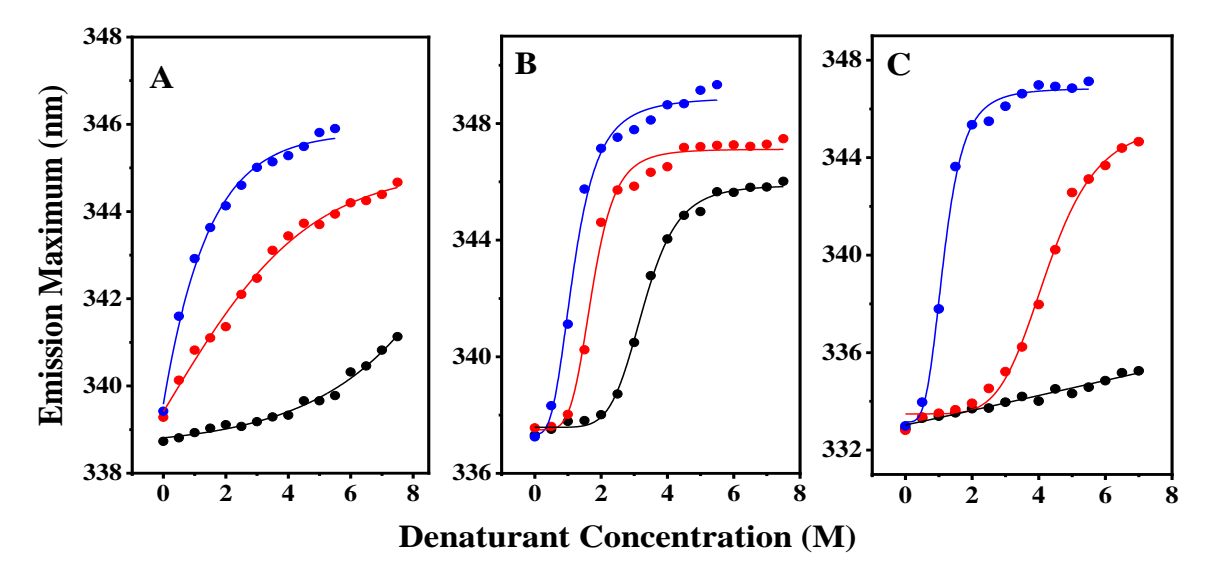


Fig.4.11. Chemical unfolding of DSP-1. Change in emission maximum of DSP-1 as a function of denaturant concentration under different conditions. (A) Native DSP-1; (B) DSP-1 reduced with 10 mM DTT; (C) DSP-1 in presence of 20 mM PrC. The denaturants used are: (●) urea; (●) GdmCl; (●) GdmSCN.

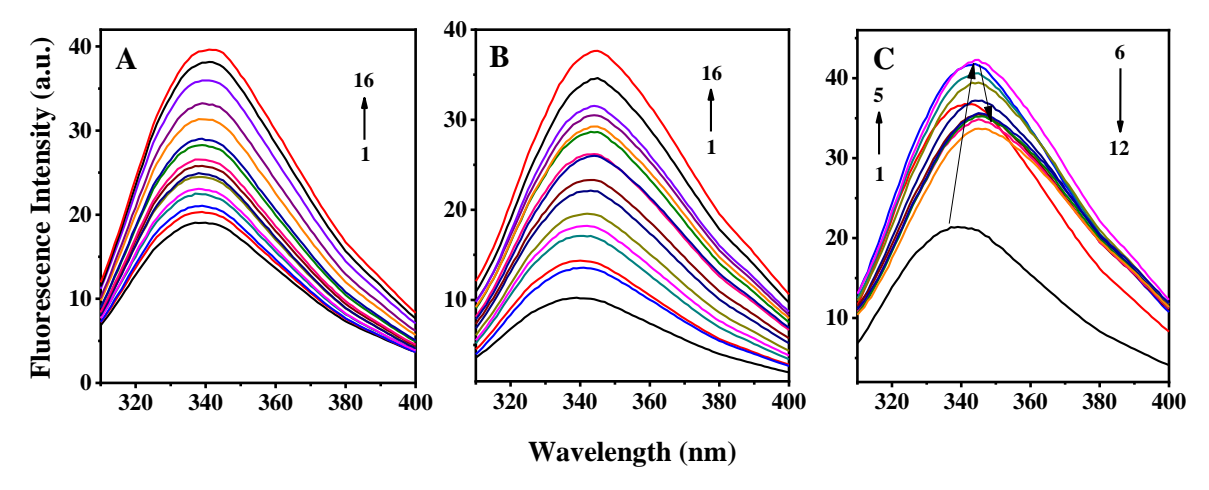


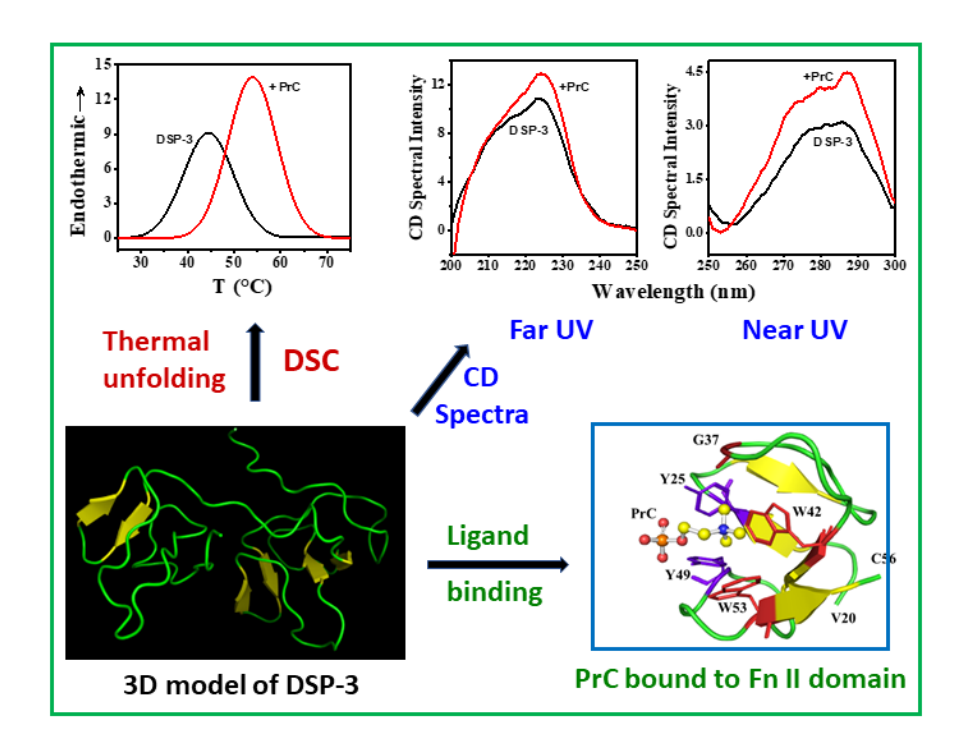
Fig. 4.12. Chemical unfolding of DSP-1. Fluorescence spectra corresponding to the chemical unfolding experiments of DSP-1 in the presence of various concentrations of (A) urea (10 M stock), (B) GdmCl (8 M stock) and (C) GdmSCN (6 M stock). Spectrum 1 is that of DSP-1 alone and spectra $2 \rightarrow 16/12$ correspond to those recorded in the presence of increasing concentration of the denaturants up to highest possible concentration.

4.5. Conclusion

In summary, in the present study intrinsic fluorescence characteristics of DSP-1 alone and upon binding with phosphorylcholine, Lyso-PC, and diacyl PC with short and long acyl chains have been investigated. Results of quenching the intrinsic fluorescence of DSP-1 by neutral and ionic quenchers indicate that the Trp residues of DSP-1 are shielded upon ligand binding of PrC and choline phospholipids. Lyso-PC and DMPC provided much higher protection than the other soluble ligands, which is consistent with short segments of the protein containing one or more tryptophan residues partially penetrating the DMPC membranes or Lyso-PC micelles. Time-resolved fluorescence studies indicate that the microenvironment of Trp residues in DSP-1 is more heterogeneous than in PDC-109, but comparable to that in HSP-1/2. Chemical unfolding studies employing chaotropic agents show that disulfide bonds in the FnII domains of DSP-1 prevent its complete unfolding, and that polydispersity and ligand binding also modulate the cooperativity of the unfolding transition.

Chapter 5

Primary structure determination and physicochemical characterization of DSP-3, a phosphatidylcholine binding glycoprotein of donkey seminal plasma



S. Alim, M. Laitaoja, S. S. Pawar, T. R. Talluri, J. Jänis, M. J. Swamy*

Int. J. Biol. Macromol. (under review)

5.1. Summary

Major proteins of the seminal plasma in a variety of mammals such as bovine PDC-109, equine HSP-1/2, and donkey DSP-1 contain fibronectin type-II (FnII) domains and are referred to as FnII family proteins. In this study, another FnII family protein, DSP-3, present in the donkey seminal plasma, has been purified and characterized. High-resolution mass spectrometric studies revealed that DSP-3 contains 106 amino acid residues and is heterogeneously glycosylated with multiple acetylations on the glycans. Interestingly, DSP-1 exhibits significantly higher homology to HSP-1 (104 identical residues) than to DSP-3 (72 identical residues). CD spectroscopic and differential scanning calorimetric (DSC) studies showed that DSP-3 unfolds at ~45°C and binding of phosphorylcholine (PrC) – the head group moiety of choline phospholipids – increases the thermal stability. Analysis of DSC data suggested that unlike PDC-109 and DSP-1 which exist as mixtures of polydisperse oligomers, DSP-3 most likely exists as a monomer. Ligand binding studies monitoring changes in protein intrinsic fluorescence indicated that DSP-3 binds lysophosphatidylcholine with ~80-fold higher affinity than PrC. Binding of DSP-3 to erythrocytes (a model cell membrane) – mediated by a specific interaction with choline phospholipids – leads to membrane perturbation, suggesting that its binding to sperm plasma membrane could be physiologically significant.

5.2. Introduction

In mammalian reproduction, seminal plasma carries spermatozoa from the male to the female uterus where it fuses with the egg, resulting in fertilization. In this process, proteins of the seminal plasma play important roles in various stages of fertilization, viz. sperm capacitation, sperm-zona pellucida interaction and establishment of oviductal reservoir [Austin, 1952; Chang, 1984; Shivaji et al., 1990; Visconti, 1998; Yanagimachi, 1994; Harrison, 1996; Gwathmey, 2003]. A major fraction of the proteins present in the mammalian seminal plasma have a common characteristic structure, which comprises of an N-terminal flanking region, followed by two or four tandemly repeating FnII domains, and show high binding specificity towards choline phospholipids [Esch et al., 1983; Seidah et al., 1987; Desnoyers and Manjunath, 1992; Ramakrishnan et al., 2001; Greube et al., 2004; Fan et al., 2006]. In the last few decades, detailed studies have been carried out with seminal FnII proteins, especially the major proteins from bovine seminal plasma, PDC-109 (a mixture of non-glycosylated BSP-1 and glycosylated BSP-2) and equine seminal plasma, HSP-1/2. Results on its interaction with phospholipids indicate that PDC-109 exhibits high specificity for choline phospholipids such as phosphatidylcholine (PC) and sphingomyelin, as compared to other phospholipids such as phosphatidylglycerol, phosphatidylserine, phosphatidylethanolamine etc [Desnoyers and Manjunath, 1992; Ramakrishnan et al., 2001]. Moreover, the presence of cholesterol in the membranes was found to potentiate the interaction of PDC-109 with different phospholipids, which could be due to PC mediated interaction of cholesterol with the protein or its direct interaction with a putative CRAC domain in the protein [Swamy et al., 2002; Müller et al., 2002; Scolari et al., 2010]. Studies on PDC-109/O-phosphorylcholine (PrC) complex using single crystal X-ray diffraction showed that each PDC-109 molecule has two PC binding sites and both the binding sites are on the same face of the protein [Romero et al., 1997; Wah et al., 2002]. The major protein from equine seminal plasma, HSP-1/2, which is homologous to PDC-109, is a non-separable mixture of HSP-1 and HSP-2, which have nearly identical primary structures but differ in the number of residues in the N-terminal segment and in the extent of glycosylation [Calvete et al.,1994, 1995a, 1995b].

Interaction of PDC-109 and HSP-1/2 with choline-containing ligands, model membranes and sperm plasma membranes has been greatly characterized due to the physiological significance of these proteins with choline phospholipids [Tannert et al., 2007; Anbazhagan and Swamy, 2005; Swamy, 2004]. Various studies indicate that both these proteins are able to intercalate into lipid membranes and perturb the lipid chain dynamics [Müller et al., 1998; Gasset et al., 2000; Ramakrishnan et al., 2001; Greube et al., 2004; Anbazhagan et al., 2011]. Studies on membrane perturbation by PDC-109, HSP-1/2 and DSP-1 using erythrocyte cells and model membranes indicate that these proteins are able to destabilize them [Damai et al., 2010; Kumar and Swamy, 2016c; Alim, 2022].

Recently, it has been observed that PDC-109 and HSP-1/2 exhibit chaperone-like activity (CLA) by protecting various target proteins against thermal, chemical and oxidative stress and hence can act as small heat shock proteins (*shsps*) [Sankhala and Swamy, 2010; Sankhala et al., 2012; Kumar and Swamy, 2016b & c]. It was also found that the CLA is modulated by a variety of factors including oligomeric status of the protein and its hydrophobicity, ligand/membrane binding, pH and ionic strength and that the membrane destabilizing activity and the CLA of these proteins are inversely correlated by a *pH switch* [Sankhala and Swamy, 2010; Sankhala et al., 2011, 2012; Kumar and Swamy, 2016b & c; Kumar et al., 2018]. Mutational studies indicated that conserved core tryptophan residues of FnII domains are essential for the membrane-perturbing and chaperone-like activities of PDC-109 [Singh et al., 2020]. In other studies it was found that glycosylation differentially modulates the membrane-perturbing and chaperone-like activities of PDC-109, with the glycosylated protein expressing higher CLA whereas the non-glycosylated protein exhibited higher membrane perturbing activity [Singh et al., 2019].

From the above, it can be seen that the major FnII proteins of mammalian seminal plasma play very important roles in priming spermatozoa for fertilization as well as in protecting other seminal plasma proteins from inactivation or misfolding as exemplified by PDC-109 and HSP-1/2. Therefore, it is important to purify the major FnII proteins from others mammal seminal plasma and characterize them in detail and to develop structure-function relationships among them. Such studies are likely to lead to a better understanding

of the functional roles played by them. With this motive, in the current study we have purified another major protein from donkey seminal plasma, DSP-3, and characterized it using biochemical and biophysical methods. Primary structure of DSP-3, derived from mass spectrometric studies showed that this protein belongs to the seminal FnII type family. Using various biophysical techniques, we studied the secondary and tertiary structures of this protein, investigated its thermal stability and characterized the binding of PrC and lyso-phosphatidylcholine (Lyso-PC) to it. The results indicate that DSP-3 exhibits membrane destabilizing activity against model cell membranes and that the thermal unfolding temperature of DSP-3 increases significantly upon PrC/Lyso-PC binding. These observations suggest that DSP-3 may play a physiologically important role in fertilization.

5.3. Materials and Methods

5.3.1. Materials

Phosphorylcholine chloride (calcium salt) and heparin-agarose type-I affinity matrix were obtained from Sigma (St. Louis, MO, USA). *p*-aminophenyl phosphorylcholine-agarose column was purchased from Pierce Chemicals (Oakville, Ontario, Canada). DMPC and Lyso-PC from egg yolk were obtained from Avanti Polar Lipids (Alabaster, AL, USA). All other chemicals were purchased from local suppliers.

5.3.2. Purification of DSP-3

In a previous report, we described the purification of DSP-1, DSP-2 and DSP-3, the three most abundant proteins in the donkey seminal plasma, using a modified procedure reported previously for HSP-1/2 with slight modifications [Sankhala, 2012]. The same procedure is employed here for the purification of DSP-3 and the details are given in section 2.3.1 (Chapter 2). The purified protein was dialyzed against 50 mM Tris/HCl buffer containing 150 mM NaCl and 5 mM EDTA, pH 7.4 (TBS). The homogeneity of the purified protein was assessed by SDS-PAGE [Laemmli, 1970].

5.3.3. Mass spectrometry

Mass spectrometric characterization of DSP-3 was done using a protocol similar to that employed earlier for DSP-1 reported in Chapter 2. Briefly, protein samples were buffer-

exchanged to 20 mM ammonium acetate (pH 7.4) using PD-10 desalting columns (Cytiva Europe GmbH). Additional purification was done using size-exclusion chromatography (SEC) on Äktapurifier 100 instrument (Amersham Pharmacia Biotech AB, Uppsala, Sweden), using a Superdex 75 column (GE Life Sciences, Sweden). Trypsin digestion was performed by incubating the protein samples overnight with sequencing grade trypsin (Sigma Aldrich, USA) at a 1:50 (w/w) trypsin-to-protein ratio using a mixture of acetonitrile (MeCN)/water (1:1, v/v) containing 10 mM dithiothreitol (DTT) as the solvent. The intact protein samples and their tryptic digests were analysed using an HPLC system (UltiMate 3000; Thermo Scientific) connected to a 12-tesla FT-ICR mass spectrometer (Bruker solariX XR; Bruker Daltonics, Germany). The proteins/peptides were eluted over an Acclaim Pepmap100 C18 (0.075 × 150 mm, 3 µm) column (Thermo Scientific) at a flow rate of 0.5 μ L/min, using a solvent gradient of 1 – 40% acetonitrile with 0.2% formic acid. Fragmentation of the peptides was performed with collision induced dissociation (CID) measurements using argon as the collision gas and previously optimized voltages. Direct infusion top-down MS/MS experiments were performed on a QTOF mass spectrometer (Bruker timsTOF; Bruker Daltonics, Germany). The instruments were controlled and the data were acquired using Chromeleon 6.80 (UltiMate 3000), ftmsControl 2.0 (solariX) or otofControl 5.1 (timsTOF) software, respectively. Postprocessing of the data and further analysis were accomplished by using Bruker DataAnalysis 5.1 software.

5.3.4. Circular dichroism spectroscopy

CD spectroscopic studies were performed using an AVIV model 420SF CD spectrometer (Lakewood, NJ, USA) fitted with a thermostatic cell holder and a thermostatic water bath at a scan speed 20 nm/min. Far- and near-UV CD spectra were recorded using a 0.2 cm path length quartz cell with samples containing DSP-3 at a concentration of 0.1 mg/mL and 0.5 mg/mL, respectively, in 10 mM Tris/HCl buffer, pH 7.4. Each spectrum recorded was the average of 6 consecutive scans from which buffer scans were subtracted. Spectra were also obtained in the presence of 20 mM PrC.

Thermal unfolding of DSP-3 was investigated by monitoring the CD spectral intensity of the protein (0.1 mg/mL) at 224 nm and the temperature was increased from 25

to 80° C at a scan speed 1° /min. The effect of binding of different ligands such as PrC, Lyso-PC or DMPC, on the thermal stability of DSP-3 was investigated by incubating 0.1 mg/mL protein for ~30 min with 50 mM PrC, or 100 μ M DMPC or 100 μ M Lyso-PC before the temperature scans were performed.

5.3.5. Computational modelling

The amino acid sequence of DSP-3 determined by mass spectrometry was submitted to I-TASSER server (http://zhanglab.dcmb.med.umich.edu/I-TASSER) to build a 3-dimensional structural model of the protein. The crystal structure of PDC-109 (pdb code: 1H8P) was used as a scaffold template. In addition, binding of PrC to the two FnII domains of DSP-3 was also studied *in silico* using the I-TASSER server.

5.3.6. Differential scanning calorimetry

DSC measurements were performed using a Nano DSC equipment from TA instruments (New Castle, Delaware, USA) described earlier [Mondal and Swamy, 2020]. DSP-3 (0.5 mg/mL) in TBS was heated from 20 to 80°C at a scan rate of 1°/min under a constant pressure of 3.0 atmosphere. Buffer baseline scan was subtracted from all the sample data to eliminate the contribution from buffer to the calorimetrically measured heat capacity of the protein. To investigate the effect of PrC binding, DSP-3 was pre-incubated with different concentrations of PrC and experiments were carried out under similar conditions and the thermograms were analyzed using the 'Gaussian Model' in the DSC data analysis software provided by the instrument manufacturer.

5.3.7. Steady-state fluorescence studies

Steady state fluorescence measurements were performed using a JASCO PF-8500 fluorescence spectrometer at room temperature, with both excitation and emission band pass filters set at 3 nm. All experiments were carried out with samples taken in a $1 \times 1 \times 4.5$ cm quartz fluorescence cuvette. DSP-3 (OD₂₈₀ < 0.1) in TBS was excited at 280 nm and emission spectra were recorded between 310 and 420 nm. Ligand binding experiments were performed by adding various lipids at mentioned concentrations to DSP-3 and the spectra were recorded after 3 minutes of incubation. Titrations to determine the association

constants for ligand binding were carried out by adding small aliquots of the ligand from a concentrated stock solution (100 μ M Lyso-PC, or 20 mM PrC) in TBS to DSP-3 (~0.1 OD) taken in the same buffer.

5.3.8. Erythrocyte lysis assay

Erythrocyte lysis assay to assess the ability of DSP-3 to perturb the cell membrane was performed as described earlier [Kumar and Swamy, 2016c; Damai et al., 2010]. In order to investigate the concentration dependence of the protein on cell lysis, 100 µL of 4% human erythrocytes in TBS were incubated with different concentrations of DSP-3 and the final volume was adjusted to 0.5 mL with TBS. After incubating the mixture for 1 hour at room temperature, the sample was centrifuged at 3000 rpm for 10 min. The supernatant was collected and optical density was checked at 415 nm – which corresponds to absorption of the haem moiety - using a Shimadzu UV-3600 UV-Vis NIR spectrophotometer. For investigating the kinetics of erythrocyte membrane disruption, 150 µg/mL of DSP-3 was incubated with 100 µL of 4% RBC suspension in different vials and incubated for different time intervals (5-300 min) before measuring absorbance as described above. To investigate the effect of ligands on erythrocyte membrane disruption, DSP-3 was pre-incubated with PrC, Lyso-PC and choline chloride (ChCl) prior to its addition to the erythrocyte suspension, and the experiment was carried out as described above. Results from a minimum of three independent experiments have been presented along with standard deviations.

5.3.9. Microscopy

Images of human erythrocytes in the presence of DSP-3 were obtained using a LSM 880 confocal microscope (Jena, Germany) as described earlier [Kumar and Swamy, 2016c] and in Chapter 2. To investigate the effect of DSP-3 on the cell morphology and membrane integrity, a 0.04% suspension of human erythrocytes in TBS was incubated with 150 μ g/ml of protein. After incubation, 50 μ l aliquots of the mixture were taken at 60 min and 90 min, spotted on a clean glass slip (Thermo Fisher) and shifted to the confocal stage for imaging. The erythrocyte suspension in TBS alone was used as the control. To investigate the effect

of ligand binding, DSP-3 was pre-incubated with 20 mM PrC, or 20 µM Lyso-PC or 20 mM ChCl for 10 min before its addition to the erythrocyte suspension.

5.3.10. Preparation of liposomes

Lipids taken in a glass tube were dissolved in either dichloromethane or dichloromethane-methanol mixture (2:1, v/v) and were dried under a gentle stream of nitrogen gas and then by vacuum desiccation for 3-4 h. The lipid film was hydrated with buffer to give the desired lipid stock concentration. Small unilamellar vesicles (SUVs) were prepared by homogenizing the lipid mixture with 3-4 freeze-thaw cycles followed by sonication of the lipid suspension for 30 min in a bath sonicator above their transition temperature.

5.4. Results and Discussion

5.4.1. Purification of DSP-3

DSP-3 was purified from donkey seminal plasma by a procedure similar to that used for the purification of HSP-1/2 and DSP-1, using affinity chromatography on heparin-agarose and *p*-aminophenyl phosphorylcholine-agarose (PPC-agarose), followed by RP-HPLC (see Fig. 2.2, Chapter 2) [Sankhala et al., 2012; Alim et al., 2022]. The purified protein was dialyzed against TBS and finally stored at 4 °C. All experiments were performed in TBS unless specified otherwise.

5.4.2. Primary structure of DSP-3

LC-MS measurements showed that DSP-3 is expressed as a heterogeneous mixture of different proteoforms (Fig. 5.1 & Fig. 5.2), which is similar to that observed with DSP-1 (see Chapter 2). The observed intact masses for DSP-3 were around 14.3 to 16.3 kDa, which are somewhat smaller than for DSP-1 (see Chapter 2). In addition, similar peak patterns originating from multiple acetylations (+42 Da) were observed for each detected DSP-3 glycoform. Trypsin digestion and the subsequent LC-MS/MS analysis were only able to partially determine the sequence of the DSP-3 with peptides best matching to those predicted for *Equus asinus* mRNA sequence of 014723760.1, which was used as a model template when assigning the peptides.

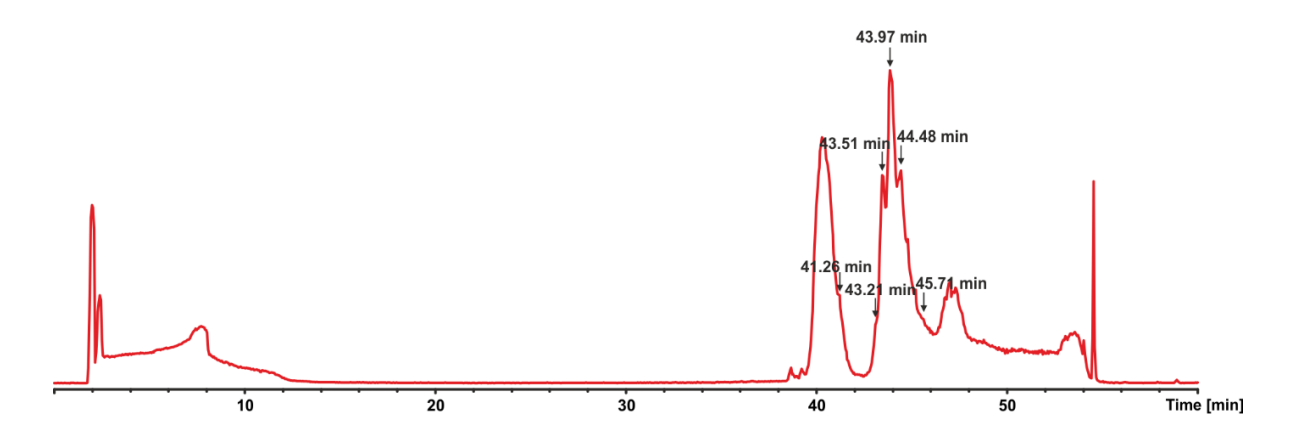


Fig. 5.1. Total ion chromatogram of the LC ESI FT-ICR MS/MS analysis of intact DSP-3. Different glycoforms of DSP-3 have been indicated with arrows with retention times indicated. The other chromatographic peaks are small molecule impurities.

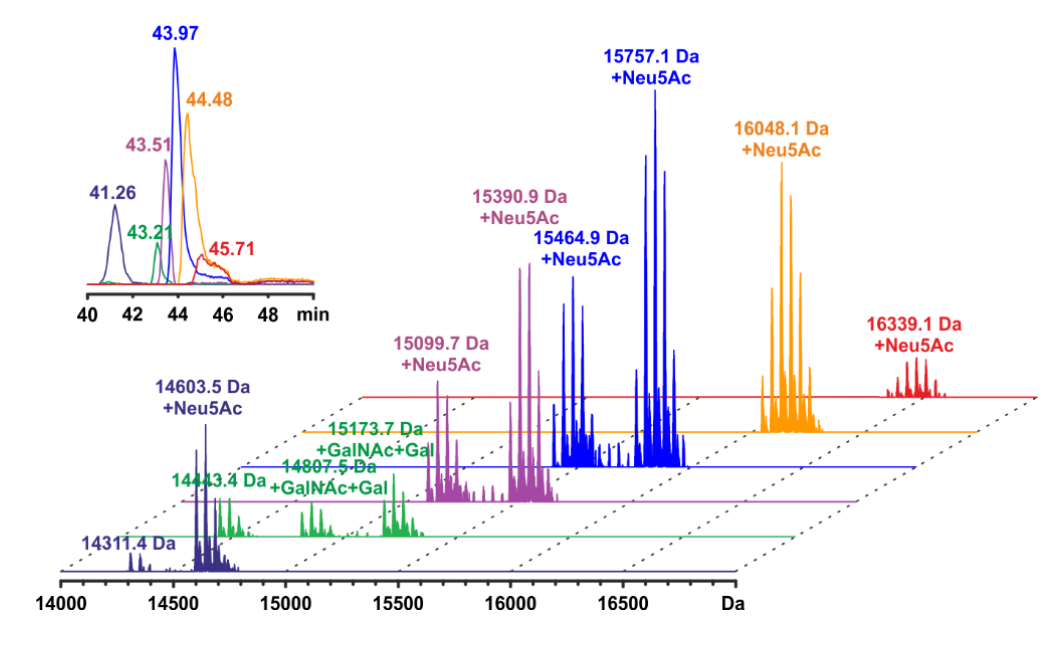


Fig. 5.2. LC ESI FT-ICR mass analysis of DSP-3. Deconvoluted mass spectra of different glycoforms of DSP-3, eluting at around 41.26, 43.21, 43.51, 43.97, 44.48, and 45.71 min are shown. The inset shows the corresponding extracted ion chromatograms (for the total ion chromatogram, see Fig. 5.2). Color code used in the mass spectra connects the glycoforms to the peaks in the inset. The peak patterns for each glycoform are due to multiple protein acetylations (+42 Da). The most abundant isotopic masses are given for the non-acetylated proteoforms of the each detected glycoform.

Table 5.1. Tryptic peptides identified for DSP-3 by LC–ESI FT-ICR MS/MS.

m/z	z	m _{exp, mono} (Da)	m _{calc, mono} (Da)	Error (ppm)	Sequence	MS/MS fragments
531.2338	2	1060.4531	1060.4536	-0.47	YCVAEDYAK	496.238 (y ₄), 625.279 (y ₅), 696.315 (y ₆), 795.382 (y ₇), 898.389 (y ₈)
419.7029	4	1674.7823	1674.7824	-0.06	SGKWRYCVAEDYAK	441.208 (b ₇ ⁺⁺), 490.742 (b ₈ ⁺⁺), 526.261 (b ₉ ⁺⁺), 590.782 (b ₁₀ ⁺⁺), 648.296 (b ₁₁ ⁺⁺)
468.5520	3	1402.6340	1402.6340	0.00	WRYCVAEDYAK	218.150 (y ₂), 381.213 (y ₃), 496.240 (y4), 625.282 (y ₅), 696.319 (y ₆), 795.387 (y ₇)
658.3040	3	1971.8902	1971.8898	0.20	TGSFHRWCSLTENYSGK	568.273 (y ₅), 697.315 (y ₆), 798.362 (y ₇), 911.447 (y ₈), 998.478 (y ₉)
567.5884	3	1699.7433	1699.7413	1.18	TGSFHRWCSLTENY	588.275 (b ₁₀ ⁺⁺), 638.799 (b ₁₁ ⁺⁺), 703.320 (b ₁₂ ⁺⁺), 760.342 (b ₁₃ ⁺⁺), 872.418 (b ₇), 975.426 (b ₈), 1062.457 (b ₉), 1175.542 (b ₁₀)
592.9387	3	1775.7944	1775.7937	0.39	TDNQCVFPFDYSGKR	485.243 (y ₈ ⁺⁺), 558.777 (y ₉ ⁺⁺), 608.311 (y ₁₀ ⁺⁺), 659.816 (y ₁₁ ⁺⁺), 723.846 (y ₁₂ ⁺⁺), 780.866 (y ₁₃ ⁺⁺)
540.5000	4	2157.9708	2157.9691	0.79	TGSFHRWCSLTENYSGK W	333.192 (y ₂), 390.213 (y ₃), 477.245 (y4), 640.309 (y ₅), 703.319 (b ₁₂ ⁺⁺), 760.340 (b ₁₃ ⁺⁺), 841.872 (b ₁₄ ⁺⁺)
782.3863	2	1562.7580	1562.7551	1.86	LIPWCSVTPNYDR	664.304 (y ₅), 765.352 (y ₆), 864.421 (y ₇), 951.451 (y ₈), 1054.462 (y ₉)
684.0747	4	2732.2698	2732.2679	0.70	SGKWRYCVAEDYAKCFF PFVYR (ox)	437.250 (y ₃), 584.319 (y ₄), 681.371 (y ₅)
706.9887	3	2117.9444	2117.9390	2.55	YCVAEDYAKCFFPFVYR (ox)	341.190 (y ₅ ⁺⁺), 414.724 (y ₆ ⁺⁺), 584.319 (y ₄), 681.371 (y ₅), 828.439 (y ₆)
816.3642	5	4076.7847	4076.7743	2.55	GRTYHTCTTDGSFFLIPW CSVTPNYDRDGGWKYC M	714.303 (b ₁₃ ⁺⁺), 787.838 (b ₁₄ ⁺⁺), 844.380 (b ₁₅ ⁺⁺), 900.921 (b ₁₆ ⁺⁺)
616.5421	4	2462.1391	2462.1340	2.07	WRYCVAEDYAKCFFPFV YR	338.182 (y ₂), 437.251 (y ₃), 584.319 (y ₄), 681.371 (y ₅), 828.439 (y ₆), 975.508 (y ₇), 1078.518 (y ₈)
970.9204	4	3879.6526	3879.6466	1.55	TYHTCTTDGSFFLIPWCS VTPNYDRDGGWKYCM (Mox)	902.892 (y ₁₅ ⁺⁺), 946.909 (y ₁₆ ⁺⁺), 998.414 (y ₁₇ ⁺⁺), 1091.453 (y ₁₈ ⁺⁺), 1139.980 (y ₁₉ ⁺⁺), 1196.522 (y ₂₀ ⁺⁺), 1253.064 (y ₂₁ ⁺⁺), 1326.597 (y ₂₂ ⁺⁺)
731.8311	4	2923.2954	2923.2946	0.27	TYHTCTTDGSFFLIPWCS VTPNYDR	567.252 (y ₄), 664.305 (y ₅), 765.355 (y ₆), 864.421 (y ₇), 951.453 (y ₈), 1054.461 (y ₉), 1337.592 (y ₁₁)
707.6602	3	2119.9587	2119.9536	2.41	YCVAEDYAKCFFPFVYR	437.251 (y ₃), 584.319 (y ₄), 681.371 (y ₅), 778.373 (y ₁₂ ⁺⁺), 828.440 (y ₆), 842.894 (y ₁₃ ⁺⁺), 878.915 (y ₁₄ ⁺⁺), 927.947 (y ₁₅ ⁺⁺), 979.451 (y ₁₆ ⁺⁺)
731.3265	4	2921.2768	2921.2800	-1.10	TYHTCTTDGSFFLIPWCS VTPNYDR	453.209 (y ₃), 567.252 (y ₄), 664.304 (y ₅), 765.352 (y ₆)
966.4194	4	3861.6485	3861.6371	2.96	TYHTCTTDGSFFLIPWCS VTPNYDRDGGWKYCM (ox)	1138.472 (y ₁₉ ⁺⁺), 1195.010 (y ₂₀ ⁺⁺), 1251.555 (y ₂₁ ⁺⁺), 1325.090 (y ₂₂ ⁺⁺)
966.9243	4	3863.6679	3863.6517	4.19	TYHTCTTDGSFFLIPWCS VTPNYDRDGGWKYCM	902.892 (y ₁₅ ⁺⁺), 946.909 (y ₁₆ ⁺⁺), 998.414 (y ₁₇ ⁺⁺), 1091.453 (y ₁₈ ⁺⁺), 1139.980 (y ₁₉ ⁺⁺), 1196.522 (y ₂₀ ⁺⁺), 1253.064 (y ₂₁ ⁺⁺), 1326.597 (y ₂₂ ⁺⁺)

Peptides marked with (ox) were found to contain a disulfide bridge and (Mox) refers to the oxidized methionine.



Fig.5.3. The complete amino acid sequence of DSP-3 with the identified tryptic peptides and their monoisotopic masses indicated. The disulfide linkages shown are based on the similarity with other homologous mammalian seminal FnII proteins, PDC-109 and HSP-1/2. The *N*-terminal extension part is most likely missing due to the observed protein modifications (glycosylations/acetylations) and was characterized by additional top-down MS experiments.

Thereby, the primary structure of DSP-3 was found to be similar to the other seminal plasma proteins (Fig. 5.3). As in the case of DSP-1, the *N*-terminal part of the sequence was determined by top-down MS/MS experiments [Chapter 2; Alim et al., 2022]. The disulfides were not reduced to limit the fragmentation to the *N*-terminal part only. The intact protein ions at $m/z \sim 1500$ were isolated and fragmented at a collision energy of 60 eV. This resulted mainly in small fragments corresponding to the released glycans (Fig. 5.4) as well as large protein ions (\sim 12 kDa) with a complete removal of glycans. The glycan fragmentation showed small *N*-acetylgalactosamine (GalNAc) and galactose (Gal) containing fragments, further modified by sialic acid (Neu5Ac) or acetylated sialic acid (Neu5, xAc₂) residues. These structures indicate that there are multiple *O*-glycosylation

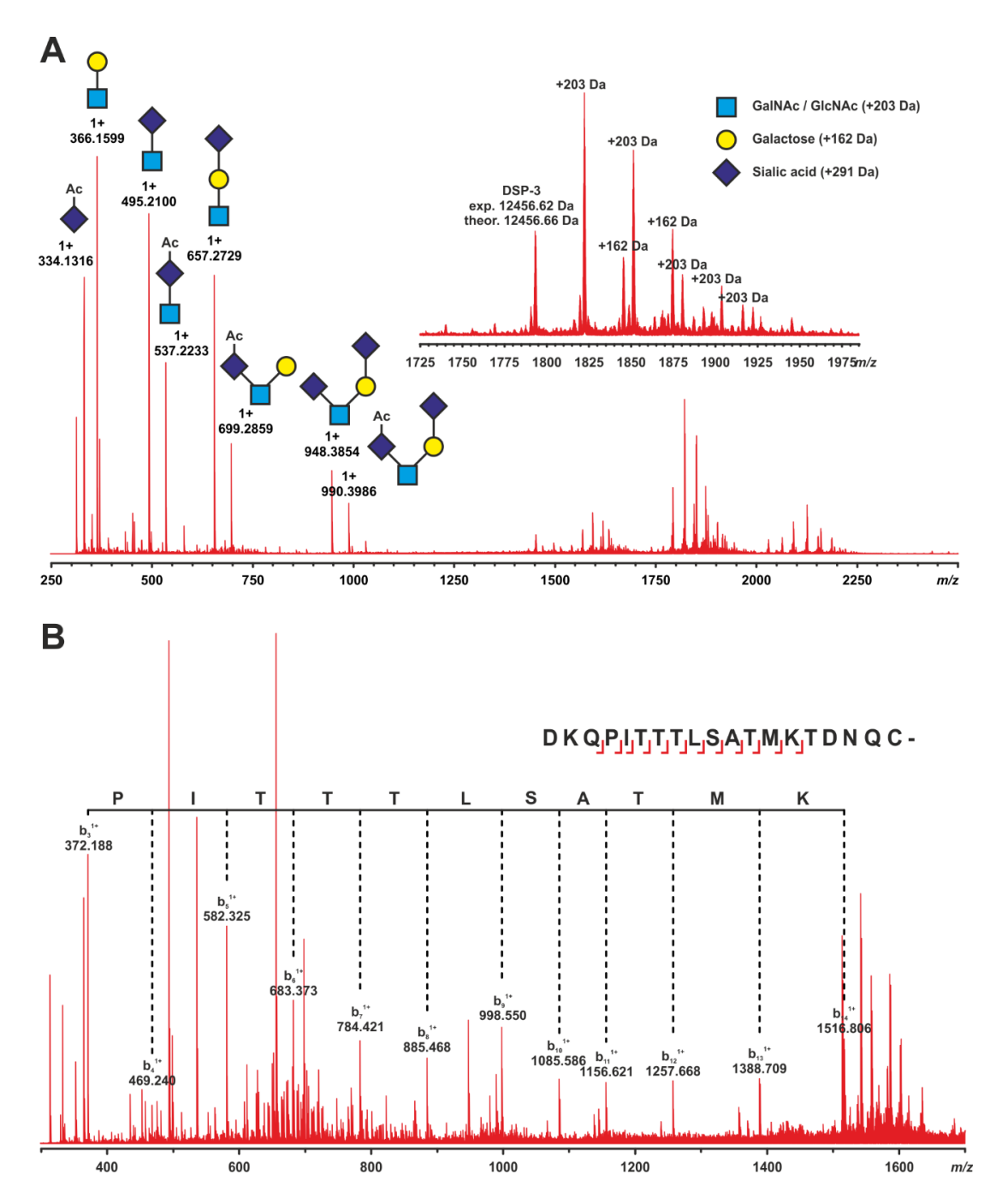


Fig. 5.4. Top-down MS/MS spectra of DSP-3. (**A**) Low energy CID shows mainly the fragmentation of the O-glycan structures. Additionally, high mass ions are observed in m/z ~1850, resulting from the sequential removal of glycosylations, up to the bare amino acid chain of DSP-3. (Ac=acetylation) (**B**) The protein signal m/z ~1550 was isolated for high-energy CID which shows the fragmentation of the N-terminal part of the protein, showing the N-terminal residues of DSP-3.

sites in the *N*-terminal part of DSP-3, similar to some of the other seminal plasma proteins [Calvete et al., 1995a, 1996; Jois and Manjunath, 2010]. For the large protein ions observed, the smallest fragment had a mass of 12456.62 Da, which corresponds to the full amino acid chain of DSP-3 without attached glycans. When the collision energy was increased to 70 eV, additional fragments from the *N*-terminal part were observed which allowed a partial sequencing of the *N*-terminal region. The determined sequence showed a partial match with the recently updated *Equus asinus* mRNA sequence (044614940.1). It is likely that the genes and intron/exon use of *Equus hemionus* is different from that of *Equus asinus*. By considering some variations in the amino acid sequence, one tryptic peptide could be associated with this region to ultimately discover the complete sequence of DSP-3. The mass calculated from the amino acid sequence of DSP-3, without the associated glycans, is 12456.66 Da, which perfectly matches with the experimental mass obtained from the top-down MS measurements.

Comparison of the primary structure of DSP-3 with that of a number of FnII proteins isolated from the seminal plasma of several other mammals, namely bull, horse, pig, mouse, donkey and human, employing multiple sequence alignment is given in Fig. 5.5. This comparison shows that when DSP-1 and equine seminal plasma protein, HSP-1 are compared, only 2 residues are different. On the other hand, a comparison of DSP-1 and DSP-3 showed that only 72 residues are exactly identical, whereas next best match is found with BSP-A3, with 53 identical residues (second highest). Thus, it is interesting that DSP-3 differs considerably with all other seminal FnII proteins (as compared to DSP-1). However, importantly all 8 Cys residues that form the characteristic disulfide bonds in the two FnII domains are conserved among all the proteins. In addition, all the 4 core tryptophan residues which have been shown to be important for the choline phospholipid binding and chaperone-like activities of PDC-109 [Singh et al., 2020], are also conserved in all the above proteins.

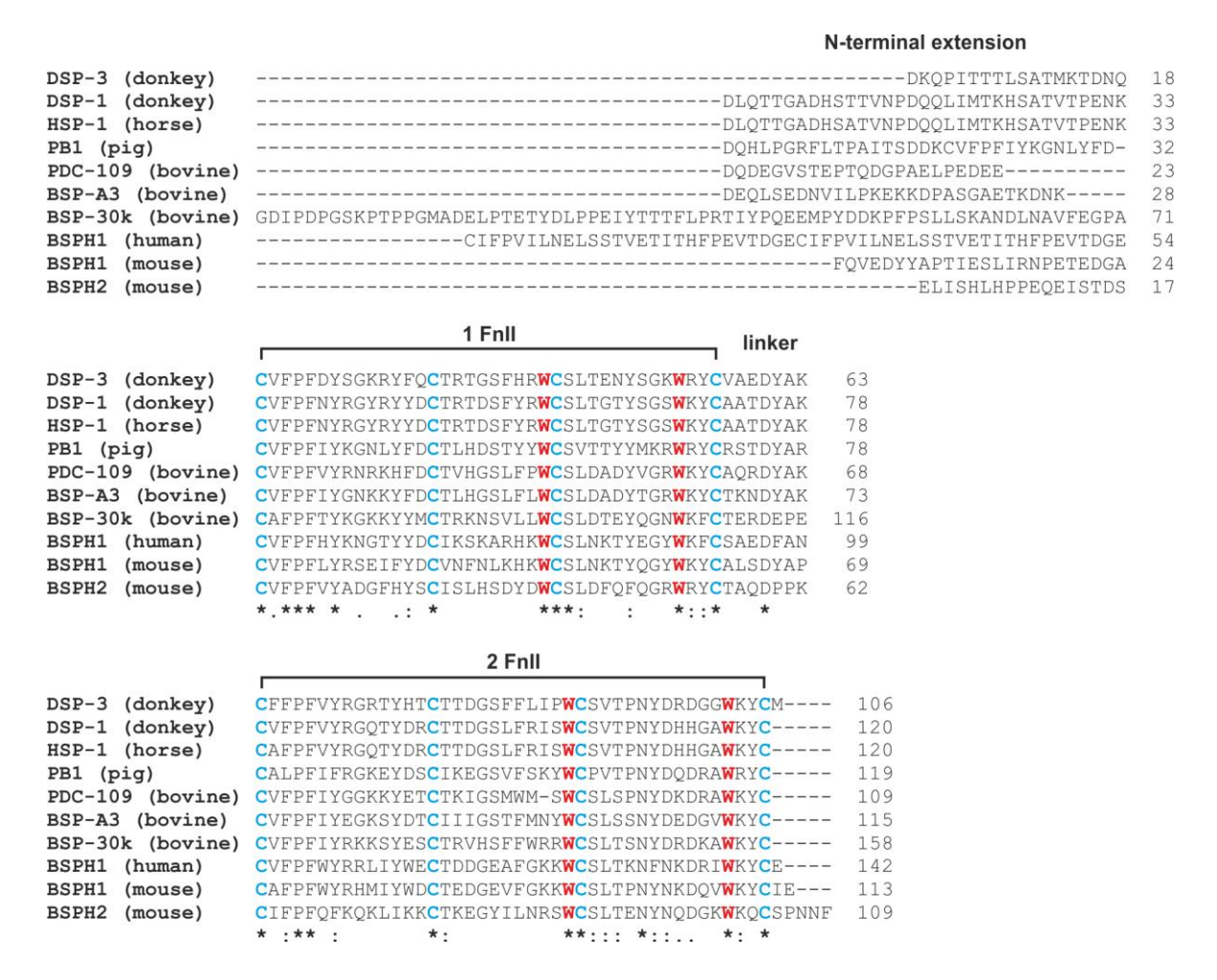


Fig. 5.5. Multiple sequence alignment of the primary structure of DSP-3 with seminal plasma FnII proteins of various mammals. Only proteins containing 2 FnII domains have been selected. All sequences were taken from EMBL-EBI database and aligned using Clustal Omega program (https://www.ebi.ac.uk/Tools/msa/clustalo/) without signal peptide sequences. The proteins (with database IDs in parentheses) are: HSP-1 (SP:P81121); porcine (pig) seminal plasma protein, PB1 (SP:P80964); bovine seminal plasma proteins PDC-109 (SP:P02784), BSP-A3 (SP:P04557) and BSP-30k (SP:P81019); human seminal plasma protein, BSPH1 (SP:Q075Z2); mouse seminal plasma proteins, BSPH1 (SP:Q3UW26) and BSPH2 (SP:Q0Q236). Conserved cysteine residues involved in disulfide bonds are shown in bold cyan, conserved core tryptophans are shown in bold red. Residues that are fully conserved across all species (*) and residues that are similar (: and .) are indicated.

5.4.3. Secondary and tertiary structure of DSP-3

The secondary and tertiary structures of DSP-3 were characterized by CD spectroscopy. Far-UV CD spectra of DSP-3 alone and in the presence of 20 mM PrC – the head group moiety of its physiological ligand, phosphatidylcholine – are shown in Fig. 5.6A. The far-UV CD spectrum of DSP-3 alone (black) is characterized by a broad positive asymmetric band with its maximum at 224 nm and a couple of shoulders at ~216 nm and 210 nm. In the presence of 20 mM PrC, the spectral intensity at 224 nm increases, whereas the spectral intensity decreases slightly below 205 nm (red). The near-UV CD spectrum of DSP-3 is quite broad, possibly due to the presence of several overlapping bands with maxima in the 275-290 nm region, and exhibits a maximum at ~286 nm (Fig. 5.6B).

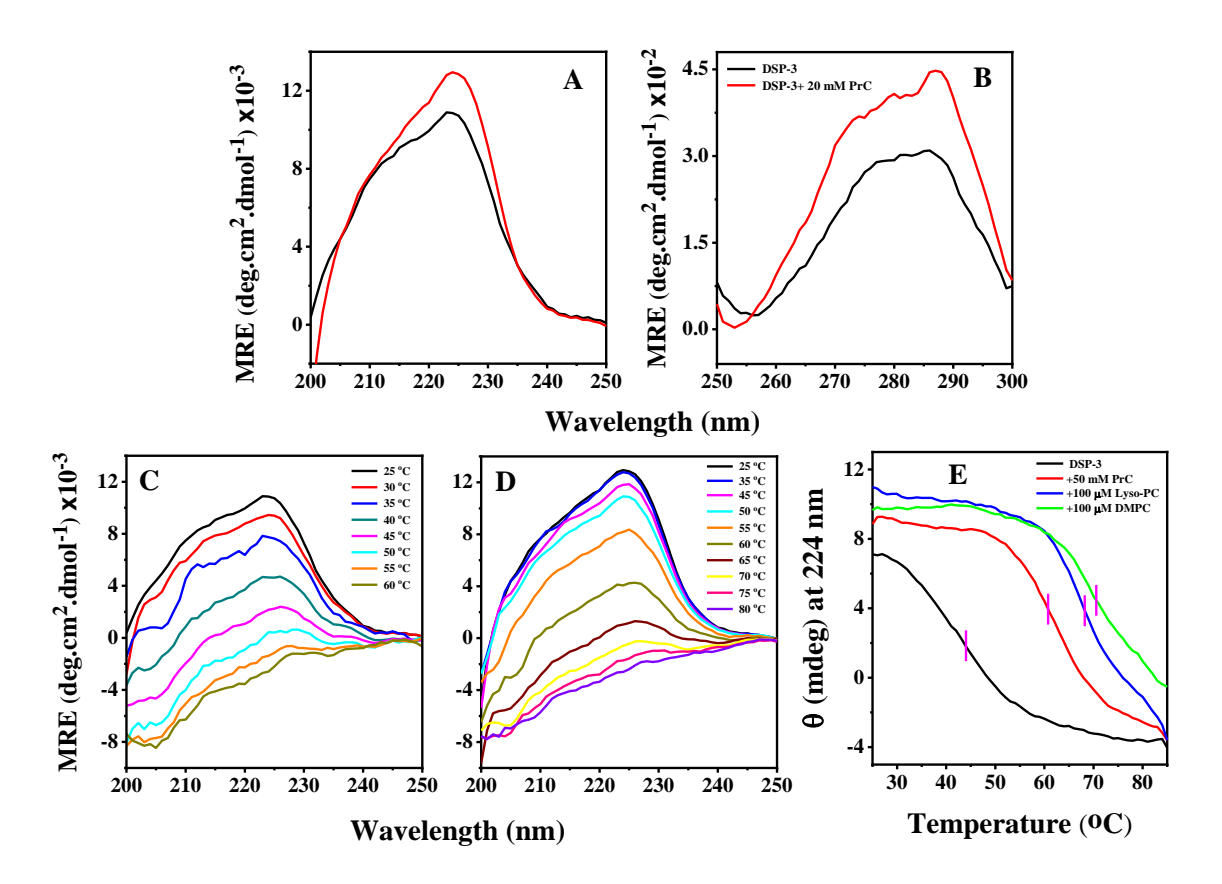


Fig.5.6. Circular dichroism spectroscopic studies of DSP-3. (**A**, **B**) Far- and near-UV CD spectra, respectively, of DSP-3 alone (black) and in the presence of 20 mM PrC (red). (**C**, **D**) Far-UV CD spectra of DSP-3 in the absence and presence of 20 mM PrC, respectively, recorded at different temperatures. (**E**) Effect of different ligands on the thermal stability of DSP-3. Thermal scans were obtained by recording the CD signal intensity of the protein at

224 nm as the temperature was increased at a scan rate of 1°/min. A fixed concentration of protein (0.1 mg/mL) was incubated with different ligands. Black, DSP-3 alone; red, + 50 mM PrC, blue, + 100 μ M Lyso-PC; green, + 100 μ M DMPC.

In the presence of 20 mM PrC, the spectral intensity increases significantly and exhibits a more distinct maximum at ~287 nm, although the overall spectrum is quite broad indicating the presence of several underlying, overlapping bands. Further, in the presence of 20 µM Lyso-PC and 20 µM DMPC the spectral intensity increases in both the cases, although no major changes are observed in the shape of the spectrum (Fig. 5.7). The positive band in the far-UV CD spectrum of DSP-3 could not be analyzed to obtain the content of various secondary structural elements of the protein, due to lack of suitable reference dataset, as was the case with the other major mammalian seminal plasma proteins, namely PDC-109, HSP-1/2 and DSP-1 [Gasset et al., 1997; Sankhala et al., 2012; Alim et al., 2022].

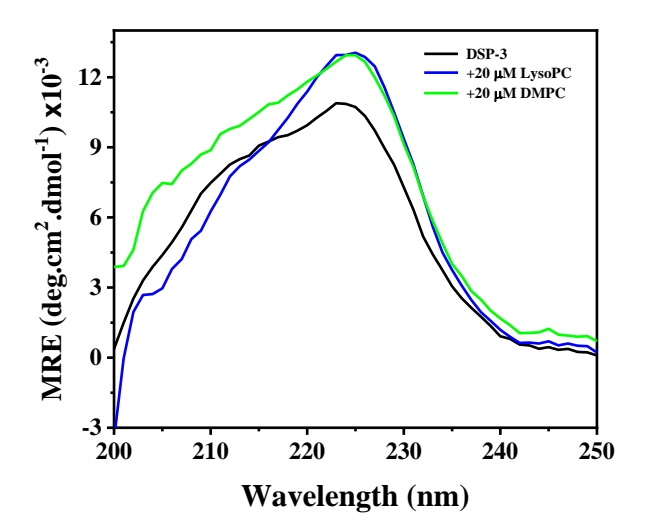


Fig. 5.7. Far-UV CD spectra of DSP-3 in the absence and presence of 20 μ M Lyso-PC and 20 μ M DMPC.

Far UV CD spectra of DSP-3 recorded at various temperatures between 25 and 60°C show a gradual decrease in the spectral intensity with increase in temperature, suggesting a gradual loss of the secondary structure of the protein (Fig. 5.6C). Broadly similar changes were seen in the near UV CD spectra (Fig. 5.8A). In contrast, in the presence of 20 mM PrC only moderate changes are seen in the far- as well as near-UV CD

spectra between 25 and 50°C, whereas significant decrease in signal intensity was observed with further increase in temperature in the range of 55-70°C (Fig. 5.6D & Fig. 5.8B). Further increases in temperature led to only moderate changes in the spectral intensity. The thermal stability of DSP-3 and the effect of ligand binding were also investigated by monitoring the CD signal intensity of the protein at 224 nm while the temperature is continuously varied. CD thermal scans recorded in the absence and presence of different ligands, viz., PrC, Lyso-PC and DMPC are shown in Fig. 5.6E. The signal intensity of native DSP-3 decreases with the steepest decline being seen at ~45°C, which is taken as the midpoint of thermal unfolding of the protein. In the presence of 50 mM PrC the midpoint of unfolding shifted to ~61°C, whereas in the presence of 100 μM concentrations of Lyso-PC and DMPC it shifted to ~68°C and ~70°C, respectively.

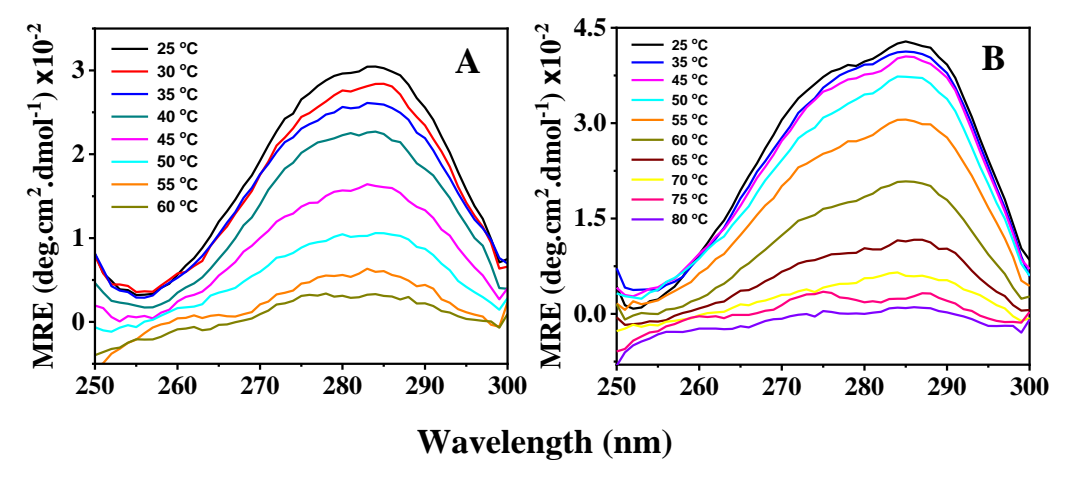


Fig. 5.8. Near-UV CD spectra of DSP-3 at different temperatures (25-80°C). (**A**) Protein alone, and (**B**) in the presence of 20 mM PrC.

5.4.4. Computational modelling of DSP-3 structure and binding of PrC

As the secondary structure of DSP-3 could not be determined from the near-UV CD spectra, we used computational methods to obtain 3-dimensional structural model of DSP-3 using Iterative Threading ASSEmbly Refinement (I-TASSER) program (http://zhanglab.dcmb.med.umich.edu/I-TASSER) using the reported crystal structure of PDC-109 (pdb code: 1h8p) as the template. The modeled structure of DSP-3 is shown in Fig. 5.9, together with the modeled structures of DSP-1, HSP-1 and PDC-109, taken from

our earlier studies on DSP-1 (Chapter 2) and HSP-1/2 [Sankhala et al., 2012]. A careful observation of the models indicates that the overall structure of DSP-3 is very similar to those of PDC-109, HSP-1 and DSP-1. Further, the relative content of various secondary structures of the three proteins, deduced from the computational models are rather similar, with all three proteins containing very little α -helix and about 20-25% β -sheet, whereas \sim 70% of the residues are in β -turns and unordered structures (Table 5.2).

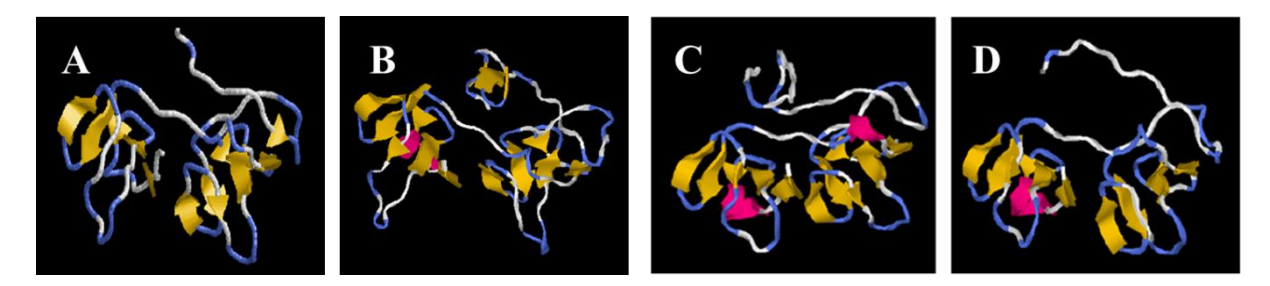


Fig. 5.9. Three dimensional structural models of DSP-3 (**A**), DSP-1 (**B**), HSP-1 (**C**) and PDC-109 (**D**). The structures were generated by computational modelling using the I-TASSER program available online (http://zhanglab.dcmb.med.umich.edu/I-TASSER) using the reported crystal structure of PDC-109 (pdb code: 1h8p) as the template. The models of DSP-1, HSP-1 and PDC-109, taken from our previous work [Sankhala et al., 2012 and chapter 2], are shown here for comparison.

Table 5.2. Secondary structure of DSP-3, DSP-1, HSP-1 and PDC-109 were estimated from computational modelling using the I-TASSER server. Secondary structure data of PDC-109 deduced from its crystal structure (pdb code: 1h8p) is also given for comparison.

Protein	α-helix	β-sheet	β-turns + unordered structures
DSP-3	-	20.8	79.2
DSP-1	3.3	25.0	71.7
HSP-1	5.8	25.0	69.1
PDC-109 (from	3.7	23.8	72.4
modelling)			
PDC-109 (from	9.2	22.9	67.8
crystal structure)			

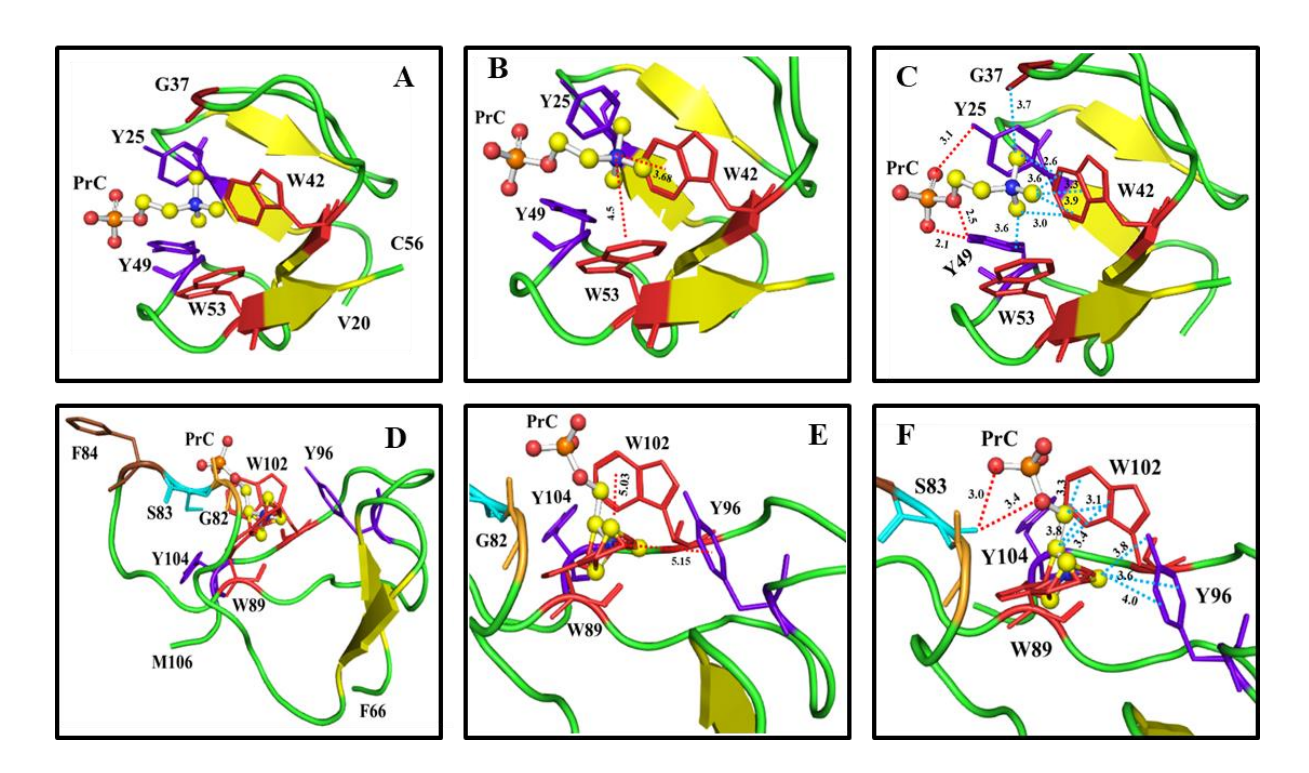


Fig. 5.10. Structure of the FnII domains of DSP-3 with bound PrC, generated using I-TASSER. The structures have been visualized using PyMOL. The side chains of binding site residues are shown in stick format. (**A**) Binding to FnII domain-I with interacting residues labeled. (**B**) Cation- π interaction of the quaternary ammonium group with W42 and W53 are indicated by red dotted lines. (**C**) Hydrogen bonds between the hydroxyls of Y25 and Y49 and the phosphate oxygens are shown in red dotted lines and the possible C-H··· π and C-H···O interactions are shown as blue dotted lines. (**D**) Binding to FnII domain-II with interacting residues labeled. (**E**) The cation- π interaction of the quaternary ammonium group with W89, W102 and Y96 are indicated by red dotted lines. (**F**) Hydrogen bonds between the hydroxyls of S98 and the phosphate oxygen are shown as red dotted lines and the possible C-H···· π and C-H···O interactions are as blue dotted lines.

Along with building a 3-D model of DSP-3 we also investigated the binding of PrC to its FnII domains using the I-TASSER server. The structures of DSP-3 domain-I and domain-II with bound PrC molecules are shown in Fig. 5.10A and 5.10D, respectively. PrC binding to DSP-3 is mediated by multiple weak interactions including cation- π , O-H···O and C-H···O hydrogen bonds as well as C-H··· π interactions. Besides the classical hydrogen bonds where N-H and O-H groups form weak interactions with O and N atoms of other groups, recent work has demonstrated that C-H···O, cation- π and C-H··· π

interactions also stabilize protein structure and protein-ligand interactions[Mahadevi and Sastry, 2013; Horowitz and Trievel, 2012; Brandl et al., 2001]. The cation-π interactions in the two FnII domains are shown in Figs. 5.10B and 5.10E, whereas the H-bonding and C-H···π interactions are shown in Figures 5.10C and 5.10F. It is observed that in first FnII domain of DSP-3, 4 out of the 5 residues that interact with PrC, namely Y25, Y49, W42 and W53 are fully conserved, whereas G37 is highly conserved among the FnII proteins whose sequences are used for comparison in the multiple sequence alignment shown in Fig. 5.5. Similarly, in the second FnII domain, W89, W102 and Y96 which interact with PrC are fully conserved whereas S83 which forms an important O-H···O hydrogen bond with PrC is conserved among 6 out of 9 sequences.

5.4.5. Thermal denaturation of DSP-3 and the effect of ligand binding

DSC studies were performed to investigate the thermal unfolding of DSP-3 in more detail as well as to obtain the thermodynamic parameters associated with it. Thermograms of DSP-3 alone and in the presence of different concentrations of PrC are shown in Fig. 5.11. The thermogram of native DSP-3 show a single thermotropic transition centred at ~44.5 °C (Fig. 5.11A). In comparison, DSP-1 showed two thermotropic transitions centred at ~32 and 43 °C, which were assigned to dissociation of oligomers and unfolding of the monomer (see Chapter 2). Absence of the minor transition before the major transition and the excellent fit of the endothermic peak in the thermogram to a single component indicate that DSP-3 exists as a monomer in solution. Further, this observation also indicates that the thermal unfolding of DSP-3 is a two-state transition, wherein the protein goes from a fully folded form to a completely unfolded state. The transition temperature determined from the DSC is also in excellent agreement with that estimated from CD thermal scans which showed a steep decrease in the spectral intensity at 224 nm at 45 °C. Further, in the presence of PrC, the temperature and enthalpy associated with the unfolding transition of DSP-3 shift to higher values with increase in the concentration of the ligand (Fig.5.11B, Table 5.3). These observations are similar to those made with DSP-1 and PDC-109 [Alim et al., 2022; Gasset et al., 1997]. The thermotropic transition temperature of DSP-3 shifted from 44.5 °C in the absence of PrC to ~60.9 °C in the presence of 50 mM PrC, with a concomitant increase in the transition enthalpy from 123 kJ/mol to 213 kJ/mol. These results strongly suggest that PrC binding stabilizes the structure of DSP-3, resulting in an increase in its unfolding temperature.

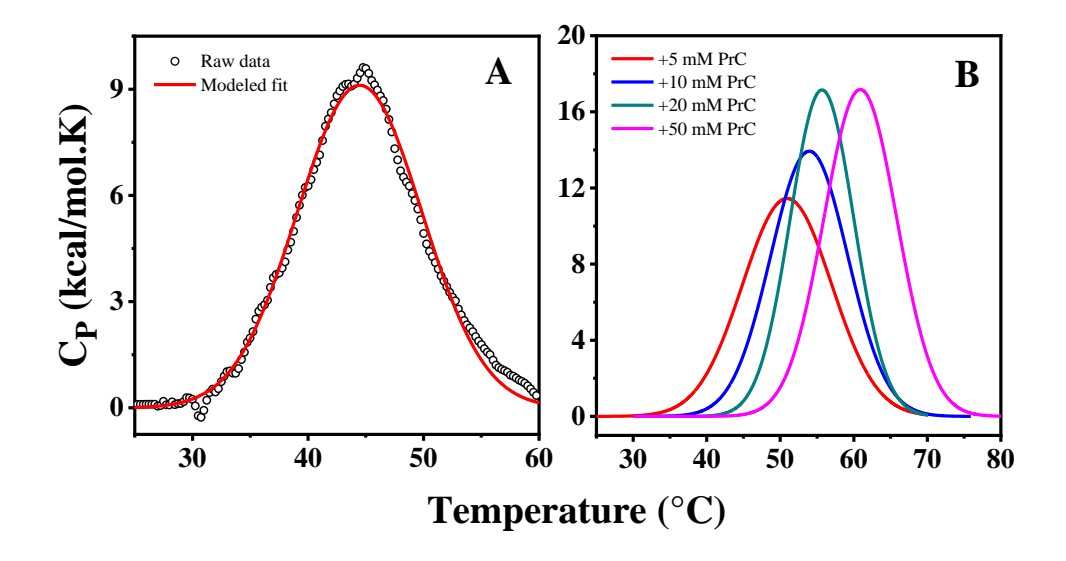


Fig. 5.11. Thermal unfolding of DSP-3. (**A**) DSC thermogram of native DSP-3. Open circles correspond to the experimental data and the red line corresponds to a fit of the experimental to the Gaussian model. (**B**) Thermograms of DSP-3 in the presence of different concentration of PrC: 5 mM (red), 10 mM (blue), 20 mM (dark cyan) and 50 mM (magenta).

Table-5.3. Transition temperatures of DSP-3 in presence of PrC derived from DSC studies. Protein (0.5 mg/mL) in the absence and presence of 5-50 mM PrC was used to obtain the transition temperature (T_m). Values given are averages from 2 or 3 independent scans with standard deviations given in parentheses.

Samples	T _{m1} (°C)	ΔH_1 (kJ/mol)
Native DSP-3	44.5 (±0.6)	123 (±14)
+5 mM PrC	51.2 (±0.5)	173 (±13)
+10 mM PrC	53.9 (±0.3)	182 (±10)
+20 mM PrC	55.6 (±0.4)	186 (±15)
+50 mM PrC	60.9 (±0.3)	213 (±12)

5.4.6. Intrinsic fluorescence studies on the binding of Lyso-PC and PrC to DSP-3

The binding of PrC and Lyso-PC to DSP-3 was investigated by monitoring ligand induced changes in the intrinsic fluorescence intensity of the protein. Fluorescence spectra corresponding to the titration with Lyso-PC and PrC are given in Fig. 5.12A & B and plots reporting the analysis of the titration data for Lyso-PC binding are given in Fig. 5.13, and for the binding of PrC are given in Fig. 5.14. To simplify the discussion, only the data analysis corresponding to the binding of Lyso-PC will be discussed below, since analysis of the data for PrC is essentially identical. Addition of small aliquots of Lyso-PC led to incremental increases in the emission intensity of the protein (Fig. 5.12A) along with a small blue shift in the emission maximum and the difference spectra obtained by subtracting the spectrum of the protein alone from the spectra recorded in the presence of increasing concentrations of Lyso-PC are shown in Fig. 5.13A. A plot of change in fluorescence emission intensity (Δ F) at 333 nm versus the ligand concentration showed saturation behaviour (Fig. 5.13B).

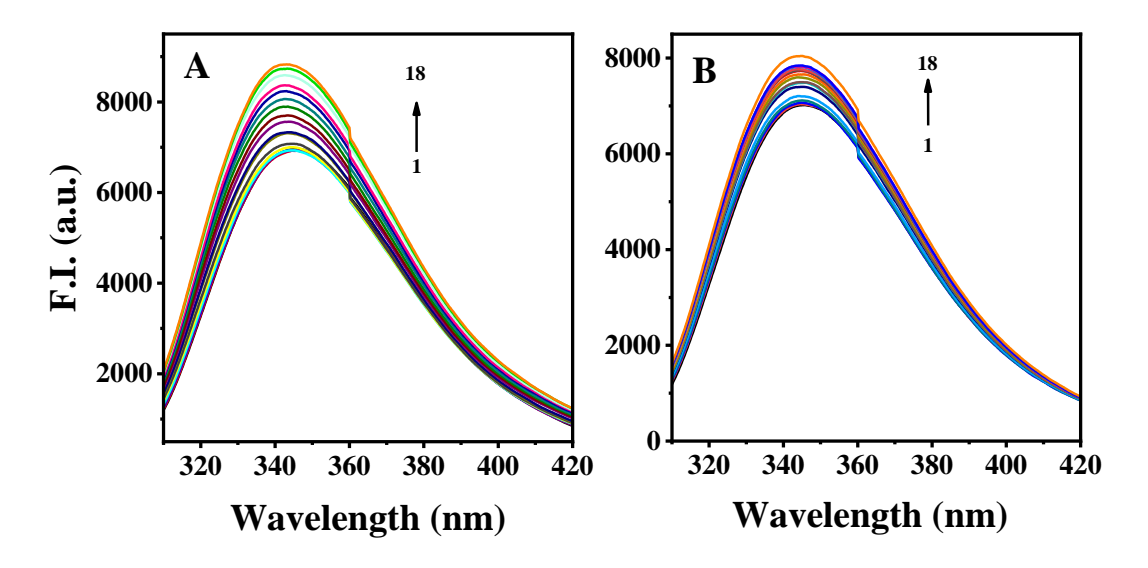


Fig. 5.12. Fluorescence titration of DSP-3 with Lyso-PC and PrC. (**A**) Fluorescence emission spectra of DSP-3 alone (curve 1) and in presence of different concentration of Lyso-PC (curves 2-18). The highest concentration of Lyso-PC in the titration mixture was 11.11 μM. (**B**) Fluorescence emission spectra of DSP-3 alone (curve 1) and in presence of different concentration of PrC (curves 2-18). The highest concentration of PrC in the titration mixture was 2.5 mM.

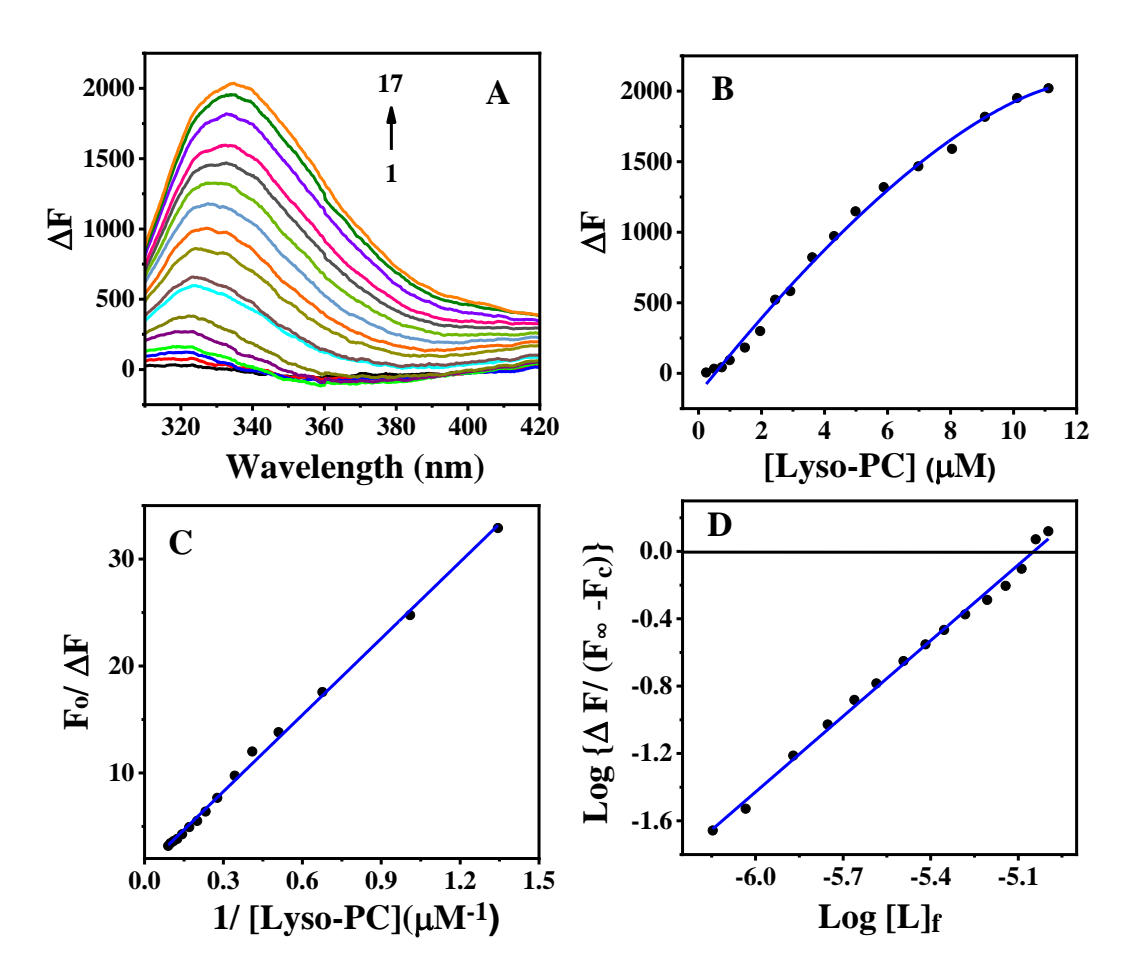


Fig. 5.13. Fluorescence titration to determine the association constant, K_a **for Lyso-PC binding to DSP-3.** (**A**) Fluorescence difference spectra of DSP-3 obtained in the presence of various concentrations of Lyso-PC. (**B**) Binding curve obtained by plotting ΔF versus [Lyso-PC]. (**C**) A double reciprocal plot of $F_o/\Delta F$ versus 1/[Lyso-PC]. From the Y-intercept of the plot, F_∞ , the fluorescence intensity of the protein at saturation binding is obtained. (**D**) A plot of [log { $\Delta F/(F_\infty$ - F_c)] versus log [L]_f. From the X-intercept of the plot the association constant, K_a , for Lyso-PC binding to DSP-3 is obtained. See text for details.

In order to obtain the association constant, K_a , the titration data was analysed by the Chipman plot as described earlier for the interaction these ligands to PDC-109 and DSP-1 [Anbazhagan and Swamy, 2005; Alim et al., 2022]. In brief, a plot of $1/\Delta F$ versus $1/[L]_t$, yielded a straight line (Fig. 5.13C). Here ΔF (= $|F_c - F_o|$) refers to the change in fluorescence intensity at any point of the titration and F_o and F_c correspond to the fluorescence intensity of DSP-3 alone and in the presence of ligand, respectively, and [L]_t

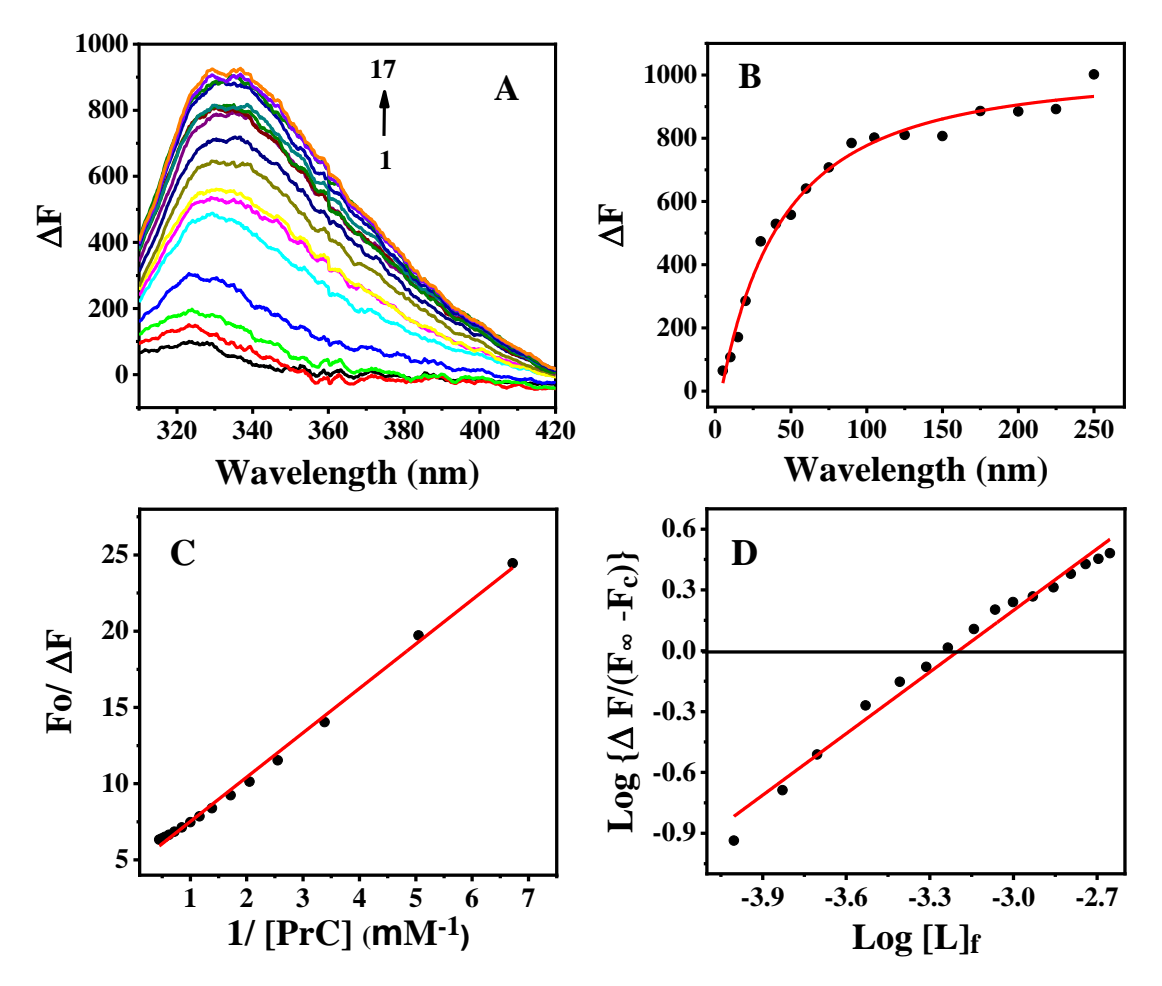


Fig. 5.14. Fluorescence titration for the binding of DSP-3 with PrC. (**A**) Fluorescence difference spectra for the titration of DSP-3 with PrC at room temperature. 1-17 correspond to difference spectra obtained in the presence of increasing concentrations of PrC. (**B**) Binding curve for the interaction of DSP-3 with PrC. The change in fluorescence intensity (ΔF) at 332 nm was plotted as a function of PrC concentration. The solid line corresponds to a 'hyperbolaGen' fit of experimental data. (**C**) A double reciprocal plot of $F_o/\Delta F$ versus 1/[PrC]. From the Y-intercept of the plot, the fluorescence change at saturation binding (ΔF_∞) is obtained. (**D**) A plot of log { $\Delta F/(F_\infty - F_c)$ } versus log [L]_f for the binding of PrC to DSP-3. X-intercept of the plot gives pK_a (-3.197) value for the titration, from which association constant, K_a was estimated as 1.573×10^3 M⁻¹.

is the corresponding total ligand concentration. From the ordinate intercepts of this plot, F_{∞} , fluorescence intensity of the sample at infinite concentration, was calculated. The titration data was further analysed according to following expression [Anbazhagan and Swamy, 2005; Chipman et al., 1967]:

$$Log \{\Delta F/(F_{\infty}-F_c)\} = Log K_a + Log [L]_f$$
(5.1)

where [L]_f, the free ligand concentration, is given by:

$$[L]_{f} = [L]_{t} - \{(\Delta F/\Delta F_{\infty})[P]_{t}\}$$

$$(5.2)$$

where $[L]_t$ and $[P]_t$ are total ligand concentration and total protein concentration, respectively, and ΔF_{∞} (= $|F_{\infty} - F_{\circ}|$) is the change in fluorescence intensity at infinite concentration (at saturation binding). From the X-intercepts of plots of log { $\Delta F/(F_{\infty} - F_{c})$ } versus log $[L]_f$, the association constant, K_a for the binding of Lyso-PC and PrC to DSP-3 were determined (Fig. 5.13D and Fig. 5.14D). The association constants thus obtained were $1.08 (\pm 0.04) \times 10^5 \,\mathrm{M}^{-1}$ for Lyso-PC and $1.39 (\pm 0.08) \times 10^3 \,\mathrm{M}^{-1}$ for PrC (averages of two independent titrations). These results show that DSP-3/Lyso-PC association is almost 80-times stronger than the DSP-3/PrC interaction.

The blue shift observed in the fluorescence emission of DSP-3 upon interaction with PrC is similar to the results obtained with PDC-109 [Anbazhagan and Swamy, 2005]. This indicates that the microenvironment around Trp residues involved in the lipid binding becomes more hydrophobic in nature upon binding of these ligands containing choline moiety.

5.4.7. Spectrophotometric and microscopic studies on DSP-3 binding to erythrocytes

To investigate the effect of DSP-3 binding on the cell membrane, human erythrocytes were taken as a model cell system, as both spermatozoa and erythrocytes of different mammalian species consist of high proportion of choline phospholipids [Damai et al., 2010; Mann and Lutwak-Mann, 1981; Holt and North, 1985; Parks et al.,1987; Martínez and Morros,1996]. Binding of DSP-3 to erythrocytes caused the disruption of membrane structure which led to cell lysis and release of haemoglobin into the solution. This was monitored by measuring absorption at 415 nm corresponding to the haem in the released haemoglobin [Damai et al., 2010]. After incubation with DSP-3, the amount of haemoglobin released from erythrocytes increased in a sigmoidal fashion and reached saturation at ~100 µg/mL concentration of DSP-3, indicating concentration-dependent

membrane destabilization (Fig. 5.15A). Kinetics of DSP-3 induced erythrocyte destabilization, which was monitored over time periods of 5-300 min, indicating that the release of haemoglobin increased with increase in incubation time up to 180 min and then levelled off (Fig. 5.15B). These results indicate that DSP-3 binding destabilizes the erythrocyte membrane in a time- and concentration-dependent manner.

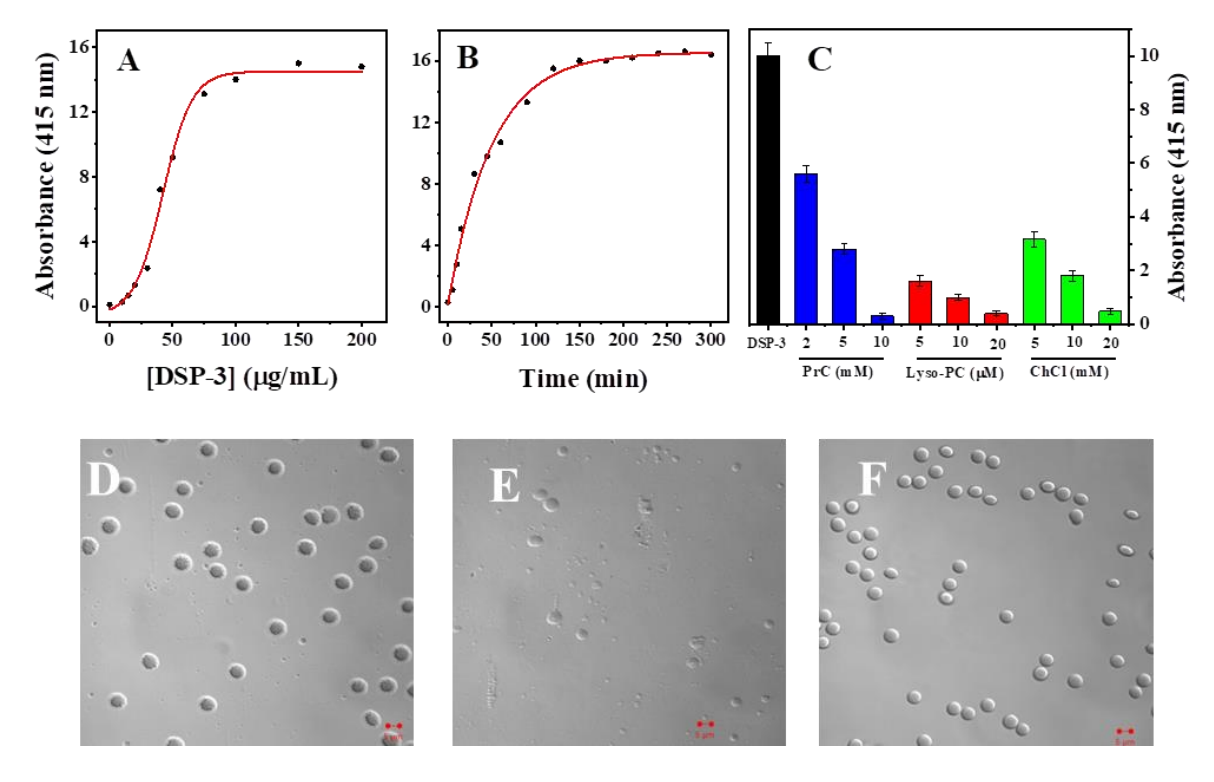


Fig. 5.15. Effect of DSP-3 on human erythrocyte membrane. (**A**) Effect of increasing the concentration of DSP-3 on erythrocyte lysis. (**B**) Kinetics of erythrocyte lysis induced by DSP-3. The protein concentration in each sample was 100 μg/mL. (**C**) Erythrocyte lysis induced by DSP-3 alone and upon pre-incubation with different concentrations of Lyso-PC, PrC and choline chloride. Absorbance at 415 nm was measured to detect the haemoglobin released upon cell lysis. (**D-F**) Microscopic images of human erythrocytes under different conditions: (**D**) in TBS buffer alone, (**E**) upon incubation for 60 min with 100 μg/mL DSP-3 and (**F**) pre-incubated with 100 μg/mL DSP-3 in presence of 20 mM PrC for 60 min. Scale bar = 5 μm.

In further studies aimed at investigating the effect of ligand binding to DSP-3 on its ability to induce erythrocyte lysis, the protein was pre-incubated with different concentrations of PrC, Lyso-PC, or choline chloride, which can block the phospholipid

binding site of DSP-3 and prevent its binding to the choline phospholipids on the erythrocyte membrane. In these experiments it was observed that erythrocyte lysis was decreased in the presence of these choline-containing ligands (Fig. 5.15C), clearly indicating that DSP-3 induced destabilization is mediated by the binding of DSP-3 to the choline phospholipids present on the erythrocyte membrane. While 20 μ M concentration of Lyso-PC could inhibit the erythrocyte lysis by >90%, similar inhibition was achieved by PrC and choline chloride only at 10 mM and 20 mM concentrations, respectively (Fig. 5.15C). Thus, these observations are consistent with the significantly higher association constant estimated for the binding of Lyso-PC to DSP-3 over PrC.

The erythrocyte membrane lysis induced by DSP-3 was also investigated by light microscopy using a confocal microscope. In these studies, images of human erythrocytes were taken in buffer and upon pre-incubation with DSP-3 alone as well as in the presence of ligands at different time intervals. Images of erythrocytes in buffer alone show well-defined morphology (Fig. 5.15D), whereas upon incubation with DSP-3 for 60 minutes, very few erythrocytes were seen together with some cell membrane fragments, indicating that the most of the erythrocyte were lysed and the cell membranes were fragmented (Fig. 5.15E). In samples where DSP-3 was pre-incubated with 20 mM PrC before its addition to the sample, all erythrocytes were intact (Fig. 5.15F), indicating that binding of PrC to DSP-3 inhibited its binding to choline phospholipids on the erythrocyte cell membrane, resulting in the inhibition of membrane destabilizing activity of the protein.

FnII proteins are the major macromolecules in the seminal plasma of various mammals and have been implicated in priming the spermatozoa for fertilization by inducing cholesterol efflux from sperm plasma membranes, which is a crucial step in sperm *capacitation*. Therefore, FnII proteins from the seminal plasma of various mammals have been isolated and purified and some of them have been characterized in considerable detail employing biochemical and biophysical approaches [Swamy, 2004; Plante et al., 2016]. In particular, their interaction with model membranes containing choline phospholipids, which are their physiological ligands, as well as sperm plasma membranes and small molecules containing the choline moiety, such as choline and phosphoryl choline, were investigated by spectroscopic methods, isothermal titration calorimetry as

well as other physical methods such as surface plasmon resonance [Müller et al., 1998; Gasset et al., 2000; Anbazhagan and Swamy, 2005; Ramakrishnan et al., 2001; Swamy et al., 2002; Thomas et al., 2003]. The recent discovery that these proteins display chaperone-like activity (CLA) in a manner similar to small heat shock proteins (*shsps*) led to increased interest in these proteins as they appear to be the only proteins in seminal plasma that exhibit the ability to protect other proteins against various kinds of stress conditions, viz., thermal, chemical and variation of pH [Kumar and Swamy, 2016c; Sankhala and Swamy, 2010; Sankhala et al, 2012]. In light of this, the present study reporting the purification and characterization of another major seminal FnII protein present in the donkey seminal plasma is quite significant.

5.5. Conclusion

In summary, in the present work we have characterized DSP-3, another major protein from donkey seminal plasma in addition to DSP-1, belonging to the seminal FnII protein family and characterized its primary, secondary and tertiary structure by experimental and computational approaches. DSP-3 exhibits significantly higher homology to HSP-1 than DSP-1. It is a glycoprotein which is heterogeneously O-glycosylated and contains acetylated sialic acid residues. Differential scanning calorimetric studies have shown that DSP-3 unfolds in a two-state transition from a folded structure to the unfolded form and that ligand binding stabilizes the protein structure, and significantly increase in the transition temperature and enthalpy. Fluorescence titrations on the binding of PrC and Lyso-PC indicated that DSP-3 exhibits considerably higher binding affinity towards Lyso-PC than PrC. Additionally, the ability of DSP-3 to bind to choline phospholipids on cell membranes was investigated employing human erythrocytes as a model system, which showed that DSP-3 is capable of inducing membrane destabilization and can cause erythrocyte lysis. This would be physiologically quite relevant since similar activity on sperm cell membrane has been implicated in inducing acrosome reaction in spermatozoa which is a crucial step in sperm *capacitation* in various mammals [Plante, 2016].

Chapter 6

General Discussion, Conclusions and Future Prospects



6.1. General Discussion and Conclusion

The thesis mainly describes the purification, molecular characterization, chaperone-like activity and ligand binding effect of two major donkey seminal plasma proteins, DSP-1 and DSP-3, which belong to the FnII family proteins. Chemical unfolding, steady-state fluorescence studies and time-resolved fluorescence measurements are also reported.

During mammalian fertilization, proteins of the seminal plasma play important roles in various stages, viz. sperm capacitation, sperm-zona pellucida interaction and establishment of the oviductal reservoir [Austin, 1952; Chang, 1984; Shivaji et al., 1990; Visconti, 1998; Yanagimachi, 1994]. The major proteins present in the seminal plasma of many mammals (e.g., bull, horse, pig etc) have a common characteristic structure, which comprises of an N-terminal flanking region, followed by two or four tandemly repeating FnII domains, and show high binding specificity towards choline phospholipids [Esch et al., 1983; Desnoyers and Manjunath, 1992; Ramakrishnan et al., 2001; Greube et al., 2004; Fan et al., 2006]. Studies on the major bovine seminal plasma protein PDC-109 in complex with O-phosphorylcholine (PrC) using single crystal X-ray diffraction showed that each PDC-109 molecule has two PC binding sites and both the binding sites are on the same face of the protein [Romero et al., 1997; Wah et al., 2002]. The major protein from equine seminal plasma, HSP-1/2, which is homologous to PDC-109, is a non-separable mixture of HSP-1 and HSP-2, which have nearly identical primary structures but differ in the number of residues in the N-terminal segment and in the extent of glycosylation [Calvete et al.,1994, 1995a, 1995b]. Recent studies have indicated that the major seminal plasma proteins from bovine, PDC-109, and horse, HSP-1/2 exhibit chaperone-like activity by protecting the target enzyme against various chemical, thermal and oxidative stress conditions. This CLA was found to be modulated by various factors such as pH, membrane binding, the presence of surfactants, etc. [Damai et. al., 2010; Sankhala et. al., 2011; Kumar and Swamy 2017b &c; Kumar et al., 2018]. Further, it was found that the CLA and membrane destabilizing activity of these proteins is inversely correlated to each other and are regulated by a 'pH switch' [Kumar and Swamy 2016c; Kumar et al., 2018]. It has been shown that glycosylation differentially modulates the membrane-perturbing and chaperone-like activities of PDC-109, with the glycosylated protein expressing higher

CLA whereas the non-glycosylated protein exhibited higher membrane perturbing activity and also the conserved core tryptophan residues of FnII domains are essential for the membrane-perturbing and chaperone-like activities of this protein [Singh et al., 2019, 2020].

Therefore, it is important to investigate and characterize the major FnII type proteins from the seminal plasma proteins of other mammals, in order to develop structurefunction relationships for them and to identify common features responsible for their functional activities. In pursuit of this objective, we have purified 3 major proteins from the donkey seminal plasma (named DSP-1, DSP-2, and DSP-3). In the studies reported in this thesis, two of these proteins – DSP-1 and DSP-3 – were characterized using various biochemical and biophysical tools. Results of studies on the molecular characterization including ligand binding specificity of DSP-1 have been reported in *Chapter 2*. Mass spectrometric and computational modelling studies yielded the amino acid sequence of DSP-1 and showed that it is homologous to other mammalian seminal plasma proteins, including bovine PDC-109 and equine HSP-1/2. Besides the amino acid sequence, highresolution LC-MS analysis indicated that the protein is heterogeneously glycosylated and also contains multiple acetylations, occurring in the attached glycans. Structural and thermal stability studies on DSP-1 using CD spectroscopy and differential scanning calorimetry revealed that the protein unfolds at ~43°C and binding to phosphorylcholine (choline phospholipids head group moiety), increasing its thermal stability. Intrinsic fluorescence titrations results showed that DSP-1 recognizes lyso-phosphatidylcholine with over 100-fold higher affinity than PrC and interaction of DSP-1 with erythrocytes, a model cell membrane, revealed that DSP-1 binding is mediated by a specific interaction with choline phospholipids and results in membrane perturbation, suggesting that binding of this protein to sperm plasma membrane is likely to be physiologically significant.

In *Chapter 3*, we have reported studies on the chaperone like activity of DSP-1. These studies reveled that DSP-1 protects various proteins from unfolding and inactivation against heat and oxidative stress conditions. It was observed that DSP-1 exhibits CLA by protecting various target proteins such as alcohol dehydrogenase, lactate dehydrogenase, and carbonic anhydrase from their heat-induced aggregation. G6PD lost its activity in the

presence of thermal stress conditions, whereas, pre-incubation with DSP-1 the activity was regained to ~92%, which indicates that DSP-1 can protect G6PD from thermal denaturation. DSP-1 can also protect the loss of activity of some enzymes such as G6PD and ADH, against oxidative stress conditions. Further observations also indicated that polydispersity and hydrophobicity are key factors that can modulate the CLA of DSP-1. It was also observed that DSP-1/DOPC mixture which formed lipoprotein complexes, prevented the aggregation better than DSP-1 alone, Since this mixture can exists *in vivo* as it is likely to be a main byproduct of DSP-1 induced sperm capacitation and hence could play a crucial role as CLA under *in vivo* conditions. These results show that choline phospholipids induce a different effect on the structure and function of DSP-1 as compared to that induced by PrC. Pre-incubation of DSP-1 with PrC shows a decrease in polydisperse nature as well as surface hydrophobicity due to the direct interaction of PrC with the aromatic amino acids in the binding pocket of the DSP-1, which decreased CLA as compared to native DSP-1.

Chapter 4 deals with the investigation of the heterogeneity of microenvironment around the tryptophan residues in the major FnII protein of donkey seminal plasma, DSP-1, in the native state and upon ligand binding employing fluorescence methods. Steady-state and time-resolved fluorescence studies on the quenching of the protein intrinsic fluorescence employing neutral and ionic quenchers revealed that the environment of the tryptophan residues in DSP-1 is less heterogeneous as compared to other homologous seminal plasma FnII proteins PDC-109 (bovine) and HSP-1/2 (equine). The quenching was decreased by ligand binding with choline containing lipids, with Lyso-PC and DMPC providing stronger shielding of the Trp residues than the soluble ligand, phosphorylcholine, which is most likely because segment(s) of the protein containing one or more Trp residues penetrate into the hydrophobic interior of the lipid membrane/micelles, thus shielding the Trp residues from the quencher. Studies on chaotrope-induced unfolding of DSP-1 revealed that disulfide bonds in the FnII domains of the protein prevent its complete unfolding, and that cooperativity of unfolding is also modulated by polydispersity of the protein.

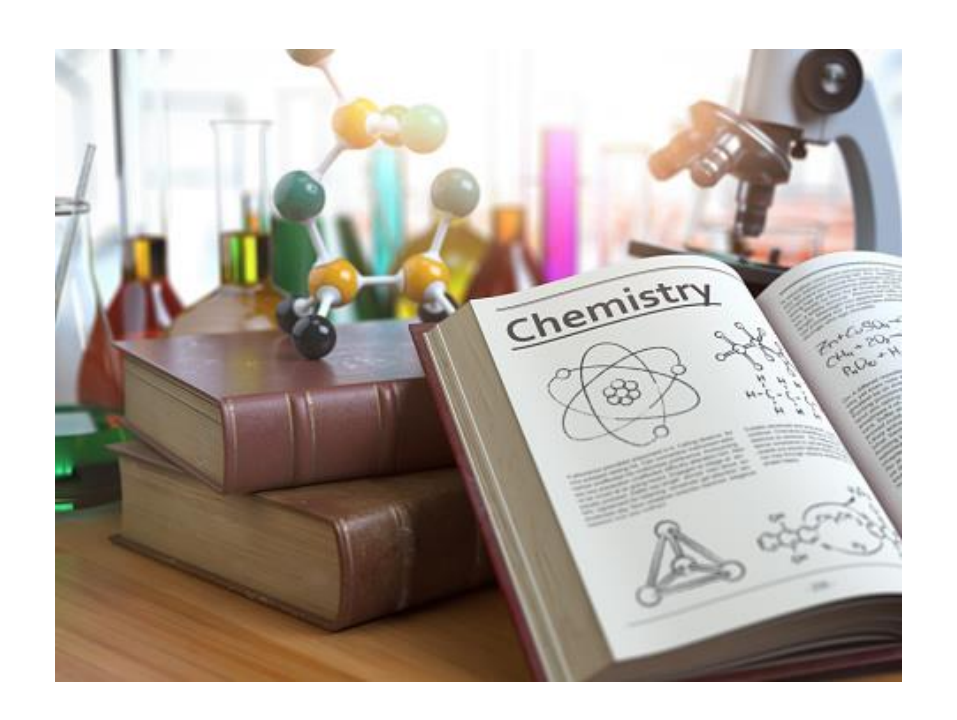
In *Chapter 5*, the primary structure of DSP-3, determined by mass spectrometric studies, and results on the physicochemical characterization of this protein, by experimental and computational approaches are reported. Interestingly, both DSP-1 and DSP-3 exhibit significantly higher homology to HSP-1 than among themselves. DSP-3 is also a glycoprotein which is heterogeneously O-glycosylated and contains acetylated sialic acid residues. However, DSC studies have shown that DSP-3 exhibits a single unfolding transition, corresponding to a two-state transition from a folded structure to the unfolded form and that ligand binding stabilizes the protein structure, and significantly increases the transition temperature and enthalpy. Fluorescence titrations on the binding of PrC and Lyso-PC indicated that DSP-3 exhibits considerably higher binding affinity towards Lyso-PC than PrC. Additionally, the ability of DSP-3 to bind to choline phospholipids on cell membranes was investigated employing human erythrocytes as a model system, which showed that DSP-3 is capable of inducing membrane destabilization and can cause erythrocyte lysis. This would be physiologically quite relevant since similar activity on sperm cell membrane has been implicated in inducing acrosome reaction in spermatozoa which is a crucial step in sperm *capacitation* in various mammals [Plante et al., 2016].

6.2. Future Prospects

In this studies, we have reported purification and biophysical/biochemical characterization of major donkey seminal plasma proteins, DSP-1 and DSP-3, which are belong to FnII family. DSP-1 and DSP-3 both can interact with choline containing phospholipids and DSP-1 exhibits chaperone-like activity. We can investigate the chaperone-like activity of DSP-3 using various target proteins against thermal and oxidative stress conditions. Further, we may find out the effect of various pH and molecular crowding on chaperone-like activity of, and ligand binding on DSP-1 and DSP-3. We can also determine the thermodynamics parameters (like binding constants, binding stoichiometry, changes in enthalpy, entropy and Gibb's free energy) associated with binding of various phospholipids to DSP-1 and DSP-3 using isothermal calorimetric titration (ITC). Further, it will also be interesting to investigate the effect of ionic liquids and osmolytes on the confirmation and activity of these proteins.

References

References



Aktas, M.; Danne, L.; Möller, P. and Narberhaus, F., Membrane lipids in Agrobacterium tumefaciens: biosynthetic pathways and importance for pathogenesis, *Frontiers in Plant Science*, 2014, **5**, 109.

Alim, S.; Kumar, C.S.; Laitaoja, M.; Talluri, T. R.; Jänis, J.; Swamy, M. J., Purification, molecular characterization and ligand binding properties of the major donkey seminal plasma protein DSP-1, *Int. J. Biol. Macromol.*, 2022, **194**, 213-222.

Anbazhagan, V.; Swamy, M.J., Thermodynamics of phosphorylcholine and lysophosphatidylcholine binding to the major protein of bovine seminal plasma, PDC-109, *FEBS Lett.*, 2005, **579**, 2933-2938.

Anbazhagan, V.; Damai, R.S.; Paul, A.; Swamy, M.J., Interaction of PDC-109, the major protein from bovine seminal plasma, with phospholipid membranes and soluble ligands investigated by fluorescence approaches, *Biochim. Biophys. Acta.*, 2008, **1784**, 891–899.

Anbazhagan, V.; Sankhala, R.S.; Singh, B.P.; Swamy, M.J., Isothermal titration calorimetric studies on the interaction of the major bovine seminal plasma protein, PDC-109 with phospholipid membranes, *PLoS ONE*, 2011, **6**, e25993.

Arcelay, E.; Salicioni, A.M.; Wertheimer, E.; Visconti, P.E., Identification of proteins undergoing tyrosine phosphorylation during mouse sperm capacitation, *Int. J. Dev. Biol.*, 2008, **52**, 463–72.

Armenteros, J. J. A.; Tsirigos, K. D.; Sønderby, C. K.; Petersen, T. N.; Winther, O.; Brunak, S.; von Heijne, G.; Nielsen, H., SignalP 5.0 improves signal peptide predictions using deep neural networks, *Nat. Biotechnol.*, 2019, **37**, 420-423.

Arnoult, C.; Zeng, Y.; Florman, H.M., ZP3-dependent activation of sperm cation channels regulates acrosomal secretions during mammalian fertilization, *J. Cell. Biol.*, 1996, **134**, 637-645.

Austin, C. R., The capacitation of the mammalian sperm, *Nature*, 1952, **170**, 326.

Baker, M.E., The PDC-109 protein from bovine seminal plasma is similar to the gelatin-binding domain of bovine fibronectin and a kringle domain of human tissue-type plasminogen activator, *Biochem. Biophys. Res. Commun.*, 1985, **130**, 1010-1014.

Bakthisaran, R.; Tangirala, R.; Rao, Ch. M., Small heat shock proteins: role in cellular functions and physiology, *Biochim. Biophys. Acta.*, 2015, **1854**, 291-319.

Baumber, J.; Ball, B.A.; Gravance, C.G.; Medina, V.; Davies-Morel, M.C.G., The effect of reactive oxygen species on equine sperm motility, viability, acrosomal integrity, mitochondrial membrane potential, and membrane lipid peroxidation, *J. Androl.*, 2001, **21**, 895-902.

Belhocine, T. Z.; and Prato, F.S., Transbilayer phospholipids molecular imaging, *EJNMMI Research*, 2011, **1**, 17.

Brandl, M.; Weiss, M.S. Jabs, A.; Sühnel, J.; Hilgenfeld, R., C-H··· π -interactions in proteins, *J. Mol. Biol.*, 2001, **307**, 357-377.

Calvete, J.J.; Nessau, S.; Mann, K.; Sanz, L.; Sieme, H.; Klug, E.; Töpfer-Petersen, E., Isolation and biochemical characterization of stallion seminal plasma proteins, *Reprod. Domest. Anim.*, 1994, **29**, 411-426.

Calvete, J.J.; Raida, M.; Sanz, L.; Wempe, F.; Scheit, K.-H.; Romero, A.; Töpfer-Petersen, E., Localization and structural characterization of an oligosaccharide *O*-linked to bovine PDC-109, *FEBS Lett.*, 1994, **350**, 203-206.

Calvete, J.J.; Mann, K.H.; Schafer, W.; Sanz, L.; Reinert, M., Nessau, S.; Töpfer-Petersen, E., Amino acid sequence of HSP-1, a major protein of stallion seminal plasma: effect of glycosylation on its heparin-and gelatin-binding capabilities, *Biochem. J.*, 1995a, **310**, 615-622.

Calvete, J.J.; Reinert, M.; Sanz, L.; Töpfer-Petersen, E., Effect of glycosylation on the heparin-binding capability of boar and stallion seminal plasma proteins, *J. Chromatogr.*, 1995b, **711**, 167-173.

Calvete, J.J.; Mann, K.; Sanz, L.; Raida, M.; Tdpfer-Petersen, E., The primary structure of BSP-30K, a major lipid-, gelatin-, and heparin-binding glycoprotein of bovine seminal plasma, *FEBS Lett.*, 1996, **399**, 147-152.

Cevc, G.; Seddon, J. M.; Marsh, D., The mechanism of regulation of membrane phase behaviour, structure and interactions by lipid headgroups and electrolyte solution, *Faraday Discuss Chem. Soc.*, 1986, **81**, 179-189.

Chang, M.C., Fertilizing capacity of spermatozoa deposited into the fallopian tubes, *Nature*, 1951, **168**, 697-698.

Chipman, D.M.; Grisaro, V.; Sharon, N., Binding of oligosaccharides containing *N*-acetylglucosamine and *N*-acetylmuramic acid to lysozyme: the specificity of binding subsites, *J. Biol. Chem.*, 1967, **242**, 4388-4394.

Clermont, Y.; Oko, R.; Hermo L., "Cell Biology of Mammalian Spermatogenesis," In: C. Desjardins and L.L. Ewing, Eds., Cell and Molecular Biology of the Testis, *Oxford University Press, New York*, 1993, pp. 332-376.

Damai, R.S.; Anbazhagan, V.; Babu Rao, K.; Swamy, M.J., Fluorescence studies on interaction of choline binding domain B of the major bovine seminal plasma protein, PDC-109 with phospholipid membranes, *Biochim. Biophys. Acta.*, 2009, **1794**, 1725-1733.

Damai, R. S.; Sankhala, R. S.; Anbazhagan, V.; Swamy, M.J., ³¹P-NMR and AFM studies on the destabilization of cell and model membranes by the major bovine seminal plasma protein, PDC-109, *IUBMB Life*, 2010, **62**: 841-851.

Das, S.; Samanta, A., On direct synthesis of high quality APbX3 ($A = Cs^+$, MA^+ and FA^+ ; $X = Cl^-$, Br^- and Γ) nanocrystals following a generic approach, *Nanoscale*, 2022, **14**, 9349–9358.

Demchenko, A. P., The red-edge effects: 30 years of exploration, *Luminescence*, 2002, **17**, 19–42.

Desnoyers, L.; Manjunath, P., Major proteins of bovine seminal plasma exhibit novel interactions with phospholipids, *J. Biol. Chem.*, 1992, **267**, 10149-10155.

Ellis, R. J., Proteins as molecular chaperones, *Nature*, 1987, **328**, 378-379.

Ellis, R.J.; van der Vies, S.M., Molecular chaperones, *Annu. Rev. Biochem.*, 1991, **60**, 321-347.

Esch, F. S.; Ling, N. C.; Bohlen, P.; Ying, S. Y., Guillemin, R., Primary structure of PDC-109, a major protein constituent of bovine seminal plasma, *Biochem. Biophys. Res. Commun.*, 1983, **113**, 861-867.

Escriba, P. V., Membrane-Lipid Therapy: A New Approach in Molecular Medicine, *Trends Mol. Med.*, 2006, **12**, 34-43.

Escriba, P. V.; Gonzalez-Ros, J. M.; Goni, F. M.; Kinnunen, P. K. J.; Vigh, L.; Sanchez-Magraner, L.; Fernandez, A. M.; Busquets, X.; Horvath, I.; Barcelo-Coblijn, G., Membranes: A Meeting Point for Lipids, Proteins and Therapies, *J. Cell. Mol. Med.*, 2008, **12**, 829-875.

Fan, J.; Lefebvre, J.; Manjunath, P., Bovine seminal plasma proteins and their relatives: A new expanding superfamily in mammals, *Gene*, 2006, **375**, 63-74.

Fawcett, D.K., The mammalian spermatozoon, *Developmental Biology*, 1975, **44**, 394-436.

Fishman, E.L.; Kyoung, J.; Quynh, P. H. N.; Kong, D.; Royfman. R.; Anthony R. C.; Khanal, S.; Miller, A. L.; Simerly, C.; Schatten, G.; Loncarek, J.; Mennella, V.; Avidor-Reiss, T., A novel atypical sperm centriole is functional during human fertilization, *Nature Commun.*, 2018, **9**, 2210.

Florman, H.M.; Arnoult, C.; Kazan, I. G.; Li, C.; O'Toole, C.M.B., A perspective on the control of mammalian fertilization by egg-activated ion channels in sperm: a tale of two channels, *Biol. Reprod.*, 1998, **59**, 12-16.

Gadella, B.M.; Luna, C., Cell biology and functional dynamics of the mammalian sperm surface, *Theriogenology*, 2014, **81**, 74-84.

Gadêlha, H.; Hernández-Herrera, P.; Montoya, F.; Darszon, A.; Corkidi, G., Human sperm uses asymmetric and anisotropic flagellar controls to regulate swimming symmetry and cell steering, *Sci. Adv.*, 2020, **6**, 5168.

Gasset, M.; Saiz, J. L.; Sanz, L.; Gentzel, M.; Töpfer-Petersen, E.; Calvete, J.J., Conformational features and thermal stability of bovine seminal plasma protein PDC-109 oligomers and phosphoryl choline bound complexes, *Eur. J. Biochem.*, 1997, **250**, 735-744.

Gasset, M.; Magdaleno, L.; Calvete, J.J., Biophysical study of the perturbation of model membrane structure caused by seminal plasma protein PDC-109, *Arch. Biochem. Biophys.*, 2000, **374**, 241-247.

Georgopoulos, C.P.; Hendrix, R.W.; Casjens, S.R.; Kaiser, A.D., Host participation in bacteriophage lambda head assembly, *J. Mol. Bid.*, 1973, **76**, 45-60.

Gervasi, M. G.; Visconti, P. E., Chang's meaning of capacitation: A molecular perspective, *Mol. Reprod. Dev.*, 2016, **83**, 860-874.

Gething, M. J.; Sambrook, J., Protein folding in the cell, *Nature*, 1992, **355**, 33-45.

Gimeno-Martos, S.; Santorromán-Nuez, M.; Cebrián-Pérez, J.A.; Muiño-Blanco, T.; Pérez-Pé, R.; Casao, A., Involvement of progesterone and estrogen receptors in the ram sperm acrosome reaction, *Domestic Animal Endocrinology*, 2021, **74**, 106527.

Glover, J.R.; Lindquist, S., Hsp104, Hsp70, and Hsp40: a novel chaperone system that rescues previously aggregated proteins. *Cell*, 1998, *94*, 73-82.

Greube, A.; Müller, K.; Töpfer-Petersen, E., A. Herrmann, P. Müller, Influence of the bovine seminal plasma protein PDC-109 on the physical state of membranes, *Biochemistry*, 2001, **40**, 8326-8334.

Greube, A.; Müller, K.; Töpfer-Petersen, E., A. Herrmann, P. Müller, Interaction of Fn type II proteins with membranes: stallion seminal plasma protein SP-1/2, *Biochemistry*, 2004, **43**, 464-472.

Goloubinoff, P.; Mogk, A.; Peres Ben Zvi, A.; Tomoyasu, T.; Bukau, B., Sequential mechanism of solubilization and refolding of stable protein aggregates by a bichaperone network, *Proc. Natl. Acad. Sci. USA*, 1999, **96**, 13732-13737.

Gwathmey, T.M.; Ignotz, G.G.; Suarez, S.S., PDC-109 (BSP-A1/A2) promotes bull sperm binding to oviductal epithelium in vitro and may be involved in forming the oviductal sperm reservoir, *Biol. Reprod.*, 2003, **69**, 809-815.

Harrison, R.A.P., Capacitation mechanisms and the role of capacitation as seen in eutherian mammals, *Reprod. Fertil. Dev.*, 1996, **8**, 581-596.

Hartl, F.U., Molecular chaperones in cellular protein folding, *Nature*, 1996, **381**, 571-579.

Hendrix, R. W., Purification and properties of GroEL, a host protein involved in bacteriophage assembly, *J. Mol. Biol.*, 1979, **129**, 375-392.

Hernandez-Gonzalez, E. O.; Sosnik, J.; Edwards, J.; Acevedo, J. J.; Mendoza-Lujambio, I., Sodium and epithelial sodium channels participate in the regulation of the capacitation-associated hyperpolarization in mouse sperm, *J. Biol. Chem.*, 2006, **281**, 5623-33.

Hendershot, L.; Wei, J.; Gaut, J.; Melnick, J.; Aviel, S.; Argon, Y., Inhibition of immunoglobulin folding and secretion by dominant negative BiP ATPase mutants, *Proc. Natl. Acad. Sci. USA*, 1996, **93**, 5269-5274.

Hill, R.B.; Flanagan, J.M.; Prestegard, J.H., 1H and 15N magnetic resonance assignments, secondary structure, and tertiary fold of *Escherichia coli* DnaJ (1–78), *Biochemistry*, 1995, **34**, 5587-5596.

Hohn, T.; Hohn, B.; Engel, A.; Wurtz, M.; Smith, P. R., Isolation and characterization of the host protein GroE involved in bacteriophage lambda assembly, *J. Mol. Biol.*, 1979, **129**, 359-373.

Horowitz, S.; Trievel, R.C., Carbon-oxygen hydrogen bonding in biological structure and function, *J. Biol. Chem.*, 2012, **287**, 41576-41582.

- Horwitz, J., Alpha-crystallin can function as a molecular chaperone, *Proc. Natl. Acad. Sci. USA*, 1992, **89**, 10449-10453.
- Holt, W.V.; North, R.D., Determination of lipid composition and thermal phase transition temperature in an enriched plasma membrane fraction from ram spermatozoa, *J. Reprod. Fertil.*, 1985, **73**, 285-294.
- Huta Y.; Nitzan Y.; Breitbart H., Ezrin protects bovine spermatozoa from spontaneous acrosome reaction, *Theriogenology*, 2020, **151**, 119-127.
- Ickowicz, D.; Finkelstein, M.; Breitbart, H., Mechanism of sperm capacitation and the acrosome reaction: Role of protein kinases, *Asian Journal of Andrology*. 2012, **14**(6), 816-821.
- Jois, P.S.; Manjunath, P., The N-terminal part of Binder of SPerm 5 (BSP5), which promotes sperm capacitation in bovine species is intrinsically disordered, *Biochem. Biophys. Res. Commun.*, 2010, **394**, 1036-1041.
- Kumar, C. S.; Sivaramakrishna, D.; Ravi, S. K.; Swamy, M. J., Fluorescence investigations on choline phospholipid binding and chemical unfolding of HSP- 1/2, a major protein of horse seminal plasma, *J. Photochem. Photobiol. B Biol.*, 2016a, **158**, 89-98.
- Kumar, C. S.; Swamy, M. J., HSP-1/2, a major horse seminal plasma protein, acts as a chaperone against oxidative stress, *Biochem. Biophys. Res. Commun.*, 2016b, **473**, 1058-1063.
- Kumar, C. S.; Swamy, M. J., A pH switch regulates the inverse relationship between membranolytic and chaperone-like activities of HSP-1/2, a major protein of horse seminal plasma, *Biochemistry*, 2016c, **55**, 3650-3657.
- Kumar, C. S.; Swamy, M. J., Differential modulation of chaperone-like activity of HSP-1/2, a major protein of horse seminal plasma by anionic and cationic surfactants, *Int. J. Biol. Macromol.*, 2017a, **96**, 524-531.
- Kumar, C. S.; Swamy, M. J., Modulation of chaperone-like and membranolytic activities of major horse seminal plasma protein HSP-1/2 by L-carnitine, *J. Biosci.*, 2017b, **42**, 469-479.
- Kumar, C. S.; Singh, B. P.; Alim, S.; Swamy, M. J., Factors influencing the chaperone-like activity of major proteins of mammalian seminal plasma, equine HSP-1/2 and bovine PDC-109: Effect of membrane binding, pH and ionic strength, *Adv. Exp. Med. Biol.*, 2018, **5**, 53-68.

Kumar, M. S.; Reddy, P. Y.; Sreedhar, B.; Reddy, G. B., αB-Crystallin assisted reactivation of glucose-6-phosphate dehydrogenase upon refolding, *Biochem. J.*, 2005, **391**, 335-341.

Lakowicz (Ed.), J.R., Principles of Fluorescence Spectroscopy, second ed. Kluwer Academic Publishers, *New York*, 1999, pp. 1-698.

Laemmli, U.K., Cleavage of structural proteins during the assembly of the head of bacteriophage T4, *Nature*, 1970, **227**, 680-685.

Laitaoja, M.; Sankhala, R. S.; Swamy, M. J.; Jänis J., Top-down mass spectrometry reveals new sequence variants of the major bovine seminal plasma protein PDC-109, *J. Mass Spectrom*, 2012, **47**, 853-859.

Langer T, Pfeifer G, Martin J, Baumeister W, Hartl FU. 1992. Chaperoninmediated protein folding: GroES binds to one end of the GroEL cylinder, which accommodates the protein substrate within its central cavity. *EMBO J.* **11,** 4757-4765.

Laufen, T., Mayer, M.P., Beisel, C., Klostermeier, D., Mogk, A., Reinstein, J., and Bukau, B., Mechanism of regulation of Hsp70 chaperones by DnaJ cochaperones. *Proc. Natl. Acad. Sci. USA*, 1999, **96**, 5452-5457.

Laskey, R. A.; Honda, B. M.; Mills, A. D.; Finch, J. T., Nucleosomes are assembled by an acidic protein which binds histones and transfers them to DNA, *Nature*, 1978, **275**, 416-20.

Leahy, T.; Gadella, B. M., Sperm surface changes and physiological consequences induced by sperm handling and storage, *Reproduction*, 2011a, **142**, 759-78.

Leahy, T.; Gadella, B.M., Capacitation and Capacitation-like Sperm Surface Changes Induced by Handling Boar Semen, *Reprod. Dom. Anim.*, 2011b, **46**, 7-13.

Lee, G. J.; Roseman, A. M.; Saibil, H. R.; Vierling, E., A small heat shock protein stably binds heat-denatured model substrates and can maintain a substrate in a folding-competent state, *EMBO J.*, 1997, **16**, 659-671.

Mahadevi, A.S.; Sastry, G.N., Cation– π interaction: Its role and relevance in chemistry, biology, and material science, *Chem. Rev.*, 2013, **113**, 2100-2138.

Manc ek-Keber, M.; Jerala, R., Structural similarity between the hydrophobic fluorescent probe and lipid A as a ligand of MD-2, *FASEB J.*, 2006, **20**, 1836-1842.

Manjunath, P.; Sairam, M. R.; Uma, J., Purification of four gelatin-binding proteins from

bovine seminal plasma by affinity chromatography, *Biosci. Rep.*, 1987a, **7**, 231-238.

Manjunath, P.; Sairam, M. R., Purification and biochemical characterization of three major acidic proteins (BSP-A1, BSP-A2 and BSP-A3) from bovine seminal plasma, *Biochem. J.*, 1987b, **241**, 685-692.

Manjunath, P.; Marcel, Y. L.; Uma, J.; Seidah, N. G.; Chretien, M.; Chapdelaine, A., Apolipoprotein A-I binds to a family of bovine seminal plasma proteins, *J. Biol. Chem.*, 1989, **264**, 16853-16857.

Manjunath, P.; Chandonnet, L.; Leblond, E.; Desnoyer, L., Major proteins of bovine seminal vesicles bind to spermatozoa, *Biol. Reprod.*, 1994, **50**, 27-37.

Manjunath, P.; Nauc, V.; Bergeron, A.; Menard, M., Major proteins of bovine seminal plasma bind to the low density lipoprotein fraction of hen's egg yolk, *Biol Reprod.*, 2002, **67,** 1250-1258.

Manjunath, P.; Thérien, I., Role of seminal plasma phospholipid-binding proteins in sperm membrane lipid modification that occurs during capacitation, *J. Reprod. Immunol.*, 2002, **53**, 109-119.

Mann, T.; Lutwak-Mann (Eds), C., Male Reproductive Function and Semen, Springer-Verlag, Berlin, 1981, pp. 495.

Martínez, P.; Morros, A., Membrane lipid dynamics during human sperm capacitation, *Front. Biosci.*, 1996, **1**, 103-117.

Martin, J.; Langer T., Chaperonin-mediated protein folding at the surface of groEL through a 'molten globule'-like intermediate, *Nature*. 1991, **352**, 36-42.

Men, L; Wang, Y., The oxidation of yeast alcohol dehydrogenase-1 by hydrogen peroxide in vitro, *J. Proteome Res.*, 2007, **6**, 216-225.

<u>Ménard</u>, S.; <u>Pupa</u>, S.M.; <u>Campiglio</u>, M.; <u>Tagliabue</u>, E., Biologic and therapeutic role of HER2 in cancer, *Oncogene*, 2003, **22(42):**6570-6578.

Meyer, E., Internal water molecules and H-bonding in biological macromolecules: A review of structural features with functional implications, *Protein Sci.*, 1992, **1**, 1543-1562.

Mitchell, L.A.; Nixon, B.; Aitken, R.J., Analysis of chaperone proteins associated with human spermatozoa during capacitation, *Mol. Hum. Reprod.*, 2007, **13**, 605-613.

- Mondal, S.; Swamy, M.J., Purification, biochemical/biophysical characterization and chitooligosaccharide binding to BGL24, a new PP2-type phloem exudate lectin from bottle gourd (*Lagenaria siceraria*), *Int. J. Biol. Macromol.*, 2020, **164**, 3656-3666.
- Moreau, R.; Thérien, I.; Lazure, C.; Manjunath, P., Type II domains of BSP- A1/-A2 proteins: binding properties, lipid efflux, and sperm capacitation potential, *Biochem. Biophys. Res. Commun.*, 1998, **246**, 148-154.
- Morgan, D.J.; Weisenhaus, M.; Shum,S.; Sua, T.; Zheng, R.; Zhang, C.; Shokat, K.M.; Hille, B.; Babcock, D.F.; McKnight, G.S., A chemical-genetic approach to study the role of PKA in specific tissues: Analysis of sperm capacitation, *Proc Natl Acad Sci USA*, 2008, **105**, 20740-20745.
- Moparthi, S.B.; Fristedt, R.; Mishra, R.; Almstedt, K.; Karlsson, M.; Hammarstrom, P.; Carlsson, U., Chaperone activity of Cyp18 through hydrophobic condensation that enables rescue of transient misfolded molten globule intermediates, *Biochemistry*, 2010, **49**, 1137-1145.
- Mosher, D.F., Assembly of fibronectin into extracellular matrix, *Curr. Opin. Struct. Biol.*, 1993, **3**, 214-222.
- Mukherjee, S.; Chattopadhyay, A., Wavelength-selective fluorescence as a novel tool to study organization and dynamics in complex biological systems, *J. Fluoresc.*, 1995, **5**, 237-346.
- Müller, P.; Erlemann, K.-R.; Müller, K.; Calvete, J. J.; Topfer-Petersen, E.; Marienfeld, K.; Herrmann, A., Biophysical characterization of the interaction of bovine seminal plasma protein PDC-109 with phospholipid vesicles, *Eur. Biophys. J.*, 1998, **27**, 33-41.
- Müller, P.; Greube, A.; Töpfer-Petersen, E.; Herrmann, A., Influence of the bovine seminal plasma protein PDC-109 on cholesterol in the presence of phospholipids, *Eur. Biophys. J.*, 2002 **31**, 438-447.
- Muthana, S. M.; Campbell, C. T.; Gildersleeve, J. C., Modifications of glycans: biological significance and therapeutic opportunities, *ACS Chem. Biol.*, 2012, **7**, 31-43.
- Nkhoma, E.T.; Poole, C.; Vannappagari, V.; Hall, S.A.; Beutler, E., The global prevalence of glucose-6-phosphate dehydrogenase deficiency: a systematic review and meta-analysis, *Blood Cells Mol. Dis.*, 2009, **42**, 267-278.

Ou, B.; Hampsch-Woodill, M.; Flanagan, J.; Deemer, E.K.; Prior, R.L.; Huang, D-J., Novel fluorometric assay for hydroxyl radical prevention capacity using fluorescein as the probe, *J. Agric. Food Chem.*, 2002, **50**, 2772-2777.

Ozhogina, O. A.; Trexler, M.; Bányai, L.; Llinás, M.; Patthy, L., Origin of fibronectin type II (FN2) modules: structural analyses of distantly-related members of the kringle family idey the kringle domain of neurotrypsin as a potential link between FN2 domains and kringles, *Protein Sci.*, 2001, **10**, 2114-2122.

Palleros, D. R.; Reid, K. L.; Shi, L.; Welch, W. J.; Fink, A. L., ATP induced protein Hsp70 complex dissociation requires K1 but not ATP hydrolysis, *Nature*, 1993, **365**, 664-666.

Pal, S.K.; Zewail, A. H., Dynamics of water in biological recognition, *Chem. Rev.*, 2004, **104**, 2099-2123.

Parks, J.E.; Arion, J.A.; Foote, R.H., Lipids of plasma membrane and outer acrosomal membrane from bovine spermatozoa, *Biol. Reprod.*, 1987, **37**, 1249-1258.

Phillips, D.M. In: Hamilton D.W, Greep R.O (eds) Handbook of physiology, Sect 7: Endocrinology, *vol V. Am Physiol Soc, Washington DC*, 1975, pp 405-420.

Plante, G.; Prud'homme, B.; Fan, J.; Lafleur, M.; Manjunath, P., Evolution and function of mammalian binder of sperm protein, *Cell Tissue Res.*, 2016, **363**, 105-127.

Privalov, P.L.; Crane-Robinson, C., Role of water in the formation of macromolecular structures, *Eur. Biophys. J.*, 2017, **46**, 203-224.

Prodromou, C.; Roe, S. M.; Piper, P. W.; Pearl, L. H.; A molecular clamp in the crystal structure of the N-terminal domain of the yeast Hsp90 chaperone, *Nature Struct. Biol.*, 1997, **4**, 477-482.

Pushkin, A.; Tsuprun, V.; Solojeva, N.; Shubin, V.; Evstigneeva, Z.; Kretovich, W., High molecular weight pea leaf protein similar to the groE protein of *Escherichia coli*, *Biochim. Biophys. Acta.*, 1982, **704**, 379-384.

Qian, Y. Q.; Patel, D.; Hartl, F.U.; Mccoll, D.J., Nuclear magnetic resonance solution structure of the human Hsp40 (HDJ-1) J-domain, *J. Mol. Biol.*, 1996, **260**, 224-235.

Rajaraman, K.; Raman, B.; Rao, Ch.M., Molten-globule state of carbonic anhydrase binds to the chaperone-like alpha-crystallin, *J. Biol. Chem.*, 1996, **271**, 27595-27600.

Ramakrishnan, M.; Anbazhagan, V.; Pratap, T.K.; Marsh, D.; Swamy, M.J., Membrane insertion and lipid-protein interactions of bovine seminal plasma protein PDC-109 investigated by spin-label electron spin resonance spectroscopy, *Biophys. J.*, 2001, **81**, 2215-2225.

Rask-Andersen, M.; Masuram, S.; Schioth, H.B., The Druggable Genome: Evaluation of Drug Targets in Clinical Trials Suggests Major Shifts in Molecular Class and Indication, *Annu. Rev. Pharmacol. Toxicol.*, 2014, **54**, 9-26.

Romero, A.; Varela, P.F.; Topfer-Petersen, E.; Calvete, J.J., Crystallization and preliminary X-ray diffraction analysis of bovine seminal plasma PDC-109, a protein composed of two fibronectin type II domains, *Proteins*, 1997, **28**, 454-456.

Rosenzweig, R.; Nillegoda, N.B.; Mayer, M.P.; Bukau, B.; The Hsp70 chaperone network, *Nat Rev Mol Cell Biol*, 2019, **20(11)**, 665-680.

Saalmann A, Munz S, Ellerbrock K, Ivell R, Kirchhoff C, Novel sperm-binding proteins of epididymal origin contain four fibronectin type II-modules. *Mol Reprod Dev.* 2001, **58**, 88–100.

Sáez-Espinosa, P.; López-Huedo, A.; Robles-Gómez, L.; Huerta-Retamal, N.; Aizpurua, J.; Gómez-Torres, M.J., Characterization of Human Spermatic Subpopulations by ConA-Binding Sites and Tyrosine Phosphorylation during in vitro Capacitation and Acrosome Reaction, *Cells Tissues Organs*, 2021, **210**, 1-9.

Saggiorato, G.; Alvarez, L.; Jikeli, J.F.; Kaupp, U.B.; Gompper, G.; Elgeti, J., Human sperm steer with second harmonics of the flagellar beat, *Nature Commun.*, 2017, **8**, 1415.

Salicioni, A.M.; Platt, M.D.; Wertheimer, E.V.; Arcelay, E.; Allaire, A.; Sosnik, J.; Visconti, P.E., Signalling pathways involved in sperm capacitation, *Soc Reprod Fertil Suppl.* 2007, **65**, 245-259.

Sankhala, R. S.; Swamy, M.J., The major protein of bovine seminal plasma, PDC-109 is a molecular chaperone, *Biochemistry*, 2010, **49**, 3908-3918.

Sankhala, R.S.; Damai, R.S.; Swamy, M.J., Correlation of membrane binding and hydrophobicity to the chaperone-like activity of PDC-109, *PLoS ONE*, 2011a, **6**, e17330.

Sankhala, R.S.; Damai, R.S.; Anbazhagan, V.; Kumar, C.S.; Bulusu, G.; Swamy, M.J., Biophysical investigations on the interaction of the major bovine seminal plasma protein, PDC-109, with heparin, *J. Phys. Chem. B.*, 2011b, **115**, 12954-12962.

- Sankhala, R.S.; Kumar, C.S.; Singh, B.P.; Arangasamy, A.; Swamy, M.J., HSP-1/2, a major protein of equine seminal plasma, exhibits chaperone-like activity, *Biochem. Biophys. Res. Commun.*, 2012, **427**, 18-23.
- Scheit, A.K.H.; Kemme, M.; Aumuller, G.; Seitz, J.; Hagendorff, G.; Zimmer, M., The major protein of bull seminal plasma: biosynthesis and biological function, *Biosci. Rep.*, 1988, **8**, 589-608.
- Scolari, S.; Müller, K.; Bittman, R.; Hermann, A.; Müller, O., Interaction of mammalian seminal plasma protein, PDC-109 with cholesterol: implications for a putative CRAC domain, *Biochemistry*, 2010, **49**, 9027-9031.
- Seidah, N.G.; Manjunath, P.; Rochemont, J.; Sairam, M.R.; Chrétien, M., Complete amino acid sequence of BSP-A3 from bovine seminal plasma. Homology to PDC-109 and to the collagen-binding domain of fibronectin, *Biochem. J.*, 1987, **243**, 195-203.
- Selvaraj, V.; Asano, A.; Buttke, D.E.; McElwee, J.L.; Nelson, J.L.; Wolff, C.A.; Merdiushev, T.; Fornés, M.W.; Cohen, A.W.; Lisanti, M.P.; Rothblat, G.H.; Kopf, G.S.; Travis, A.J., Segregation of micron-scale membrane sub-domains in live murine sperm, *J. Cell. Physiol.*, 2006, **206**, 636-646.
- Sheluho, D.; Ackerman, S.H., An accessible hydrophobic surface is a key element of molecular chaperone action of Atp11p, *J. Biol. Chem.*, 2001, **276** (**43**), 39945–39949.
- Shivaji, S., Scheit, K. H., Bhargava, P. M., Proteins of seminal plasma, *Wiley*, *New York*, 1990.
- Singer, S. J., The molecular organization of membranes, *Ann. Rev. Bioch.*, 1974, **43**, 805-833.
- Singer, S. J.; Nicolson, G. L., The fluid mosaic model of the structure of cell membrane, *Science*, 1972, **175**, 720-731.
- Singh, B. P.; Saha, I.; Nandi, I.; Swamy, M. J., Spermine and spermidine act as chemical chaperones and enhance chaperone-like and membranolytic activities of bovine seminal plasma protein, PDC-109, *Biochem. Biophys. Res. Commun.*, 2017, **493**, 1418-1424.
- Singh, B.P.; Sankhala, R.S.; Asthana, A.; Ramakrishna, T.; Rao, Ch.M.; Swamy, M. J., Glycosylation differentially modulates membranolytic and chaperone-like activities of PDC-109, the major protein of bovine seminal plasma, *Biochem. Biophys. Res. Commun.*, 2019, **511**, 28-34.

- Singh, B.P.; Asthana, A.; Basu, A.; Ramakrishna, T.; Rao, Ch.M.; Swamy, M.J., Conserved core tryptophans of FnII domains are crucial for the membranolytic and chaperone-like activities of bovine seminal plasma protein, PDC-109, *FEBS Lett.*, 2020, **594**, 509-518.
- Skorstengaard, K.; Holtet, T.L.; Etzerodt, M.; Thargersen, H.C., Collagen-binding recombinant fibronectin fragments containing type II domains., *FEBS Letters*, 1994, **343**, 47-50.
- Smoot, A.L.; Panda, M.; Brazil, B.T.; Buckle, A.M.; Fersht, A.R.; Horowitz, P.M., The Binding of bis-ANS to the isolated GroEL apical domain fragment induces the formation of a folding intermediate with increased hydrophobic surface not observed in tetradecameric GroEL, *Biochemistry*, 2001, **40**, 4484-4492.
- Song, S.H.; Shin, D. H.; Her, Y. S.; Oh, M. H.; Baek, J. W.; Sung, S.; Eum, J. H.; Heo, Y.; Kim, D. S., Effect of phosphodiesterase type 5 inhibitors on sperm motility and acrosome reaction: An in vitro study, *Investig. Clin. Urol.*, 2021, **62**, 354-360.
- Sun, Y.; MacRae, T.M.; The small heat shock proteins and their role in human disease, *FEBS J* 2005, **272(11)**, 2613-2627.
- Swamy, M. J.; Marsh, D.; Anbazhagan, V.; Ramakrishnan, M., Effect of cholesterol on the interaction of seminal plasma protein, PDC-109 with phosphatidylcholine membranes, *FEBS Lett.*, 2002, **528**, 230-234.
- Swamy, M. J., Interaction of bovine seminal plasma proteins with model membranes and sperm plasma membranes, *Curr. Sci.*, 2004, **87**, 203-212.
- Szweda, L.I.; Stadtman, E.R., Iron-catalyzed oxidative modification of glucose-6-phosphate dehydrogenase from Leuconostoc mesenteroides. Structural and functional changes, *J. Biol. Chem.*, 1992, **267**, 3096-3100.
- Tanguy, E.; Kassas, N.; Vitale, N., Protein–Phospholipid Interaction Motifs: A Focus on Phosphatidic Acid, *Biomolecules*, 2018, **8**, 20.
- Tannert, A.; Kurz, A.; Erlemann, K. R.; Müller, K.; Herrmann, A.; Schille, J.; Töpfer-Petersen, E.; Manjunath, P.; Müller, P., The bovine seminal plasma protein PDC-109 extracts phosphorylcholine-containing lipids from the outer membrane leaflet, *Eur. Biophys. J.*, 2007, **36**, 461-475.
- Thérien, I.; Bleau, G.; Manjunath, P., Phosphatidylcholine-binding proteins of bovine seminal plasma modulate sperm capacitation of spermatozoa by heparin, *Biol. Reprod.*,

1995, **52**, 1372-1379.

Thérien, I.; Souberand, S.; Manjunath, P., Major Proteins of Bovine Seminal Plasma Modulate Sperm Capacitation High-Density Lipoprotein, *Biol. Reprod.*, 1997, **57**, 1080-1088.

Thérien, I.; Moreau, R.; Manjunath, P., Major proteins of bovine seminal plasma and high-density lipoprotein induce cholesterol efflux from epididymal sperm, *Biol. Reprod.*, 1998, **59**, 768-776.

Thomas, C.J.; Anbazhagan, V.; Ramakrishnan, M.; Sultan, N.; Surolia, I.; Swamy, M.J., Mechanism of membrane binding by the bovine seminal plasma protein, PDC-109. A surface plasmon resonance study, *Biophys. J.*, 2003, **84**, 3037-3044.

Töpfer-Petersen, E.; Ekhlasi-Hundrieser, M.; Kirchhoff, C.; Leeb, T.; Sieme, H., The role of stallion seminal proteins in fertilization, *Anim. Reprod. Sci.*, 2005, **89**, 159-170.

Vali Z.; Patthy, P., The fibrin-binding site of human plasminogen. Arginines 32 and 34 are essential for fibrin affinity of the kringle 1 domain, *J. Biol. Chem.*, 1984, 259 (22) 1369-13694.

Visconti, P.E., Bailey, J.L., Moore, G.D., Pan. D., Olds-Clarke, P. & Kopf, G.S., Capacitation of mouse spermatozoa: Correlation between the capacitation state and protein tyrosine phosphorylation. *Development*. 1995, **121**, 1129-1137.

Visconti, P.E.; Calantino-Hormer, H.; Moore, G.D.; Bailey, J.L.; Ning, X.; Fornes, M.; Kopf, G.S., The molecular basis of sperm capacitation, *J. Androl.*, 1998, **19**, 242-248.

Visconti, P. E., Understanding the molecular basis of sperm capacitation through kinase design, *Proc Natl Acad Sci USA*, 2009, **106**, 667-668.

Voellmy, R.; Boellmann F., Chaperone regulation ofheat shock protein response, *Adv Exp Med Biol.*, 2007, **594**, 88-99.

Von Fellenberg, R.; Zweifel, H. R.; Grunig, G.; Pellegrini, A., Proteinase inhibitors of horse seminal plasma. A high molecular mass, acid-soluble proteinase inhibitor, *Biol. Chem. Hoppe. Seyler.*, 1985, **366**, 705-712.

Wah, D.A.; Fernández-Tornero, C.; Sanz, L.; Romero, A.; Calvete, J.J., Sperm coating mechanism from the 1.8 Å crystal structure of PDC-109-phosphorylcholine complex, *Structure*, 2002, **10**, 505-514.

Wang, X.; Venable, J.; La Pointe, P.; Hutt, D.; Koulov, A.; Coppinger, J.; Gurkan, C.; Kellner, W.; Matteson, J.; Plutner, H.; Riordan, J. R.; Kelly, J. W.; Yates, J. R.; Balch, W. E., Hsp90 cochaperone Aha1 down regulation rescues misfolding of CFTR in cystic fibrosis, *Cell*, 2006, **127**, 803-815.

Ward, C. R.; Storey, B. T.; Kopf G. S., Selective activation of Gi1 and Gi2 in mouse sperm by the zona pellucida the ovum's extracellular matrix, *J. Biol. Chem.*, 1994, **269**, 13254-13258.

Wassarman, P.M., The biology and chemistry of fertilization, *Science*, 1987, 235, 553-560.

Wickner, S.; Hoskins, J.R., Chaperones, molecular, *Encyclopedia of Biological Chemistry*, 2004, **1**, 387-392

Yanagimachi, R., Mammalian fertilization, in: E. Knobil, J. Neill (Eds.), Physiology of Reproduction, *Raven Press*, *New York*, 1994, pp. 189-317.

Zigo, M.; Maňásková-Postlerová, P.; Zuidema, D.; Kerns, K.; Jonáková, V.; Tůmová, L.; Bubeníčková, F.; Sutovsky, P., Porcine model for the study of sperm capacitation, fertilization and male fertility, *Cell Tissue Res.*, 2020, **380**, 237-262.

Purification and Structural and Functional Characterization of The Major Donkey Seminal Plasma Proteins, DSP-1 and DSP-3

by Sk Alim

Submission date: 29-Dec-2022 12:15PM (UTC+0530)

Submission ID: 1987233609

File name: Sk Alim Thesis for Plagiarism check-29-12-22.pdf (4.8M)

Word count: 26336 Character count: 143393

Purification and Structural and Functional Characterization of The Major Donkey Seminal Plasma Proteins, DSP-1 and DSP-3

ORIGINALITY REPORT

47% SIMILARITY INDEX

14%

INTERNET SOURCES

47%

PUBLICATIONS

2%

STUDENT PAPERS

PRIMARY SOURCES

Sk Alim, Sudheer K. Cheppali, Mikko Laitaoja, Thirumala Rao Talluri, Janne Jänis, Musti J. Swamy. "Purification, molecular characterization and ligand binding properties of the major donkey seminal plasma protein DSP-1", International Journal of Biological Macromolecules, 2022

Publication

Prof. Musti J. Swamy
School of Chemistry
University of Hyderabad
Hyderabad – 500 046, India

C. Sudheer Kumar, D. Sivaramakrishna, Hydera Sanjay K. Ravi, Musti J. Swamy. "Fluorescence investigations on choline phospholipid binding and chemical unfolding of HSP-1/2, a major protein of horse seminal plasma", Journal of Photochemistry and Photobiology B: Biology, 2016

Publication

pubmed.ncbi.nlm.nih.gov

Prof. Musti J. Swamy
School of Chemistry

"Biochemical and Biophysical Roles of Certerabad - 500 046, India Surface Molecules", Springer Science and

Prof. Musti J. Swamy School of Chemistry University of Hyderabad Hyderabad – 500 046, India

- Sk Alim, Sudheer K. Cheppali, Mikko Laitaoja,
 Thirumala Rao Talluri, Janne Jänis, Musti J.
 Swamy. "Purification, molecular
 characterization and ligand binding properties
 of the major donkey seminal plasma protein
 DSP-1", International Journal of Biological
 Macromolecules, 2021
 Publication

 Sk Alim, Sudheer K. Cheppali, Mikko Laitaoja,
 1 %

 Prof. Musti J. Swamy
 School of Chemistry
 University of Hyderabad
 Hyderabad 500 046, India
- 6 www.science.gov
 Internet Source 1 %
- Rajani S. Damai, V. Anbazhagan, K. Babu Rao, Musti J. Swamy. "Fluorescence studies on the interaction of choline-binding domain B of the major bovine seminal plasma protein, PDC-109 with phospholipid membranes", Biochimica et Biophysica Acta (BBA) Proteins and Proteomics, 2009

C. Sudheer Kumar, Musti J. Swamy. "A pH Switch Regulates the Inverse Relationship between Membranolytic and Chaperone-like Activities of HSP-1/2, a Major Protein of Horse Seminal Plasma", Biochemistry, 2016

Publication

V. Anbazhagan, Rajani S. Damai, Aniruddha Paul, Musti J. Swamy. "Interaction of the

<1%

major protein from bovine seminal plasma, PDC-109 with phospholipid membranes and soluble ligands investigated by fluorescence approaches", Biochimica et Biophysica Acta (BBA) - Proteins and Proteomics, 2008 Publication

10	datospdf.com Internet Source	<1%
11	C. Sudheer Kumar, Musti J. Swamy. "HSP-1/2, a major horse seminal plasma protein, acts as a chaperone against oxidative stress", Biochemical and Biophysical Research Communications, 2016 Publication	<1%
12	Submitted to University of Hyderabad, Hyderabad Student Paper	<1%
13	baadalsg.inflibnet.ac.in Internet Source	<1%
14	repository.ias.ac.in Internet Source	<1%
15	Rajeshwer Singh Sankhala, Musti J. Swamy. "The Major Protein of Bovine Seminal Plasma, PDC-109, Is a Molecular Chaperone", Biochemistry, 2010 Publication	<1%

Publication

A. Venugopal, C. Sudheer Kumar, Nadimpalli 17 Siva Kumar, Musti J. Swamy. "Kinetic and biophysical characterization of a lysosomal α-I -fucosidase from the fresh water mussel, Lamellidens corrianus", International Journal of Biological Macromolecules, 2017

cancerres.unboundmedicine.com 18 Internet Source

Bhanu Pratap Singh, Ishita Saha, Indrani 19 Nandi, Musti J. Swamy. "Spermine and spermidine act as chemical chaperones and enhance chaperone-like and membranolytic activities of major bovine seminal plasma protein, PDC-109", Biochemical and Biophysical Research Communications, 2017 **Publication**

<1%

Kumar, C. Sudheer, and Musti Joginadha 20 Swamy. "A pH switch regulates the inverse relationship between membranolytic and chaperone-like activities of HSP-1/2, a major protein of horse seminal plasma", Biochemistry, 2016.

Publication

Olga A. Ozhogina, Mária Trexler, László Bányai, Miguel Llinás, László Patthy. "Origin of fibronectin type II (FN2) modules: Structural analyses of distantly-related members of the kringle family idey the kringle domain of neurotrypsin as a potential link between FN2 domains and kringles", Protein Science, 2001 Publication	<1%
pubag.nal.usda.gov Internet Source	<1%
Akkaladevi Narahari, Musti J. Swamy. "Tryptophan exposure and accessibility in the chitooligosaccharide-specific phloem exudate lectin from pumpkin (Cucurbita maxima). A fluorescence study", Journal of Photochemistry and Photobiology B: Biology, 2009 Publication	<1%
Heat Shock Proteins, 2015. Publication	<1%
"Biochemical Roles of Eukaryotic Cell Surface Macromolecules", Springer Science and Business Media LLC, 2015 Publication	<1%
faraday.ee.emu.edu.tr Internet Source	<1%

27	Rajeshwer S. Sankhala, Rajani S. Damai, V. Anbazhagan, C. Sudheer Kumar, Gopalakrishnan Bulusu, Musti J. Swamy. "Biophysical Investigations on the Interaction of the Major Bovine Seminal Plasma Protein, PDC-109, with Heparin", The Journal of Physical Chemistry B, 2011	<1%
28	David A. Wah, Carlos Fernández-Tornero, Libia Sanz, Antonio Romero, Juan J. Calvete. "Sperm Coating Mechanism from the 1.8 Å Crystal Structure of PDC-109- Phosphorylcholine Complex", Structure, 2002	<1%
29	V. Anbazhagan, Musti J. Swamy. "Thermodynamics of phosphorylcholine and lysophosphatidylcholine binding to the major protein of bovine seminal plasma, PDC-109", FEBS Letters, 2005 Publication	<1%
30	lib.bioinfo.pl Internet Source	<1%
31	Soumavo Ghosh, Saptarshi Biswas, Antonio Bauzá, Miquel Barceló-Oliver, Antonio Frontera, Ashutosh Ghosh. " Use of Metalloligands [CuL] (H L = Salen Type Di- Schiff Bases) in the Formation of Heterobimetallic Copper(II)-Uranyl Complexes:	<1%

Photophysical Investigations, Structural Variations, and Theoretical Calculations ", Inorganic Chemistry, 2013

Publication

32	intl.biophysj.org Internet Source	<1%
33	C. Sudheer Kumar, Musti J. Swamy. "Differential modulation of the chaperone-like activity of HSP-1/2, a major protein of horse seminal plasma by anionic and cationic surfactants", International Journal of Biological Macromolecules, 2017 Publication	<1%
34	Rajani S. Damai. "31P NMR and AFM studies on the destabilization of cell and model membranes by the major bovine seminal plasma protein, PDC-109", IUBMB Life, 11/2010 Publication	<1%
35	cyberleninka.org Internet Source	<1%
36	Anbazhagan, V "Thermodynamics of phosphorylcholine and lysophosphatidylcholine binding to the major protein of bovine seminal plasma, PDC-109", FEBS Letters, 20050523 Publication	<1%

37	N. Srivastava, A. Jerome, S.K. Srivastava, S.K. Ghosh, Amit Kumar. "Bovine seminal PDC-109 protein: An overview of biochemical and functional properties", Animal Reproduction Science, 2013 Publication	<1%
38	Sneha Sudha Komath, Musti J. Swamy. "Fluorescence quenching, time-resolved fluorescence and chemical modification studies on the tryptophan residues of snake gourd (Trichosanthes anguina) seed lectin", Journal of Photochemistry and Photobiology B: Biology, 1999 Publication	<1%
39	www.pubfacts.com Internet Source	<1%
40	Nabil Ali Mohammed Sultan, M. Kavitha, Musti J. Swamy. "Purification and physicochemical characterization of two galactose-specific isolectins from the seeds of ", IUBMB Life, 2009 Publication	<1%
41	Nabil Ali Mohammed Sultan, Musti J. Swamy. "Fluorescence quenching and time-resolved fluorescence studies on Trichosanthes dioica	<1%

42	Tereza Vařilová. "Affinity liquid chromatography and capillary of seminal plasma proteins", Jo Separation Science, 05/2006 Publication	electroph	noresis	<1%
43	Submitted to University of Syd	ney		<1%
44	Submitted to Stanmore College Student Paper	e		<1%
45	WMC Maxwell, SP de#Graaf, ReG Evans. "Seminal plasma effection handling and female fertility", Proceedings, 2019 Publication	cts on sp	erm	<1%
46	eftms2022.campus.ciencias.ulisboa.pt Internet Source			<1%
47	hdl.handle.net Internet Source			<1%
Exclud	de quotes On Exclude	matches <	< 14 words	

Exclude bibliography On

List of Publications:

- Kumar, C.S.; Singh, B.P.; <u>Alim, S.</u> and Swamy, M.J., Factors Influencing the Chaperone-Like Activity of Major Proteins of Mammalian Seminal Plasma, Equine HSP-1/2 and Bovine PDC-109: Effect of Membrane Binding, pH and Ionic Strength, *Adv. Expt. Med. Biol.* 2018, 1112, 53-68.
- Damera, D.P.; Kaja, S.; Janardhanam, L.S.L; <u>Alim, S.</u>; Venuganti, V.V.K. and Nag, A., Synthesis, Detailed Characterization, and Dual Drug Delivery Application of BSA Loaded Aquasomes, *ACS Appl. Bio Mater.* 2019, 2, 4471–4484.
- 3. Bhuvanachandra, B.; Sivaramakrishna, D.; <u>Alim, S.;</u> Preethiba, G.; Rambabu, S.; Swamy, M.J. and Podile, A.R., New Class of Chitosanase from Bacillus amyloliquefaciens for the Generation of Chitooligosaccharides, *J. Agric. Food Chem.* 2021, **69**, 78–87.
- 4. <u>Alim, S.</u>; Chappali, S.K.; Laitaoja, M.; Talluri, T.R.; Janis, J. and Swamy, M.J., Purification, Molecular Characterization and Ligand Binding Properties of the Major Donkey Seminal Plasma Protein DSP-1, *Int. J. Biol. Macromol.* 2022, **194**, 213–222.
- 5. Bhuvanachandra, B.; Sivaramakrishna, D.; <u>Alim, S.</u>; Swamy, M.J. and Podile, A.R., Deciphering the Thermotolerance of Chitinase O from Chitiniphilus Shinanonensis by in vitro and in Silico Studies, *Int. J. Biol. Macromol.* 2022, **210**, 44–52.
- 6. Alim, S.; Das, S. and Swamy, M.J., Probing the Chemical Unfolding of and Phospholipid Binding to the Major Protein of Donkey Seminal Plasma, DSP-1 by Fluorescence Spectroscopy, *J. Photochem. Photobiol. A: Chemistry*, (Under Review).
- 7. Alim, S.; M. Laitaoja, Pawar, S.S.; Talluri, T.R.; Janis, J. and Swamy, M.J., Primary Structure Determination and Physicochemical Characterization of DSP-3, a Phosphatidylcholine Binding Glycoprotein of Donkey Seminal Plasma Protein, *Int. J. Biol. Macromol.* (Under Review).

8. <u>Alim, S.</u> \$; Cheppali, C.K. \$; and Swamy, M.J., Chaperone-like Activity of the Major Donkey Seminal Plasma Protein DSP-1is Modulated by Ligand Binding, Polydispersity and Hydrophobicity, (**To be Communicated**). (\$These two authors equally contributed).

Conferences/ Presentations:

1. Purification, Biophysical Characterization, Lipid Binding Properties and Chaperonelike Activity of the Major Donkey Seminal Plasma Protein, DSP-1.

<u>Poster presentation</u>: International Conference on Frontier Area of Science and Technology (ICFACT-2022), 12th India-Japan Science and Technology Seminar organized by Indian JSPS Alumni Association (IJAA), 9-10 September, 2022, University of Hyderabad, Hyderabad, India.

2. Molecular Characterization, Ligand Binding Properties and Chaperone-like Activity of a Major Donkey Seminal Plasma Protein, DSP-3.

<u>Poster presentation</u>: CHEMFEST-2022 19th Annual in-house Symposium, 22-23 April, 2022, School of Chemistry, University of Hyderabad, Hyderabad, India.

3. Purification, Molecular Characterization and Lipid Binding Properties of the Major Donkey Seminal Plasma Protein, DSP-1.

<u>Poster presentation</u>: 44th Indian Biophysical Society Annual Meeting 30th March–1st April, 2022 (hybrid mode) at ACTREC, Navi Mumbai, India.

4. Major Protein from Donkey Seminal Plasma, DSP-1 Exhibits Membrane Binding Specificity and Chaperone-like Activity.

<u>Oral presentation:</u> CHEMFEST-2021 18th Annual in-house Symposium, 19-20 March, 2021, School of Chemistry, University of Hyderabad, Hyderabad, India.

5. The Major Protein of Donkey Seminal Plasma, DSP-1 Exhibits Chaperone-like Activity.

<u>Poster presentation</u>: 43rd Indian Biophysical Society Annual Meeting 15-17 March, 2019, IISER Kolkata, Kolkata, India.

6. The Major Protein of Donkey Seminal Plasma, DSP-1 Exhibits Chaperone-like Activity and Ligand Binding Activities.

<u>Poster presentation</u>: CHEMFEST-2019 16th Annual in-house Symposium, 22-23 February, 2019, School of Chemistry, University of Hyderabad, Hyderabad, India.

7. The Major Protein of Donkey Seminal Plasma, DSP-1 Exhibits Chaperone-like Activity.

<u>Poster presentation</u>: CHEMFEST-2017 14th Annual in-house Symposium, 3-4 March, 2017, School of Chemistry, University of Hyderabad, Hyderabad, India.

FISEVIER

Contents lists available at ScienceDirect

International Journal of Biological Macromolecules

journal homepage: www.elsevier.com/locate/ijbiomac





Purification, molecular characterization and ligand binding properties of the major donkey seminal plasma protein DSP-1

Sk Alim^a, Sudheer K. Cheppali^a, Mikko Laitaoja^b, Thirumala Rao Talluri^c, Janne Jänis^b, Musti J. Swamy^{a,*}

- a School of Chemistry, University of Hyderabad, Hyderabad 500046, India
- ^b Department of Chemistry, University of Eastern Finland, FI-80101 Joensuu, Finland
- ^c Equine Production Campus, ICAR-NRC on Equines, Bikaner 334001, Rajasthan, India

ARTICLE INFO

Keywords: Fibronectin type-2 protein Mass spectrometry Differential scanning calorimetry

ABSTRACT

Fibronectin type-II (FnII) family proteins are the major proteins in many mammalian species including bull, horse and pig. In the present study, a major FnII protein has been identified and isolated from donkey (*Equus hemionus*) seminal plasma, which we refer to as <u>Donkey Seminal Plasma</u> protein-1 (DSP-1). The amino acid sequence determined by mass spectrometry and computational modeling studies revealed that DSP-1 is homologous to other mammalian seminal plasma proteins, including bovine PDC-109 (also known as BSP-A1/A2) and equine HSP-1/2. High-resolution LC-MS analysis indicated that the protein is heterogeneously glycosylated and also contains multiple acetylations, occurring in the attached glycans. Structural and thermal stability studies on DSP-1 employing CD spectroscopy and differential scanning calorimetry showed that the protein unfolds at \sim 43 °C and binding to phosphorylcholine (PrC) – the head group moiety of choline phospholipids – increases its thermal stability. Intrinsic fluorescence titrations revealed that DSP-1 recognizes lysophosphatidylcholine with over 100-fold higher affinity than PrC. Further, interaction of DSP-1 with erythrocytes, a model cell membrane, revealed that DSP-1 binding is mediated by a specific interaction with choline phospholipids and results in membrane perturbation, suggesting that binding of this protein to sperm plasma membrane could be physiologically significant.

1. Introduction

In mammals, fertilization occurs when spermatozoa from male fuse with the egg in the female uterus. Upon ejaculation, during their journey through the female genital tract, spermatozoa undergo a series of ultrastructural and biochemical changes, termed as *capacitation*, which is poorly understood at the molecular level [1–3]. In several mammals, a family of proteins present in the seminal plasma called seminal FnII or BSP (binder of sperm) proteins play a major and crucial role in sperm capacitation. All these proteins have a common characteristic structure comprising of an *N*-terminal flanking region, followed by two or four tandemly repeating fibronectin type-II (FnII) domains, and show greater binding specificity towards choline phospholipids [4–6]. Among the seminal FnII proteins, the major proteins from bovine seminal plasma, PDC-109 and equine seminal plasma, HSP-1/2 have been studied in great detail. Studies on its interaction with phospholipids indicate that

PDC-109 exhibits high specificity for choline phospholipids such as phosphatidylcholine (PC) and sphingomyelin, as compared to other phospholipids such as phosphatidylgylcerol, phosphatidylserine, phosphatidylethanolamine etc. [4,5]. In addition, presence of cholesterol in the membranes was found to potentiate the interaction of PDC-109 with different phospholipids, suggesting that PC might mediate the interaction between PDC-109 and cholesterol [7]. Single crystal X-ray diffraction studies on PDC-109/O-phosphorylcholine (PrC) complex revealed that each PDC-109 molecule has two PC binding sites and both the binding sites are on the same face of the protein [8]. HSP-1/2, the major protein from horse seminal plasma and a homologue of PDC-109, is a non-separable mixture of HSP-1 and HSP-2 [9]. The primary structure of these two proteins is nearly identical but differ in the number of residues in the *N*-terminal segment and in the extent of glycosylation [9–11].

The interaction of PDC-109 with different phospholipids especially choline phospholipids has been investigated in detail along with its

E-mail address: mjswamy@uohyd.ac.in (M.J. Swamy). URL: http://chemistry.uohyd.ac.in/~mjs/ (M.J. Swamy).

 $^{^{\}ast} \ \ Corresponding \ author.$

interaction with other small molecules. Binding of PrC is shown to result in a more closed conformation along with reducing the polydisperse nature of these seminal FnII proteins [8,12]. Interaction of PDC-109 and HSP-1/2 with choline-containing ligands, model membranes and sperm plasma membranes has been greatly characterized in view of their physiological significance [13–15]. Studies have shown that both these proteins are able to intercalate into lipid membranes and perturb the lipid chain dynamics [5,6,16]. Studies on membrane perturbation by PDC-109 and HSP-1/2 using supported and model cell membranes show that these proteins cause membrane destabilization, which mimic their activity in vivo [17,18].

Recent studies have shown that PDC-109 and HSP-1/2 can also act as small heat shock proteins (*shsps*), by exhibiting chaperone-like activity (CLA) by protecting various target proteins against thermal, chemical and oxidative stress [18–21]. This CLA was found to be modulated by various factors such as membrane binding, pH, presence of surfactants etc. [17,22–25]. Further, it was found that the CLA and membrane destabilizing activity of these proteins are inversely correlated to each other and are regulated by a '*pH switch*' [18,25]. In addition, it has been shown that glycosylation differentially modulates the membrane-perturbing and chaperone-like activities of PDC-109, with the glycosylated protein exhibited higher membrane perturbing activity [26]. Importantly, mutational studies have shown that conserved core tryptophan residues of FnII domains are essential for the membrane-perturbing and chaperone-like activities of this protein [27].

From the foregoing it is quite clear that the major FnII proteins of mammalian seminal plasma play crucial roles not only in priming spermatozoa for fertilization, but also in protecting other seminal plasma proteins from misfolding/inactivation as exemplified by the bovine protein, PDC-109 and the equine protein, HSP-1/2. Therefore, it is important to purify the major FnII proteins from the seminal plasma of other mammals and characterize them in detail, in order to develop structure-function relationships in this class of proteins and to identify common features that are critical for their functional activities. With this objective, in the present study, we have purified the major protein from donkey seminal plasma, DSP-1 and characterized its biochemical and ligand binding properties. The primary structure of DSP-1, derived from mass spectrometric studies revealed that this protein belongs to the seminal FnII protein family. Furthermore, the protein was posttranslationally modified by multiple O-glycosylations with acetylated sialic acid residues. By employing various biophysical techniques we studied the secondary and tertiary structures of DSP-1, investigated its thermal stability and characterized the binding of PrC and lysophosphatidylcholine (Lyso-PC). These studies revealed that DSP-1 recognizes the choline head group of phospholipids and exhibits membrane destabilizing activity against model cell membranes. Ligand binding results in a significant increase in the thermal unfolding temperature of DSP-1 and also leads to an increase in its resistance to chemical denaturation.

2. Materials and methods

2.1. Materials

Choline chloride, phosphorylcholine chloride (calcium salt) and heparin-agarose type-I affinity matrix were obtained from Sigma (St. Louis, MO, USA) and p-aminophenyl phosphorylcholine-agarose column was purchased from Pierce Chemicals (Oakville, Ontario, Canada). Lyso-PC from egg yolk was obtained from Avanti Polar Lipids (Alabaster, AL, USA). All other chemicals were purchased from local suppliers and were of the highest purity available.

2.2. Purification of DSP-1

DSP-1 was purified from donkey seminal plasma using a modified

procedure reported previously for HSP-1/2 [20]. Freshly ejaculated semen from healthy donkeys was obtained from the Equine Production Campus, ICAR-National Research Centre on Equines (Bikaner, India). Seminal plasma was separated from spermatozoa by centrifugation of the semen at 1500 rpm in an Eppendorf 5810R centrifuge for 20 min at 4 °C. The supernatant was collected and then seminal plasma was further clarified by centrifugation again at 6000 rpm for 15 min at 4 °C. The collected seminal plasma was frozen in liquid nitrogen and stored at $-80\ ^{\circ}\mathrm{C}$ until further use.

2.2.1. Affinity chromatography on heparin-agarose

About 15 mL of clear donkey seminal plasma was diluted to 50 mL with 50 mM Tris/HCl, pH 7.4, containing 150 mM NaCl, 5 mM EDTA and 0.025% sodium azide (TBS) and double loaded on to a heparinagarose column which was pre-equilibrated with TBS buffer. The column was washed with the same buffer till absorbance of the column effluent at 280 nm was $\leq\!0.05$, following which the bound proteins were eluted with TBS containing 20 mM PrC. The fractions with high protein content were pooled and dialyzed against TBS to remove PrC.

2.2.2. Affinity chromatography on p-aminophenyl phosphorylcholineagarose (PPC-agarose)

The heparin bound-fraction obtained in the previous step was applied to a p-aminophenyl phosphorylcholine column pre-equilibrated with TBS. After extensive washing with TBS till the unbound proteins are completely removed (A_{280nm} of the column effluent \leq 0.05), the bound protein fraction was eluted with 20 mM PrC in TBS. The eluted proteins were dialyzed against TBS to remove PrC and concentrated using an Amicon filter (3 kDa cutoff).

2.2.3. Reverse-phase high-performance liquid chromatography

The proteins bound to PPC-agarose affinity matrix were further purified using reverse-phase high-performance liquid chromatography (RP-HPLC) on a Shimadzu LC 1080 (Shimadzu corporation, Tokyo, Japan) as described earlier for HSP-1/2 purification [10,20]. PPCagarose bound, concentrated protein mixture was dialyzed extensively against double distilled water containing 0.1% trifluoroacetic acid (TFA) and RP-HPLC was performed using a Luna RP-100C-18 column (250 \times 4.6 mm, 5 µM particle size) from Phenomenex (California, USA). The column was pre-equilibrated with 0.1% TFA in milli-Q water (solution A, 75%) and acetonitrile (solution B, 25%). A flow rate of 1.0 mL/min was maintained throughout. A gradient of 25-60% acetonitrile containing 0.1% TFA was used as the mobile phase. After sample loading, the column was run using the following program: 25% B for 5 min, followed by a gradient of 25-30% B over 5 min and 30-35% B over another 25 min and a gradient of 35-60% B over 10 min. Three individual peaks obtained were collected manually, dialyzed against TBS and concentrated using an Amicon concentrator (3 kDa cutoff filter) and stored at 4 °C. Finally, purity of the proteins was checked using 15% sodium dodecyl sulfate-polyacrylamide gel electrophoresis (SDS-PAGE)

2.3. Mass spectrometry

For mass spectrometry experiments, the protein samples were first buffer exchanged to 20 mM ammonium acetate (pH 7.4) using PD-10 desalting columns (Cytiva Europe GmbH). Further purification was performed by using size exclusion chromatography (SEC) on an Äktapurifier 100 instrument (Amersham Pharmacia Biotech AB, Uppsala, Sweden), using a Superdex 75 column (GE Life Sciences, Sweden). The proteins were eluted at a flow rate of 1.0 mL/min using 20 mM ammonium acetate solution (pH 7.4) as the elution buffer. The samples were further concentrated using Vivaspin2 concentrators (Sartorius Stedim Biotech GmbH, Germany). Trypsin digestion was performed by incubating the protein samples overnight with sequencing grade trypsin (Sigma Aldrich, USA) at a 1:50 (w/w) trypsin-to-protein

ratio using an acetonitrile (MeCN)/water (1:1, ν/ν) solvent containing 10 mM dithiothreitol (DTT).

The intact protein samples and the tryptic digests were analysed using an HPLC system (UltiMate 3000; Thermo Scientific) connected to a 12-tesla FT-ICR mass spectrometer (Bruker solariX-XR; Bruker Daltonics, Germany). The proteins/peptides were eluted over an Acclaim Pepmap100 C18 (0.075 \times 150 mm, 3 $\mu m)$ column (Thermo Scientific) at a flow rate of 0.5 µL/min, using a solvent gradient of 1–40% acetonitrile with 0.2% formic acid. For the direct infusion measurements, a standard Apollo-II electrospray (ESI) ion source was used, operated at a flow rate of 2 μ L/min. In the LC-MS/MS, experiments, a Bruker nano-ESI nebulizer was connected to the ion source. The drying gas temperature was set at 200 °C and a flow rate to 4 L/min. Additional top-down MS (i.e., intact protein MS/MS) experiments were performed on a QTOF mass spectrometer (Bruker timsTOF; Bruker Daltonics, Germany). The peptide or protein ions were fragmented by collision-induced dissociation (CID), using previously optimized fragmentation voltages. The instruments were controlled and the data were acquired using Chromeleon 6.80 (Ultimate 3000), ftmsControl 2.0 (solariX) or otofControl 5.1 (timsTOF) software, respectively. The data post-processing and further analysis was accomplished by using Bruker DataAnalysis 4.4/5.1 software.

The NCBI database was searched for the sequences similar to PDC-109, while limiting a species to donkey. Four possible predicted sequences were found, belonging to *Equus asinus* (accession codes 014723761.1, 014723758.1, 014723760.1, and 014723757.1). The signal peptide prediction was done with SignalP 5.1 (http://www.cbs.dtu.dk/services/SignalP/) [29].

2.4. Circular dichroism spectroscopy

CD spectroscopic studies were performed using a Jasco 810 spectropolarimeter (Jasco Corporation, Tokyo, Japan) fitted with a thermostatted cell holder and a thermostatic water bath at a scan speed of 30 nm/min. Far- and near-UV CD spectra were recorded using a 0.2 cm path length quartz cell with samples containing DSP-1 at a concentration of 0.1 mg/mL and 0.5 mg/mL, respectively in 10 mM Tris/HCl buffer, pH 7.4. Each spectrum recorded was the average of 8 consecutive scans from which buffer scans were subtracted. Spectra were also obtained in the presence of up to 50 mM PrC.

Thermal unfolding of DSP-1 was investigated by monitoring the CD spectral intensity of the protein (0.1 mg/mL) at 225 nm, while the temperature was increased from 25 to 80 $^{\circ}$ C at a scan speed of 1 $^{\circ}$ C/min. Effect of PrC binding on the thermal stability of DSP-1 was investigated by incubating a fixed concentration protein (0.1 mg/mL) for $\sim\!30$ min with varying concentrations of PrC (10–50 mM) before the temperature scans were performed.

2.5. Computational modeling

The amino acid sequence of DSP-1 determined by the mass spectrometric studies was submitted to I-TASSER server (http://zhanglab.dcmb.med.umich.edu/I-TASSER) to build a 3-dimensional structural model of the protein. The crystal structure of PDC-109 (pdb code: 1H8P) was used as a scaffold template. In addition, binding of PrC to the two FnII domains of DSP-1 was also studied in silico using the I-TASSER server.

2.6. Differential scanning calorimetry

Differential scanning calorimetric (DSC) measurements were performed using a Nano DSC from TA instruments (New Castle, Delaware, USA) described earlier [30]. DSP-1 (1 mg/mL) in TBS was heated from 20 to 80 $^{\circ}\text{C}$ at a scan rate of 1 $^{\circ}\text{C/min}$ under a constant pressure of 3.0 atm. Buffer base line scan was subtracted from all the sample data to eliminate the contribution from buffer to the calorimetrically measured

heat capacity of the protein. To investigate the effect of PrC binding, DSP-1 was pre-incubated with different concentrations of PrC and experiments were carried out under similar conditions and the thermograms were analysed using 'Gaussian Model' in the DSC data analysis software provided by the manufacturer.

2.7. Steady-state fluorescence studies

Steady state fluorescence measurements were performed using a Spex model Fluoromax-4 fluorescence spectrometer at room temperature, with excitation and emission band pass filters set at 2 and 3 nm, respectively. All experiments were carried out with samples taken in a 1 \times 1 \times 4.5 cm quartz fluorescence cuvette. DSP-1 (0.05 mg/mL) in TBS was excited at 280 nm and emission spectra were recorded between 310 and 400 nm. Titrations to determine the association constants for the binding of ligands were carried out by adding small aliquots of 100 μM Lyso-PC and 20 mM PrC in TBS to DSP-1 solution in the same buffer. Fluorescence spectra were recorded after a 3-minute incubation period.

2.8. Erythrocyte lysis assay

Effect of DSP-1 binding on the erythrocyte membranes (lysis) was investigated by absorption spectroscopy as described earlier [17,18]. A 0.04% suspension of human erythrocytes in TBS was incubated with varying concentrations of DSP-1 and the final volume was adjusted to 0.5 mL with TBS. After incubating the mixture for 90 min, the sample was centrifuged at 3000 rpm for 10 min. The supernatant was collected and its absorbance at 415 nm, corresponding to haem moiety was measured using an Agilent Cary 100 spectrophotometer equipped with a Peltier device for temperature control. For investigating the kinetics of erythrocyte membrane disruption, 150 μg/mL of DSP-1 was incubated with 0.04% RBC suspension in different vials and incubated for different time intervals (5-300 min) before measuring absorbance as described above. To investigate the effect of ligands on erythrocyte lysis, DSP-1 was pre-incubated with PrC, Lyso-PC and choline chloride prior to its addition to the erythrocyte suspension, and the experiment was carried out as described above. Results from a minimum of three independent experiments have been presented along with standard deviations.

2.9. Microscopy

Images of human erythrocytes in presence of DSP-1 were obtained using a Leica TCS SP2 confocal microscope (Heidelberg, Germany) as described earlier [18]. To investigate the effect of DSP-1, a 0.04% suspension of human erythrocytes in TBS was incubated with 150 $\mu g/mL$ of protein. After incubation, 50 μL aliquots of the mixture were taken at 45 min and 90 min, spotted on a clean glass slip (Thermo Fisher) and shifted to confocal stage for imaging. The erythrocyte suspension in TBS alone was used as the control. To investigate the effect of ligand binding, DSP-1 was pre-incubated with 20 mM PrC for 10 min before its addition to the erythrocyte suspension.

3. Results and discussion

3.1. Purification of DSP-1

DSP-1 was purified from donkey seminal plasma by a procedure similar to that used for the purification of HSP-1/2, using affinity chromatography on heparin-agarose and p-aminophenyl phosphorylcholine-agarose (PPC-agarose), followed by RP-HPLC (Fig. S1, Fig. 1A). Heparin-bound and PPC-agarose-bound fraction gave three major peaks when subjected to RP-HPLC. Among the three peaks, the first peak showed highest intensity (Fig. 1A), and migrated as a single band in SDS-PAGE corresponding to a molecular weight of \sim 20 kDa (Fig. 1B). Hence we named this as \underline{D} onkey \underline{S} eminal \underline{P} lasma protein-1 (DSP-1). The second and third peaks also migrated as single bands with

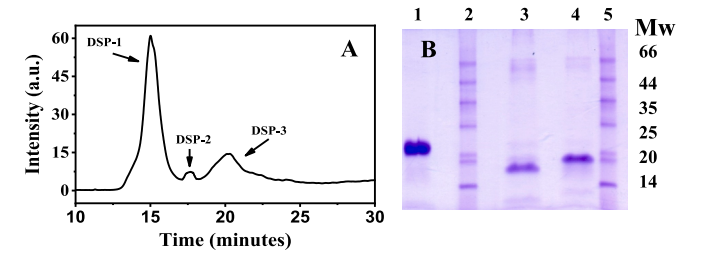


Fig. 1. (A) RP-HPLC chromatogram of heparin-bound and PPC-agarose-bound fraction showing three major peaks. (B) SDS-PAGE of purified donkey seminal plasma proteins: lane 1, DSP-1; lanes 2 & 5, molecular weight markers; lane 3, DSP-2; lane 4, DSP-3.

approximate molecular masses of 16 kDa and 18 kDa, respectively and we refer to them as DSP-2 and DSP-3, respectively (Fig. 1B).

3.2. Mass spectrometric studies

3.2.1. LC-MS

Our previous studies on PDC-109 employing top-down mass spectrometry revealed the presence of several sequence variants [31]. Since DSP-1 exhibited similar characteristics, we expected it to be homologous to PDC-109 and also contain several different proteoforms. Hence, we chose to characterize the primary structure of the protein by employing a combination of database search for proteins similar to PDC-109 in the donkey and sequence analysis of peptides derived by enzymatic fragmentation of DSP-1. The direct infusion ESI FT-ICR MS measurements with DSP-1 showed that the protein is expressed as highly heterogeneous mixture of different proteoforms (Fig. S2). Furthermore, additional peak patterns with 42 Da spacing were observed in the mass spectra, suggesting heterogeneous acetylation of the peptide chain or the attached glycans. For DSP-1, the observed protein masses were around 18.1-20.4 kDa, consistent with the SDS-PAGE analyses. In addition, unidentified polymeric substances, with a repeating unit of 44 Da (indicative of PEG-like compounds), were observed in the samples, which complicated the analysis. Therefore, further LC-MS experiments were performed with intact DSP-1, which confirmed the presence of different glycoforms with multiple acetylations (Fig. 2). Protein deglycosylation experiments using PNGase-F did not change the appearance of the mass spectra, suggesting O-glycosylation, similar to that observed with PDC-109 and HSP-1 [9,32]. The mass spectra also indicated that each DSP-1 glycoform was similarly acetylated.

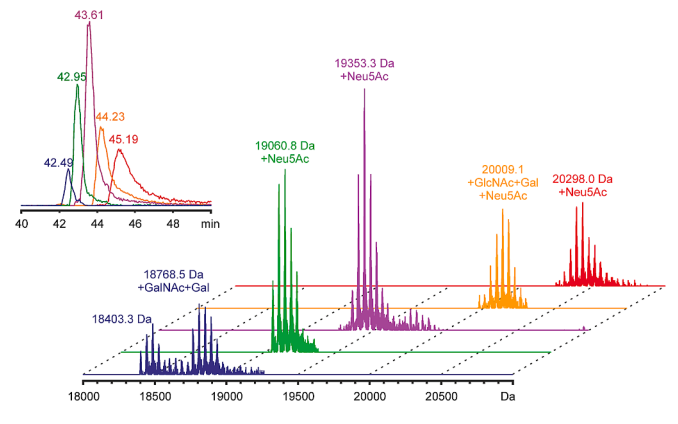


Fig. 2. LC ESI FT-ICR mass analysis of DSP-1. Deconvoluted mass spectra of different glycoforms of DSP-1, eluting at 42.49, 42.95, 43.61, 44.23, and 45.19 min are shown. The inset shows the corresponding extracted ion chromatograms (for the total ion chromatogram, see Supporting Information). The peak patterns observed for different glycoforms are due to multiple protein acetylations (+42 Da). The most abundant isotopic masses are given for the lowest mass species for each glycoform (i.e., the non-acetylated forms).

Since the protein sequences for donkey are very limited and the databases contain mostly predicted sequences based on mRNA, trypsin digestion, and subsequent LC-MS/MS analysis enabled only a partial sequencing and preliminary protein identification. Only peptides from the two FnII domains and the linker between them were found in the mass spectra, possibly due to the presence of a detergent and/or heterogeneous glycosylation suppressing the signals of the *N*-terminal peptides. The eluted peptides did not show typical glycan fragmentation patterns, indicating that *N*-terminal part of the protein was the likely location of the attached glycans, similar to the homologous proteins from other species. Fig. 3 shows the MS/MS sequencing of a peptide obtained from the tryptic digest of DSP-1. The identified peptide, along with other peptides sequenced (Table S2), matched the predicted sequence of 014723758.1 (Fig. 4), thus confirming similarity of these proteins to those from different species.

Based on the expected sequence, the mass of the intact peptide chain of DSP-1 would be 13,954.28 Da, and thus the observed post-translational modifications (glycans, acetylations) covers about 4.0–6.4 kDa of the mass of the native protein.

3.2.2. Top-down MS

To determine the *N*-terminal sequence of the protein, top-down MS experiments were performed. In top-down MS, intact protein ions are isolated and further subjected to MS/MS experiments for sequencing and identifying post-translational modifications. As the fragmentation preferentially occurs in disordered or loop regions, disulfides in DSP-1 were not reduced in order to limit the fragmentation to the mobile linker region and the *N*-terminal part (see Section 3.4 for protein models). All top-down MS experiments were performed on a high-resolution QTOF mass spectrometer to obtain high fragmentation efficiency for intact protein ions. To maximize the fragment ion intensity,

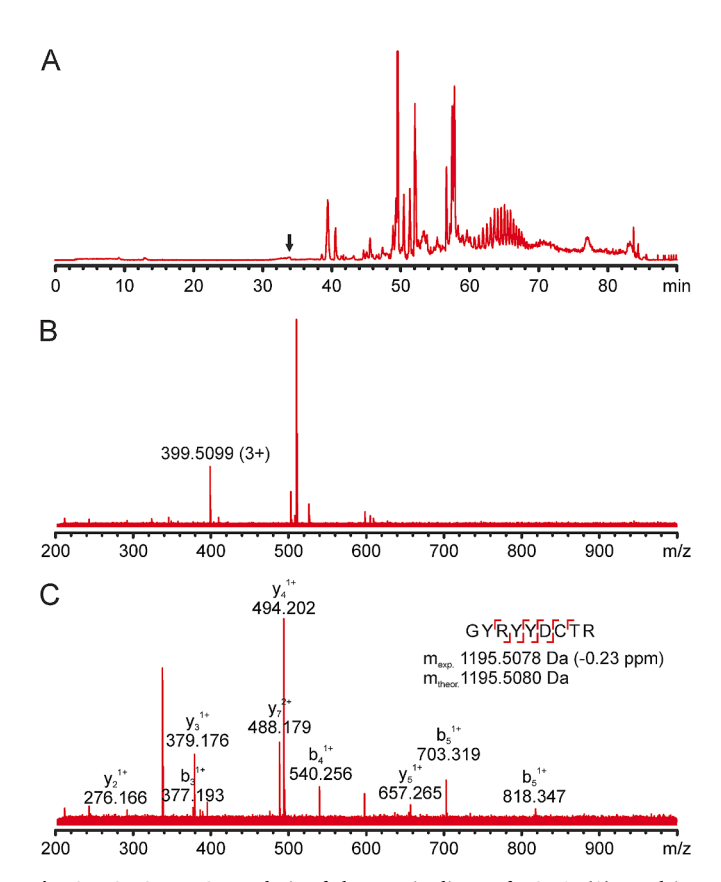


Fig. 3. LC ESI FT-ICR analysis of the tryptic digest of DSP-1. (A) Total ion chromatogram (polymeric impurities are seen at 60-70 min), (B) isolation of a triply charged peptide eluting at 34 min (m/z 399.5099) and (C) MS/MS fragmentation of the peptide with the identified b and y fragments.

predicted signal peptide MAPRIGIFLIWAGTCIFLQLDHVDG-

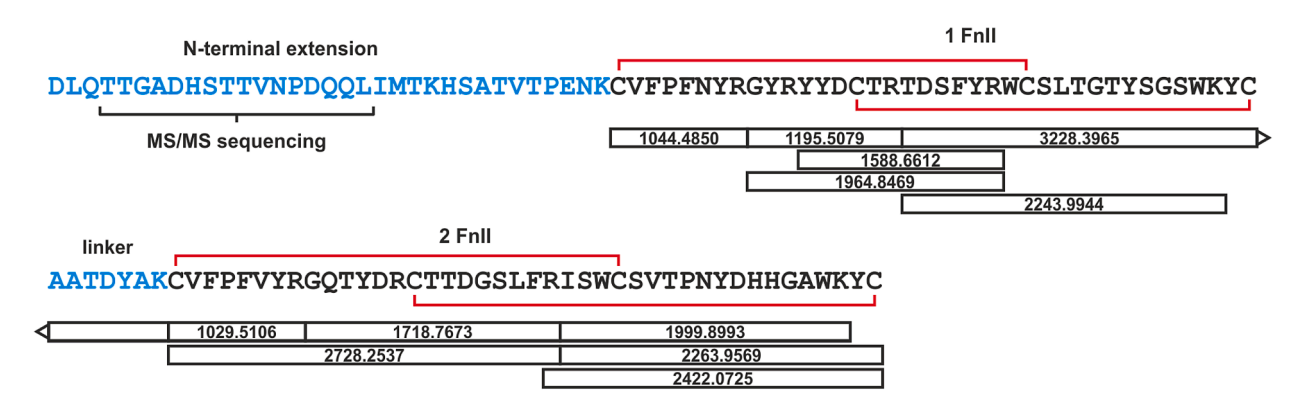


Fig. 4. Putative amino acid sequence of DSP-1 with the identified tryptic peptides and their monoisotopic masses indicated. The disulfide linkages shown are based on similarity with those observed in other homologous mammalian seminal FnII proteins PDC-109 and HSP-1/2. The *N*-terminal extension part is most likely missing due to the observed protein modifications (glycosylation/acetylations), and was characterized by additional top-down MS experiments.

top-down experiments were performed without a precursor ion isolation.

In low-energy conditions, (collision energy \sim 50 eV) the mass spectra showed mainly small fragment ions with m/z values corresponding to different glycan fragments (Fig. S3A). The fragmentation of glycopeptides typically results in the cleavage of glycosidic bonds, and the subsequent formation of different oligosaccharides depending on the glycan structures. These fragments can be used for the glycan structure annotations; however, information on the glycan locations within the polypeptide chain are lost. Although there is also a plausible *N*-glycosylation site (NKC) in DSP-1, based on the sequence and type of glycosylations observed in other homologous proteins, it is highly likely that the protein contains O-glycosylation. Since the O-glycans are typically small, containing only a few carbohydrate residues, it is assumed that there are multiple sites in DSP-1 where the glycans are attached, most likely threonine and serine residues as observed in PDC-109, HSP-1 and BSP-30-kDa protein [9,32,33]. Similar to BSP-30k, we observed several Nacetylgalactosamine (GalNAc) and galactose (Gal) containing di- and trisaccharides which are further modified by attachment of sialic acid or acetylated sialic acid residues (Neu5Ac/Neu5, xAc2) residues. This further proves that glycosylation in DSP-1 occurs in the solvent-exposed serine or threonine residues within the *N*-terminal region, similar to the other homologous proteins. In addition, heterogeneous acetylation occurs in the attached sialic acid residues, observed only in top-down MS/ MS experiments [34].

Moreover, large (\sim 14 kDa) fragment ions were also observed at $m/z\sim2000$, corresponding to the protein fragments resulting from the complete glycan removals from the polypeptide chain. Among these ions, a fragment ion with a mass of 13,954.33 Da was observed, matching to the proposed amino acid sequence of DSP-1. In high-energy conditions (collision energy \sim 170 eV), additional fragments corresponding to the N-terminal region were detected in the mass spectra (Fig. S3B), further verifying the proposed sequence of DSP-1. The MS/MS spectra also proved that the observed acetylations occur only in the sialic acid residues attached to glycans and no fragment ions corresponding to the acetylation occurring in the peptide chain were observed. In addition, the MS/MS experiments suggest that there are no major sequence variants of DSP-1 present in the sample, and the observed heterogeneity is solely a result of the heterogeneous O-glycosylation with multiple acetylations.

Multiple sequence alignment of the primary structure of DSP-1 with the seminal plasma FnII proteins from other mammals, viz., bull, horse, pig, mouse and human is given in Fig. 5. From this alignment it can be seen that the primary structure of DSP-1 exhibits highest homology to

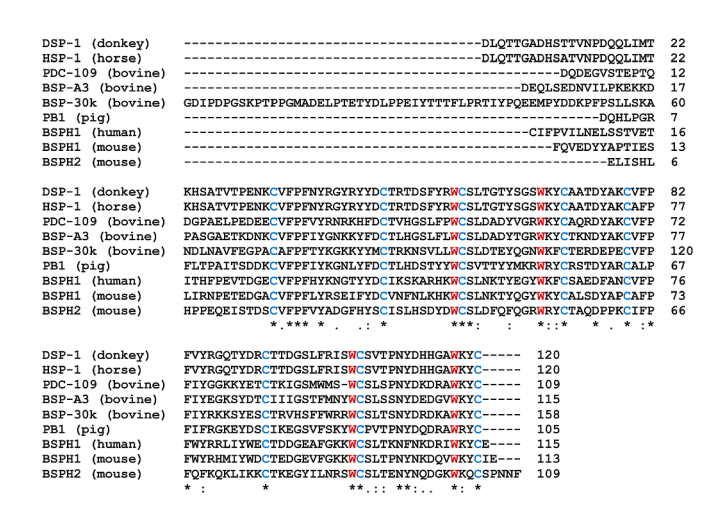


Fig. 5. Multiple sequence alignment of the primary structure of DSP-1 with the seminal plasma FnII proteins from different mammalian species. Only proteins containing 2 FnII domains have been selected. All sequences were taken from EMBL-EBI database and aligned using Clustal Omega program (https://www. ebi.ac.uk/Tools/msa/clustalo/) without the signal sequences. The different proteins used in the alignment (with database IDs in brackets) are: horse seminal plasma protein, HSP-1 (SP:P81121); porcine (pig) seminal plasma protein, PB1 (SP:P80964); bovine seminal plasma proteins PDC-109 (SP: P02784), BSP-A3 (SP:P04557) and BSP-30k (SP:P81019); human seminal plasma protein, BSPH1 (SP:Q075Z2); mouse seminal plasma proteins, BSPH1 (SP:Q3UW26) and BSPH2 (SP:Q0Q236). Conserved cysteine residues involved in disulfide bonds are shown in bold cyan, conserved core tryptophans are shown in bold red. Residues that are fully conserved across all species (*) and residues that are similar (: and .) are indicated. (For interpretation of the references to colour in this figure legend, the reader is referred to the web version of this article.)

the amino acid sequence of HSP-1, with only two residues differing between the two proteins, wherein Ala-11 and Ala-80 in HSP-1 are replaced by Thr residues in DSP-1. Extensive homology is also seen among all these proteins, with all the 8 Cys residues involved in disulfide bond formation in the FnII domains as well as the 4 core Trp residues that have been shown to be crucial for ligand binding and chaperone-like activity of PDC-109 [27] being conserved among all these proteins.

3.3. Secondary and tertiary structure of DSP-1

The secondary and tertiary structures of DSP-1 were characterized by CD spectroscopy. Far-UV CD spectra of DSP-1 alone and in the presence of 50 mM PrC, the head group moiety of its physiological ligand, phosphatidylcholine are shown in Fig. 6A. The spectrum of DSP-1 alone (black) is characterized by a broad positive asymmetric band with maxima at 226 nm and 220 nm and two shoulders at $\sim\!212$ nm and 209 nm. In the presence of PrC (red), these bands shift to 225, 217 and 207 nm without major changes in the spectral intensity. The near-UV CD spectrum of DSP-1 contains three overlapping positive bands with maxima at $\sim\!260$ nm, $\sim\!274$ nm and $\sim\!288$ nm (Fig. 6B). The positive band in far-UV CD spectrum of DSP-1 could not be analysed to obtain the secondary structural elements of the protein, due to lack of suitable reference dataset, as was the case with PDC-109 [12].

Far-UV CD spectra of DSP-1 recorded at various temperatures between 25 and 55 °C show that the spectral intensity decreases steadily with increase in temperature suggesting a gradual loss of the secondary structure of the protein (Fig. 6C). Broadly similar changes were seen in the near UV CD spectra (Fig. S4A). In contrast, in the presence of 50 mM PrC, only moderate changes were seen in the far- as well as near-UV CD spectra between 25 and 55 °C, whereas significant decrease in signal intensity was observed with further increase in temperature with large decrease being seen between 60 and 70 °C (Figs. 6D, S4B). The thermal stability of DSP-1 and the effect of ligand binding on it was also investigated by monitoring the CD signal intensity of the protein at 225 nm as a function of temperature in the absence and presence of different concentrations of PrC (Fig. 6E). The signal intensity of native DSP-1 decreases with the steepest decline being seen at ~43 °C (black line), which is taken as the midpoint of thermal unfolding of the protein. In the presence of 10 mM PrC the unfolding shifted to $\sim \! 58~^{\circ} \text{C}$ (red line) and upon further increase in the concentration of PrC to 20 and 50 mM, the unfolding temperature further shifted to ${\sim}62~^{\circ}\text{C}$ (green) and 64 $^{\circ}\text{C}$ (violet), respectively.

3.4. Computational modeling of DSP-1 structure and binding of PrC

As the secondary structure of DSP-1 could not be determined from the near-UV CD spectra, we used computational methods to obtain a 3dimensional structural model of DSP-1 using Iterative Threading AS-SEmbly Refinement (I-TASSER) server (http://zhanglab.dcmb.med. umich.edu/I-TASSER) using the reported crystal structure of PDC-109 (pdb code: 1h8p) as the template. The modeled structure of DSP-1 is shown in Fig. 7 together with the modeled structures of PDC-109 and HSP-1, taken from our earlier study on HSP-1/2 [20]. A careful observation of the models indicates that the overall structure of DSP-1 is very similar to those of HSP-1 and PDC-109. Further, the relative content of various secondary structures of the three proteins, deduced from the computational models are rather similar, with all three proteins containing very little α -helix and about 25% β -sheet, whereas \sim 70% of the residues are present in β -turns and unordered structures (Table 1). In addition, comparison of the relative content of various secondary structural elements of PDC-109 - deduced from its crystal structure -

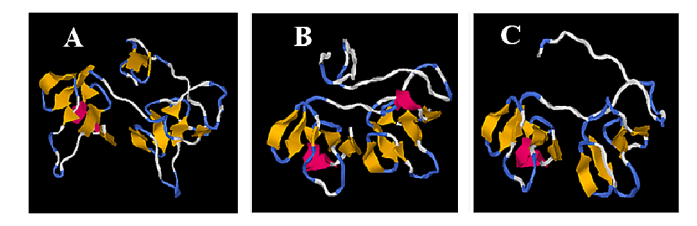


Fig. 7. Three-dimensional structures of DSP-1 (A), HSP-1 (B) and PDC-109 (C) generated by I-TASSER server.

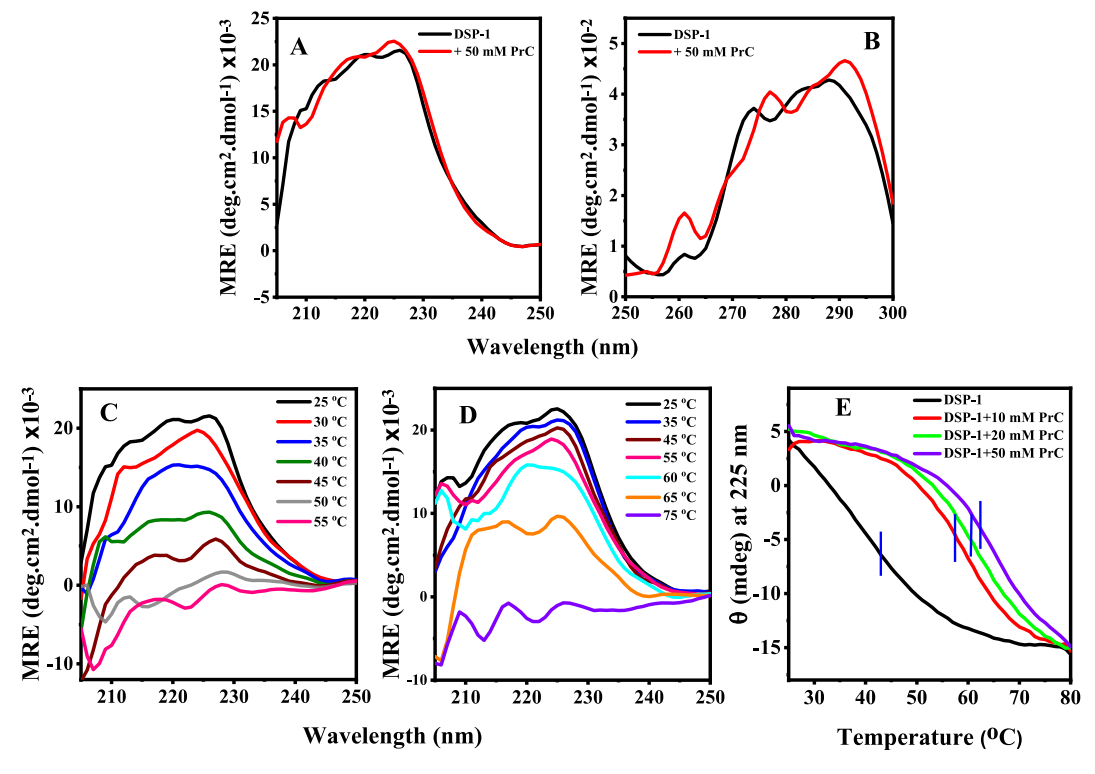


Fig. 6. CD spectroscopic studies of DSP-1. (A, B) Far- and near-UV CD spectra of DSP-1 alone (black) and in the presence of 50 mM PrC (red). Far-UV CD spectra of DSP-1 at various temperatures in absence (C) and presence (D) of 50 mM PrC. (E) Effect of PrC on the thermal stability of DSP-1. The CD signal intensity of the protein at 225 nm was recorded as the temperature was increased at a scan rate of 1° /min. Protein concentration was 0.1 mg/mL in all samples. Concentration of PrC in different samples is: black, 0 mM; red, 10 mM; green, 20 mM; violet, 50 mM. (For interpretation of the references to colour in this figure legend, the reader is referred to the web version of this article.)

Table 1Secondary structure of DSP-1, HSP-1 and PDC-109 estimated from computational modeling using the I-TASSER server. Secondary structure of PDC-109 determined from the crystal structure (pdb code: 1h8p) is also given for comparison.

Protein	α-Helix	β-Sheet	β-Turns + unordered structures
DSP-1	3.3	25.0	71.7
HSP-1	5.8	25.0	69.1
PDC-109 (from modeling)	3.7	23.8	72.4
PDC-109 (from crystal structure)	9.2	22.9	67.8

with the results obtained in the present modeling studies shows a very good correlation (Table 1).

Along with building a 3-D model of DSP-1 we also investigated the binding of PrC to its FnII domains using the I-TASSER server. The structures of the first and second FnII domains of DSP-1 with bound PrC molecules are shown in Fig. 8A and D, respectively. The binding of PrC is mediated by multiple weak interactions including cation- π , O-H···O and C-H···O hydrogen bonds as well as C-H··· π interactions. The cation- π interactions in the two FnII domains are shown in Fig. 8B and E, whereas the H-bonding and C-H $\cdots\pi$ interactions are shown in Fig. 8C and F. It is noteworthy that in the first FnII domain of DSP-1, 4 out of the 5 residues that interact with PrC, namely Y40, Y64, W57 and W68 are fully conserved, whereas D52 is highly conserved among the FnII proteins whose sequences are used for comparison in the multiple sequence alignment shown in Fig. 5. Similarly, in the second FnII domain, W104, Y111 and W117, which interact with PrC are fully conserved whereas S98 which forms an important O-H O hydrogen bond with PrC is conserved in 6 out of 9 sequences.

3.5. Thermal denaturation of DSP-1 and the effect of ligand binding

To investigate the thermal unfolding of DSP-1 in more detail, especially to obtain the thermodynamic parameters associated with it,

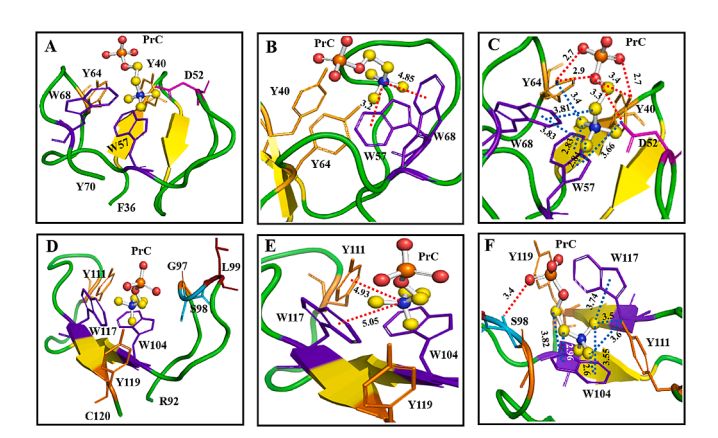


Fig. 8. Structure of the FnII domains of DSP-1 with bound PrC, generated using I-TASSER. The structures have been visualized using PyMOL. (A) The side chains of residues involved in ligand binding (domain-I) Y40, Y64, D52, W57 and W68 are shown in stick format; (B) the cation- π interaction of the quaternary ammonium group with W57 and W68 are indicated by red dotted lines; (C) hydrogen bonds between the hydroxyls of Y40 and Y64 and the phosphate oxygens are shown in red dotted lines and the possible CH- π and CH-O interactions are in blue dotted line; (D) the site chains of residues involved in ligand binding (domain-II) G97, S98, L99, W104, W117, Y111 and Y119 are shown in stick format; (E) the cation- π interaction of the quaternary ammonium group with Y111 and W117 are indicated by red dotted lines and (F) hydrogen bonds between the hydroxyls of S98 and the phosphate oxygen is shown in red dotted line and the possible CH- π and CH-O interactions are in blue dotted line. (For interpretation of the references to colour in this figure legend, the reader is referred to the web version of this article.)

differential scanning calorimetric studies were performed. Thermograms of DSP-1 alone and in the presence of different concentrations of PrC are shown in Fig. 9. The thermogram of native DSP-1 exhibits two thermotropic transitions centred at \sim 32.4 (\pm 0.2) and 43.1 (\pm 0.3) $^{\circ}$ C (Fig. 9A). The transition occurring at the lower temperature could be attributed to the dissociation of the oligomeric form of DSP-1 to monomers whereas the higher temperature transition can be attributed to the complete unfolding of the monomer. This suggests that the thermal unfolding of DSP-1 is a three-state transition with two partially overlapping, yet distinct transitions. That the higher temperature transition corresponds to the protein unfolding is supported by the results of CD spectroscopic studies which showed a steep decrease in the spectral intensity at 225 nm at 43 °C. Importantly, in the presence of PrC, the thermogram of DSP-1 exhibits only a single transition. These observations are similar to those made with PDC-109 and indicate that binding of PrC decreases the polydisperse nature of DSP-1 [12]. In the presence of different concentrations of PrC, the transition temperature and transition enthalpy increased with increasing concentrations of the ligand (Fig. 9B, Table S1). The temperature corresponding to the major thermotropic transition of DSP-1 shifted from 43.1 (± 0.3) °C in the absence of PrC to \sim 60.6 (\pm 0.3) °C in the presence of 50 mM PrC, with a concomitant increase in the transition enthalpy from 258 kJ/mol to 411 kJ/mol. These observations strongly suggest that PrC binding stabilizes the structure of DSP-1 and increases its unfolding temperature.

3.6. Fluorescence studies on the binding of PrC and Lyso-PC to DSP-1

To obtain quantitative information on ligand binding to DSP-1, we performed fluorescence spectroscopic studies in which DSP-1 was titrated with PrC and Lyso-PC in separate experiments and changes in the protein intrinsic fluorescence properties have been monitored. Fluorescence spectra corresponding to the titration with PrC are given in Fig. S5 and plots reporting the analysis of the titration data are given in Fig. 10 and the corresponding plots for the binding of Lyso-PC are given in Fig. S6. It was observed that addition of each aliquot of PrC resulted in a small decrease in the emission intensity of the protein (Fig. S5) with a concomitant blue shift in the emission maximum, and a plot of change in fluorescence emission intensity at 360 nm (Δ F) versus the ligand concentration showed saturation behaviour (Fig. 10B). For Lyso-PC binding, due to a larger blue shift in the emission maximum, the difference spectra showed a maximum centred around 317 nm and a minimum centred around 365 nm (Fig. S6A). Therefore, the change in fluorescence

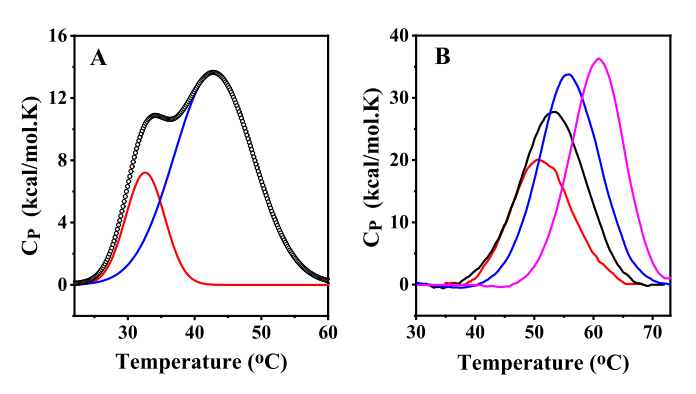


Fig. 9. Differential scanning calorimetry of DSP-1. (A) DSC thermogram of native DSP-1. Open circles correspond to the experimental data and the red and blue lines correspond to the deconvoluted components. (B) Thermograms of DSP-1 in presence of different concentration of PrC: 5 mM (red), 10 mM (black), 20 mM (blue) and 50 mM (purple). The thermogram of DSP-1 alone could be best fitted to two thermotropic transitions centred at about 32 °C (red line) and 43 °C (blue line). Thermograms obtained in the presence of PrC could be fitted satisfactorily to a single transition. (For interpretation of the references to colour in this figure legend, the reader is referred to the web version of this article.)

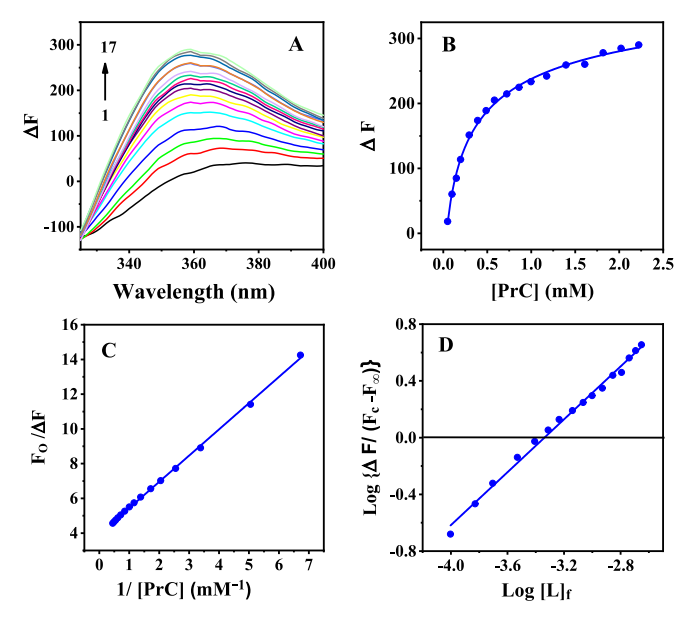


Fig. 10. Fluorescence titration to determine the association constant, K_a for PrC binding to DSP-1. (A) Fluorescence difference spectra of DSP-1 obtained in the presence of various concentrations of PrC. (B) Binding curve obtained by plotting ΔF versus [PrC]. (C) A double reciprocal plot of $F_o/\Delta F$ versus 1/[PrC]. From the Y-intercept of the plot F_∞ , the fluorescence intensity of the protein at saturation binding is obtained. (D) A double log plot of [log $\{\Delta F/(F_c - F_\infty)\}$] versus log [L]_F. From the X-intercept of the plot the association constant, K_a for PrC binding to DSP-1 is obtained. See text for details.

intensity at 317 nm was used to obtain the binding curve (Fig. S6B).

The titration data was further analysed using the Chipman plot in order to obtain the association constant, K_a as described earlier for the interaction of these ligands to PDC-109 [14,35]. In brief, a plot of $1/\Delta F$ versus $1/[L]_t$ where ΔF (= $|F_o-F_c|$) refers to the change in fluorescence intensity at any point of in the titration and F_o and F_c correspond to the fluorescence intensity of DSP-1 alone and in the presence of ligand (PrC or Lyso-PC), respectively, and $[L]_t$ is the corresponding total ligand concentration (Figs. 10C, S6C). From the ordinate intercept of the plot, F_∞ , fluorescence intensity of the sample at infinite concentration, was calculated. The titration data was further analysed according to the following expression [14,35]:

$$Log \{\Delta F/(F_c - F_\infty)\} = log K_a + log [L]_f$$
(1)

where [L]_f, the free ligand concentration, is given by:

$$[L]_f = [L]_t - \left\{ (\Delta F / \Delta F_{\infty})[P]_t \right\} \tag{2}$$

where [L]_t and [P]_t are total ligand concentration and total protein concentration, respectively, and ΔF_{∞} (=F_o - F_{\infty}) is the change in fluorescence intensity at infinite concentration (saturation). From the X-intercepts of plots of log {\Delta F / (F_c - F_{\infty})} versus log [L]_f the association constant, K_a for the binding of PrC and Lyso-PC to DSP-1 were determined (Figs. 10D, S6D). The association constants thus obtained were 2.16 (±0.03) × 10³ M⁻¹ for PrC and 2.72 (±0.09) × 10⁵ M⁻¹ for Lyso-PC (averages of two independent titrations). These results show that DSP-1 binding of Lyso-PC is two orders of magnitude stronger than its association with PrC.

The blue shift observed in the fluorescence emission of DSP-1 upon interaction with PrC and Lyso-PC is similar to the results obtained with PDC-109 and HSP-1/2 [14,36]. This indicates that the microenvironment around Trp residues involved in the lipid binding becomes more hydrophobic upon binding of these ligands containing choline moiety.

3.7. Spectrophotometric and microscopic studies on DSP-1 binding to erythrocytes

To investigate the effect of DSP-1 binding on the cell membrane, human erythrocytes were taken as a model cell system since both erythrocytes and spermatozoa of different mammalian species contain a high proportion of choline phospholipids [37–40]. Binding of DSP-1 to erythrocytes disrupted their membrane structure and led to cell lysis and release of haemoglobin into the solution. This process was monitored by measuring absorption at 415 nm corresponding to the haem bound to haemoglobin [17]. When erythrocytes were incubated with DSP-1 the amount of haemoglobin released increased with increasing concentration of DSP-1, indicating concentration-dependent membrane destabilization, and reached saturation at \sim 250 µg/mL (Fig. 11A). Kinetics of DSP-1 induced erythrocyte destabilization, monitored over time periods of 5-300 min showed that the release of haemoglobin increased with increasing incubation time up to 240 min and then remained constant (Fig. 11B). These results show that DSP-1 can destabilized the erythrocyte membrane in a time- and concentration-dependent manner.

Further, to examine the specificity of erythrocyte lysis induced by DSP-1, the protein was pre-incubated with different concentrations of Lyso-PC, PrC and choline chloride, which can block its phospholipid binding site, thus hindering its binding to the erythrocyte membrane. In these experiments a decrease in the erythrocyte lysis was observed (Fig. 11C), clearly establishing that DSP-1 induced erythrocyte lysis is due to membrane perturbation by this protein, which is mediated by its binding to choline phospholipids present on the erythrocyte membrane. While 50 µM Lyso-PC could inhibit the cell lysis by >90%, similar inhibition was achieved only at 1-2 mM concentrations of PrC, whereas inhibition by choline chloride was considerably weaker even at 50 mM concentration (Fig. 11C). These observations are consistent with the significantly higher association constant estimated for the binding of Lyso-PC to DSP-1 than PrC. Interestingly, incubation with \geq 200 μ M Lyso-PC resulted in strong lysis of the erythrocytes (not shown). This is most likely due to the detergent-like activity of this amphiphile.

Erythrocyte membrane lysis induced by DSP-1 was also investigated by confocal microscopy. In these studies, human erythrocytes were imaged in buffer and upon pre-incubation with DSP-1 at different time intervals. Images of erythrocytes alone in buffer show well-defined morphology (Fig. 11D), whereas upon incubation with DSP-1 for 90 min, no erythrocytes were observed and only few membrane fragments

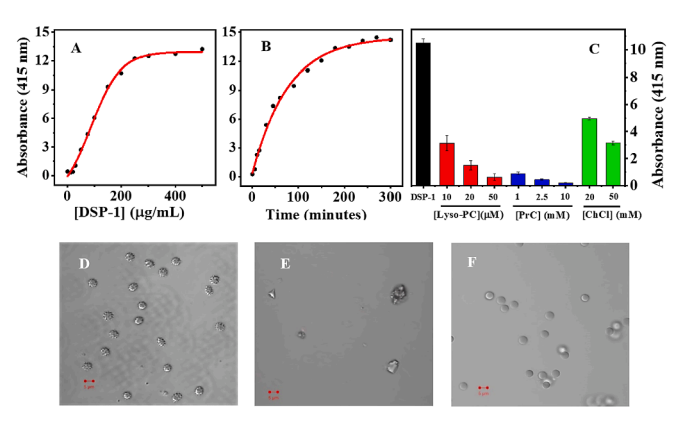


Fig. 11. Effect of DSP-1 on human erythrocyte membrane. (A) Effect of increasing the concentration of DSP-1 on erythrocyte lysis. (B) Kinetics of erythrocyte lysis induced by DSP-1. The protein concentration in each sample was 100 $\mu g/mL$. (C) Erythrocyte lysis induced by DSP-1 alone and upon preincubation with different concentrations of Lyso-PC, PrC and choline chloride. Absorbance at 415 nm was measured to detect the haemoglobin released upon cell lysis. (D-F) Confocal images of human erythrocytes under different conditions: (D) in TBS buffer alone, (E) upon incubation for 90 min with 200 $\mu g/mL$ DSP-1 and (F) upon incubation with 200 $\mu g/mL$ DSP-1 and 20 mM PrC for 60 min. Scale bar $=5~\mu m$.

were visible indicating that most of the erythrocyte were lysed and their membranes were broken down to smaller fragments (Fig. 11E). Preincubation of DSP-1 with 20 mM PrC prevented the erythrocyte lysis (Fig. 11F), clearly establishing that binding of DSP-1 to choline phospholipids on the erythrocyte membrane is obligatory for its membrane perturbing activity.

Seminal FnII proteins constitute the major protein fraction in the seminal plasma of various mammals. The seminal FnII proteins from a number of mammals have been isolated, purified and characterized, both structurally and functionally using various biochemical and biophysical methods [13,41]. Extensive studies were carried out to investigate their interaction with choline phospholipids, their physiological ligand. Their role in cholesterol efflux and 'sperm capacitation' has been the main focus of investigation in a majority of these studies [4-8,14-18]. The recent discovery of chaperone-like activity (CLA) of the seminal FnII proteins has grouped them into small heat shock protein (shsp) family and a more significant role/function of these proteins has been postulated as they are the only proteins that exhibit protection towards other proteins against various stress conditions in the seminal plasma [19-21]. In this context, the present study reporting the purification and characterization of a major seminal FnII protein present in the donkey seminal plasma assumes relevance. Further work to characterize the chaperone-like activity of DSP-1 is currently underway in our laboratory.

In summary, we successfully purified DSP-1, a major protein from donkey seminal plasma that belongs to seminal FnII protein family and carried out primary, secondary, tertiary and quaternary structural characterization of this protein. The protein was observed to be heterogeneously modified by O-glycosylation with acetylated sialic acid residues. Thermal unfolding studies have shown that DSP-1 exhibits polydispersity along with structural flexibility that is intrinsic in nature and plays a major role in its structural stability. Binding of PrC and Lyso-PC to DSP-1 has been characterized by fluorescence titrations and it was found that DSP-1 exhibits higher binding strength towards PrC and Lyso-PC as compared to PDC-109. Binding of PrC to DSP-1 not only results in a thermal stabilization of the protein but also reduces its polydisperse nature. Furthermore, membrane perturbing activity of DSP-1 was investigated under in vivo-mimicking conditions with model cell membranes (erythrocytes) and it was found that DSP-1 induces membrane destabilization and causes cell lysis. This could be of considerable physiological significance since similar activity of FnII proteins on sperm cell membrane has been reported to be important for inducing acrosome reaction in spermatozoa and subsequent sperm 'capacitation' in various mammals [41]. Since the role of seminal FnII proteins is expanding beyond their role in sperm capacitation as shsps and other regulatory activities, DSP-1 functions and activities will be explored in that direction. Currently, CLA of DSP-1 is being investigated indicating its role as a shsp, which exhibits chaperone activity against various client proteins.

CRediT authorship contribution statement

Sk Alim: Investigation; Data curation; Formal analysis; Methodology; Writing - original draft.

Sudheer K. Cheppali: Investigation; Methodology; Writing - part of original draft.

Mikko Laitaoja: Investigation - mass spectrometric studies; Writing - part of original draft.

Thirumala Rao Talluri: Methodology - sample collection and processing.

Janne Jänis: Resources; Supervision - mass spectrometric studies; Funding acquisition; Writing - review & editing.

Musti J. Swamy: Conceptualization, Project administration; Resources; Supervision; Funding acquisition; Writing - review & editing.

Declaration of competing interest

The authors declare that they have no conflicts of interest with the contents of this article.

Acknowledgements

This work was supported by research grants from the DST (India) and IoE program of the UGC (India) from the University of Hyderabad to MJS. SA is the recipient of a Maulana Azad National Fellowship from UGC (India). SKC was a Senior Research Fellow of CSIR (India). Financial and infrastructure support from the UGC (through the UPE-II and CAS programs) and the DST (through the PURSE and FIST programs) are gratefully acknowledged. The FT-ICR MS facility is supported by Biocenter Finland/FINStruct, Biocenter Kuopio, the European Regional Development Fund (grant A70135) and the EU's Horizon 2020 Research and Innovation Programme (EU FT-ICR MS project; grant 731077).

Appendix A. Supplementary data

Supplementary data to this article can be found online at https://doi.org/10.1016/j.ijbiomac.2021.11.177.

References

- P.E. Visconti, H. Calantino-Hormer, G.D. Moore, J.L. Bailey, X. Ning, M. Fornes, G. S. Kopf, The molecular basis of sperm capacitation, J. Androl. 19 (1998) 242–248.
- [2] R. Yanagimachi, Mammalian fertilization, in: E. Knobil, J. Neill (Eds.), Physiology of Reproduction, Raven Press, New York, 1994, pp. 189–317.
- [3] R.A.P. Harrison, Capacitation mechanisms and the role of capacitation as seen in eutherian mammals, Reprod. Fertil. Dev. 8 (1996) 581–596.
- [4] L. Desnoyers, P. Manjunath, Major proteins of bovine seminal plasma exhibit novel interactions with phospholipids, J. Biol. Chem. 267 (1992) 10149–10155.
- [5] M. Ramakrishnan, V. Anbazhagan, T.V. Pratap, D. Marsh, M.J. Swamy, Membrane insertion and lipid-protein interactions of bovine seminal plasma protein PDC-109 investigated by spin-label electron spin resonance spectroscopy, Biophys. J. 81 (2001) 2215–2225.
- [6] A. Greube, K. Müller, E. Töpfer-Petersen, A. Herrmann, P. Müller, Interaction of fn type II proteins with membranes: stallion seminal plasma protein SP-1/2, Biochemistry 43 (2004) 464–472.
- [7] M.J. Swamy, D. Marsh, V. Anbazhagan, M. Ramakrishnan, Effect of cholesterol on the interaction of seminal plasma protein, PDC-109 with phosphatidylcholine membranes, FEBS Lett. 528 (2002) 230–234.
- [8] D.A. Wah, C. Fernández-Tornero, L. Sanz, A. Romero, J.J. Calvete, Sperm coating mechanism from the 1.8 Å crystal structure of PDC-109-phosphorylcholine complex, Structure 10 (2002) 505–514.
- [9] J.J. Calvete, K.H. Mann, W. Schafer, L. Sanz, M. Reinert, S. Nessau, E. Töpfer-Petersen, Amino acid sequence of HSP-1, a major protein of stallion seminal plasma: effect of glycosylation on its heparin-and gelatin-binding capabilities, Biochem. J. 310 (1995) 615–622.
- [10] J.J. Calvete, S. Nessau, K. Mann, L. Sanz, H. Sieme, E. Klug, E. Töpfer-Petersen, Isolation and biochemical characterization of stallion seminal plasma proteins, Reprod. Domest. Anim. 29 (1994) 411–426.
- [11] J.J. Calvete, M. Reinert, L. Sanz, E. Töpfer-Petersen, Effect of glycosylation on the heparin-binding capability of boar and stallion seminal plasma proteins, J. Chromatogr. A 711 (1995) 167–173.
- [12] M. Gasset, J.L. Saiz, L. Sanz, M. Gentzel, E. Töpfer-Petersen, J.J. Calvete, Conformational features and thermal stability of bovine seminal plasma protein PDC-109 oligomers and phosphoryl choline bound complexes, Eur. J. Biochem. 250 (1997) 735–744.
- [13] M.J. Swamy, Interaction of bovine seminal plasma proteins with model membranes and sperm plasma membranes, Curr. Sci. 87 (2004) 203–212.
- [14] V. Anbazhagan, M.J. Swamy, Thermodynamics of phosphorylcholine and lysophosphatidylcholine binding to the major protein of bovine seminal plasma, PDC-109, FEBS Lett. 579 (2005) 2933–2938.
- [15] A. Tannert, A. Kurz, K.R. Erlemann, K. Müller, A. Herrmann, J. Schille, E. Töpfer-Petersen, P. Manjunath, P. Müller, The bovine seminal plasma protein PDC-109 extracts phosphorylcholine-containing lipids from the outer membrane leaflet, Eur. Biophys. J. 36 (2007) 461–475.
- [16] V. Anbazhagan, R.S. Sankhala, B.P. Singh, M.J. Swamy, Isothermal titration calorimetric studies on the interaction of the major bovine seminal plasma protein, PDC-109 with phospholipid membranes, PLoS ONE 6 (2011), e25993.
- [17] R.S. Damai, R.S. Sankhala, V. Anbazhagan, M.J. Swamy, 31P-NMR and AFM studies on the destabilization of cell and model membranes by the major bovine seminal plasma protein, PDC-109, IUBMB Life 62 (2010) 841–851.
- [18] C.S. Kumar, M.J. Swamy, A pH switch regulates the inverse relationship between membranolytic and chaperone-like activities of HSP-1/2, a major protein of horse seminal plasma, Biochemistry 55 (2016) 3650–3657.

- [19] R.S. Sankhala, M.J. Swamy, The major protein of bovine seminal plasma, PDC-109 is a molecular chaperone, Biochemistry 49 (2010) 3908–3918.
- [20] R.S. Sankhala, C.S. Kumar, B.P. Singh, A. Arangasamy, M.J. Swamy, HSP-1/2, a major protein of equine seminal plasma, exhibits chaperone-like activity, Biochem. Biophys. Res. Commun. 427 (2012) 18–23.
- [21] C.S. Kumar, M.J. Swamy, HSP-1/2, a major horse seminal plasma protein, acts as a chaperone against oxidative stress, Biochem. Biophys. Res. Commun. 473 (2016) 1058–1063.
- [22] R.S. Sankhala, R.S. Damai, M.J. Swamy, Correlation of membrane binding and hydrophobicity to the chaperone-like activity of PDC-109, PLoS ONE 6 (2011), e17330.
- [23] C.S. Kumar, M.J. Swamy, Differential modulation of chaperone-like activity of HSP-1/2, a major protein of horse seminal plasma by anionic and cationic surfactants, Int. J. Biol. Macromol. 96 (2017) 524–531.
- [24] C.S. Kumar, M.J. Swamy, Modulation of chaperone-like and membranolytic activities of major horse seminal plasma protein HSP-1/2 by L-carnitine, J. Biosci. 42 (2017) 469–479.
- [25] C.S. Kumar, B.P. Singh, S. Alim, M.J. Swamy, Factors influencing the chaperone-like activity of major proteins of mammalian seminal plasma, equine HSP-1/2 and bovine PDC-109: effect of membrane binding, pH and ionic strength, Adv. Exp. Med. Biol. 5 (2018) 53-68.
- [26] B.P. Singh, R.S. Sankhala, A. Asthana, T. Ramakrishna, Ch.M. Rao, M.J. Swamy, Glycosylation differentially modulates membranolytic and chaperone-like activities of PDC-109, the major protein of bovine seminal plasma, Biochem. Biophys. Res. Commun. 511 (2018) 28–34.
- [27] B.P. Singh, A. Asthana, A. Basu, T. Ramakrishna, Ch.M. Rao, M.J. Swamy, Conserved core tryptophans of FnII domains are crucial for the membranolytic and chaperone-like activities of bovine seminal plasma protein, PDC-109, FEBS Lett. 594 (2020) 509–518.
- [28] U.K. Laemmli, Cleavage of structural proteins during the assembly of the head of bacteriophage T4, Nature 227 (1970) 680–685.
- [29] J.J.A. Armenteros, K.D. Tsirigos, C.K. Sønderby, T.N. Petersen, O. Winther, S. Brunak, G. von Heijne, H. Nielsen, SignalP 5.0 improves signal peptide predictions using deep neural networks, Nat. Biotechnol. 37 (2019) 420–423.

- [30] S. Mondal, M.J. Swamy, Purification, biochemical/biophysical characterization and chitooligosaccharide binding to BGL24, a new PP2-type phloem exudate lectin from bottle gourd (Lagenaria siceraria), Int. J. Biol. Macromol. 164 (2020) 3656–3666.
- [31] M. Laitaoja, R.S. Sankhala, M.J. Swamy, J. Jänis, Top-down mass spectrometry reveals new sequence variants of the major bovine seminal plasma protein PDC-109, J. Mass Spectrom. 47 (2012) 853–859.
- [32] J.J. Calvete, M. Raida, L. Sanz, F. Wempe, K.-H. Scheit, A. Romero, E. Töpfer-Petersen, Localization and structural characterization of an oligosaccharide Olinked to bovine PDC-109, FEBS Lett. 350 (1994) 203–206.
- [33] J.J. Calvete, K. Mann, L. Sanz, M. Raida, E. Tdpfer-Petersen, The primary structure of BSP-30K, a major lipid-, gelatin-, and heparin-binding glycoprotein of bovine seminal plasma, FEBS Lett. 399 (1996) 147–152.
- [34] S.M. Muthana, C.T. Campbell, J.C. Gildersleeve, Modifications of glycans: biological significance and therapeutic opportunities, ACS Chem. Biol. 7 (2012) 31–43
- [35] D.M. Chipman, V. Grisaro, N. Sharon, Binding of oligosaccharides containing N-acetylglucosamine and N-acetylmuramic acid to lysozyme: the specificity of binding subsites, J. Biol. Chem. 242 (1967) 4388–4394.
- [36] C.S. Kumar, D. Sivaramakrishna, S.K. Ravi, M.J. Swamy, Fluorescence investigations on choline phospholipid binding and chemical unfolding of HSP- 1/ 2, a major protein of horse seminal plasma, J. Photochem. Photobiol. B Biol. 158 (2016) 89–98.
- [37] T. Mann, C. Lutwak-Mann (Eds.), Male Reproductive Function and Semen, Springer-Verlag, Berlin, 1981, 495pp.
- [38] W.V. Holt, R.D. North, Determination of lipid composition and thermal phase transition temperature in an enriched plasma membrane fraction from ram spermatozoa, J. Reprod. Fertil. 73 (1985) 285–294.
- [39] J.E. Parks, J.A. Arion, R.H. Foote, Lipids of plasma membrane and outer acrosomal membrane from bovine spermatozoa, Biol. Reprod. 37 (1987) 1249–1258.
- [40] P. Martínez, A. Morros, Membrane lipid dynamics during human sperm capacitation, Front. Biosci. 1 (1996) 103–117.
- [41] G. Plante, B. Prud'homme, J. Fan, M. Lafleur, P. Manjunath, Evolution and function of mammalian binder of sperm protein, Cell Tissue Res. 363 (2016) 105–127.